

**Small Core Heterocyclic Carbamates and Carboxamides:  
Resistance-breaking Acetylcholinesterase Inhibitors Targeting the Malaria Mosquito,  
*Anopheles gambiae***

Astha Verma

Dissertation submitted to the faculty of the Virginia Polytechnic Institute and State University in  
partial fulfillment of the requirements for the degree of

**Doctor of Philosophy**

In

**Chemistry**

Paul R. Carlier, Committee Chair  
David G. I. Kingston  
James M. Tanko  
Webster L. Santos

April 22<sup>nd</sup>, 2014  
Blacksburg, VA

Keywords: Acetylcholinesterase, 1,2-azoles, *Anopheles gambiae*, heterocyclic carbamates and carboxamides, isoxazole, insecticide treated nets, malaria, pyrazoles, propoxur, insecticide resistance, species-selective inhibitors.

Copyright © Astha Verma

**Small Core Heterocyclic Carbamates and Carboxamides:  
Resistance-breaking Acetylcholinesterase Inhibitors Targeting the Malaria Mosquito,  
*Anopheles gambiae***

Astha Verma

ABSTRACT

Malaria is one of the deadliest diseases known to mankind. In 2010, 219 million cases were reported, and 666,000 deaths were attributed to this disease. In the past, pyrethroid-treated mosquito nets have shown efficacy in reducing malaria transmission in many malaria endemic regions. However, an upsurge in the mosquito population that is resistant to pyrethroids threatens to compromise the efficacy of pyrethroid-treated bed nets. In an effort to develop another class of insecticide with a different mode of action, we have explored three classes of five membered heterocyclic carbamates (isoxazol-3-yl, pyrazol-5-yl, and pyrazol-4-yl), and 3-oxoisoxazole-2(3*H*)-carboxamide as acetylcholinesterase inhibitors (AChE) targeting wild type (G3) and resistant (Akron) malaria mosquito *Anopheles gambiae* (*Ag*). Isoxazole carboxamide and carbamates were obtained regioselectively through judicious use of two different protocols. The final products were characterized and identified using <sup>1</sup>H and <sup>13</sup>C NMR, and mass spectroscopy. In addition, the carboxamide structure was confirmed using X-ray diffraction. Several of the novel carbamates and carboxamides evaluated exhibited excellent toxicity towards susceptible G3 and resistant Akron strain *An. gambiae* (**48f** LC<sub>50</sub> G3 = 41 µg/mL, LC<sub>50</sub> Akron = 58 µg/mL, and **47i** LC<sub>50</sub> G3 = 38 µg/mL, LC<sub>50</sub> Akron = 40 µg/mL). Hence, achieving the resistance-breaking goal. On the contrary, the commercial aryl methylcarbamates currently approved for indoor residual sprays (IRS) showed no potency towards the resistant strain *An. gambiae* (LC<sub>50</sub> G3 = 16-42 µg/mL, and LC<sub>50</sub> Akron >5,000 µg/mL). Further, we observed low toxicological

cross-resistance ratios (RR) for the toxic isoxazol-3-yl and pyrazol-4-yl carbamates, and 3-oxoisoxazole-2(3*H*)-carboxamides (RR = 0.5-2.0). Amongst the commercial AChE inhibitors approved for IRS, only aldicarb exhibited such low RR (RR = 0.5), whereas the RR for commercial aryl methylcarbamates exceed 130-fold. The low RR observed for these novel heterocyclic inhibitors would certainly be favorable for a new anticholinesterase-based mosquitocide targeting both the susceptible and resistant strain mosquitoes. Although the overall selectivity (*Ag* vs *human*) did not exceed 24-fold, the heterocyclic carbamates and carboxamides synthesized by the author showed appreciable inhibition of resistant AChE (G119S) in comparison to commercial aryl carbamates, which showed no inhibition at all.

During the course of this project, the isoxazol-3-yl and pyrazol-5-yl methylcarbamates proved to be unstable, and thus could not be isolated. The synthesis of pyrazol-4-yl methylcarbamates using *N*-methylcarbamoyl chloride proved particularly challenging due to the formation of by-products called allophanates. The similar R<sub>f</sub> of the by-product and the desired final product made the isolation laborious and time-consuming. We have successfully overcome this problem by employing a new protocol, where triphosgene served as the carbonylating agent and *N*-methylamine in THF was used as the amine source. In addition, we have also developed another one-pot protocol for a safer synthesis of pyrazol-4-yl methylcarbamates utilizing 1,1-carbonyldiimidazole (CDI), and *N*-methylamine hydrogen chloride salt. With the pyrazol-4-yl core, apart from achieving excellent toxicity towards both strains of *An. gambiae*, we have also achieved excellent *Ag*AChE vs *h*AChE selectivity (*Ag* vs *h* >100-fold). Due to our continued interest in developing this core, we have devised a convenient, scalable, no-column approach for the synthesis an intermediate **103** that can be utilized to synthesize these compounds more efficiently.

## Acknowledgements

“It is not the destination but the journey that matters”. In my case though the destination is definitely important, the journey would not have been achievable and memorable without the presence of the people mentioned here.

First and foremost, I would like to thank my advisor, Professor Paul R. Carlier, for his immense support and guidance throughout my Ph.D. program at the Virginia Tech. I often wonder, whether I won half the battle when I chose him as my mentor. He groomed me into a successful chemist as well as a confident individual. His hands-off training method developed me into an independent researcher and a critical thinker. However, he was always available for guidance when needed. I truly appreciate the emotional support he has given me during my difficult times, whether it was during visa issues or when I lacked self-confidence. Professional integrity, righteousness, patience, and punctiliousness would be amongst the many qualities I admired in him, and I will emulate in my future endeavors.

My sincere gratitude goes to my committee members: Dr. Kingston, Dr. Santos, and Dr. Tanko. Their valuable feedback and research ideas during committee meetings always stimulated me towards better performance. Their suggestions and comments on my writing have been instrumental in the refinement of my thesis. I would like to thank Dr. Bloomquist and his research group for sharing their expertise in entomology and for providing the contact toxicity data. I would also like to acknowledge our Molsoft LLC collaborators for performing the docking studies on my compounds. My special thanks to Dr. Carla Slebodnick for providing me the X-ray crystal structures of my compounds. The thermal ellipsoid drawings provided by her, have always been helpful in nailing down the final structures of my compounds. Moreover, I

wholeheartedly appreciate her patience during the back and forth email conversations we had while solving my queries.

I would like to thank all of my colleagues cum friends in Carlier research group especially Dr. Dawn M. Wong, Maryam, and Eugene. Dr. Dawn Wong was always there whenever I needed moral support or more insights on enzyme kinetics. Thank you for patiently listening to me and always showing me the light at the end of the tunnel. Maryam, I am truly going to miss our getaways to buffalo wild wings after the group meetings!!! Eugene, it has always been a pleasure chit chatting with you, be it about chemistry or our usual leg pulling.

I would also like to thank all my friends outside my work life. My friend Navi provided me useful guidance during the initial years of my Ph.D. I still remember his critical comments on my writing style and my presentation style that helped me improve on both the departments. Big thanks to Shraddha for all the sumptuous dinners, especially during the busy days of my thesis writing. Many thanks to my good friend Swapnil for lending me his car during my late-nights in lab. Working till 2 a.m. would not have been possible without his support. I also thank my friends Ninad, Neeraj, and Pavithra for the fun-filled time in Blacksburg. My undergraduate friends (Manasi, Sonali, Krittika, Nidhi, Priyanka, and Jyoti) provided me their priceless support through WhatsApp during my difficult times, even though they were in different places. Gladly, they no longer have to say, “you are almost there, Astha”.

Last but not least, I would like to acknowledge my family for their continued support and trust in me. I am able to reach this far because of their sincere enthusiasm in providing me good education. I am grateful for all the sacrifices my parents have made; from sacrificing their sleep to give me early morning tea during my exam days to sending their children overseas in search of a better future and giving up the idea of meeting them every few months. While they have

motivated me to strive for excellence in studies, they made sure I did not lose my sanity under academic pressure.

Without the contribution of each one of you, I would not have been Doctor Astha Verma.

Thank you All!

## **Dedication**

*To*

*My mother & father,*

*Pramila Verma & Ranjit Singh Verma,*

*for their love, understanding, and encouragement*

## Table of Contents

<b>Chapter 1: Malaria-An overview .....</b>	<b>1</b>	
<b>1.1</b>	Introduction .....	1
<b>1.2</b>	Socio-economic burden of malaria.....	2
<b>1.3</b>	The malaria parasites.....	4
<b>1.4</b>	The life cycle of the Plasmodium parasite .....	5
<b>1.5</b>	Malaria prevention and control .....	7
<b>1.5.1</b>	Vaccine development .....	7
<b>1.5.2</b>	Antimalarial drug development.....	8
<b>1.5.3</b>	Vector control.....	9
<b>1.6</b>	Vector control using insecticides .....	12
<b>1.6.1</b>	Voltage-gated sodium channel blockers.....	12
<b>1.6.1.1</b>	Organochlorines .....	12
<b>1.6.1.2</b>	Pyrethroids.....	13
<b>1.6.2</b>	Acetylcholinesterase inhibitors .....	16
<b>1.6.2.1</b>	Introduction to acetylcholinesterase (AChE) system .....	16
<b>1.6.3</b>	Role of AChE inhibitors.....	21
<b>1.6.3.1</b>	Organophosphates (OP) .....	21
<b>1.6.3.2</b>	Carbamates .....	25
<b>1.6.3.3</b>	Insecticidal resistance in <i>Anopheles gambiae</i> to AChE inhibitors.....	30
<b>1.7</b>	Bibliography .....	32
<b>Chapter 2: Exploring 3-oxoisoxazole-2(3H)-carboxamides and isoxazol-3-yl carbamates as mosquitoicide .....</b>	<b>45</b>	
<b>2.1</b>	An overview of Chapter 2 .....	45
<b>2.2</b>	Bioassays .....	45
<b>2.2.1</b>	Tarsal contact toxicity assay.....	45
<b>2.2.2</b>	Enzyme inhibition .....	47
<b>2.3</b>	Rationale and objective behind the synthesis of five membered heterocyclic carboxamides and carbamates .....	50

<b>2.4</b>	3-oxoisoxazole-2( <i>3H</i> )-carboxamides and isoxazol-3-yl carbamates .....	56
<b>2.5</b>	Characterization of the 3-oxoisoxazole-2( <i>3H</i> )-carboxamide and isoxazol-3-yl carbamates.....	77
<b>2.6</b>	Tarsal contact toxicity of 3-oxoisoxazole-2( <i>3H</i> )-carboxamides and isoxazol-3-yl carbamates.....	81
<b>2.7</b>	Enzyme inhibition by 3-oxoisoxazole-2( <i>3H</i> )-carboxamides and isoxazol-3-yl carbamates.....	88
<b>2.8</b>	Conclusion.....	100
<b>2.9</b>	Bibliography .....	101
 <b>Chapter 3: Exploring pyrazol-5-yl and pyrazol-4-yl carbamates as mosquitocide.</b> .....		<b>110</b>
<b>3.1</b>	Introduction .....	110
<b>3.2</b>	Synthesis of pyrazol-5-yl carbamates.....	113
<b>3.3</b>	Toxicity and enzyme inhibition studies on pyrazol-5-yl dimethylcarbamates.....	118
<b>3.4</b>	Synthesis of pyrazol-4-yl carbamates.....	121
<b>3.5</b>	Toxicity and enzyme inhibition studies on pyrazole-4-yl methylcarbamates .....	127
<b>3.6</b>	An efficient protecting group protocol for the synthesis of pyrazol-4-yl carbamates	131
<b>3.7</b>	Conclusion.....	141
<b>3.8</b>	Bibliography .....	142
 <b>Chapter 4: Future research project ideas.....</b>		<b>149</b>
 <b>Chapter 5: Experimental procedures and analytical data for Chapter 2.....</b>		<b>156</b>
<b>5.1</b>	Materials.....	156
<b>5.2</b>	General procedure for the synthesis of acyl Meldrum's acids <b>44a-f, k, m, o</b> using acid chlorides.....	156
<b>5.3</b>	General procedure for the synthesis of acyl Meldrum's acids <b>44g-j, l, n</b> using acids	161
<b>5.4</b>	General procedure for the synthesis of <i>N,O</i> -diBoc-protected $\beta$ -keto hydroxamic acids <b>45c, d, k, l, o</b> .....	165
<b>5.5</b>	General procedure for the synthesis of <i>N,O</i> -diBoc-protected $\beta$ -keto hydroxamic acids <b>45a, b, e, g-j, m</b> .....	168

<b>5.6</b>	General procedure for the synthesis of 5-substituted isoxazol-3-ols <b>46a-o</b> .....	175
<b>5.7</b>	General procedure for the synthesis of <i>N,N</i> -dimethyl-3-oxoisoxazole-2(3 <i>H</i> )-carboxamide <b>47a-p</b> .....	183
<b>5.8</b>	General procedure for the synthesis of isoxazol-3-yl dimethylcarbamate .....	191
<b>5.9</b>	General procedure for the synthesis of <i>N</i> -methyl-3-oxoisoxazole-2(3 <i>H</i> )-carboxamide.....	200
<b>5.10</b>	Synthesis of <i>N</i> -substituted derivatives of <b>46h</b> .....	208
<b>5.11</b>	X-ray crystallographic analysis .....	216
<b>5.12</b>	Bibliography .....	219
 <b>Chapter 6: Experimental procedures and analytical data for Chapter 3.....</b>		<b>220</b>
<b>6.1</b>	Materials.....	220
<b>6.2</b>	Experimental section for chapter 3 section 3.2 .....	220
<b>6.3</b>	Experimental section for chapter 3 section 3.4 .....	230
<b>6.4</b>	Experimental section for chapter 3 section 3.6 .....	248
<b>6.5</b>	Bibliography .....	257

## List of Figures

<b>Figure 1.1:</b>	Global distribution of malaria.....	2
<b>Figure 1.2:</b>	The malaria transmission cycle.....	6
<b>Figure 1.3:</b>	Anti-malarial drugs: Chloroquine, sulphadoxine, pyrimethamine, mefloquine, and artemisinin.....	8
<b>Figure 1.4:</b>	Some of the recommended insecticides for IRS malaria vector control.....	10
<b>Figure 1.5:</b>	Insecticide treated mosquito net.....	11
<b>Figure 1.6:</b>	Natural product, pyrethrin and their synthetic analogs called pyrethroids. ....	14
<b>Figure 1.7:</b>	Simplified catalytic cycle of substrate hydrolysis by acetylcholinesterase (AChE).....	16
<b>Figure 1.8:</b>	Ribbon diagram of 3-D structure of <i>TcAChE</i> (PDB Code 2ace).....	17
<b>Figure 1.9:</b>	Simplified diagram of the active-site gorge of <i>TcAChE</i> . .....	18
<b>Figure 1.10:</b>	Acetylcholine manually docked in the active site of the enzyme AChE (PDB ID 2ace).....	20
<b>Figure 1.11:</b>	Organophosphorus compounds: Insecticides and nerve agents.....	22
<b>Figure 1.12:</b>	The bioactivation of parathion ( <b>16</b> ) to paraoxon ( <b>22</b> ) through cytochrome P450 mediated desulfuration.....	23
<b>Figure 1.13:</b>	Structure of antidote 2-PAM.....	24
<b>Figure 1.14:</b>	Phosphorylation and aging of AChE .....	25
<b>Figure 1.15:</b>	Structure of physostigmine and carbaryl .....	25
<b>Figure 1.16:</b>	General mechanism of pseudo-irreversible inhibition of cholinesterase by carbamates.....	26
<b>Figure 1.17:</b>	Alignment of <i>T. californica</i> , human, <i>An. gambiae</i> (ace-1), and <i>D. melanogaster</i> (ace-2). .....	29
<b>Figure 1.18:</b>	(A) Distribution of carbamate resistance across Africa from 2000-2013. (B) Distribution of pyrethroid resistance across Africa from 2000-2013. ....	30
<b>Figure 2.1:</b>	Tubes used in WHO filter paper toxicity assays.....	46
<b>Figure 2.2:</b>	Structure of commercial carbamates ( <b>8</b> , <b>9</b> , <b>27-29</b> ), and previously reported aryl methylcarbamates ( <b>30-32</b> ) .....	50

<b>Figure 2.3:</b>	Computational modelling of (A) terbam ( <b>28</b> ) in the active site of susceptible enzyme. (B) terbam ( <b>28</b> ) in the active site of G119S enzyme. (C) aldicarb ( <b>29</b> ) in the active site of G119S enzyme .....	55
<b>Figure 2.4:</b>	Biologically active isoxazol-3-ols.....	56
<b>Figure 2.5:</b>	Structure of Meldrum's acid <b>42</b> , and its misinterpreted structure <b>43</b> .....	60
<b>Figure 2.6:</b>	$^1\text{H}$ NMR of <b>45a</b> in $\text{CDCl}_3$ showing keto-enol tautomerism. ....	64
<b>Figure 2.7:</b>	Tautomeric representation of isoxazol-3-ols .....	68
<b>Figure 2.8:</b>	Anisotropic displacement ellipsoid drawings (50%) of X-ray structure of compound <b>46m</b> . .....	68
<b>Figure 2.9:</b>	A) $^1\text{H}$ NMR of dimethylcarboxamide ( <b>47a</b> ), dimethylcarbamate ( <b>48a</b> ), and 2-isopropoxyphenyl dimethylcarbamate ( <b>67</b> ). B) $^{13}\text{C}$ NMR of dimethylcarboxamide ( <b>47a</b> ), dimethylcarbamate ( <b>48a</b> ), and 2-isopropoxyphenyl dimethylcarbamate ( <b>67</b> ). ....	78
<b>Figure 2.10:</b>	Characteristic chemical shift differences of <i>H</i> -4 in carboxamides and carbamates, as illustrated by <b>47k</b> , <b>49k</b> , and <b>48k</b> , respectively. ....	79
<b>Figure 2.11:</b>	Anisotropic displacement ellipsoid drawings (50%) of X-ray structure of compound <b>49k</b> . .....	80
<b>Figure 2.12:</b>	Anisotropic displacement ellipsoid drawings (50%) of X-ray structure of compound <b>47e</b> . ....	80
<b>Figure 2.13:</b>	Structure of the synthesized dimethylcarboxamide <b>47d</b> , and <b>68</b> , a known potent AChE trifluoromethylketone inhibitor (TFK). ....	96
<b>Figure 2.14:</b>	Tetrahedral adduct formed after the attack of AChE (mouse) active site serine S203 on carbonyl carbon of <b>68</b> and <b>47d</b> . ....	98
<b>Figure 2.15:</b>	Chemical structures of previously reported serine hydrolase inhibitors.....	99
<b>Figure 3.1:</b>	Marketed drugs containing pyrazole core as the basic moiety. ....	110
<b>Figure 3.2:</b>	Degradation pathways of fipronil ( <b>75</b> ) in animals and plants. ....	111
<b>Figure 3.3:</b>	Commercially available agrochemicals containing pyrazole as the basic moiety .....	112
<b>Figure 3.4:</b>	Chemdraw representation of pyrazol-5-yl and pyrazol-4-yl carbamates.....	113

<b>Figure 3.5:</b>	Computational modeling of (A) terbam ( <b>28</b> ) in the active site of susceptible enzyme. (B) terbam ( <b>28</b> ) in the active site of G119S enzyme. (C) <i>S</i> -enantiomer of pyrazol-4-yl methylcarbamate ( <b>99a</b> ) in the active site of G119S enzyme .....	131
<b>Figure 3.6:</b>	Proposed applicability of an efficient synthesis of pyrazol-4-ol. ....	133
<b>Figure 4.1:</b>	Potent serine hydrolase inhibitors.....	150
<b>Figure 4.2:</b>	Schemes depicting the synthesis of desired <i>1H</i> -1,2,3 triazole ureas .....	152
<b>Figure 4.3:</b>	Synthesis of 3,5-disubstituted- <i>1H</i> -1,2,4-triazole .....	153

## List of Tables

<b>Table 2.1:</b>	Bimolecular rate constants $k_i$ for inactivation of rAgAChE (WT, G119S), and hAChE.....	51
<b>Table 2.2:</b>	Tarsal and topical contact toxicity to WT (G3) and Akron strain <i>An. gambiae</i> .....	53
<b>Table 2.3:</b>	Isolated yields for the synthesis of acylated Meldrum's acids <b>44</b> .....	61
<b>Table 2.4:</b>	Isolated yields for the synthesis of $\beta$ -keto hydroxamic acids <b>45a-o</b> from acylated Meldrum's acids <b>44a-o</b> .....	63
<b>Table 2.5:</b>	Isolated yields of 5-substituted isoxazol-3-ols <b>46</b> .....	67
<b>Table 2.6:</b>	Isolated yields of 5-substituted 3-oxoisoxazole-2(3H)-carboxamide <b>47</b> , and isoxazol-3-yl dimethylcarbamates <b>48</b> .....	69
<b>Table 2.7:</b>	Isolated yields of 5-substituted-N-methyl-3-oxoisoxazole-2(3H)-carboxamide <b>49</b> .....	72
<b>Table 2.8:</b>	Tarsal contact toxicity of 5-substituted <i>N,N</i> -dialkyl-3-oxoisoxazole-2(3H)-carboxamides to G3 and Akron strain of <i>An. gambiae</i> .....	82
<b>Table 2.9:</b>	Tarsal contact toxicity of 5-substituted isoxazol-3-yl dialkylcarbamates to G3 and Akron strain of <i>An. gambiae</i> .....	85
<b>Table 2.10:</b>	Inactivation rate constants $k_i$ of 5-substituted <i>N,N</i> -dialkyl-3-oxoisoxazole-2(3H)-carboxamides for rAgAChE (WT and G119S), & rhAChE.....	89
<b>Table 2.11:</b>	Inactivation rate constants $k_i$ of 5-substituted isoxazol-3-yl dialkylcarbamates for rAgAChE (WT and G119S), & rhAChE.....	92
<b>Table 3.1:</b>	Half-life of 1-isopropyl-3-methyl-1 <i>H</i> -pyrazol-5-yl methylcarbamate ( <b>86b</b> ) at various pH values as reported by Gubler et al .....	115
<b>Table 3.2:</b>	Isolated yields of alkyl hydrazine sulfate salt <b>90b-d</b> .....	116
<b>Table 3.3:</b>	Isolated yields of <i>N</i> -alkyl pyrazol-5-one <b>85b-d</b> .....	117
<b>Table 3.4:</b>	Isolated yields of <i>N</i> -alkyl pyrazol-5-yl dimethylcarbamate <b>82b-d</b> .....	118
<b>Table 3.5:</b>	Tarsal contact toxicity pyrazol-5-yl dimethylcarbamates to G3 and Akron strain of <i>An. gambiae</i> . .....	119
<b>Table 3.6:</b>	Inactivation rate constants $k_i$ ( $\text{mM}^{-1} \text{ min}^{-1}$ ) for AgAChE (WT and G119S), and rhAChE. ....	120
<b>Table 3.7:</b>	Synthesis of <i>N</i> -substituted 4-iodopyrazole <b>93a-c,e</b> .....	122

<b>Table 3.8:</b>	Synthesis of <i>N</i> -substituted 4-benzyloxy pyrazole <b>97a-e</b> , and <i>N</i> -substituted pyrazol-4-ols <b>98a-e</b> .....	123
<b>Table 3.9:</b>	Synthesis and isolated yields of pyrazol-4-yl methylcarbamates <b>99a-c,e</b> using triphosgene and <i>N</i> -methylamine.....	125
<b>Table 3.10:</b>	Tarsal contact toxicity of pyrazol-4-yl methylcarbamates ( <b>99a-e</b> ) towards G3 and Akron strain of <i>An. gambiae</i> .....	128
<b>Table 3.11:</b>	Pyrazol-4-yl methylcarbamates ( <b>99a-e</b> ) inactivation rate constants $k_i$ for rAgAChE (WT and G119S), and rhAChE.....	129
<b>Table 3.12:</b>	Attempted deprotection of PMB, and PMP protected 4-(benzyloxy)-1 <i>H</i> -pyrazole.....	138

## List of Schemes

<b>Scheme 2.1:</b> Ellman assay for the chlorimetric determination of AChE acitivity.....	47
<b>Scheme 2.2:</b> Kinetic scheme explaining mechanism of AChE by pseudo-irreversible carbamate inhibitors.....	48
<b>Scheme 2.3:</b> Synthesis of 5-methylisoxazol-3-ol ( <b>39</b> ).....	57
<b>Scheme 2.4:</b> Simplified mechanism leading to the formation of the desired isoxazol-3-ols, and undesired isoxazol-5-ones .....	59
<b>Scheme 2.5:</b> Possible pathways for the formation of $\beta$ -keto hydroxamic acids <b>45</b> .....	66
<b>Scheme 2.6:</b> Regioselective synthesis of 5-substituted 3-oxoisoxazole-2( <i>3H</i> )-carboxamide <b>47</b> , and isoxazol-3-yl dimethylcarbamates <b>48</b> .....	69
<b>Scheme 2.7:</b> Synthesis of 5-substituted 3-oxoisoxazole-2( <i>3H</i> )-carboxamide <b>49</b> .....	72
<b>Scheme 2.8:</b> Attempted synthesis of <i>N</i> -benzyl- <i>N</i> -methyl-3-oxo-5-(pentan-2-yl)isoxazole-2( <i>3H</i> )-carboxamide and 5-(pentan-2-yl)isoxazol-3-yl benzyl(methyl) carbamate using disuccinimidyl carbonate ( <b>50</b> ) as a carbonylating agent.....	74
<b>Scheme 2.9:</b> Attempted synthesis of <i>N</i> -substituted-5-neopentyl-3-oxoisoxazole-2( <i>3H</i> )-carboxamide, and 5-neopentylisoxazol-3-yl- <i>N</i> -substituted carbamate using carbonyl diimidazole ( <b>52</b> ) as a carbonylating agent .....	75
<b>Scheme 2.10:</b> Synthesis of 5-(2-pentyl)- <i>N</i> -substituted-3-oxoisoxazole-2( <i>3H</i> )-carboxamide, and 5-(2-pentyl)-isoxazol-3-yl- <i>N</i> -substituted carbamate using triphosgene.....	76
<b>Scheme 2.11:</b> Synthesis of 5-(2-pentyl)- <i>N</i> -substituted-3-oxoisoxazole-2( <i>3H</i> )-carboxamide and -(2-pentyl)-isoxazol-3-yl- <i>N</i> -substituted carbamate from commercially available carbamoyl chlorides.....	77
<b>Scheme 3.1:</b> Synthesis of 3-methyl-1-phenylpyrazol-5-one .....	113
<b>Scheme 3.2:</b> Synthesis of 3-methyl-1-phenylpyrazol-5-yl dimethylcarbamate ( <b>82a</b> ) and methylcarbamate ( <b>86a</b> ). ....	114
<b>Scheme 3.3:</b> Synthesis of 4-iodo-1-(3-methoxybutyl)-1 <i>H</i> -pyrazole ( <b>93d</b> ). ....	122
<b>Scheme 3.4:</b> Synthesis of pyrazol-4-yl methylcarbamate using <i>N</i> -methylcarbamoyl chloride.....	124
<b>Scheme 3.5:</b> Synthesis of pyrazol-4-yl methylcarbamate using CDI, and <i>N</i> -methyamine hydrogenchloride salt.....	126

<b>Scheme 3.6:</b> Proposed scheme for the synthesis of pyrazol-4-ols.....	134
<b>Scheme 3.7:</b> (A) Protection of 4-iodopyrazole using trityl, and PMB protecting group. (B) Attempted protection of 4-iodopyrazole using PMP group. (C) Protection of pyrazole using PMP group.....	135
<b>Scheme 3.8:</b> Cu-catalyzed benzyloxylation of <b>97f</b> , <b>97g</b> , <b>97h</b> .....	136
<b>Scheme 3.9:</b> De-protection of <b>97f</b> using TFA .....	137
<b>Scheme 3.10:</b> A no-column protocol for the synthesis of <b>103</b> using <i>N</i> -trityl-4-iodopyrazole ..	140
<b>Scheme 3.11:</b> An illustrative example to demonstrate the applicability of synthesized <b>103</b> intermediate.....	141

## List of Abbreviations

- AChE: Acetylcholinesterase  
ACh: Acetylcholine  
ATCh: Acetylthiocholine  
AD: Alzheimer's disease  
*An. gambiae*: *Anopheles gambiae*  
ACT: Artemisinin-based combination therapy  
CDI: Carbonyl diimidazole  
CAS: Catalytic active site  
CDC: Center for Disease Control and Prevention  
CNS: Central nervous system  
DALYs: Disability-adjusted life years  
DDT: Dichlorodiphenyltrichloroethane  
*D. melanogaster*: *Drosophila melanogaster*  
DTNB: (5,5'-dithiobis)-2-nitrobenzoic acid  
GDP: Gross domestic product  
HSL: Hormone sensitive lipase inhibitor  
HPPD: 4-hydroxyphenylpyruvate dioxygenase  
IRS: Indoor-residual spraying  
ITNs: Insecticide-treated nets  
kdr: Knockdown resistance  
MCs: Methyl carbamates  
*M. domestica*: *Musca domestica*  
NTE: Neurotoxic esterase  
OPs: Organophosphates  
OPIDN: Organophosphate induced delayed neuropathy  
PAS: Peripheral anionic site  
PBO: Piperonyl butoxide  
PMB: *p*-methoxybenzyl  
PMP: *p*-methoxyphenyl

RR: Resistance ratio

TLC: Thin layer chromatography

Trt: Trityl

TNB: 5-thio-2-nitrobenzoic acid

*T. californica*: Torpedo californica

WHO: World Health Organization

WHOPES: World Health Organization Pesticide Evaluation Scheme

## **Chapter 1: Malaria-An overview**

### **1.1 Introduction**

Vector-borne diseases are present in more than 100 countries, predominantly in the tropics, subtropical, and warm temperate regions.<sup>1</sup> According to DALYs (disability-adjusted life years), which is a metric to express the sum of the number of years lost due to ill-health or premature death in a population, one-sixth of the world's infection is attributed to vector-borne diseases.<sup>2</sup> In fact, 90% of this fraction is due to mosquito-transmitted agents, where the malaria parasite contributes more to the burden than any other pathogen.<sup>2</sup> Today more than 40% of the world's population lives under the risk of contracting malaria.<sup>3</sup> According to World Health Organization (WHO) estimates, malaria killed nearly 655,000 people in 2010, mostly children under the age of five.<sup>4</sup> According to a recent study, the actual mortality numbers are almost double of what is reported because many cases go unreported or undiagnosed.<sup>5</sup>

The history of this disease can be traced back to ancient times. Several characteristic symptoms that almost certainly described malaria appear in Chinese documents dating from 2700 BC and goes as far back as the sixth century BC Hindu texts.<sup>6</sup> Malaria was widely recognized in Greece by the 4<sup>th</sup> century BCE. Early Greeks including Homer (850 BC), Empedocles of Agrigentum (550 BC), and Hippocrates (400 BC), were aware of the principal symptoms like poor health and paroxysmal fevers associated with enlarged stiff spleen that were often seen in people living in marshy places.<sup>6-7</sup> For this reason, for over 2,500 years it was mistakenly believed that the malaria fevers were caused by the miasmas rising from the swamps.<sup>6</sup> Hence, the name mal'aria, which means bad or spoiled air, although this name has been largely disputed.<sup>6</sup> The first major breakthrough in malaria research was achieved in 1880, when Charles Louis Alphonse Laveran, a French army surgeon, discovered the malaria parasite

in the blood of malaria patients.<sup>8</sup> For this discovery, he was awarded the Nobel Prize in Medicine in 1907.<sup>8</sup> In 1897, Ronald Ross, a British officer in Indian Medical Service, established the role of mosquitoes in transmitting malaria.<sup>6</sup> He received the Nobel Prize in 1902 for his work on malaria.<sup>7</sup> After these pioneering discoveries, it was believed that a cure for this disease was not far away, however till today many parts of the world are still struggling to fight the burden of this disease.

## 1.2 Socio-economic burden of malaria

The burden of malaria is very unevenly distributed. From the global transmission map (Figure 1.1), it is clear that the disease is centered in the tropics, with a reach into subtropical regions in the five continents.<sup>9</sup>

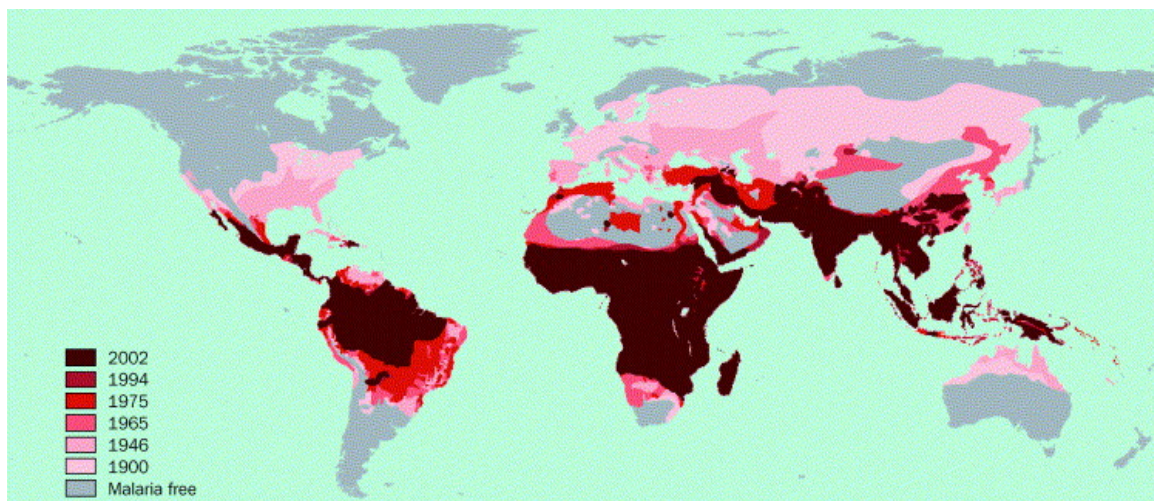


**Figure 1.1:** Global distribution of malaria.<sup>10</sup> With copyright permission from Elsevier.

Attempts to eliminate or at least suppress the disease have been successful in temperate zones which are characterized by strong seasonality and cold winters. Apart from climatic features, factors like socio-economic development, improved housing (especially the provision

of screened door and windows) combined with the efforts at better environmental management such as eliminating the breeding grounds of vector mosquitoes have played a crucial role in eliminating malaria from temperate zone countries.<sup>9</sup> Conversely, the vector control methods that succeeded in the temperate zones have repeatedly failed in the tropical regions. In the tropics, climatic conditions provide a favorable habitat for the breeding of mosquitoes. Subsequently, frequent exposure to the infected vector mosquitoes each night leads to high inoculation rates, which in turn, when combined with the long duration of the parasite survival in the host leads to a population saturated with the infection.<sup>9</sup>

Malaria endemic countries are generally poorer than non-malarious countries and also have a lower economic growth rate.<sup>9</sup> However, it remains unclear whether it is the poverty that promotes malaria or it is the malaria that causes poverty by hampering the economic growth. It is possible that the causation goes in both directions. In 1995, the global distribution of per-capita gross domestic product (GDP) showed a striking correlation between poverty and malaria. The average GDP in countries with intensive malaria was US\$1,526 as compared to US\$8,268 in the countries which were not intensively malarious.<sup>11</sup> Poverty can certainly be held accountable for the large malaria transmission in the poor countries. While people in the developed countries can spend more on the prevention methods such as bed nets or insecticides, there is also more funding from the government for the malaria control programmes as compared to that in poor countries.<sup>12</sup> However, economic development alone is not enough, otherwise, the wealthy countries like Oman and United Arab Emirates could have easily eliminated the disease.<sup>9</sup>

Malaria imposes broad social costs by bringing changes in the household behavior in response to the disease, for example, factors like schooling, migration, demography and saving.<sup>11</sup> Adults have been shown to develop some immunity to the disease symptoms in malaria endemic

regions. However, the mortality remains high amongst young children, especially under the age of five. This high infant and child mortality rates leads to a disproportionately high fertility rates and, thus an overall high population growth in the malaria endemic regions.<sup>9</sup> Parents have more children to replace the ones lost to this disease or to have a certain number of surviving kids so as to guarantee at least one male heir. This hypothesis is also known as the “child-survivor hypothesis”.<sup>9</sup>

### 1.3 The malaria parasites

Malaria is caused by an infection from the protozoan parasite *Plasmodium*. The five species of *Plasmodium* that affect humans are: *Plasmodium falciparum*, *Plasmodium vivax*, *Plasmodium malariae*, *Plasmodium ovale* and *Plasmodium knowlesi*.<sup>13</sup> The usual symptoms of uncomplicated malaria caused by all the species of *Plasmodium* are chills, headache/muscle ache, fever, vomiting, diarrhea; a clinical picture that also represents many other childhood infections.<sup>14, 15</sup> The severity of the symptoms and the course of the clinical attack often depend on the species and the strain of the plasmodium parasite.

*P. falciparum* is the most prevalent and lethal malaria parasite especially in sub-Saharan Africa, and is responsible for over 90% of the malaria deaths.<sup>16</sup> Out of 90% of the deaths caused by *P. falciparum*, 80% occur in children under the age of five. If left untreated, *P. falciparum* infection can lead to severe malaria, which in the case of adults is characterized by multi-organ failure, including renal failure.<sup>14</sup> However, in children, severe malaria usually leads to coma, respiratory distress (deep breathing), severe anemia, and cerebral malaria.<sup>17</sup> Respiratory distress signs have been established as a powerful predictor of a fatal outcome in *P. falciparum* malaria.<sup>14</sup>

<sup>18</sup> *P. vivax* is the second most common species with a strong hold in Asia and South America.<sup>19</sup> Most of the cases occur outside of Africa because a high proportion of African population lack

the Duffy blood antigen that is expressed on the surface of the red blood cells and is a necessary receptor for the parasite (*P. vivax*) invasion of erythrocytes.<sup>18</sup> Often termed as benign malaria, the lethality of *P. vivax* has been highly underestimated. Recent estimates suggest that malaria caused by *P. vivax* is more widespread. In comparison to *P. falciparum*, the infection caused by *P. vivax* is more difficult to control and eradicate because the parasite can remain dormant for months (as a hypnozoite, which is a dormant stage in the life cycle of the parasite) in the liver causing relapses.<sup>10, 18, 20</sup> The third species, *P. malariae*, doesn't form hypnozoite but it persists for decades as a blood stage infection without showing any symptoms.<sup>20</sup> The infection with *P. malariae* is less common when compared to the infection with *P. falciparum* or *P. vivax*; although it does occur in malaria-endemic areas.<sup>18</sup> *Plasmodium ovale* is rare outside Africa. The fifth species, *Plasmodium knowlesi*, which was originally known as the monkey parasite, is now known to infect humans in some areas such as Malaysia.<sup>21</sup>

#### 1.4 The life cycle of the *Plasmodium* parasite

The *Plasmodium* parasite is transmitted to human by a female mosquito. The male *Anopheles* mosquito is not a vector for malaria transmission, as they feed exclusively on plants and nectar.<sup>22</sup>

The malaria causing *Plasmodium* parasite has a complex life cycle. It consists of numerous transitions and stages (Figure 1.2).<sup>6</sup>

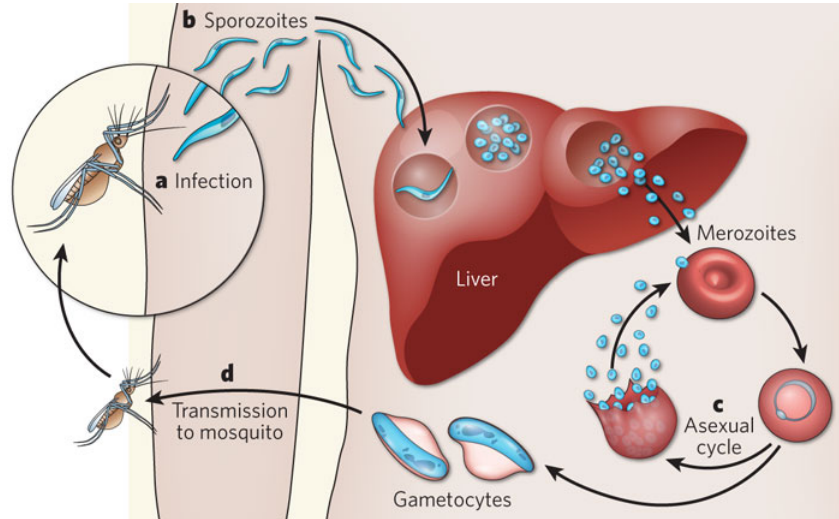


**Figure 1.2:** The malaria transmission cycle.<sup>23</sup> With copyright permission from Nature Publishing Group.

- 1) **Liver stage** – The infection of the human host begins with the inoculation of the parasites (sporozoites) into the blood stream. Within 30 minutes, the sporozoites invade the liver and start replicating (schizonts). The liver stage of the infection lasts for about approximately 5-10 days where each sporozoite undergoes a phase of asexual multiplication to yield tens of thousands of merozoites, which then invade the red blood cells.
- 2) **Blood stage** – During the blood stage of the infection, the merozoites again undergo repeated cycles of asexual multiplication to infect more red blood cells. This stage is responsible for the high malaria fevers and the pathology.
- 3) **Transmission stage** – As the infection progresses some parasites further develop into male and female sexual forms called gametocytes, which circulate in the peripheral blood until a female anopheline mosquito takes them up during blood feeding. In case of *P.vivax*, the sexual forms (gametocytes) are produced earlier in the life cycle in comparison to *P.falciparum*, this makes it more easily transmissible.<sup>18</sup>

4) **Mosquito Stage** – When ingested by mosquitoes, the gametocytes mature into a female and male gametes that fuse in the mosquito gut to form a zygote (not shown in Figure 1.2). This is the beginning of a new process called sporogony, in which new sporozoites are formed to infect the next human host.

## **1.5 Malaria prevention and control**

Malaria control relies on three factors that are elaborated below:

### **1.5.1 Vaccine development**

Currently there is no approved malaria vaccine. An effective and safe malaria vaccine is essential to accelerate the efforts to eliminate and eradicate malaria. Malaria vaccine development has been greatly hampered due to scarcity of research funding and the sheer complexity of the malaria parasite and its life cycle.<sup>1, 24</sup> Amongst all the vaccine candidate against human malaria evaluated so far, RTS,S is the most advanced front runner (developed by GlaxoSmithKline, PATH and the Bill and Melinda Gates Foundation). RTS,S is a pre-erythrocytic vaccine.<sup>24</sup> The exact mechanism by which a pre-erythrocytic vaccine works is still unclear. It is possible that the RTS,S vaccine temporarily reduces the number of merozoites emerging after the liver stage infection.<sup>25</sup> This leads to prolonged exposure to low dose of asexual blood stage parasites, thereby helping the immune system to develop the blood stage immunity naturally.<sup>25</sup> This vaccine is now in Phase III clinical trials. The initial results showed 50% reduction in severe malaria cases in older age group (5 to 17 months) and approximately 37% in younger children (6-12 weeks).<sup>26</sup> However, it is unclear if RTS,S will meet the specific goals of 50 and 80% efficacy set forth in the global malaria vaccine development road map.<sup>27</sup>

### 1.5.2 Antimalarial drug development

Malaria is a curable infectious disease and an antimalarial drug that can cure this disease will be highly valuable. However, the successful implementation of current antimalarial drugs is often hampered by factors such as low efficacy, drug resistance,<sup>13</sup> safety issues (counterfeit drugs), and affordability (especially in poorer nations).<sup>28</sup> Although, chloroquine (**1**) and sulphadoxine-pyrimethamine (**2, 3**) (Figure 1.3) are still the first and second line of treatment for acute uncomplicated malaria, respectively; they fail in some countries due to drug resistance.<sup>13-14</sup>

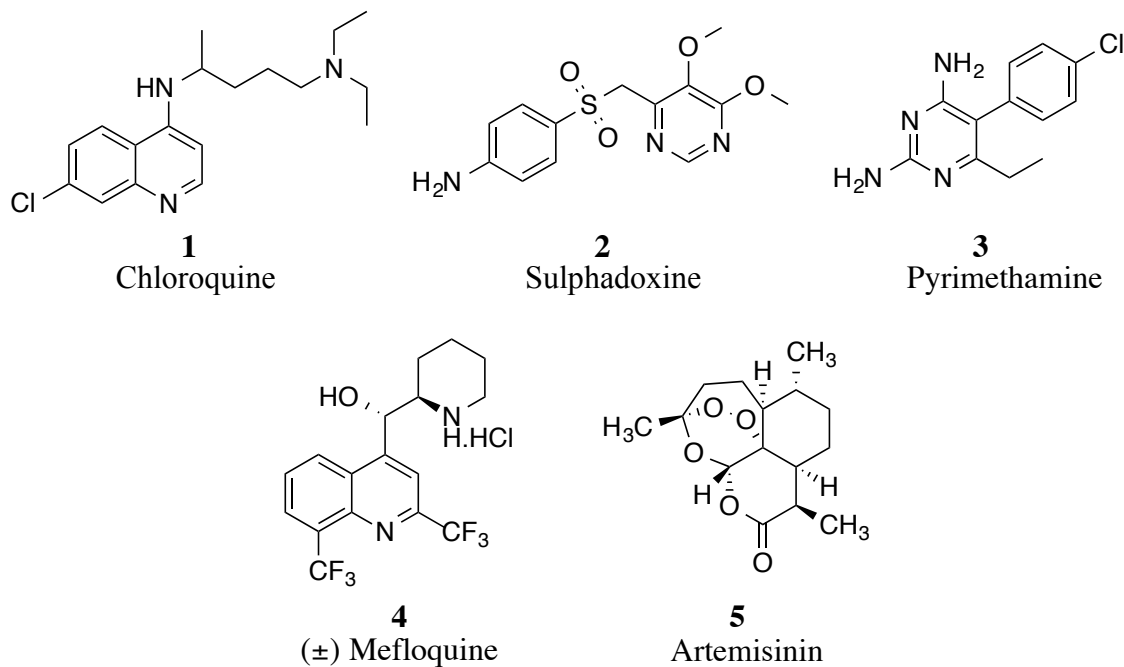


**Figure 1.3:** Anti-malarial drugs: Chloroquine, sulphadoxine, pyrimethamine, mefloquine, and artemisinin.

Resistance has also emerged to newer derivatives such as mefloquine (**4**) which been developed to treat drug resistant strains of *P. falciparum*.<sup>14</sup> In contrast to some antimalarial drugs, artemisinin (**5**) is extremely potent and acts rapidly against the blood stages of the parasite and

has an additional advantage of killing gametocytes, and therefore, decreasing parasite transmission.<sup>29-30</sup> In order to limit the emergence of resistance development, these drugs are used in combination with a second drug.<sup>14</sup> In theory, the different mechanism of action of the combined drugs enables the combination to kill parasites that have resistance to only one of the components of the combination. If the partner drug is selected carefully, artemisinin-based combination therapy (ACT) has shown 95% efficacy in curing malaria and is also well tolerated by the patients. However, this technique is not infallible and there are several reports of emerging resistance to artemisinin too.<sup>13</sup> Also, the high cost of ACT (approximately 10 to 20 times that of chloroquine) limits its use in the poorer regions.<sup>18</sup> Therefore, there is an urgent need for developing new anti-malarial drugs that target all the stages of the parasite or to explore an alternative malaria control strategy such as vector control.

### **1.5.3 Vector control**

Prevention is always better than cure and the same goes for malaria. The major hurdle to global malaria eradication is the parasites' strong hold in Africa. The unusually high populations of an ideal and highly efficient vector, which can provide a safe abode for the parasite to reproduce and then transmit to the human population, adds to the burden and sometimes may even negate the impact of drugs and vaccines. Hence, in order to achieve a definitive end to malaria transmission, the population of the malaria vector must be controlled. The control of mosquitoes has long relied on the use of indoor residual sprays (IRS) and insecticide treated nets (ITNs). In the past, high coverage with either of these interventions has resulted in the community-wide suppression of the malaria transmission.<sup>10, 31</sup>

In IRS, a stable formulation of the insecticide is applied to the walls, and roofs of the houses and domestic animal shelters. This reduces the life span of the female mosquitoes,

thereby reducing the malaria transmission.<sup>32</sup> The first IRS campaign was started after World War II and was highly successful.<sup>33</sup> To date, IRS forms an integral part of malaria control strategy in 25 out of the 42 malaria endemic countries in the WHO African regions.<sup>33</sup> The success of this strategy depends highly on the extensive and sustained coverage, the right time of spraying (which is usually before the transmission season starts), and also on the susceptibility of the targeted vectors species to the insecticide used.<sup>32</sup> Currently 12 insecticides have been approved by WHO for IRS, which includes dichlorodiphenyltrichloroethane (DDT) (**6**), malathion (**7**), bendiocarb (**8**), propoxur (**9**), deltamethrin (**10**).<sup>34</sup> (Figure 1.4)

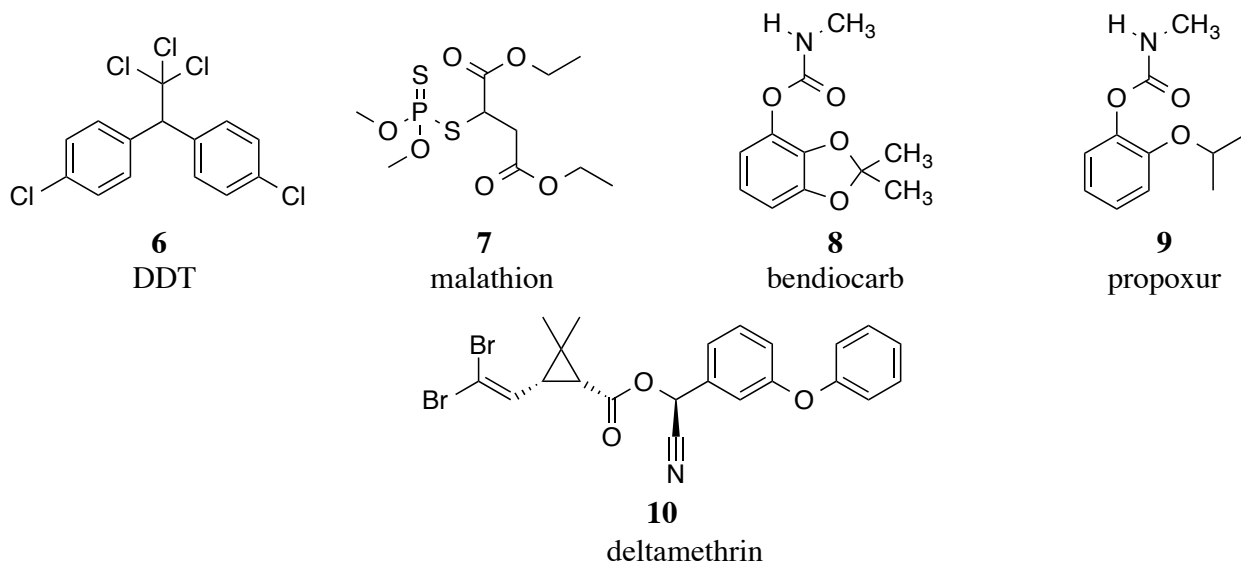


**Figure 1.4:** Some of the recommended insecticides for IRS malaria vector control.<sup>32</sup>

Mosquito nets are an old technology and have been effective to reduce malaria transmission by providing a physical barrier between the human and the infected vector. However, they are not perfect barriers, and hence, insecticide treated nets were invented, which

not only deter the mosquito-human contact by providing a barrier but also reduce the vector populations by killing the mosquito with residual insecticidal activity.<sup>32</sup>



**Figure 1.5:** Insecticide treated mosquito net. Image credit: Deborah Carlier.

ITNs were twice as effective as the untreated nets, and also provided greater than 70% protection when compared to the cases with no nets.<sup>35</sup> ITNs have been shown to reduce child mortality by 16-63%, especially in children under the age of 5 years in several large-scale studies.<sup>36-37</sup> These nets lose efficacy due to repeated washing. So, regular retreatment of the nets with insecticides is required to maintain the efficacy of the ITNs. This was difficult to sustain on a large scale<sup>14</sup> and hence, led to the advent of the long lasting nets in which the insecticide is incorporated into the net fibers. These nets maintain their biological activity for 3 to 5 years depending on the type of the fiber used for the net.<sup>32</sup>

Despite the proven success of IRS and ITNs in malaria control in the past, the rising insecticide resistance in the mosquito population insecticide poses a serious threat to IRS and

ITN programs. The current insecticides used for IRS and ITNs and the emergence of the resistance against these insecticides is discussed in detail in the next segment.

## **1.6 Vector control using insecticides**

The historically successful eradication of malaria in various parts of the world largely depended on the insecticides for vector control programs. The present day extensive and rapid roll out of ITNs and IRS call for a continuous efforts to develop new insecticides in addition to enhancing the effectiveness of the current insecticides. Currently, there are 4 classes of insecticides, which are approved by WHOES to be used for IRS and only one of these them is approved for ITNs.<sup>34</sup> These insecticide classes can be further divided into two categories on the basis of their mode of action: voltage gated sodium channel blockers and acetylcholinesterase inhibitors.

### **1.6.1 Voltage-gated sodium channel blockers**

The voltage-gated sodium channel is the principal molecular target for organochlorines (such as DDT) and pyrethroids. Initial contact with the insecticide delays the closing of the sodium channel, thereby prolonging the action potential and causing the neurons to fire continuously.<sup>38</sup> This causes abnormal hyper-excitability and eventually leads to paralysis and death of the insect. While DDT affects mainly the peripheral nervous system, pyrethroids affect both peripheral and central nervous systems.<sup>38</sup>

#### **1.6.1.1 Organochlorines**

DDT, an organochlorine, was discovered in 1939 by the Swiss chemist Paul Muller.<sup>38</sup> It was considered an ideal insecticide because it was cheap to produce, highly toxic to most pest insects and also durable. The last big international campaign to eradicate malaria, which ran from 1955 to 1969, relied primarily on DDT and its outstanding residual insecticide effectiveness in

house sprays.<sup>39</sup> By 1961, malaria eradication was achieved in many countries including North America, Europe, and parts of Asia, and substantial decrease in malaria were also noticed other regions.<sup>38</sup> However, by the early 1970s, the agriculture use of DDT was banned in USA, and many European countries.<sup>40</sup> Its non-agricultural usage in these countries is permitted only under emergency pest control situations. DDT is slow to degrade as its half-life can range from 22 days to 30 years in the soil.<sup>33</sup> Furthermore, DDT is highly fat-soluble so it can accumulate easily in the fats of the insects and large animals and also humans by passing up the food chain.<sup>33</sup> So far, DDT is linked to 3 human cancers (liver, pancreatic and breast) based on the results of the animal studies.<sup>32, 40</sup> In 2006, DDT was reintroduced by WHO for use in IRS for malaria control.<sup>41</sup> The reintroduction was based on an extensive research that showed that under correct usage DDT pose no health hazards.

### 1.6.1.2 Pyrethroids

Pyrethroids constitute a major class of neurotoxic insecticide. They were developed in 1980, and are synthetic analogues of the naturally occurring pyrethrum (pyrethrin I (**11**) and pyrethrin II (**12**)) found in the flowers of *Chrysanthemum cinerifolius*.<sup>42</sup> The first synthetic pyrethroid was permethrin (**13**), which was followed by deltamethrin (**10**), which turned out to be the most active insecticide at its time of discovery.<sup>42</sup>

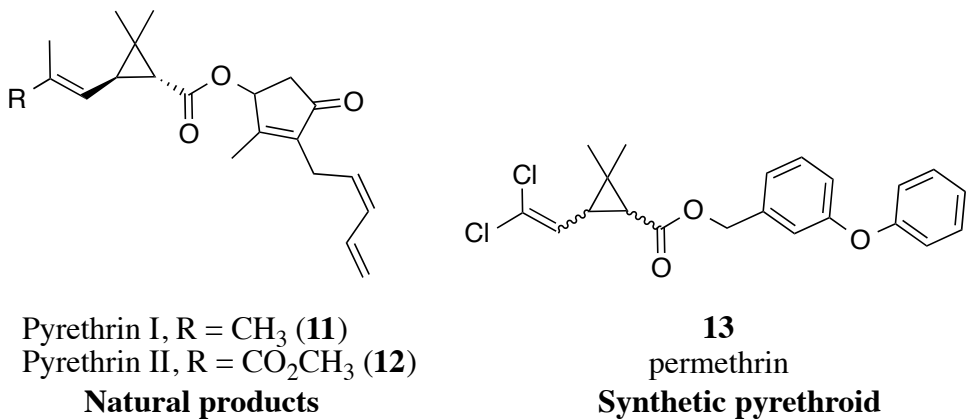


**Figure 1.6:** Natural product, pyrethrins and their synthetic analogs called pyrethroids.

Currently, six insecticides have been approved for use on ITNs and all belong to the pyrethroid class.<sup>34</sup> Furthermore, they are used in IRS, on curtains and screens, and also in coils, aerosols and mats.<sup>43, 44</sup> They have been used extensively over the past 20 years owing to their low mammalian toxicity, high insecticidal and repellent activity, limited soil persistence, and low cost.<sup>44</sup> These advantages also led to their massive overuse. Due to the continuous exposure to this class of insecticides and also to DDT (which was extensively used in agriculture to control pests), mosquitoes have developed resistance against these insecticides. This resistance is spreading at a fast pace as more and more ITNs are rolled out.

There are several mechanisms that are responsible for conferring resistance to the pyrethroids. Two main mechanisms are target site resistance and metabolic resistance.<sup>38, 44-45</sup> The target site for pyrethroids is the voltage-gated sodium channel on the insects' neurons. Any alteration in the target site can leave the insect insensitive to the effect of insecticide. In *An. gambiae*, this resistance is termed as knockdown resistance (*kdr*) as mosquitoes can tolerate prolonged exposure to pyrethroids without being knocked down. This resistance is due to the substitution of a leucine residue at 1014 codon by a phenylalanine (1014F) or a serine residue

(1014S). The mutation at 1014 is reported to alter the channel activation kinetics, thereby reducing the affinity for pyrethroids without interacting directly with the insecticide.<sup>46</sup> So far, this is the only residue associated with target site resistance to pyrethroids in *An. gambiae*. In some cases, a cross-resistance to DDT has been reported as they share the same mechanism of action.

The second mechanism that provides protection against pyrethroids is the metabolic resistance. As a result of this resistance the insecticide is either detoxified before it reaches the target site of the insect or sequestered, where an esterase having affinity for the insecticide is over expressed in the resistant strain, thereby effectively binding the insecticide, and subsequently reducing the levels of the insecticide reaching the target site.<sup>45, 47</sup> In *An. gambiae* this resistance is caused by overexpression of particular cytochrome P450 isoforms (there are 111 such isoforms in *An. gambiae*). Apart from the above two resistance mechanisms, cuticular thickening or a reduction in the permeability of the cuticles to the lipophilic insecticide, has also been identified as a minor resistance mechanism to pyrethroids. Resistance can also arise from a change in phenotype for example: a) an early exit from the house with reduction in indoor biting,<sup>48</sup> b) a change of host preference,<sup>48</sup> and c) a shift in biting time behavior,<sup>49</sup> all which would reduce contact with insecticides.

Current ITNs rely exclusively on pyrethroids. The widespread resistance against this class of insecticide is a big threat to current malaria control measures. Hence, there is an urgent need to explore another biological target such as acetylcholinesterase, which has not been explored to its potential.

## 1.6.2 Acetylcholinesterase inhibitors

### 1.6.2.1 Introduction to acetylcholinesterase (AChE) system

Acetylcholinesterase (AChE) is an important enzyme, both in humans and insects. The principal role of AChE is to catalyze the hydrolysis of the neurotransmitter acetylcholine (ACh) (14). This enzyme is responsible for the termination of nerve impulse transmission at the cholinergic synapses in the central nervous system (CNS) of both humans and insects.<sup>50</sup> A highly simplified catalytic cycle of the hydrolysis of the substrate ACh is shown in Figure 1.7. The acylation of the active site serine and the hydrolysis of the acylated enzyme are both fast processes.<sup>51</sup>

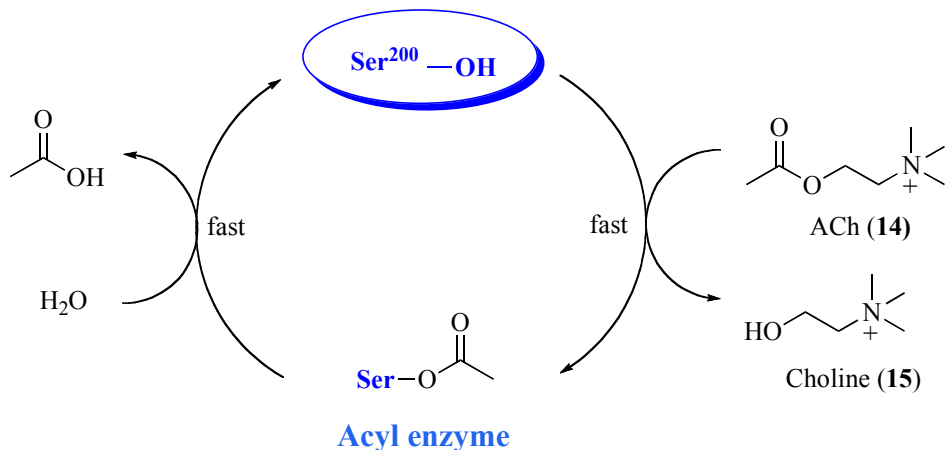


**Figure 1.7:** Simplified catalytic cycle of substrate hydrolysis by acetylcholinesterase (AChE).

The hydrolysis of the acetylated enzyme regenerates the free enzyme with the release of acetic acid. AChE is a highly efficient enzyme with a turnover of  $10^3$  - $10^4$  sec<sup>-1</sup>.<sup>52</sup> Due to its crucial role in the nervous system, it has been widely utilized as a target for nerve agents, Alzheimer drugs and insecticides like organophosphates and carbamates.

In order to understand its importance as an important biological target, it is important to understand the structure of this enzyme and to get an insight into how it works. The first crystal structure of AChE was reported by Sussman et al. and with that came a wealth of structural information (Figure 1.8).<sup>53</sup> These crystals were obtained from *Torpedo californica*, a pacific electric ray, and this species of enzyme will be referred to as *TcAChE*. Further, through out the chapter, the conventional numbering of *TcAChE* will be used, unless otherwise stated.

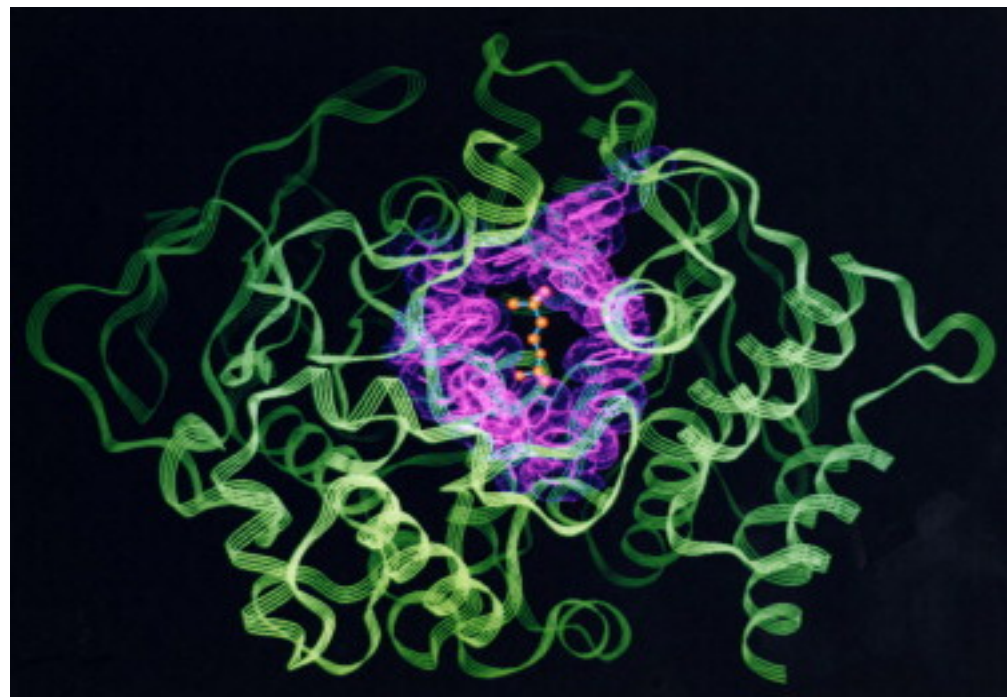


**Figure 1.8:** Ribbon diagram of 3-D structure of *TcAChE* (PDB Code 2ace). ACh bound at the bottom of the active-site gorge is shown using ball and stick diagram. The 14 conserved aromatic residues lining the gorge are shown as pink sticks and dot surface.<sup>53</sup> With copyright permission from Elsevier.

The crystal structure of AChE revealed that its active site is at the bottom of a gorge, about 20 Å deep and penetrates half way into the enzyme and widens at the base (see Figure 1.9).<sup>54</sup>

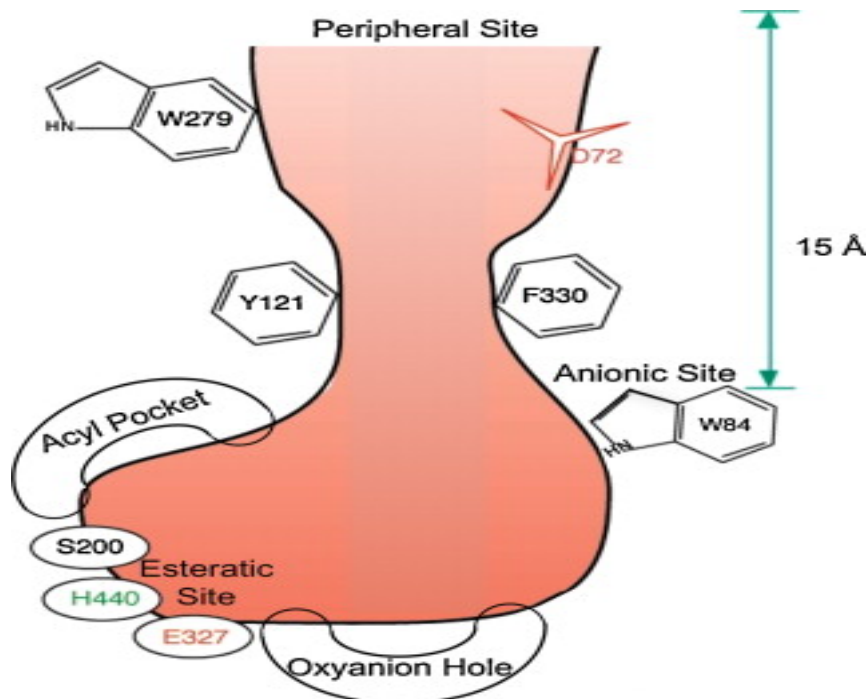


**Figure 1.9:** Simplified diagram of the active-site gorge of *TcAChE*.<sup>54</sup> With copyright permission from Elsevier.

This buried active site increases the substrate (ACh) and enzyme interactions, which in turn helps to lower the energy of the transition state. The conserved aromatic residues lining the active site accounts for ~ 40% of the cavity surface.<sup>54</sup> The diameter of the gorge at the bottleneck is only ~ 5 Å wide, which is quite narrow for the substrate ACh whose quaternary group diameter itself is 6.4 Å.<sup>53</sup> This observation raises an interesting question. How does the substrate make its way down the gorge? This dilemma was rationalized on the basis of the “aromatic guidance theory”.<sup>54</sup> The gorge is lined with aromatic residues, which makes for 70% of the gorge

surface.<sup>55</sup> This aromatic lining around the enzyme provides multiple low affinity binding sites, which traps the substrate ACh.<sup>54, 56</sup> Once it is trapped at the entrance of the gorge, it slides down the gorge via cation- $\pi$  interactions. Thus, there are two substrate-binding sites, one at the mouth of the gorge called the peripheral anionic site (PAS) and the other, which is the active site located at the bottom of the gorge called the catalytic anionic site (CAS). Rosenberry et al. have shown that PAS traps the substrate first and then it proceeds down towards the CAS.<sup>53</sup> Further, the breathing motions inside the enzyme also contribute substantially to the movement of the substrate into the CAS.<sup>55</sup>

The PAS consists of three key amino acids Try70, Asp72 and Trp279. The CAS consists of two subsites, ‘anionic’ and ‘esteratic’ subsites.<sup>53</sup>

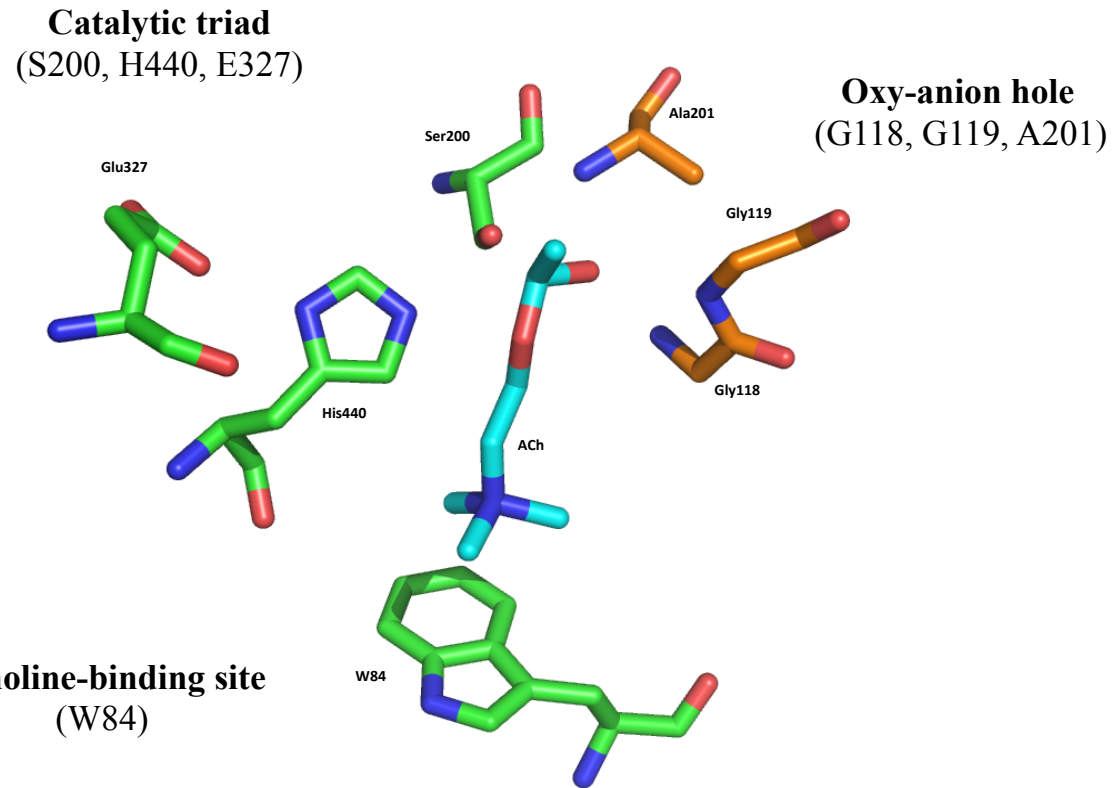


**Figure 1.10:** Acetylcholine manually docked in the active site of the enzyme AChE (PDB ID 2ace). Three of the major sub-sites in the CAS that are catalytic triad, oxy-anion hole, and choline-binding site are labelled in the figure. Image credit: Dawn Wong from Paul R. Carlier's group.

In the catalytic anionic site, also known as choline-binding pocket consisting of Trp84, Glu199, and Phe330, the quaternary ammonium moiety of ACh is stabilized mainly by cation- $\pi$  interaction with Trp84 (see Figure 1.10, Glu199, and Phe330 not shown). The esteratic subsite contains a serine hydrolase catalytic triad consisting of Ser200, His440, and Glu327. The oxyanion hole consists of Gly118, Gly119 and Ala201. These key residues help to stabilize the oxyanion in the transition state via hydrogen bonding of the main chain NH groups. Furthermore, the acyl pocket (consisting of Trp233, Phe288, Phe290 and Phe331 not shown in Figure 1.10)

contributes towards stabilizing the acetyl group through hydrophobic interactions with the methyl group of ACh.<sup>52, 57</sup> All these regions work in concert to make this enzyme so efficient.

### **1.6.3 Role of AChE inhibitors**

In humans, AChE is associated with Alzheimer's disease (AD) and other degenerative disorders.<sup>58</sup> According to the cholinergic hypothesis, the symptoms of Alzheimer's disease arise from impairment of cholinergic transmission due to low levels of the neurotransmitter ACh.<sup>59</sup> AChE inhibitors reverse this deficit by inhibiting the enzyme, thus prolonging the effect of neurotransmitter *in vivo*, and providing symptomatic relief in the early stages of AD patients.<sup>50, 60</sup> Some of the first generation AD drugs that are AChE inhibitors include the synthetic compounds like tacrine (Cognex),<sup>61</sup> the carbamates rivastigmine (Exelon),<sup>62</sup> and E2020 (donepezil, Aricept).<sup>63-64</sup>

In contrast to their helpful role as AD memory enhancers, AChE inhibitors also include some of the most dangerous natural toxins like fasciculin, and man-made nerve agents like sarin. AChE is the molecular target for two major classes of pesticides, organophosphates (OPs) and carbamates, used in the agriculture and public health sectors for pest control.<sup>65</sup> OPs and carbamates, especially methyl carbamates (MCs), contribute 40% to the total insecticides currently in use.<sup>66</sup> These insecticides play a crucial role in malaria control and are discussed in detail below.

#### **1.6.3.1 Organophosphates (OP)**

Organophosphates (OP) are structurally diverse. They share common characteristics being triesters of phosphoric acid, where the phosphorous atom is double bonded to either to an oxygen or sulfur moiety (Figure 1.11). Further, they have two alkyl side chains, and a variable leaving group X, which leaves either on hydrolysis or upon reaction with the target site esterase.

Also, having X as a strongly electronegative group (such as cyanide, halide or thiocyanate) makes these compounds highly toxic as in the case of nerve gases like tabun (**18**), sarin (**19**), soman (**20**), and VX (**21**) (**19**, **20**, and **21** are more specifically referred to as organophosphonates due to presence of P-C bond).<sup>67</sup> Although these compounds are referred to as “gases”, however, under temperate conditions they exist as liquids.<sup>67</sup> Apart from their high toxicity, their tendency to volatilize poses a significant hazard (Figure 1.11).<sup>67</sup>

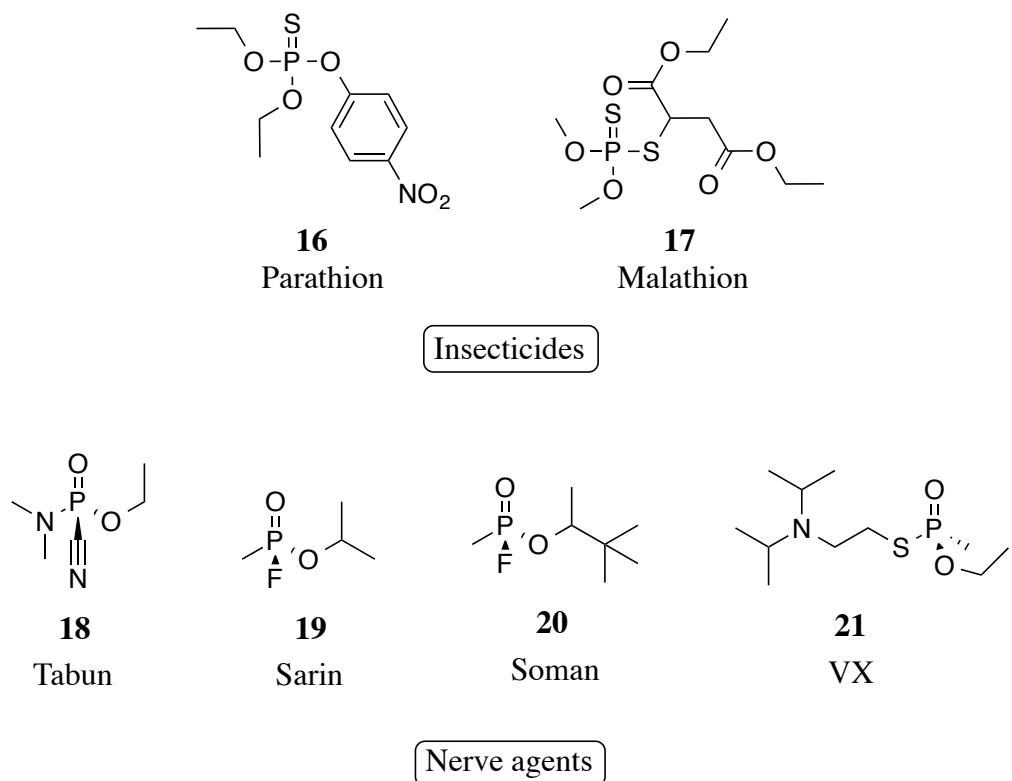


**Figure 1.11:** Organophosphorus compounds: Insecticides and nerve agents.<sup>67</sup>

Compounds with P=S are known as phosphorothionates. The P=S analogs are bio-activated to P=O analogs, called the “oxon form” through the action of cytochrome P450.<sup>68</sup> The oxons are shown to be 3-fold more potent inhibitors of AChE in vitro as compared to the parent

phosphorothionates.<sup>69</sup> Oxons although more toxic than the parent compound are less selective. Due to their high reactivity, they react with many non-target molecules at the site of their synthesis and only a small fraction makes it to the target site.<sup>68</sup>

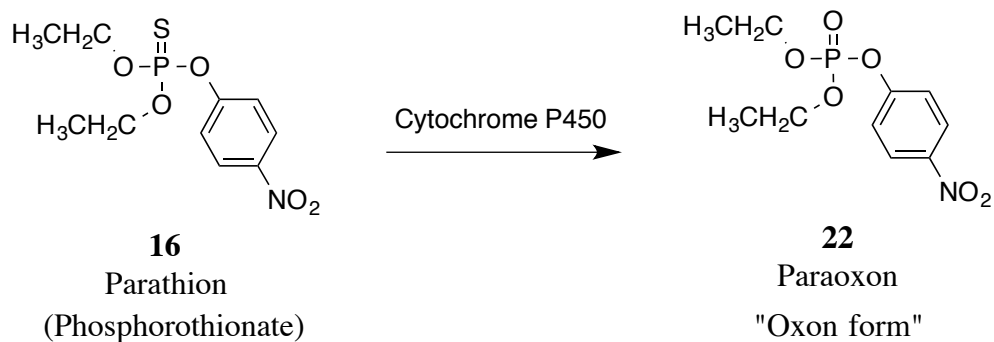


**Figure 1.12:** The bioactivation of parathion (**16**) to paraoxon (**22**) through cytochrome P450 mediated desulfuration.

The first organophosphate was synthesized in Germany before the Second World War as a highly toxic biological warfare agents.<sup>70</sup> Subsequently, many OPs were developed as insecticides with the hope that they will have manageable toxicity to mammals.<sup>33</sup> Although OP insecticides were far less toxic than the OP nerve agents, they were still very toxic to the vertebrates.<sup>71</sup> For example, when parathion, an OP insecticide, was used as a replacement for DDT, many human deaths were reported due to OP poisoning.<sup>33, 72</sup> Until now only three OP insecticides are recommended for IRS. These compounds exert their toxic effect by irreversibly inhibiting AChE.<sup>73</sup> An OP insecticide phosphorylates the enzyme by covalently binding to the serine hydroxyl group oxygen in the catalytic center, and subsequently inhibits its activity.<sup>74</sup> This results in the accumulation of ACh and further activation of nicotinic and muscarinic receptors.<sup>75</sup> The phosphorylated AChE is extremely stable. Therefore, OPs especially nerve agents are called irreversible inhibitors.

The symptoms of OP poisoning typically include agitation, muscle weakness and fasciculation, hyper salivation and sweating.<sup>73</sup> In the case of severe poisoning, a person may show symptoms of respiratory failure, unconsciousness, convulsions, confusion, and even death.<sup>73</sup> Furthermore, OP induced delayed neuropathy (OPIDN) has also been reported in case of single or multiple exposures to some OPs.<sup>76</sup> This is caused by the inhibition of more than 70% of a carboxylesterase enzyme called neurotoxic esterase (NTE).<sup>71</sup> The symptoms usually appear between 14 to 24 days after the poisoning.<sup>71</sup>

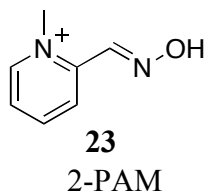


**Figure 1.13:** Structure of antidote 2-PAM.<sup>77</sup>

Fortunately, the phosphorylated enzyme can be reactivated by using AChE re-activators (antidotes) such as pralidoxime (2-PAM, see Figure 1.13 for structure).<sup>78</sup> However, re-activation is severely limited by a process called aging.<sup>77</sup> Aging occurs when the phosphorylated adduct de-alkylates to give a negatively charged adduct which is highly stabilized by interaction with His440.<sup>77,79</sup> (Figure 1.14) An aged enzyme is highly stable and cannot be reactivated by AChE reactivation.<sup>77</sup>

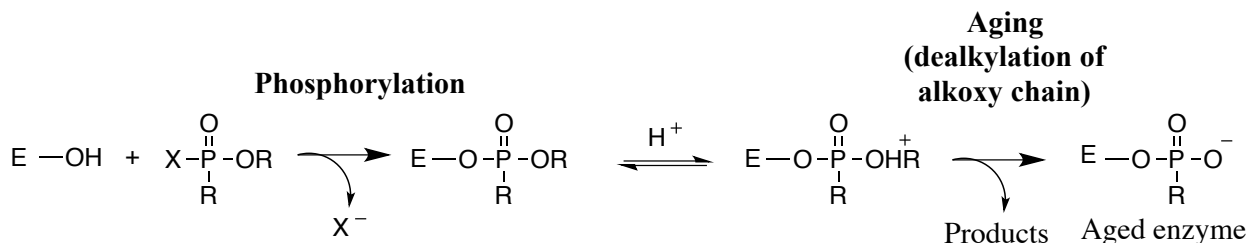


**Figure 1.14:** Phosphorylation and aging of AChE.<sup>79</sup>

Due to their acute high toxicity and concerns of OPIDN following chronic exposure, OP insecticides were not considered an attractive pharmacophore for mosquitoide development in the Carlier group.

### 1.6.3.2 Carbamates

Carbamates are esters derived from carbamic acids. The interest in the carbamates insecticides originated with tests on the alkaloid physostigmine (**23**), which was identified in 1925.<sup>80</sup> The research on developing successful carbamate insecticides was initiated by Hans Gysin in Switzerland in the 1940s.<sup>80</sup> Later Robert Metcalf and colleagues at the University of California from Riverside in 1954 developed aryl methyl carbamates (MCs).<sup>80-81</sup> Ultimately, Union Carbide discovered a very effective carbaryl called carbaryl (**24**).<sup>80</sup>

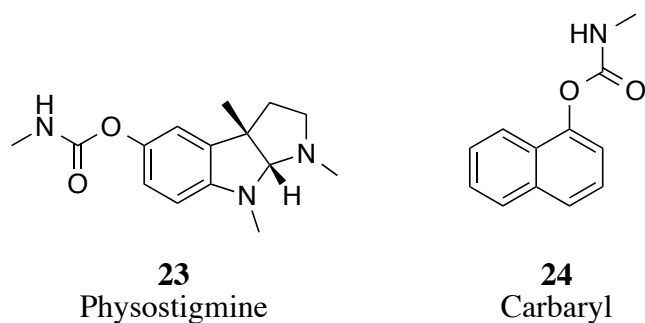


**Figure 1.15:** Structure of physostigmine and carbaryl.<sup>73</sup>

The mode of action of carbamates is very similar to that exerted by OPs. The catalytic cycle is shown in Figure 1.16. The carbamates deactivate the cholinesterase by carbamylation at the active site serine residue (**1.16a-c**). The subsequent hydrolysis of carbamylated serine regenerates the active site enzyme (**1.16d-f**). Thus, carbamates are called pseudo-irreversible inhibitors. The carbamylated AChE is less stable and regenerates the free enzyme within 30 to 40 minutes.<sup>82</sup>

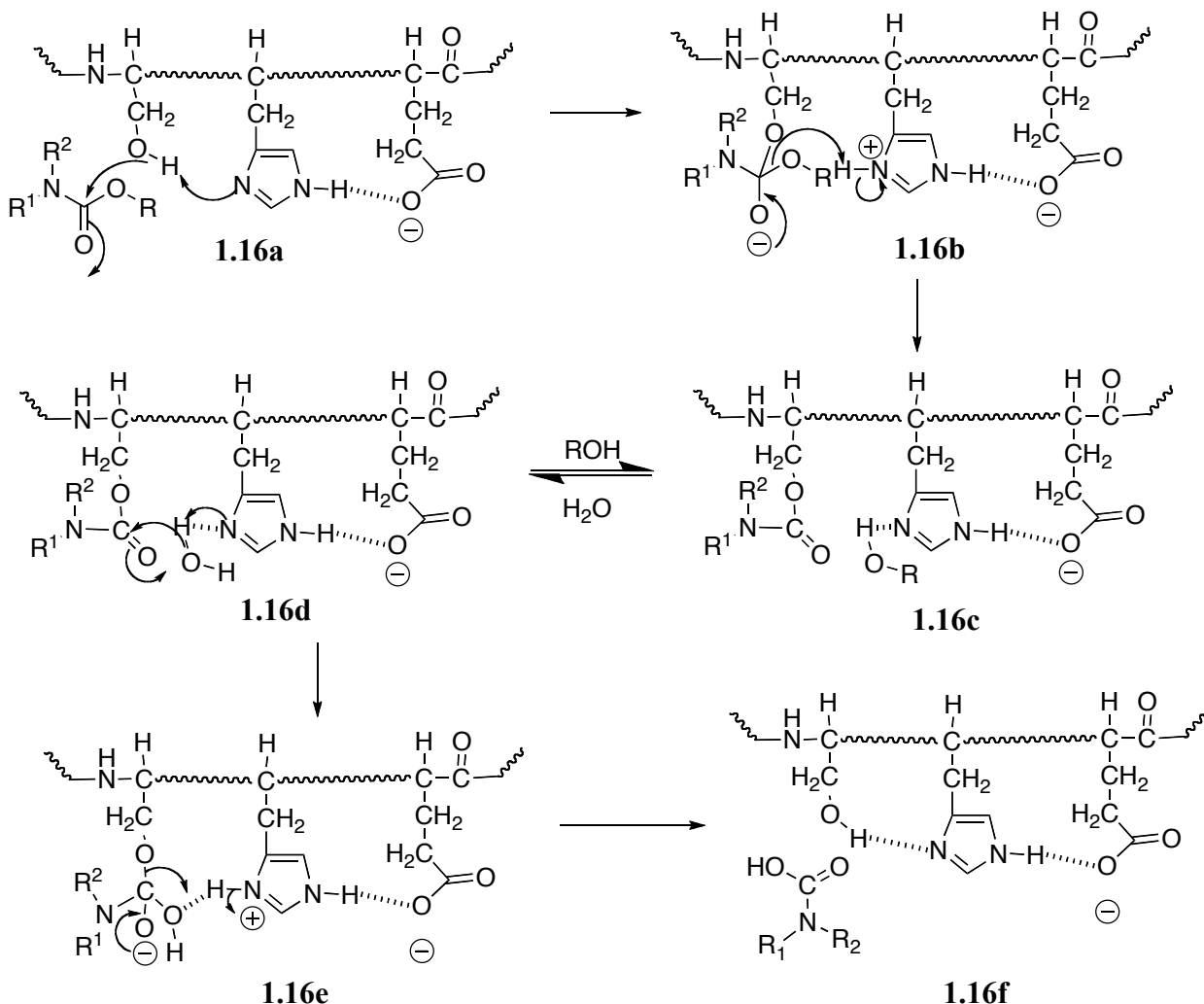


**Figure 1.16:** General mechanism of pseudo-irreversible inhibition of cholinesterase by carbamates.<sup>83</sup>

In contrast to carbamates, OPs are referred to as irreversible inhibitors of AChE. This is because the phosphorylated AChE complex is very stable and takes hours to several days to regenerate the free enzyme.

Carbamates are a better option to explore as insecticides as compared to OPs because unlike OPs there is little evidence suggesting that carbamates cause OPIDN.<sup>84, 76, 85</sup> Lotti et al. have proposed that OPIDN might occur only after exposure to repeated high doses of carbamates.<sup>85</sup> Despite this carbamates remain the weakest inhibitors of NTE amongst other NTE inhibitors. Further, they also have low dermal toxicity as compared to organophosphates.<sup>84</sup>

In spite of all favorable aspects of this class of insecticides, no carbamate insecticide has been approved for ITNs, perhaps due to their concomitant mammalian toxicity. Since AChE enzyme is present in mammals and other species with cholinergic nerves, these insecticides can have off-target toxicity.<sup>86</sup> One way to reduce off-target toxicity is to develop species-selective insecticides.<sup>87</sup>

Our strategy is to inhibit the *Anopheles gambiae* AChE (*AgAChE*) selectively by carbamylating the serine residue in the active site of the enzyme. Precedents have shown that achieving species-selectivity is an achievable goal because of various differences in the primary sequence of human AChE (*hAChE*) vs *AgAChE*. Bar-On et al. reported that the Alzheimer's drug rivastigmine was 1500-fold more inhibitory for *hAChE* over *Torpedo californica* AChE (*TcAChE*).<sup>62</sup> Pang and co-workers have extensively reviewed the literature pertaining to an insect-specific cysteine residue (C286), which is located at the mouth of AChE active site and can serve as a novel target to make specie-selective insecticide.<sup>74</sup> They recently reported a chemical compound containing a methanethiosulfonate group to preferentially form an adduct with the insect-specific cysteine residue.<sup>74</sup> This compound showed >95% inhibition of *Anopheles*

*gambiae* AChE and >80% inhibition in northern house and the yellow fever mosquitoes after 1 h exposure at 6  $\mu\text{m}$ .<sup>74</sup> Interestingly, under these conditions no inhibition of *hAChE* was observed.

The first crystal structure of *TcAChE* was reported by Sussman et al.,<sup>53</sup> and with that came considerable information. Later, a series of 3D structures of *TcAChE* bound to various inhibitors,<sup>88</sup> mouse AChE (*mAChE*)<sup>89</sup> and the fruit fly *Drosophila melanogaster* (*DmAChE*) were published.<sup>90</sup> At present, there is no crystal structure available for *AgAChE* to aid us in developing the species-selective AChE inhibitors for malaria mosquito *Anopheles gambiae*. However, the genome of *AgAChE* has been completely sequenced.<sup>91</sup> One might think that two insects AChE, more specifically *Anopheles gambiae* AChE (*AgAChE*) and *Drosophila melanogaster* (*DmAChE*), will share more similarity as compared to *AgAChE* and *human AChE* (*hAChE*). This would allow the use of the resolved crystal structures of insect AChE to predict properties of *AgAChE*. To the contrary, *DmAChE* and *AgAChE* share only 41% sequence identity (56% similarity).<sup>87</sup> The low sequence identity is due to the fact that AChE in these two species are encoded by different genes. *An. gambiae* is reported to carry two AChEs (AChE1 and AChE2), which are encoded by different genes *ace-1* and *ace-2*, respectively. However, Weill et al. have given compelling evidence that the major ACh hydrolyzing enzyme in *An. gambiae* is encoded by *ace-1* gene.<sup>91</sup> In contrast, *DmAChE* is encoded by only one gene that is *ace-2*.<sup>91</sup> The presence of single *ace* gene in *Drosophila* might be attributed to the years of evolution where at some stage it lost the *ace-1* gene. This could happen if the function of the two genes overlapped and one gene could compensate for the loss of the other.<sup>91</sup> The *AgAChE* is 49% identical with *hAChE*, which is marginally higher as compared to *DmAChE*.<sup>87</sup> But the overall low sequence identity is encouraging to meet the target goal of achieving specie selectivity. For the ease of

comparison, Figure 1.17 shows a section of few important amino acids alignment for *T. californica*, *human*, *An. gambiae*, and *D. melanogaster* AChE sequence.

		catalytic triad			oxyanion hole		choline-binding site	
		200	327	440	116	201	84	330
<i>Tc</i>	TIFGESAGGAS	<b>E</b>	<b>H</b>		YGGGF	<b>A</b>	W	FF
	203	334	447		119	204	86	337
<i>human</i>	TLFGESAGAAS	<b>E</b>	<b>H</b>		YGGGF	<b>A</b>	W	YF
	199	325	439		116	200	84	328
<i>Ag ace-1</i>	TLFGESAGAVS	<b>E</b>	<b>H</b>		FGGGF	<b>A</b>	W	YF
	238	367	480		148	239	83	370
<i>Dm ace-2</i>	TLFGESAGSSS	<b>E</b>	<b>H</b>		YGGGF	<b>A</b>	W	YF
		acyl pocket			peripheral site		flexible PAS loop	
		233	288	290	70	72	121	279
<i>Tc</i>	W	F	F		Y	D	Y	334
	236	295	297		72	74	124	286
<i>human</i>	W	F	F		Y	D	Y	341
	232	286	288		70	72	121	280
<i>Ag ace-1</i>	W	C	F		I	D	Y	332
	271	328	330		69	71	153	321
<i>Dm ace-2</i>	W	L	F		E	Y	M	374
							W	YD
							279	291
							WNVLPFD <b>S</b> IFRFS	
							286	298
							WHVLPQESVFRFS	
							280	289
							WGTL---GICEFP	
							321	331
							WNSY--SGILSFP	

**Figure 1.17:** Alignment of *T. californica*, *human*, *An. gambiae* (ace-1), and *D. melanogaster* (ace-2).<sup>87</sup> With copyright permission from Elsevier.

It can be seen that the amino acid residues are conserved in the catalytic triad, the oxyanion hole, and the choline-binding site of *hAChE* and *AgAChE*. However, potentially useful differences in the acyl pocket, peripheral site, and the flexible site loop could be exploited to achieve the species-selectivity.<sup>87</sup>

Apart from species-selectivity another major issue is the resistance towards carbamate insecticides. However, the resistance towards this class of insecticide is not as widespread when compared to pyrethroids. The following section will throw more light on the insecticidal resistance in *An. gambiae* towards this class.

### 1.6.3.3 Insecticidal resistance in *Anopheles gambiae* to AChE inhibitors.

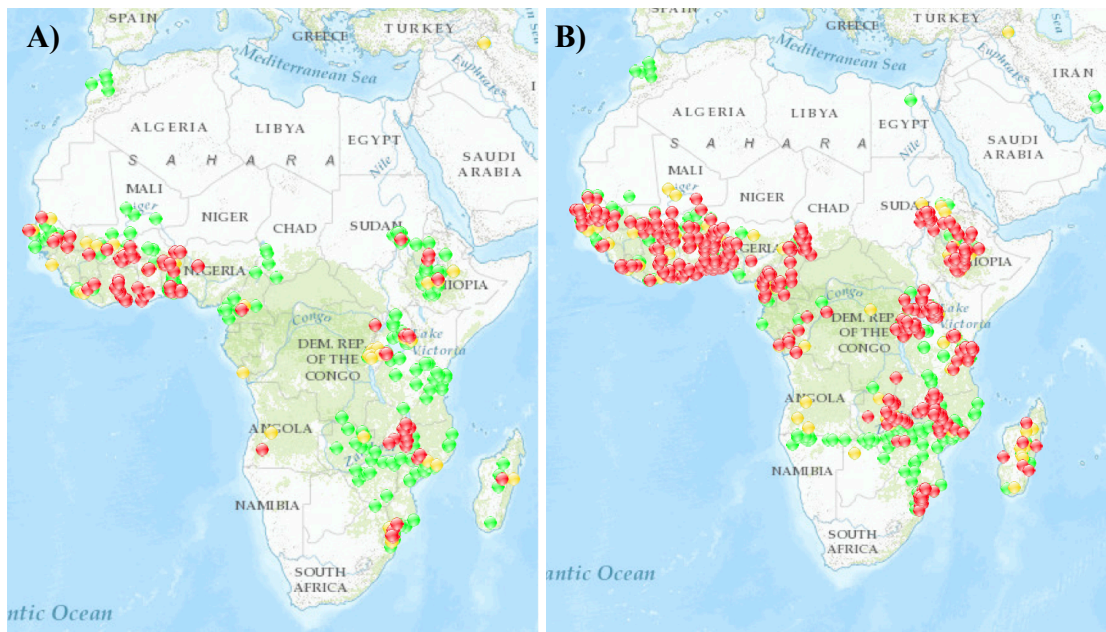


**Figure 1.18:** (A) Distribution of carbamate resistance across Africa from 2000-2013. (B) Distribution of pyrethroid resistance across Africa from 2000-2013. The red balls indicated confirmed resistance, yellow balls for possible resistance, and green balls for susceptible population. Image created using IR mapper (<http://www.irmapper.com/>).

The continuous exposure to insecticides puts pressure on the insects and subjects them to “survival of the fittest theory”. From Figure 1.18 (A), it is clear that the mosquitoes have developed resistance to carbamates too. However, as seen in Figure 1.18, the resistance to carbamates is not as extensive when compared to pyrethroid “*kdr*” resistance. The resistance to carbamate can come from either target site resistance or metabolic resistance.<sup>92, 93</sup> These mechanisms alone, or in combination can confer resistance to this class of insecticides. Russell and co-workers suggested two patterns of target site resistance towards OP/ carbamates.<sup>94</sup> Pattern I resistance can be identified by much greater resistance to carbamate insecticides such as

propoxur, carbosulfan or primicarb than to OPs such as paraoxon, malaoxon, temephos or chlorpyriphos.<sup>94</sup> Pattern II resistance is characterized by high OP resistance with either equivalent or reduced carbamate resistance.<sup>94</sup> The resistance in *An. gambiae* falls into the first category. Pattern I resistance was first reported by Weill and co-workers.<sup>91, 95</sup> They identified two AChE genes, *ace-1* and *ace-2* from *An. gambiae* genome. After comparing the entire *ace-1* coding region from susceptible and resistant strain, a single amino acid substitution was identified.<sup>95-96</sup> The glycine codon (GGC) at position 119 in the oxyanion hole at the base of the gorge of susceptible AChE-1 enzyme was replaced by a serine codon (AGC) in the resistant mosquitoes.<sup>95</sup> Interestingly, a different mutation but in the same oxyanion hole site of some carboxylesterases also provides resistance against OP insecticides.<sup>97</sup> For example, mutation of Gly119 to an Asp, Glu or His residue can make the mutant enzyme hydrolyze the phosphorylated serine in the active site faster, and thus, regenerates the free enzyme.<sup>98</sup> In these cases, it was proposed that the mutant amino acid residue acts as a general base, thereby activating the water molecule to hydrolyze the OP-enzyme faster.<sup>94</sup> However, a similar logic cannot be applied to insensitivity of carbamates due to G119S mutation because of the structural differences between carbamates/carboxyesters (which are planar around carbonyl group) and OPs (which are tetrahedral around the phosphorus).<sup>94</sup> A mutation (G119S), which might increase OP turnover might not increase carbamate turnover, as the direction of attack for hydrolysis of the enzyme-inhibitor will be different in both cases. Another possibility reported is that the substitution of glycine by serine in the active site causes a steric shift, which can either enhance the carbamate turnover or block the initial reaction of carbamates with AChE-1 in the first place.<sup>94</sup> Work in the Carlier's group suggests the later scenario.<sup>99</sup>

In conclusion, pyrethroids is the only group of insecticides, which have been approved for use at present on insecticide treated nets. However, widespread resistance against this class of insecticide can jeopardize the efficacy of ITNs, which are impregnated with pyrethroids. So, we aim to develop a new class of AChE-based inhibitors, more specifically carbamates, which will be discussed in Chapter 2. With this class of AChE inhibitors, we hope to achieve high species-selectivity (*Ag* vs *h*). Moreover, due to rise in carbamate resistant strain of *An. gambiae*, one goal will be to achieve AChE inhibition not only for the susceptible enzyme but also for the resistant enzyme (G119S). Further, since our long-term goal is to deploy these AChE-based inhibitor insecticides on ITNs, we would like these insecticides to exhibit contact toxicity towards susceptible and resistant strains of *An. gambiae*.

## 1.7 Bibliography

1. McGraw, E. A.; O'Neill, S. L., Beyond insecticides: New thinking on an ancient problem. *Nat. Rev. Micro.* **2013**, *11*, 181-193.
2. *Changing history – the world health report 2004; world health organization: Geneva, switzerland, 2004.* .
3. Kappe, S. H. I.; Vaughan, A. M.; Boddey, J. A.; Cowman, A. F., That was then but this is now: Malaria research in the time of an eradication agenda. *Science* **2010**, *328*, 862-866.
4. *World health malaria report 2011; world health organization: Geneva, switzerland, 2011.* .
5. Murray, C. J.; Rosenfeld, L. C.; Lim, S. S.; Andrews, K. G.; Foreman, K. J.; Haring, D.; Fullman, N.; Naghavi, M.; Lozano, R.; Lopez, A. D., Global malaria mortality between 1980 and 2010: A systematic analysis. *Lancet* **2012**, *379*, 413-431.

6. Cox, F., History of the discovery of the malaria parasites and their vectors. *Parasites & Vectors* **2010**, *3*, 5-14.
7. CDC. The history of malaria, an ancient disease. Centers for disease control and prevention. <http://www.cdc.gov/malaria/about/history/> (accessed January 14, 2014).
8. CDC. Laveran and the discovery of the malaria parasite. Centers for disease control and prevention. <http://www.cdc.gov/malaria/about/history/laveran.html> (accessed January 14, 2014).
9. Sachs, J.; Malaney, P., The economic and social burden of malaria. *Nature* **2002**, *415*, 680-685.
10. Hay, S. I.; Guerra, C. A.; Tatem, A. J.; Noor, A. M.; Snow, R. W., The global distribution and population at risk of malaria: Past, present, and future. *Lancet. Infect. Dis.* **2004**, *4*, 327-336.
11. Gallup, J. L.; Sachs, J. D., The economic burden of malaria. *Am. J. Trop. Med. Hyg.* **2001**, *64*, 85-96.
12. Kitron, U.; Spielman, A., Suppression of transmission of malaria through source reduction: Antianopheline measures applied in Israel, the United States, and Italy. *Rev. Infect. Dis.* **1989**, *11*, 391-406.
13. Petersen, I.; Eastman, R.; Lanzer, M., Drug-resistant malaria: Molecular mechanisms and implications for public health. *FEBS Lett.* **2011**, *585*, 1551-1562.
14. Greenwood, B. M.; Bojang, K.; Whitty, C. J. M.; Targett, G. A. T., Malaria. *Lancet* **2005**, *365*, 1487-1498.

15. Kallander, K.; Nsungwa-Sabiiti, J.; Peterson, S., Symptom overlap for malaria and pneumonia--policy implications for home management strategies. *Acta Trop.* **2004**, *90*, 211-214.
16. Gething, P. W.; Patil, A. P.; Smith, D. L.; Guerra, C. A.; Elyazar, I. R.; Johnston, G. L.; Tatem, A. J.; Hay, S. I., A new world malaria map: *Plasmodium falciparum* endemicity in 2010. *Malar. J.* **2011**, *10*, 378.
17. Schellenberg, D.; Menendez, C.; Kahigwa, E.; Font, F.; Galindo, C.; Acosta, C.; Schellenberg, J. A.; Aponte, J. J.; Kimario, J.; Urassa, H.; Mshinda, H.; Tanner, M.; Alonso, P., African children with malaria in an area of intense *Plasmodium falciparum* transmission: Features on admission to the hospital and risk factors for death. *Am. J. Trop. Med. Hyg.* **1999**, *61*, 431-438.
18. Crawley, J.; Chu, C.; Mtobe, G.; Nosten, F., Malaria in children. *Lancet* **2010**, *375*, 1468-1481.
19. Price, R. N.; Tjitra, E.; Guerra, C. A.; Yeung, S.; White, N. J.; Anstey, N. M., Vivax malaria: Neglected and not benign. *Am. J. Trop. Med. Hyg.* **2007**, *77*, 79-87.
20. Markus, M., Malaria: Origin of the term “hypnozoite”. *J. Hist. Biol.* **2011**, *44*, 781-786.
21. Cox-Singh, J.; Davis, T. M.; Lee, K. S.; Shamsul, S. S.; Matusop, A.; Ratnam, S.; Rahman, H. A.; Conway, D. J.; Singh, B., *Plasmodium knowlesi* malaria in humans is widely distributed and potentially life threatening. *Clin. Infect Dis.* **2008**, *46*, 165-171.
22. Manda, H.; Gouagna, L. C.; Nyandat, E.; Kabiru, E. W.; Jackson, R. R.; Foster, W. A.; Githure, J. I.; Beier, J. C.; Hassanali, A., Discriminative feeding behaviour of anopheles gambiae s.S. On endemic plants in western kenya. *Med. Vet. Entomol.* **2007**, *21*, 103-111.

23. Michalakis, Y.; Renaud, F., Malaria: Evolution in vector control. *Nature* **2009**, *462*, 298-300.
24. Heppner, D. G., The malaria vaccine – status quo 2013. *Travel Med. Infect. Dis.* **2013**, *11*, 2-7.
25. Crompton, P. D.; Pierce, S. K.; Miller, L. H., Advances and challenges in malaria vaccine development. *J. Clin. Invest.* **2010**, *120*, 4168-4178.
26. Mwangoka, G.; Ongutu, B.; Msambichaka, B.; Mzee, T.; Salim, N.; Kafuruki, S.; Mpina, M.; Shekalaghe, S.; Tanner, M.; Abdulla, S., Experience and challenges from clinical trials with malaria vaccines in africa. *Malar. J.* **2013**, *12*, 1-9.
27. Casares, S.; Brumeau, T.-D.; Richie, T. L., The RTS,S malaria vaccine. *Vaccine* **2010**, *28*, 4880-4894.
28. Wells, T. N. C.; Alonso, P. L.; Gutteridge, W. E., New medicines to improve control and contribute to the eradication of malaria. *Nat. Rev. Drug Discov.* **2009**, *8*, 879-891.
29. Greenwood, B. M.; Fidock, D. A.; Kyle, D. E.; Kappe, S. H. I.; Alonso, P. L.; Collins, F. H.; Duffy, P. E., Malaria: Progress, perils, and prospects for eradication. *J. Clin. Invest.* **2008**, *118*, 1266-1276.
30. Biamonte, M. A.; Wanner, J.; Le Roch, K. G., Recent advances in malaria drug discovery. *Bioorg. Med. Chem. Lett.* **2013**, *23*, 2829-2843.
31. Killeen, G.; Seyoum, A.; Sikaala, C.; Zomboko, A.; Gimnig, J.; Govella, N.; White, M., Eliminating malaria vectors. *Parasites & Vectors* **2013**, *6*, 172-181.
32. Raghavendra, K.; Barik, T.; Reddy, B. P. N.; Sharma, P.; Dash, A., Malaria vector control: From past to future. *Parasitol. Res.* **2011**, *108*, 757-779.
33. Perveen, F., *Insecticides - advances in integrated pest management*. InTech 2012.

34. Ranson, H.; Abdallah, H.; Badolo, A.; Guelbeogo, W.; Kerah-Hinzoumbé, C.; Yangalbé-Kalnoné, E.; Sagnon, N. F.; Simard, F.; Coetzee, M., Insecticide resistance in *Anopheles gambiae*: Data from the first year of a multi-country study highlight the extent of the problem. *Malar. J.* **2009**, *8*, 1-12.
35. D'Alessandro, U.; Olaleye, B. O.; McGuire, W.; Thomson, M. C.; Langerock, P.; Bennett, S.; Greenwood, B. M., A comparison of the efficacy of insecticide-treated and untreated bed nets in preventing malaria in gambian children. *Trans R. Soc. Trop. Med. Hyg.* **1995**, *89*, 596-598.
36. D'Alessandro, U.; Olaleye, B. O.; McGuire, W.; Langerock, P.; Bennett, S.; Aikins, M. K.; Thomson, M. C.; Cham, M. K.; Cham, B. A.; Greenwood, B. M., Mortality and morbidity from malaria in gambian children after introduction of an impregnated bednet programme. *Lancet* **1995**, *345*, 479-483.
37. Binka, F. N.; Kubaje, A.; Adjuik, M.; Williams, L. A.; Lengeler, C.; Maude, G. H.; Armah, G. E.; Kajihara, B.; Adiamah, J. H.; Smith, P. G., Impact of permethrin impregnated bednets on child mortality in kassena-nankana district, ghana: A randomized controlled trial. *Trop. Med. Int. Health* **1996**, *1*, 147-154.
38. Davies, T. G.; Field, L. M.; Usherwood, P. N.; Williamson, M. S., DDT, pyrethrins, pyrethroids and insect sodium channels. *IUBMB Life* **2007**, *59*, 151-162.
39. Najera, J. A.; Gonzalez-Silva, M.; Alonso, P. L., Some lessons for the future from the global malaria eradication programme (1955-1969). *PLoS Med.* **2011**, *8*, e1000412.
40. Curtis, C. F., Should DDT continue to be recommended for malaria vector control? *Med. Vet. Entomol.* **1994**, *8*, 107-112.

41. Casimiro, S.; Coleman, M.; Mohloai, P.; Hemingway, J.; Sharp, B., Insecticide resistance in *Anopheles funestus* (diptera: Culicidae) from mozambique. *J. Med. Entomol.* **2006**, *43*, 267-275.
42. Davies, T. G. E.; Field, L. M.; Usherwood, P. N. R.; Williamson, M. S., DDT, pyrethrins, pyrethroids and insect sodium channels. *IUBMB Life* **2007**, *59*, 151-162.
43. Hougard, J. M.; Zaim, S. D.; Guillet, P., Bifenthrin: A useful pyrethroid insecticide for treatment of mosquito nets. *J. Med. Entomol.* **2002**, *39*, 526-533.
44. Hemingway, J.; Hawkes, N. J.; McCarroll, L.; Ranson, H., The molecular basis of insecticide resistance in mosquitoes. *Insect Biochem. Mol. Biol.* **2004**, *34*, 653-665.
45. Ranson, H.; N'Guessan, R.; Lines, J.; Moiroux, N.; Nkuni, Z.; Corbel, V., Pyrethroid resistance in african anopheline mosquitoes: What are the implications for malaria control? *Trends Parasitol.* **2011**, *27*, 91-98.
46. O'Reilly, A. O.; Khambay, B. P.; Williamson, M. S.; Field, L. M.; Wallace, B. A.; Davies, T. G., Modelling insecticide-binding sites in the voltage-gated sodium channel. *Biochem. J.* **2006**, *396*, 255-263.
47. Kostaropoulos, I.; Papadopoulos, A. I.; Metaxakis, A.; Boukouvala, E.; Papadopoulou-Mourkidou, E., Glutathione s-transferase in the defence against pyrethroids in insects. *Insect Biochem. Mol. Biol.* **2001**, *31*, 313-319.
48. Takken, W., Do insecticide-treated bednets have an effect on malaria vectors? *Trop. Med. Int. Health* **2002**, *7*, 1022-1030.
49. Mathenge, E. M.; Gimnig, J. E.; Kolczak, M.; Ombok, M.; Irungu, L. W.; Hawley, W. A., Effect of permethrin-impregnated nets on exiting behavior, blood feeding success, and

- time of feeding of malaria mosquitoes (diptera: Culicidae) in western kenya. *J. Med. Entomol.* **2001**, *38*, 531-536.
50. McGleenon, B. M.; Dynan, K. B.; Passmore, A. P., Acetylcholinesterase inhibitors in alzheimer's disease. *Br. J. Clin. Pharmacol.* **1999**, *48*, 471-480.
51. Timchalk, C., Physiologically based pharmacokinetic modeling of organophosphorus and carbamate pesticides in toxicology of organophosphate & carbamate compounds, gupta, r. C., ed. Elsevier academic press: Burlington, ma, 2006; pp 103-125.
52. Colletier, J. P.; Fournier, D.; Greenblatt, H. M.; Stojan, J.; Sussman, J. L.; Zaccai, G.; Silman, I.; Weik, M., Structural insights into substrate traffic and inhibition in acetylcholinesterase. *EMBO J.* **2006**, *25*, 2746-2756.
53. Sussman, J. L.; Harel, M.; Frolow, F.; Oefner, C.; Goldman, A.; Toker, L.; Silman, I., Atomic structure of acetylcholinesterase from *Torpedo californica*: A prototypic acetylcholine-binding protein. *Science* **1991**, *253*, 872-879.
54. Dvir, H.; Silman, I.; Harel, M.; Rosenberry, T. L.; Sussman, J. L., Acetylcholinesterase: From 3D structure to function. *Chem. Biol. Interact.* **2010**, *187*, 10-22.
55. Silman, I.; Sussman, J. L., Acetylcholinesterase: How is structure related to function? *Chem. Biol. Interact.* **2008**, *175*, 3-10.
56. Rosenberry, T. L.; Neumann, E., Interaction of ligands with acetylcholinesterase. Use of temperature-jump relaxation kinetics in the binding of specific fluorescent ligands. *Biochemistry* **1977**, *16*, 3870-3878.
57. Harel, M.; Quinn, D. M.; Nair, H. K.; Silman, I.; Sussman, J. L., The X-ray structure of a transition state analog complex reveals the molecular origins of the catalytic power and substrate specificity of acetylcholinesterase. *J. Amer. Chem. Soc.* **1996**, *118*, 2340-2346.

58. Wong, D. M.; Greenblatt, H. M.; Dvir, H.; Carlier, P. R.; Han, Y. F.; Pang, Y. P.; Silman, I.; Sussman, J. L., Acetylcholinesterase complexed with bivalent ligands related to huperzine a: Experimental evidence for species-dependent protein-ligand complementarity. *J. Am. Chem. Soc.* **2003**, *125*, 363-373.
59. Bartus, R.; Dean, R.; Beer, B.; Lippa, A., The cholinergic hypothesis of geriatric memory dysfunction. *Science* **1982**, *217*, 408-414.
60. Haviv, H.; Wong, D. M.; Greenblatt, H. M.; Carlier, P. R.; Pang, Y. P.; Silman, I.; Sussman, J. L., Crystal packing mediates enantioselective ligand recognition at the peripheral site of acetylcholinesterase. *J. Am. Chem. Soc.* **2005**, *127*, 11029-11036.
61. Davis, K. L. P. P., Tacrine. *Lancet* **1995**, *345*, 625.
62. Bar-On, P.; Millard, C. B.; Harel, M.; Dvir, H.; Enz, A.; Sussman, J. L.; Silman, I., Kinetic and structural studies on the interaction of cholinesterases with the anti-Alzheimer drug rivastigmine. *Biochemistry* **2002**, *41*, 3555-3564.
63. Kawakami, Y.; Inoue, A.; Kawai, T.; Wakita, M.; Sugimoto, H.; Hopfinger, A. J., The rationale for E2020 as a potent acetylcholinesterase inhibitor. *Bioorg. Med. Chem.* **1996**, *4*, 1429-1446.
64. Berg, L.; Andersson, C. D.; Artursson, E.; Hömberg, A.; Tunemalm, A.-K.; Linusson, A.; Ekström, F., Targeting acetylcholinesterase: Identification of chemical leads by high throughput screening, structure determination and molecular modeling. *PLoS One* **2011**, *6*, e26039.
65. Enayati, A.; Hemingway, J., Malaria management: Past, present, and future. *Annu. Rev. Entomol.* **2010**, *55*, 569-591.

66. Casida, J. E.; Durkin, K. A., Anticholinesterase insecticide retrospective. *Chem. Biol. Interact.* **2013**, *203*, 221-225.
67. Sidell, F. R.; Borak, J., Chemical warfare agents: Ii. Nerve agents. *Ann. Emerg. Med.* **1992**, *21*, 865-871.
68. Satoh, T.; Gupta, R. C., *Anticholinesterase pesticides: Metabolism, neurotoxicity, and epidemiology*. John Wiley & Sons: New Jersey, 2011.
69. Forsyth, C. S.; Chambers, J. E., Activation and degradation of the phosphorothionate insecticides parathion and EPN by rat brain. *Biochem. Pharmacol.* **1989**, *38*, 1597-1603.
70. Lukaszewicz-Hussain, A., Role of oxidative stress in organophosphate insecticide toxicity - Short review. *Pest. Biochem. Physiol.* **2010**, *98*, 145-150.
71. Walker Jr, B.; Nidiry, J., Current concepts: Organophosphate toxicity. *Inhal. Toxicol.* **2002**, *14*, 975-990.
72. Grob, D.; Garlick, W. L.; Merrill, G. G.; Freimuth, H. C., Death due to parathion, an anticholinesterase insecticide. *Ann. Intern. Med.* **1949**, *31*, 899-904.
73. Sogorb, M. A.; Vilanova, E., Enzymes involved in the detoxification of organophosphorus, carbamate and pyrethroid insecticides through hydrolysis. *Toxicol. Lett.* **2002**, *128*, 215-228.
74. Pang, Y. P.; Brimijoin, S.; Ragsdale, D. W.; Zhu, K. Y.; Suranyi, R., Novel and viable acetylcholinesterase target site for developing effective and environmentally safe insecticides. *Curr. Drug Targets* **2012**, *13*, 471-482.
75. Aygun, D.; Erenler, A. K.; Karatas, A. D.; Baydin, A., Intermediate syndrome following acute organophosphate poisoning: Correlation with initial serum levels of muscle enzymes. *Basic Clin. Pharmacol. Toxicol.* **2007**, *100*, 201-204.

76. Lotti, M.; Moretto, A., Organophosphate-induced delayed polyneuropathy. *Toxicol. Rev.* **2005**, *24*, 37-49.
77. Worek, F.; Thiermann, H., The value of novel oximes for treatment of poisoning by organophosphorus compounds. *Pharmacol. Ther.* **2013**, *139*, 249-259.
78. Childs, A. F.; Davies, D. R.; Green, A. L.; Rutland, J. P., The reactivation by oximes and hydroxamic acids of cholinesterase inhibited by organo-phosphorus compounds *Br. J. Pharmacol.* **1955**, *10*, 462-465.
79. Masson, P.; Clery, C.; Guerra, P.; Redslob, A.; Albaret, C.; Fortier, P. L., Hydration change during the aging of phosphorylated human butyrylcholinesterase: Importance of residues aspartate-70 and glutamate-197 in the water network as probed by hydrostatic and osmotic pressures. *Biochem. J.* **1999**, *343 Pt 2*, 361-369.
80. Casida, J. E.; Quistad, G. B., Golden age of insecticide research: Past, present, or future? *Annu. Rev. Entomol.* **1998**, *43*, 1.
81. Casida, J. E., Mode of action of carbamates. *Annu. Rev. Entomol.* **1963**, *8*, 39-58.
82. Kuhr, R. J.; Dorough, H. W., *Mode of action*. CRC Press: Cleveland, OH, 1976; p 41-70.
83. Darvesh, S.; Darvesh, K. V.; McDonald, R. S.; Mataija, D.; Walsh, R.; Mothana, S.; Lockridge, O.; Martin, E., Carbamates with differential mechanism of inhibition toward acetylcholinesterase and butyrylcholinesterase. *J. Med. Chem.* **2008**, *51*, 4200-4212.
84. Jiang, Y.; Swale, D.; Carlier, P. R.; Hartsel, J. A.; Ma, M.; Ekström, F.; Bloomquist, J. R., Evaluation of novel carbamate insecticides for neurotoxicity to non-target species. *Pest. Biochem. Physiol.* **2013**, *106*, 156-161.
85. Lotti, M.; Moretto, A., Do carbamates cause polyneuropathy? *Muscle Nerve* **2006**, *34*, 499-502.

86. Grue, C. E.; Gibert, P. L.; Seeley, M. E., Neurophysiological and behavioral changes in non-target wildlife exposed to organophosphate and carbamate pesticides: Thermoregulation, food consumption, and reproduction. *Amer. Zool.* **1997**, *37*, 369-388.
87. Carlier, P. R.; Anderson, T. D.; Wong, D. M.; Hsu, D. C.; Hartsel, J.; Ma, M.; Wong, E. A.; Choudhury, R.; Lam, P. C.; Totrov, M. M.; Bloomquist, J. R., Towards a species-selective acetylcholinesterase inhibitor to control the mosquito vector of malaria, *Anopheles gambiae*. *Chem. Biol. Interact.* **2008**, *175*, 368-375.
88. Greenblatt, H. M.; Dvir, H.; Silman, I.; Sussman, J. L., Acetylcholinesterase: A multifaceted target for structure-based drug design of anticholinesterase agents for the treatment of Alzheimer's disease. *J. Mol. Neurosci.* **2003**, *20*, 369-383.
89. Bourne, Y.; Taylor, P.; Radic, Z.; Marchot, P., Structural insights into ligand interactions at the acetylcholinesterase peripheral anionic site. *EMBO J.* **2003**, *22*, 1-12.
90. Harel, M.; Kryger, G.; Rosenberry, T. L.; Mallender, W. D.; Lewis, T.; Fletcher, R. J.; Guss, J. M.; Silman, I.; Sussman, J. L., Three-dimensional structures of *Drosophila melanogaster* acetylcholinesterase and of its complexes with two potent inhibitors. *Protein Sci.* **2000**, *9*, 1063-1072.
91. Weill, M.; Fort, P.; Berthomieu, A.; Dubois, M. P.; Pasteur, N.; Raymond, M., A novel acetylcholinesterase gene in mosquitoes codes for the insecticide target and is non-homologous to the ace gene in drosophila. *Proc. Biol. Sci.* **2002**, *269*, 2007-2016.
92. Djogbenou, L.; Pasteur, N.; Akogbeto, M.; Weill, M.; Chandre, F., Insecticide resistance in the *Anopheles gambiae* complex in benin: A nationwide survey. *Med. Vet. Entomol.* **2011**, *25*, 256-267.

93. Oakeshott, J. G.; Devonshire, A. L.; Claudianos, C.; Sutherland, T. D.; Horne, I.; Campbell, P. M.; Ollis, D. L.; Russell, R. J., Comparing the organophosphorus and carbamate insecticide resistance mutations in cholin- and carboxyl-esterases. *Chem. Biol. Interact.* **2005**, *157–158*, 269-275.
94. Russell, R. J.; Claudianos, C.; Campbell, P. M.; Horne, I.; Sutherland, T. D.; Oakeshott, J. G., Two major classes of target site insensitivity mutations confer resistance to organophosphate and carbamate insecticides. *Pest. Biochem. Physiol.* **2004**, *79*, 84-93.
95. Weill, M.; Lutfalla, G.; Mogensen, K.; Chandre, F.; Berthomieu, A.; Berticat, C.; Pasteur, N.; Philips, A.; Fort, P.; Raymond, M., Comparative genomics: Insecticide resistance in mosquito vectors. *Nature* **2003**, *423*, 136-137.
96. Weill, M.; Malcolm, C.; Chandre, F.; Mogensen, K.; Berthomieu, A.; Marquine, M.; Raymond, M., The unique mutation in ace-1 giving high insecticide resistance is easily detectable in mosquito vectors. *Insect. Mol. Biol.* **2004**, *13*, 1-7.
97. Newcomb, R. D.; Campbell, P. M.; Ollis, D. L.; Cheah, E.; Russell, R. J.; Oakeshott, J. G., A single amino acid substitution converts a carboxylesterase to an organophosphorus hydrolase and confers insecticide resistance on a blowfly. *Proc. Natl. Acad. Sci. U S A* **1997**, *94*, 7464-7468.
98. Heidari, R.; Devonshire, A. L.; Campbell, B. E.; Bell, K. L.; Dorrian, S. J.; Oakeshott, J. G.; Russell, R. J., Hydrolysis of organophosphorus insecticides by in vitro modified carboxylesterase E3 from *Lucilia cuprina*. *Insect Biochem. Mol. Biol.* **2004**, *34*, 353-363.
99. Wong, D. M.; Li, J.; Chen, Q.-H.; Han, Q.; Mutunga, J. M.; Wysinski, A.; Anderson, T. D.; Ding, H.; Carpenetti, T. L.; Verma, A.; Islam, R.; Paulson, S. L.; Lam, P. C. H.; Totrov, M.; Bloomquist, J. R.; Carlier, P. R., Select small core structure carbamates

exhibit high contact toxicity to , "carbamate-resistant" strain malaria mosquitoes,  
*Anopheles gambiae* (akron). *PLoS One* **2012**, *7*, e46712.

## **Chapter 2: Exploring 3-oxoisoxazole-2(3H)-carboxamides and isoxazol-3-yl carbamates as mosquitocide.**

### **2.1 An overview of Chapter 2**

From Chapter 1, it is evident that there has been an upsurge in the mosquito population that is resistant to pyrethroids. This development threatens to compromise the efficacy of pyrethroid-treated bed nets, and has motivated the development of another class of insecticide with a different mode of action. Acetylcholinesterase (AChE) inhibitors appear promising in this regard, in view of their efficacy as an indoor wall application (“indoor residual spraying”, IRS) against adult mosquitoes. However, none of the AChE inhibitors approved for IRS have been approved for bed nets, perhaps due to the lingering concern of mammalian toxicity. A safe and effective insecticide against the susceptible and resistant strain of *Anopheles gambiae* will be needed for deployment on ITNs. We will begin Chapter 2 by giving a brief account of the efforts made by the Carlier group in the past to develop a safe AChE insecticide, their advantages, and scope for improvement. This will be followed by a rationale behind the synthesis of AChE insecticides in this project. Finally, the focus of this chapter will be on the synthesis, and pharmacology of 3-oxoisoxazole-2(3H)-carboxamides and isoxazol-3-yl carbamates. The compounds were evaluated using toxicological and enzyme inhibition assay that are discussed below.

### **2.2 Bioassays**

#### **2.2.1 Tarsal contact toxicity assay**

The author did measure *An. gambiae* tarsal contact toxicity of numerous AChE inhibitors in the course of this work. Nevertheless, a significant fraction of these determinations were performed by members of the Bloomquist group (Entomology, Virginia Tech and the University

of Florida). The tarsal contact toxicity of the synthesized compounds was determined by using standard WHO filter paper assay towards wild type (G3 strain, susceptible), and resistant (Akron strain, carbamate resistant) mosquitoes.<sup>1</sup> The test compound was dissolved in 2 mL of ethanol and impregnated on the filter paper (Whatman<sup>®</sup> No. 1) measuring 12 x 15 cm. To avoid any loss of insecticide solution being pipetted out onto the filter paper, the paper is supported on several pins attached to a cardboard sheet. Then a uniform layer of the insecticide solution is applied on the paper, being sure to dispense all 2 mL onto the paper. The paper is left to air dry for 24 hours before putting it in the exposure tube marked with a red dot in Figure 2.1. According to WHO protocol, the treated paper can be reused only five times.

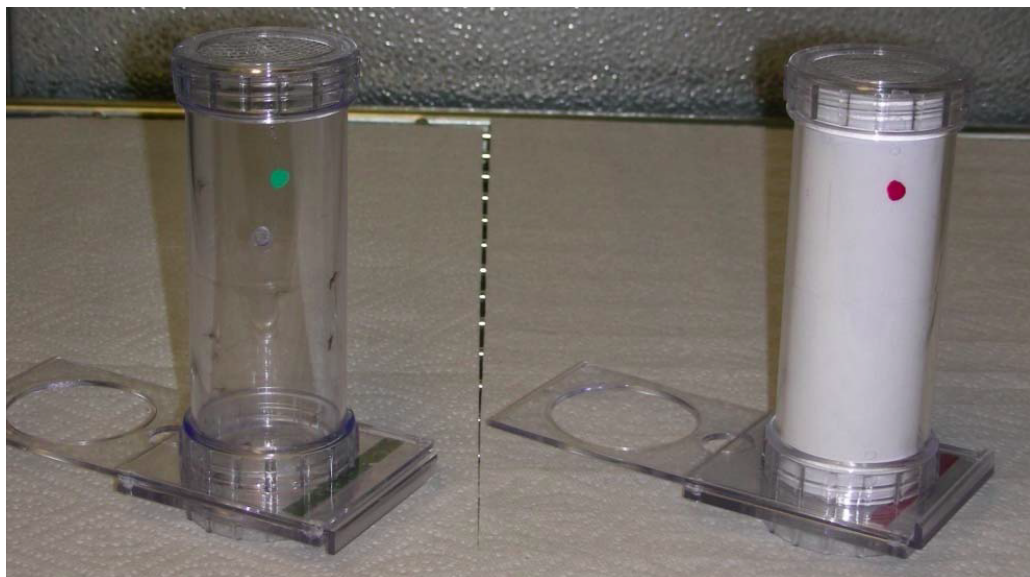
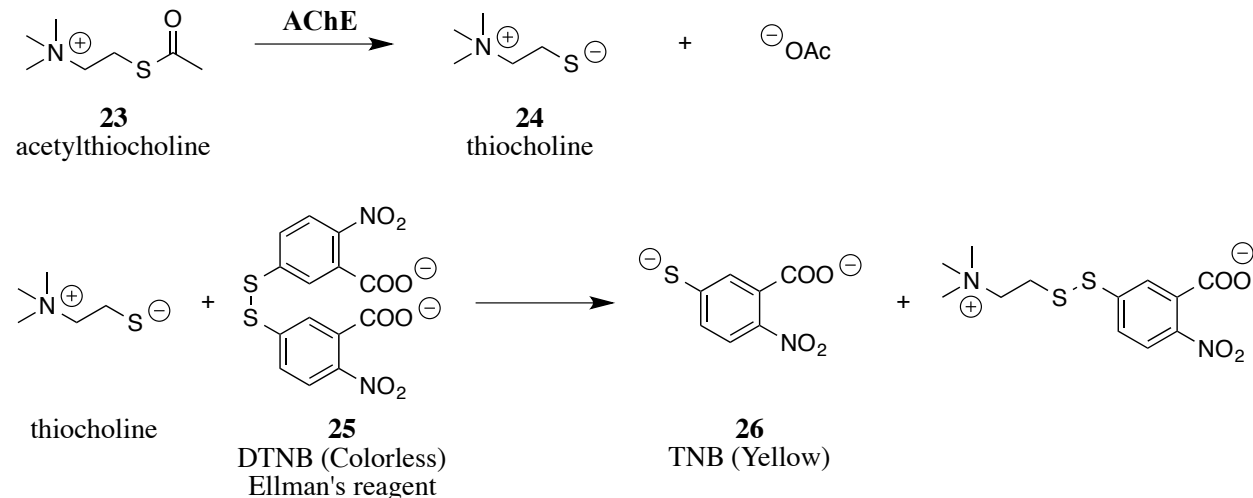


**Figure 2.1:** Tubes used in WHO filter paper toxicity assays. The one on the left is the holding tube marked with a green dot. The exposure tube with the treated paper in it is on the right, and is marked with a red dot

Experiments were performed in duplicates at each concentration. For each experiment, a batch of 25 non-blood fed, 2-5 day old female *An. gambiae* mosquitoes were used. Mosquitoes were anaesthetized by keeping them on ice for several minutes, and then were transferred to the holding tube (Figure 2.1). They were acclimatized for one hour before being gently blown into the exposure tube, where they were exposed to the treated paper for 1 hour. At the end of the exposure they were blown back into the holding tube, and any mortality due to 1 h exposure was recorded. The holding tubes were left in a dark room at  $25^{\circ}\text{C} \pm 1^{\circ}\text{C}$  with a relative humidity of  $80\% \pm 10\%$ . During the post exposure period the mosquitoes were provided with sugar water (10% w/v) on a cotton wool. The mortality was recorded after 24 hours.

## 2.2.2 Enzyme inhibition

The Ellman Assay was used to determine the inhibitory activity of isoxazol-3-yl carboxamides and carbamates (Scheme 2.1).<sup>2</sup>

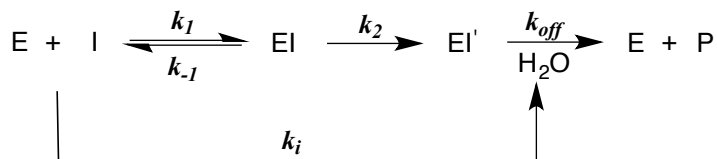


**Scheme 2.1:** Ellman assay for the chlorimetric determination of AChE acitivity.<sup>2</sup>

In the Ellman assay, acetylthiocholine **23** (ATCh) is used as a pseudo-substrate instead of acetylcholine **14** (ACh). ATCh serves as a satisfactory substitute for ACh, because it shares identical kinetic properties with the natural substrate.<sup>3</sup> Further, the progress of the enzymatic reaction could be monitored spectrophotometrically as explained below.

As shown in Scheme 2.1, the enzyme hydrolyses ATCh **23**, giving thiocholine **24**, and acetate. Thiocholine generated rapidly reacts with (5,5'-dithiobis)-2-nitrobenzoic acid (DTNB) **25** to give a yellow colored dianion of 5-thio-2-nitrobenzoic acid (TNB), which can be easily detected in a UV-visible spectrophotometer ( $\lambda = 405$  nm). Moreover, the rate of change in absorption depends on the rate of hydrolysis of ATCh, which reflects the rate of enzymatic activity.

Carbamates are pseudo-irreversible inhibitors of AChE; they inhibit the enzyme by covalently modifying the active site serine. The inhibition of AChE by carbamates is a multi-step process as shown in Scheme 2.2.



$$k_i (\text{min}^{-1}) = K_a * k_2 \quad \text{where } K_a (\text{affinity constant, mM}^{-1}) = k_{-1}/k_1$$

**Scheme 2.2:** Kinetic scheme explaining mechanism of AChE by pseudo-irreversible carbamate inhibitors.

Firstly, the carbamate forms a reversible complex with the enzyme before the carbamylation step. The rate constant for the formation enzyme-inhibitor complex is denoted by  $k_1$ , and  $k_{-1}$  is the rate constant for the dissociation of the complex. The binding constant or

affinity constant for this reversible step is denoted by  $K_a$ , which is defined as  $k_I/k_{-I}$ . In the next step, serine is carbamylated and the rate constant for this step is denoted by  $k_2$ . The rate constant  $k_{off}$  gives a measure of the hydrolysis of the carbamylated enzyme, which is a relatively slow process. Further, the apparent bimolecular rate constant  $k_i$ , is a product of  $K_a$ , and  $k_2$ , a parameter that determines how fast the enzyme is inactivated. Before we proceed to the next section, we would briefly describe the protocol employed for enzyme inhibition assays. These assays were performed by Dr. Dawn Wong in the Carlier group.

The apparent second order rate constant  $k_i$  was measured by following a progressive inactivation approach previously reported by Bar-On et al., and Reiner and Aldridge.<sup>4, 5</sup> The enzymes (rAgAChE-WT, rhAChE, and rAgAChE-G119S) were diluted in buffer A having the following composition: 0.01 M sodium phosphate containing 0.3% sodium azide (w/v), 1 mg/mL bovine serum albumin (BSA), 0.3% Triton X-100 (v/v)). The inhibitor was diluted in buffer B containing 0.01 M sodium phosphate with 0.3% sodium azide (w/v). For maximum activity and stability of the enzymes, the assay was done at pH 7.7 and at a  $23 \pm 1$  °C.<sup>5-6</sup> The enzymes were pre-incubated for typically 10 minutes at approximately 1-minute interval with five different concentrations of the inhibitor. Each inhibitor concentration was present in duplicate in a 96-well microplate. Further, for accuracy and to avoid spurious results, every experiment was repeated. After the desired incubation time, a freshly prepared solution of the substrate **23** (ATCh), and indicator **25** (DTNB), 4 and 3 mM in buffer B, respectively were added. Thereafter, during the course of the enzymatic reaction a yellow colored 2-mercapto-5-nitrobenzoic acid is produced. The enzyme activity was monitored at 405 nm at room temperature using a microplate reader. The final concentrations of substrate **23** (ATCh), and indicator **25** (DTNB) were 0.4 and 0.3 mM, respectively.

Enzyme velocities ( $v/v_0$ ) at a fixed inhibitor concentration were measured as a function of time  $t$ . Plots of  $\ln(v/v_0)$  vs incubation time  $t$  were constructed and the slope provided the pseudo first-order rate constant  $k_{\text{obs}}$  ( $\text{min}^{-1}$ ) for inactivation. For each inhibitor,  $k_{\text{obs}}$  values were determined at three or more inhibitor concentrations [I]. Finally, the slope of the plots of  $k_{\text{obs}}$  vs [I] provided the second order rate constant  $k_i$  ( $\text{mM}^{-1}\text{min}^{-1}$ ) for inactivation.

### 2.3 Rationale and objective behind the synthesis of five membered heterocyclic carboxamides and carbamates

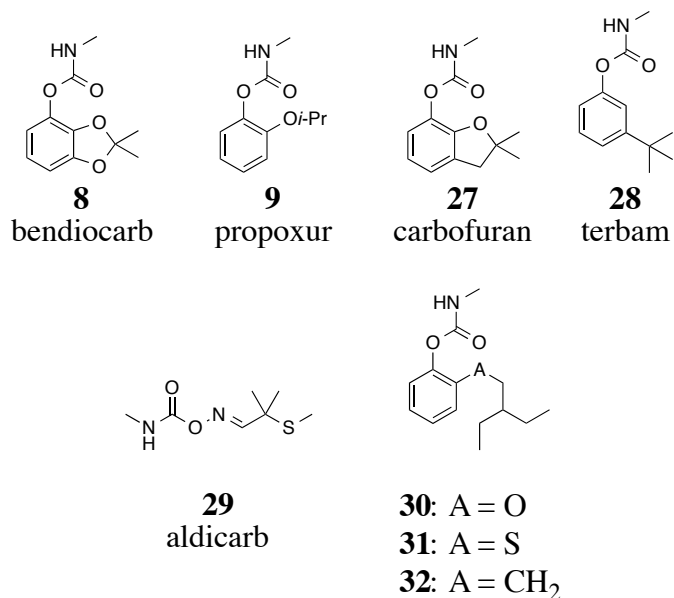


**Figure 2.2:** Structure of commercial carbamates (8, 9, 27-29), and previously reported aryl methylcarbamates (30-32).<sup>7</sup>

Significant research has been done by Carlier et al. to develop novel insecticides that can confer high selectivity for *AgAChE* over *hAChE*, and could be safer than existing anticholinesterase insecticides for use on ITNs in malaria endemic regions. The classic aryl methyl pharmacophore introduced by Metcalf, which in the past has offered high insecticidal

activity was successfully redesigned to achieve high species selectivity towards WT *An. gambiae* (G3).<sup>8, 6</sup>

**Table 2.1:** Bimolecular rate constants  $k_i$  for inactivation of rAgAChE (WT, G119S), and hAChE.

Compound	<sup>a</sup> rAgAChE $k_i$ (mM <sup>-1</sup> min <sup>-1</sup> )	<sup>a</sup> hAChE $k_i$ (mM <sup>-1</sup> min <sup>-1</sup> )	<sup>a, d</sup> G119S $k_i$ (mM <sup>-1</sup> min <sup>-1</sup> )	<sup>b</sup> WT/G119S Resistance ratio	<sup>c</sup> Ag/h selectivity
<b>9</b> (propoxur)	266 ± 9	17.0 ± 0.4	<0.037 ± 0.007	7,200 ± 1,400	16 ± 1
<b>8</b> (bendiocarb)	839 ± 22	111 ± 5	<0.055 ± 0.007	15,000 ± 2,000	7.6 ± 0.4
<b>27</b> (carbofuran)	2,620 ± 150	428 ± 12	<0.044 ± 0.020	60,000 ± 27,000	6.1 ± 0.4
<b>28</b> (terbam)	1,510 ± 100	126 ± 3	0.40 ± 0.03	3,800 ± 400	12 ± 1
<b>29</b> (aldicarb)	13.3 ± 0.3	6.5 ± 0.3	3.15 ± 0.08	4.2 ± 0.1	2.0 ± 0.1
<b>30</b>	255 ± 12	0.48 ± 0.12	<0.06 ± 0.02	4,300 ± 1,100	530 ± 130
<b>31</b>	1850 ± 100	14.5 ± 1.5	<0.046 ± 0.018	40,000 ± 17,000	130 ± 15
<b>32</b>	75.3 ± 2.7	0.75 ± 0.03	ND	ND	100 ± 5

$k_i$  measurements were done by Dr. Dawn Wong in the Carlier group. <sup>a</sup>Measured at 23 ± 1 °C, pH 7.7, 0.1% (v/v) DMSO. Values at rAgAChE (WT and G119S) and rhAChE were reported previously.<sup>6</sup> <sup>b</sup>Resistance ratio is calculated as  $k_i(\text{WT})/k_i(\text{G119S})$ . Standard error in the ratio is calculated according to a standard propagation of error formula. <sup>c</sup>Selectivity for inhibiting AgAChE (WT) vs hAChE, calculated as  $k_i(\text{AgAChE-WT})/k_i(\text{hAChE})$ , with standard error in the ratio calculated according to a standard propagation of error formula.<sup>9</sup> <sup>d</sup>G119S is the resistant AgAChE with G119S mutation.

From the  $k_i$  data in Table 2.1, it is evident that none of the commercial aryl methylcarbamates offer appreciable selectivity. Propoxur (**9**), which has been approved by WHOPES for IRS, is only 16-fold selective for WT AgAChE over hAChE. None of the other commercial carbamates (**8**, **27-29**) showed high selectivity (< 10-fold). In contrast to the commercial carbamates, a recently disclosed series of aryl methylcarbamates (e.g. **30-32**, Figure

2.2) by Carlier et al. has shown high selectivity (>100-fold) for *An. gambiae* AChE (*AgAChE*) vs human AChE (*hAChE*).<sup>6-7</sup> Compound **30** bearing a 2-(2-ethylbutoxy) group showed greater than 500-fold selectivity. This high selectivity obviously arises from the differences in the amino acid substitutions in the catalytic subunits of *AgAChE* and *hAChE*.<sup>10</sup> Although we cannot yet point to a specific group of residue substitutions that confer selectivity, we have developed a ligand-based model that is somewhat predictive of inhibition selectivity.<sup>6</sup> These compounds maintained good topical contact toxicity towards WT *An. gambiae* (Table 2.2). However, carbamate-resistant Akron strain *An. gambiae* (MR4, CDC) were shown to be insensitive to these novel aryl methylcarbamates (**30-32**), as they were to commercial aryl methylcarbamates (**8-9, 27-28**), (Table 2.2). As can be seen in Table 2.2, the LC<sub>50</sub> values for commercial carbamates (**9, 8, 27, 28**) bearing a phenyl core fell between 16-42 µg/mL for the susceptible G3 strain of *An. gambiae*; however, these compounds were not toxic towards the resistant Akron strain even when treated at concentrations up to >5,000 µg/mL.<sup>6</sup> The carbamate insensitivity of the Akron strain is known to arise from a G119S mutation in the oxyanion hole of AChE.<sup>11, 12</sup>

**Table 2.2:** Tarsal and topical contact toxicity to WT (G3) and Akron strain *An. gambiae*.

Compound	<sup>a</sup> Tarsal <i>An. gambiae</i> (G3) LC <sub>50</sub> μg/mL (95% CI)	<sup>a</sup> Tarsal <i>An. gambiae</i> (Akron) LC <sub>50</sub> μg/mL (95% CI)	Topical <i>An. gambiae</i> (G3) LD <sub>50</sub> μg/mL (95% CI) (Topical)	<sup>b</sup> Resistance ratios
<b>9</b> (propoxur)	39 (32-45)	>5,000	3.2 (2.4-4.2)	>130
<b>8</b> (bendiocarb)	16 (14-17)	>5,000	0.74 (0.52-0.97)	>310
<b>27</b> (carbofuran)	16 (11-25)	>5,000	0.85 (0.7-1.1)	>310
<b>28</b> (terbam)	37 (14-16)	>5,000	4.48 (3.6-5.4)	>130
<b>29</b> (aldicarb)	70 (66-74)	32 (30-35)	1.3 (1.1-1.6)	0.5
<b>30</b>	27% @ 1,000 μg/mL	ND	81 (64-94)	ND
<b>31</b>	27% @ 1,000 μg/mL	ND	10 (8-12)	ND
<b>32</b>	0% @ 1,000 μg/mL	ND	ND	ND

Toxicity assays were performed by members of the Bloomquist group.<sup>a</sup> Mosquitoes were exposed (1 h) to dried filter papers previously treated with ethanolic solutions of carbamates; mortality was recorded after 24 h. LC<sub>50</sub> values derived from the concentrations of inhibitor used to treat the paper and were reported previously.<sup>6</sup>

<sup>b</sup>Defined by LC<sub>50</sub> (Akron)/LC<sub>50</sub> (G3).

Thus we observed high enzymatic and toxicological resistance for these aryl methylcarbamates (**8-9, 27-28, 30-32**) (Table 2.1 and 2.2). A resistance ratio is a measure of pesticide sensitivity relative to a susceptible population.<sup>13</sup> A large resistance ratio indicates a highly resistant population.<sup>14</sup> Since all carbamate insecticides share the same mode of action (acetylcholinesterase inhibition), we see cross-resistance to these novel aryl methylcarbamates (**30-32**).<sup>15</sup>

However, an important exception to the above-mentioned commercial insecticides was aldicarb (**29**), which showed high contact toxicity towards both G3 and Akron strain *An.*

*gambiae*, and low toxicological cross-resistance (G3, LC<sub>50</sub> = 70, and Akron, LC<sub>50</sub> = 32 µg/mL, Table 2.2). The high in vivo insecticidal efficacy exhibited by aldicarb towards Akron could possibly be the result of oxidative metabolism to more toxic aldicarb sulfoxide due to up-regulated cytochrome P450 monooxygenases in resistant strain of *An. gambiae*.<sup>16</sup> Also, it is highly possible that Akron toxicity results from its smaller core structure. The G119S mutation, where glycine at position 119 has been replaced by serine, should reduce the free volume in the active site of the enzyme. Thus, inhibitors like aldicarb might fit better in the crowded active site of the resistant enzyme due to their small size as compared to the bulkier aryl methylcarbamate. Further, we took the help of computational modeling to gain insight into the binding of aryl methyl carbamate, and aldicarb in the active site of the susceptible, and the mutant enzyme. As can be seen in Figure 2.3, the six membered aromatic ring of terbam (**28**) is well accommodated in the active site of the susceptible enzyme (Figure 2.3 A); however, it encounters a steric clash with the hydroxyl group of S119 (a mutated glycine to a serine at position 119) in the mutant enzyme (Figure 2.3). In contrast to this, aldicarb due to its smaller size could fit well in the mutant enzyme, and encounters no clash with the hydroxyl of S119 (Figure 2.3 C).<sup>6</sup>

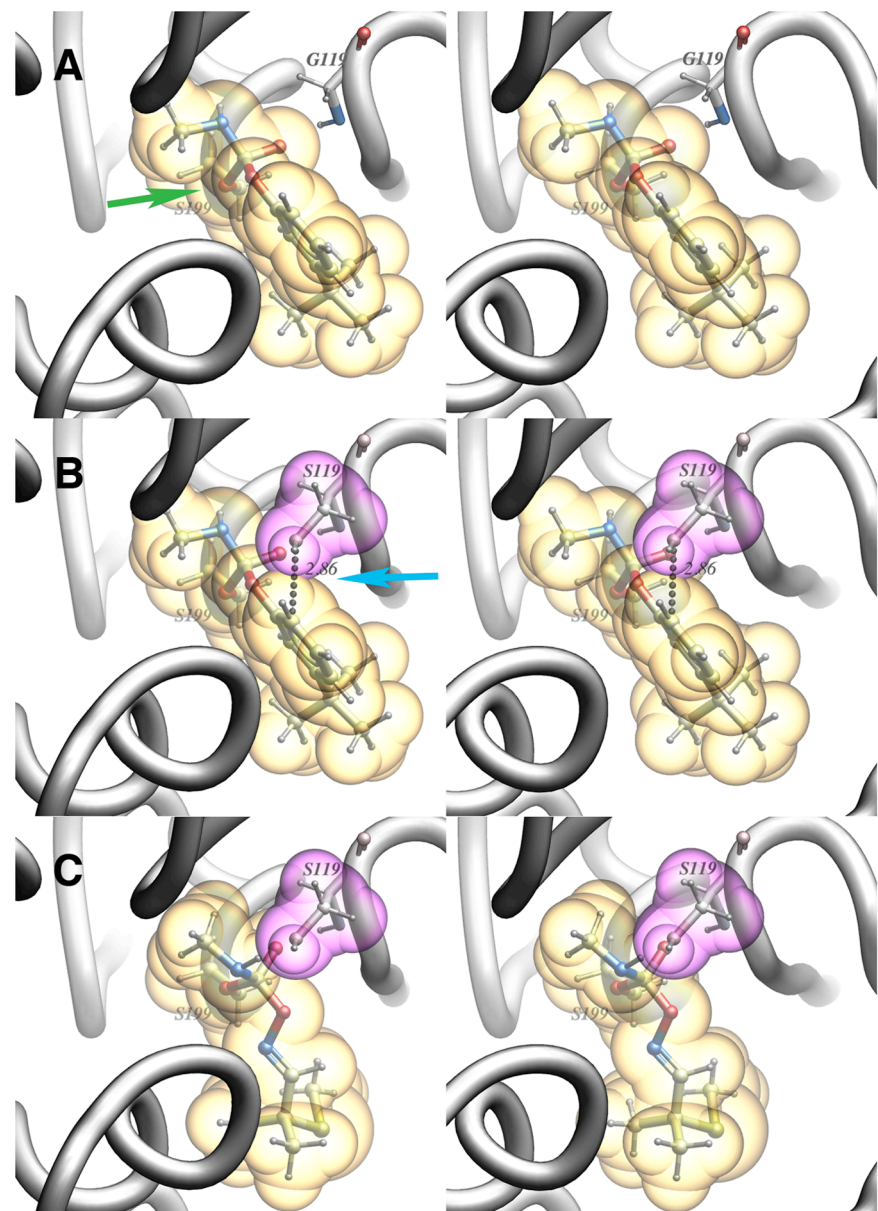


**Figure 2.3:** Computational modelling of (A) terbam (**28**) in the active site of susceptible enzyme. (B) terbam (**28**) in the active site of G119S enzyme. (C) aldicarb (**29**) in the active site of G119S enzyme.<sup>6</sup>

These findings prompted us to explore other “smaller-core” heterocyclic inhibitors that might serve as the key to combat insecticide resistance towards carbamates. In particular, isoxazol-3-yl carbamates (Chapter 2), pyrazol-5-yl, and pyrazol-4-yl carbamates (Chapter 3)

were chosen because after carbamylation of the active site serine the phenol like leaving group (i.e. heterocyclic enols) is expected to benefit from its aromaticity.

## 2.4 3-oxoisoxazole-2(3H)-carboxamides and isoxazol-3-yl carbamates

The first step in the synthesis of 3-oxoisoxazole-2(3H)-carboxamide and isoxazol-3-yl carbamates involves the synthesis of intermediate 5-substituted isoxazol-3-ols. Isoxazol-3-ol in itself is an important motif in medicinal chemistry.<sup>17, 18</sup>

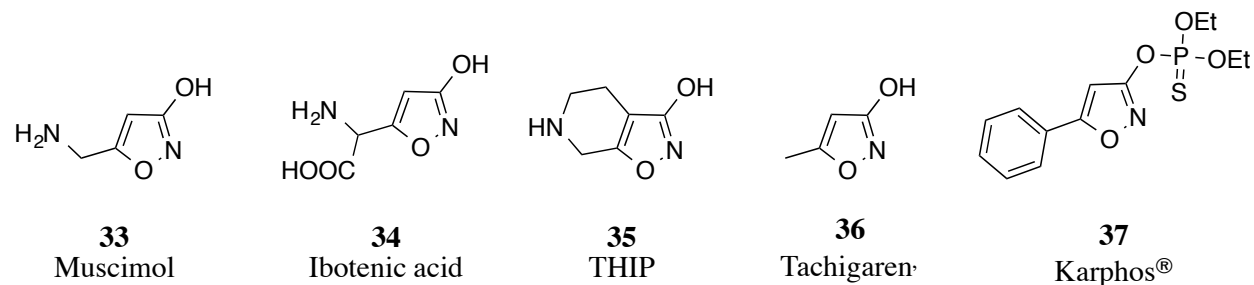
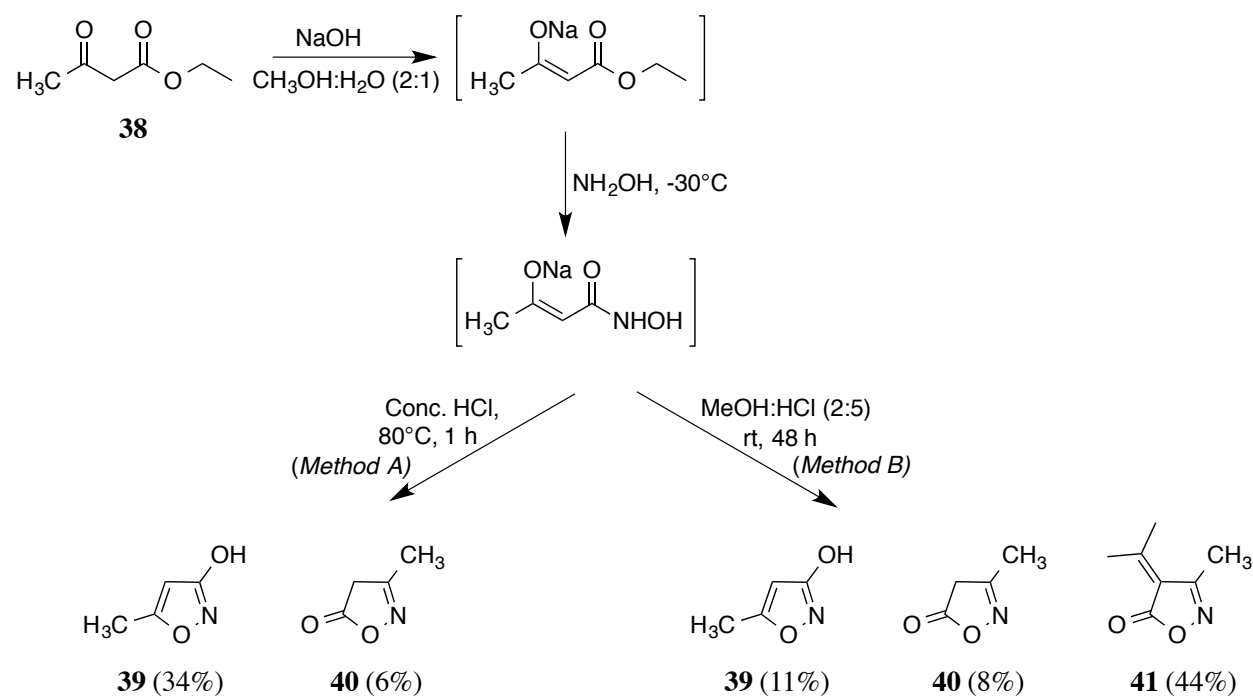


**Figure 2.4:** Biologically active isoxazol-3-ols.<sup>19-20</sup>

The unique biological properties of naturally occurring isoxazol-3-ols, muscimol (**33**) and ibotenic acid (**34**), were discovered in mid-1960s. Muscimol, a non-selective and potent agonist of 4-aminobutyric acid (GABA) receptor, was derived from a fungus, *A. pantherina* by Onda et al.<sup>21</sup> This compound served as a lead for the design, and synthesis of 4,5,6,7-tetrahydroisoxazolo[4,5-*c*]pyridin-3-ol (**35**, THIP), a specific and more potent GABA<sub>A</sub> receptor agonist.<sup>19</sup> Ibotenic acid was isolated from the species of mushroom, *Amanita strobiliformis*, and is known for its non-selective interactions with (L)-glutamate receptor in the CNS.<sup>22</sup> Further, isoxazol-3-ols are being used in agrochemical industry. 5-methylisoxazol-3-ol (**36**), also known as Tachigaren<sup>®</sup> or hymexazol, is a plant growth promoter and a soil fungicide.<sup>20</sup> The phosphorothioate of 3-hydroxy-5-phenylisoxazole (**37**, Karpbos<sup>®</sup>), is a broad spectrum

insecticide.<sup>20</sup> The versatility of this moiety, and literature precedents demonstrating its excellent agrochemical properties, makes it an interesting pharmacophore to explore from an insecticide point of view.

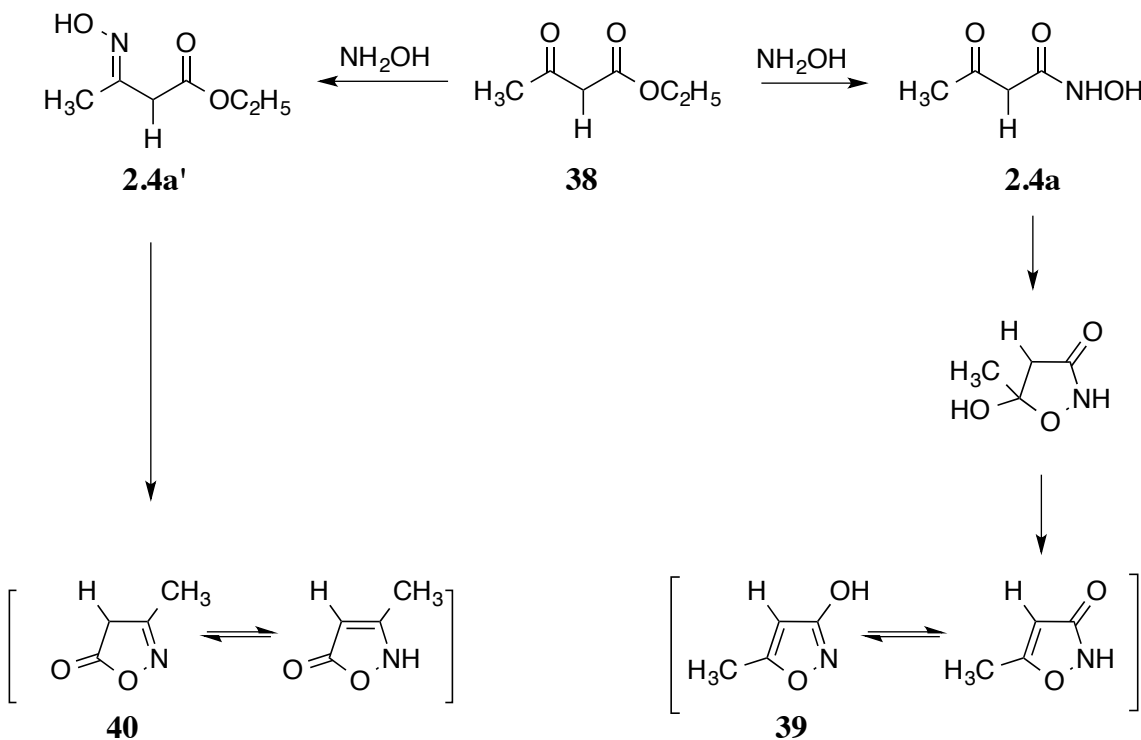
The traditional method to synthesize isoxazol-3-ols involves the reaction of  $\beta$ -keto esters with hydroxylamine. The ease of availability, and low price of the starting materials, makes it the most economical, and widely employed method for the synthesis of this moiety. We followed a literature procedure reported by Sato et al. for the synthesis of 5-methylisoxazol-3-ol (**39**) (Scheme 2.3).<sup>20</sup>



**Scheme 2.3:** Synthesis of 5-methylisoxazol-3-ol (**39**).<sup>20</sup>

Ethyl acetoacetate (**38**) was added drop wise to a solution of sodium hydroxide in methanol and water at -20 °C. The solution was stirred for 10 minutes, and then hydroxylamine (prepared from NH<sub>2</sub>OH.HCl and NaOH in water) was added at -30 °C. The reaction was allowed

to stir for 2 h before acetone was added at -20 °C to quench the residual NH<sub>2</sub>OH. This was followed by adding concentrated HCl at once, and heating the reaction mixture to 80 °C for 1 h. The reaction was cooled, poured in water, and chromatographed. Although, the literature yield of the desired product is 72%, we obtained it in 34% yield (Method A). Further, we also obtained the undesired 3-methylisoxazol-5-one **40** by-product in 6% yield. Similar observations were reported in the literature, where isoxazol-5-one was formed preferentially in the case of 2-unsubstituted β-keto esters.<sup>23</sup> The yield of the desired product dropped to 11% when less harsh conditions for cyclization were used (Method B). Further, under these conditions we obtained the undesired condensation product of **40** with acetone, which was used for quenching the excess NH<sub>2</sub>OH. The above reaction is known to proceed through two consecutive steps as shown in Scheme 2.4.<sup>24</sup>



**Scheme 2.4:** Simplified mechanism leading to the formation of the desired isoxazol-3-ols, and undesired isoxazol-5-ones.<sup>23-24</sup>

In the first step,  $\text{NH}_2\text{OH}$  attacks the  $\beta$ -keto ester (**38**) forming either intermediate (**2.4a**) or intermediate (**2.4a'**). In the subsequent step, these intermediates undergo cyclization, and dehydration upon acidification to give the final products. Compound **2.4a** is most likely the discrete intermediate for the formation of isoxazol-3-ols. In addition, Jacobsen et al. have investigated the effect of pH on the outcome of the first step of the reaction.<sup>23</sup> At a pH of 9-10, hydroxylamine predominately exists in neutral form, and preferentially attacks the ester carbonyl leading to the formation of  $\beta$ -keto hydroxamic acid, and thereby maximizing the yield of the desired isoxazol-3-ols. However, all the efforts by us to improve the yield of the desired product by varying the reaction conditions did not lead to the desired outcome. Finally, looking at the

unpredictability of this reaction, we rejected this as a suitable approach to synthesize series of 5-substituted isoxazol-3-ols.

During the literature search to find an efficient synthetic route to regioselectively synthesize 5-substituted isoxazol-3-ols, we came across a procedure reported by Sørensen et al.<sup>25</sup> They utilized the high reactivity of Meldrum's acid to synthesize  $\beta$ -keto hydroxamic acids, which can further cyclize regioselectivity to give isoxazol-3-ols exclusively. Meldrum's acid (2,2-dimethyl-1,3-dioxane-4,6-dione) was first synthesized in 1908 by A.N. Meldrum.<sup>26</sup> The structure was misinterpreted as that of a  $\beta$ -lactone (**43**), and the correct structure was assigned 40 years later by Davidson and Bernhard (Figure 2.5).<sup>27</sup>

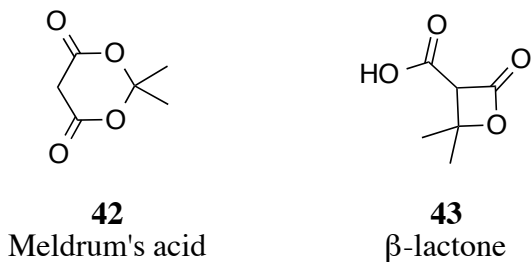
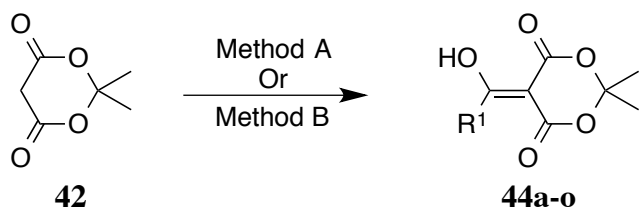


**Figure 2.5:** Structure of Meldrum's acid **42**, and its misinterpreted structure **43**.<sup>27</sup>

Meldrum's acid is well known to react readily with various electrophiles due to its remarkably high acidity ( $pK_a$  4.97 in water) as compared to malonic esters ( $pK_a$  13.7), and acetoacetic esters ( $pK_a$  10.7).<sup>28</sup> Therefore, acylation reactions of **42** can easily occur even in the absence of a base. There are many convenient, and efficient synthetic routes for the preparation of acyl Meldrum's acid from carboxylic acid chlorides and anhydrides, and by using coupling reagents like DCC, DMAP, and diethylcyanophosphonate (DECP).<sup>28-31</sup> We chose to follow the literature protocol reported by Sørensen et al. to synthesize acyl Meldrum's acids from

carboxylic acid chlorides, and carboxylic acids.<sup>25</sup> Acylated Meldrum's acids were obtained in moderate to good yield (Table 2.3).

**Table 2.3:** Isolated yields for the synthesis of acylated Meldrum's acids **44**.



**Method A:** Pyridine (2.0 equiv), DCM, 0 °C, 15 min; R<sup>1</sup>C(O)Cl (1.0 equiv), 0 °C, 1.5 h; RT, 1.5 h

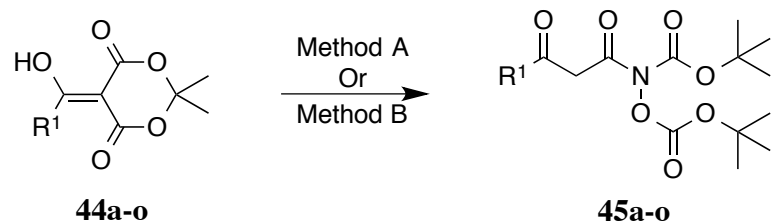
**Method B:** R<sup>1</sup>COOH (1.0 equiv), DECP (1.1 equiv), (Et)<sub>3</sub>N (3.1 equiv), DMF, 0 °C, 30 min; RT, 16 h.

Entry	R <sup>1</sup>	Method	<sup>a</sup> Product Yield (%)	Entry	R <sup>1</sup>	Method	Product Yield (%)
<b>44a</b>	—	A	83	<b>44i</b>	—	B	49
<b>44b</b>	—	A	65	<b>44j</b>	—	B	75
<b>44c</b>	—	A	63	<b>44k</b>	—	A	58
<b>44d</b>	—	A	60	<b>44l</b>	—	B	78
<b>44e</b>	—	A	77	<b>44m</b>	—	A	45
<b>44f</b>	—	A	52	<b>44n</b>	—	B	77
<b>44g</b>	—	B	86	<b>44o</b>	—	A	87
<b>44h</b>	—	B	79				

<sup>a</sup>Isolated product yields.

The subsequent thermolysis of **44a-o** with *N*, *O*-bis-*t*-Boc hydroxylamine (NHBoc(OBoc), synthesized using the literature procedure<sup>32</sup>) was initially performed using the previously reported procedure.<sup>25</sup> In this procedure, 1 equiv. of acyl Meldrum's acid **44** was reacted with 1 equiv. of NHBoc(OBoc) at 65 °C, typically for 3-16 h. However, the reaction did not proceed smoothly in every case. In some instances (e.g. **45c**, **45d**, **45k**, **45l**), the product was obtained in low yield, whereas in other cases (**45f**, **45n**), it could not be purified due to contamination with residual *N*, *O*-bis-*t*-Boc hydroxylamine. To optimize the yield for some of our substrates, we took 1 equiv. of the NHBoc(OBoc), and 1.8 equiv. of the compound **44** and heated the reaction to 90 °C for 45 min-1.5 h. The reaction time for this step is crucial to avoid loss in yield and competing side reactions. Using this modification, we could improve the yield of compound **45** for some substrates (e.g. **45a**, **45g-j**), and the product could be isolated by column chromatography except in the case of **45e**, where we proceeded to the next step with the crude product (Table 2.4). Further, based on thin-layer chromatographic (TLC) analysis, we realized that the β-keto hydroxamic (**45**) acids were not stable at room temperature for extended periods of time. Upon standing the purified colorless oil **45** degrades to give a white solid in the flask. TLC and <sup>1</sup>H NMR analysis of the contents confirmed the decomposition of **45**, and an increased in NHBoc(OBoc) spot/peak.

**Table 2.4:** Isolated yields for the synthesis of  $\beta$ -keto hydroxamic acids **45a-o** from acylated Meldrum's acids **44a-o**.



**Method A:** Acyl Meldrum's Acid (1.0 equiv), NH(Boc)(OBoc) (1.0 equiv), toluene, 65 °C, 16 h.

**Method B:** Acyl Meldrum's Acid (1.8 equiv), NH(Boc)(OBoc) (1.0 equiv), toluene, 90 °C, 1.5-2 h.

Entry	R <sup>1</sup>	Method	<sup>a</sup> Product Yield (%)	Entry	R <sup>1</sup>	Method	<sup>a</sup> Product Yield (%)
<b>45a</b>		B	72	<b>45i</b>		B	66
<b>45b</b>		A	<sup>b</sup> Crude	<b>45j</b>		B	66
<b>45c</b>		A	52	<b>45k</b>		A	33
<b>45d</b>		A	32	<b>45l</b>		A	33
<b>45e</b>		B	85 (Crude)	<b>45m</b>		B	78
<b>45f</b>		A	<sup>b</sup> Crude	<b>45n</b>		A	<sup>b</sup> Crude
<b>45g</b>		B	73	<b>45o</b>		B	43
<b>45h</b>		B	68				

<sup>a</sup>Isolated yields of the product. <sup>b</sup>Crude product contaminated with residual NH(Boc)(OBoc) was taken to the next step.

Compounds **45a-o** were characterized using  $^1\text{H}$  NMR,  $^{13}\text{C}$  NMR, and mass spectroscopy. Interestingly, in  $\text{CDCl}_3$  solution, the  $\beta$ -keto hydroxamic acids **45** exist as a *keto-enol* tautomeric mixture. A  $^1\text{H}$  NMR spectrum of **45a** is shown in Figure 2.6. The peaks of interest have been labeled. The *enol* OH appeared downfield around 13.09 ppm, and the vinylic proton showed up at 6.19 ppm. Further, the methylene protons of the *keto* tautomer appeared as a multiplet at 3.98 ppm. The *keto* form predominates in an approximately 5.5:1 ratio over the *enol* form. However, the ratio varies depending on the  $\text{R}^1$  group.

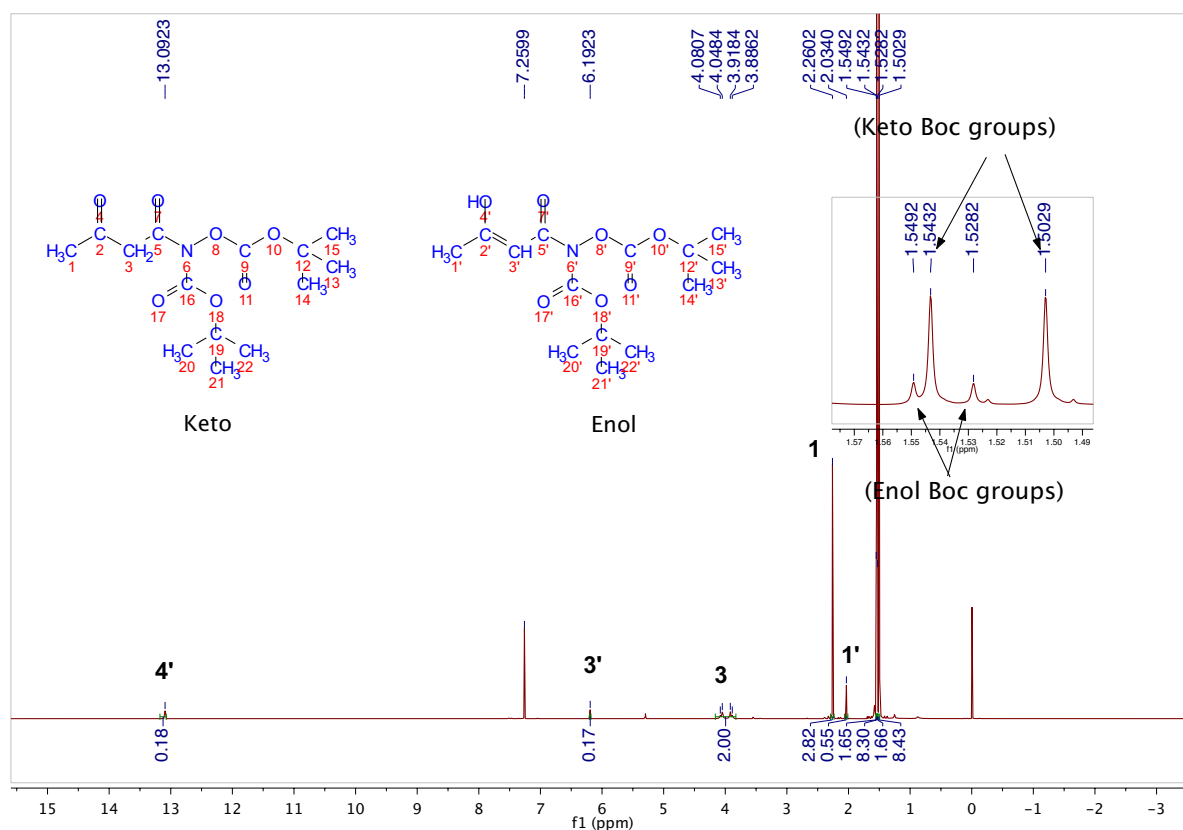
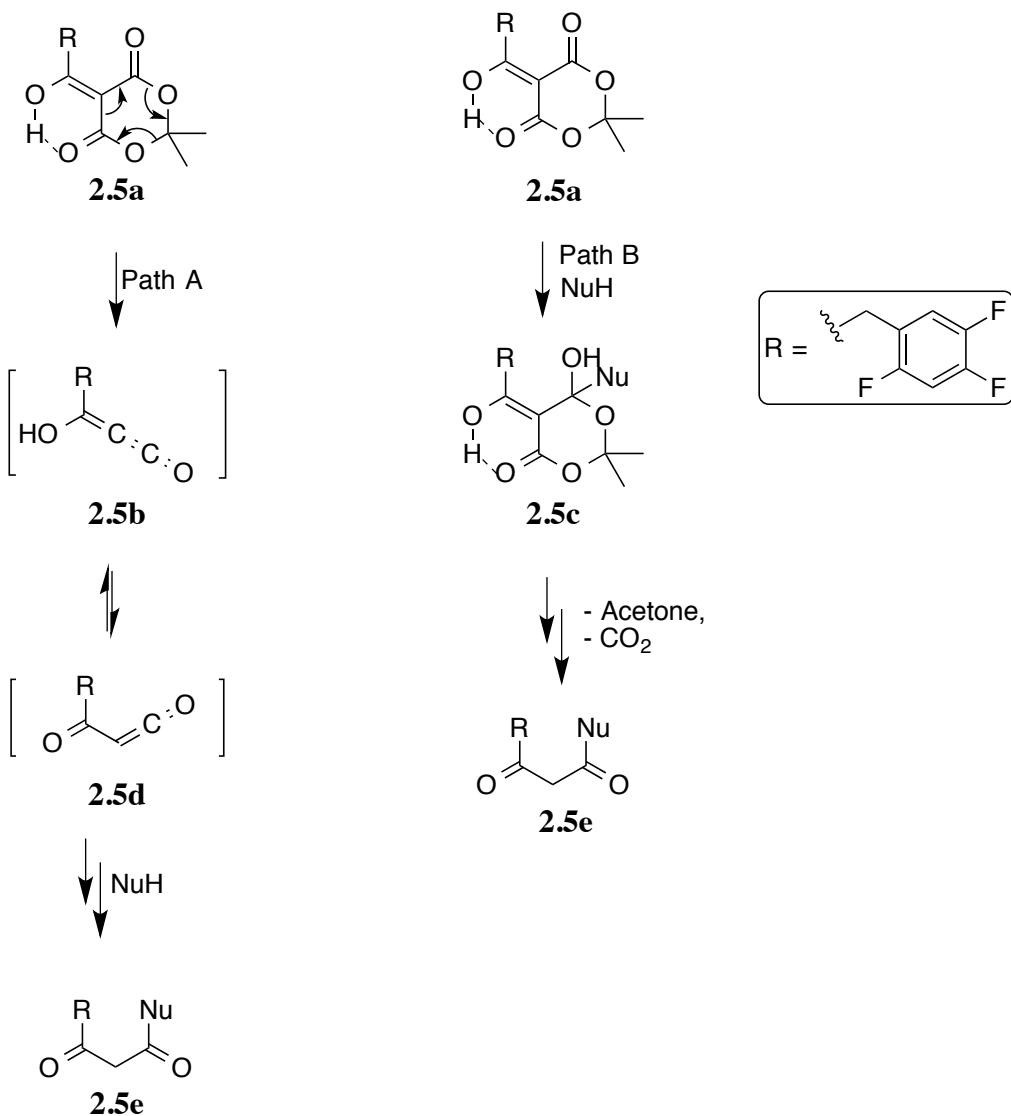


**Figure 2.6:**  $^1\text{H}$  NMR of **45a** in  $\text{CDCl}_3$  showing *keto-enol* tautomerism.

The mechanism of formation of  $\beta$ -keto hydroxamic acids is particularly interesting, and deserves a mention. Although acyl Meldrum's acid derivatives have been extensively exploited for ready access to a number of functionalized 1,3-dicarbonyl compounds; the mechanism of the reaction, however, has remained ambiguous. Till now four tentative reaction intermediates have been proposed,<sup>33</sup> out of which two that have received considerable attention: 1)  $\alpha$ -oxoketene pathway - An oxoketene **2.5d** is formed first, which subsequently reacts with the nucleophile to give the desired 1,3-dicarbonyl product **2.5e**,<sup>34-35</sup> (Path A, Scheme 2.5) 2) A nucleophilic addition-elimination pathway - The nucleophile attacks the acylated Meldrum's acid to form an intermediate **2.5c**, followed by an elimination to give the desired product **2.5e** (Path B, Scheme 2.5).<sup>28,36</sup> Xu et al. carried out an in-depth kinetic analysis to get an insight into the mechanism of this multistep process.<sup>35</sup> The acylated Meldrum's acid **2.5a** was reacted with 1 equiv. or 2 equiv. of NH(Boc)(OBoc) at 50 °C for 4 h, and the reaction rates were determined. If the reaction followed a nucleophilic addition-elimination pathway (Path B, Scheme 2.5) or if the intermediate incorporating the nucleophile was involved in the rate determining step, the rate should show a first-order dependence on [NH(Boc)(OBoc)]. However, a zero order dependence on [NH(Boc)(OBoc)] was observed, thus ruling out the Pathway B. Further, as expected, they observed first-order dependence of the reaction rate on the concentration of the acyl Meldrum's acid, which is consistent with the  $\alpha$ -oxoketene pathway A.<sup>33</sup>

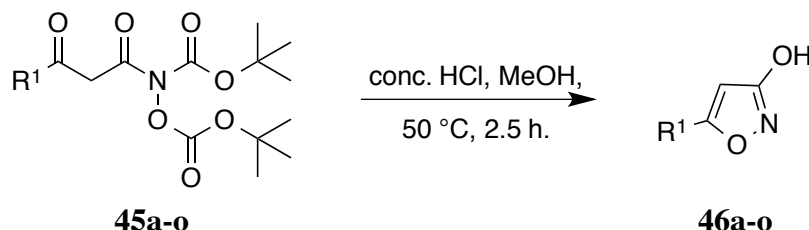


**Path A:**  $\alpha$ -oxoketene pathway    **Path B:** Nucleophilic Addition- Elimination pathway

**Scheme 2.5:** Possible pathways for the formation of  $\beta$ -keto hydroxamic acids **45**.<sup>33</sup>

The next step in the synthesis was cyclization of  $\beta$ -keto hydroxamic acids. The cyclization of **45a-o** proceeded in high yields even when the acid equivalents were reduced to half of what is reported in the literature (Table 2.5).<sup>25</sup>

**Table 2.5:** Isolated yields of 5-substituted isoxazol-3-ols **46**.



Entry	R <sup>1</sup>	<sup>a</sup> Product Yield (%)	Entry	R <sup>1</sup>	<sup>a</sup> Product Yield (%)
<b>46a</b>		75	<b>46i</b>		81
<b>46b</b>		83	<b>46j</b>		40
<b>46c</b>		47	<b>46k</b>		66
<b>46d</b>		77	<b>46l</b>		68
<b>46e</b>		61	<b>46m</b>		74
<b>46f</b>		77	<b>46n</b>		92
<b>46g</b>		70	<b>46o</b>		77
<b>46h</b>		75			

<sup>a</sup>Isolated yields of the products.

Further, isoxazol-3-ols were characterized using <sup>1</sup>H NMR, <sup>13</sup>C NMR, and IR. According to the reported literature, isoxazol-3-ols exists predominately in the OH-form in non-polar solvents, whereas the contribution from the NH-form increases in polar solvents (Figure 2.7).<sup>37</sup> In CDCl<sub>3</sub>, we observed only the OH-form, which was confirmed by an X-ray analysis (Figure 2.8).

### Tautomerism of isoxazol-3-ols

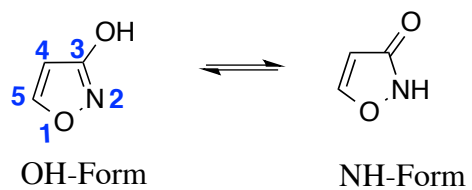


**Figure 2.7:** Tautomeric representation of isoxazol-3-ols.<sup>38</sup>

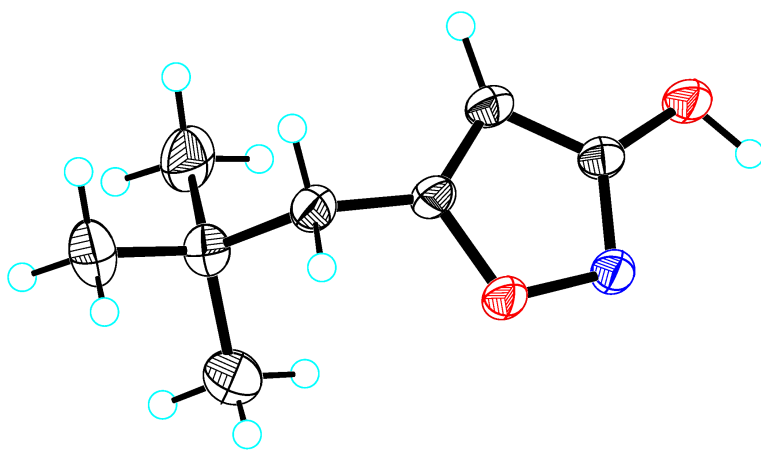


**Figure 2.8:** Anisotropic displacement ellipsoid drawings (50%) of X-ray structure of compound 46m. X-ray structure provided by Dr. Carla Slebodnick (Department of Chemistry, Virginia Tech).

The final products, 5-substituted 3-oxoisoxazole-2(3*H*)-carboxamides and isoxazol-3-yl dimethylcarbamates, were obtained regioselectively through judicious use of two different protocols. The reaction of isoxazol-3-ols **46** with dimethyl carbamoyl chloride under neutral conditions gave dimethylcarboxamides **47** as the major product, and isoxazol-3-yl dimethylcarbamate **48** as the minor product (Scheme 2.6). Compounds **47p** and **48p** were prepared from commercially available methyl 3-hydroxyisoxazol-5-carboxylate (**46p**) using the above-mentioned protocol. Under neutral conditions, the more nucleophilic ring nitrogen attacks

the carbonyl carbon of carbamoyl chloride forming dimethylcarboxamides as the major product. However, in the presence of the base  $\text{KO}t\text{-Bu}$ , **46** gave isoxazol-3-yl dimethylcarbamate **48** as the major product, with dimethylcarboxamides **47** formed in 5-16% yield (Table 2.6).

**Scheme 2.6:** Regioselective synthesis of 5-substituted 3-oxoisoxazole-2(*3H*)-carboxamide **47**, and isoxazol-3-yl dimethylcarbamates **48**.

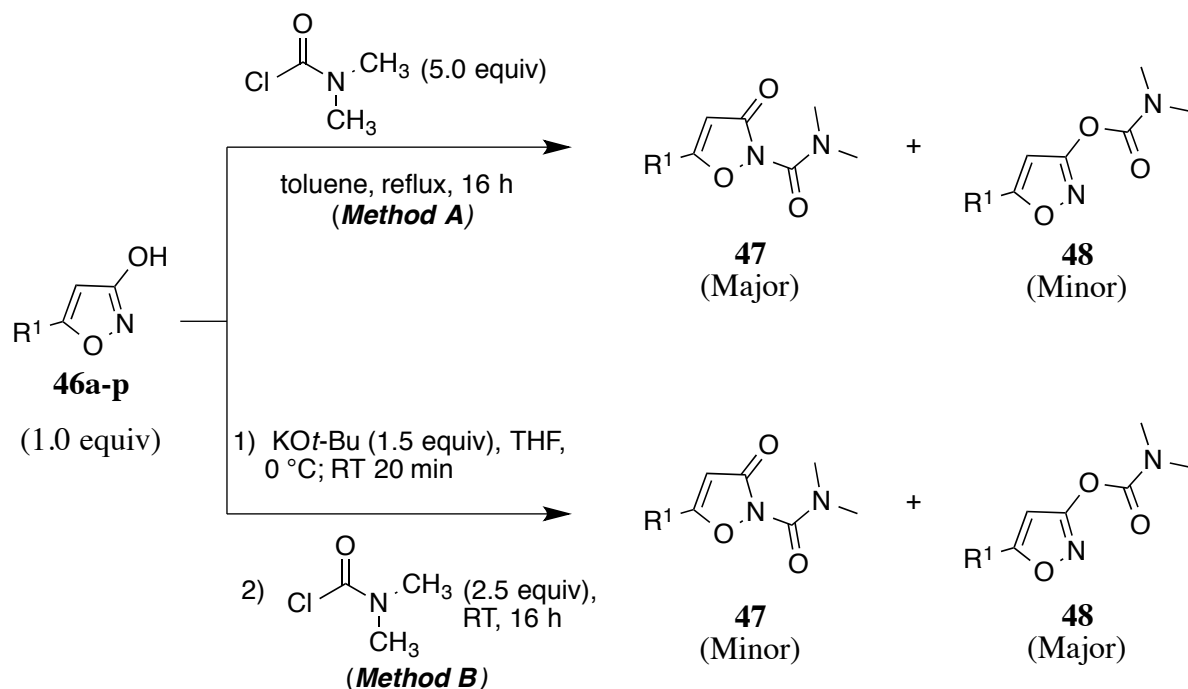


**Table 2.6:** Isolated yields of 5-substituted 3-oxoisoxazole-2(*3H*)-carboxamide **47**, and isoxazol-3-yl dimethylcarbamates **48**.

Entry	$\text{R}^1$	% <sup>a</sup> Yield of <b>47</b>	% <sup>a</sup> Yield of <b>48</b>	% <sup>a</sup> Yield of <b>47</b>	% <sup>a</sup> Yield of <b>48</b>
		Method A		Method B	
<b>a</b>		84	14	15	75
<b>b</b>		ND	ND	ND	ND

<b>c</b>		14	78	10	ND
<b>d</b>		61	21	9	80
<b>e</b>		79	20	5	89
<b>f</b>		73	17	12	82
<b>g</b>		67	29	8	82
<b>h</b>		78	11	16	84
<b>i</b>		81	14	12	83
<b>j</b>		ND	ND	ND	61
<b>k</b>		54	39	12	66
<b>l</b>		46	24	10	82
<b>m</b>		81	14	12	71
<b>n</b>		71	20	9	80
<b>o</b>		79	16	8	90
<b>p</b>	COOCH <sub>3</sub>	56	38	ND	ND

<sup>a</sup>Isolated yields of product.

Unexpectedly, reaction of **46** with methylcarbamoyl chloride under basic conditions gave methylcarboxamides **49** with no trace of the corresponding methylcarbamates (Scheme 2.7). It is

possible that hydrogen bonding between the carbamate NH and the isoxazol-3(*2H*)-one carbonyl in **49** renders the methylcarboxamides considerably more stable than the methylcarbamates. If that were the case, the methylcarbamates initially formed under basic conditions could undergo O->N carbamoyl transfer to yield the observed methylcarboxamides. In fact, we noted that methylcarboxamides **49** were themselves unstable in aqueous buffer (pH 7.7) over 30 minutes; it is therefore possible that any traces of methylcarbamate present in the reaction mixture would be even more unstable and decomposed during aqueous workup (Scheme 2.7).

**Scheme 2.7:** Synthesis of 5-substituted 3-oxoisoxazole-2(3*H*)-carboxamide **49**.

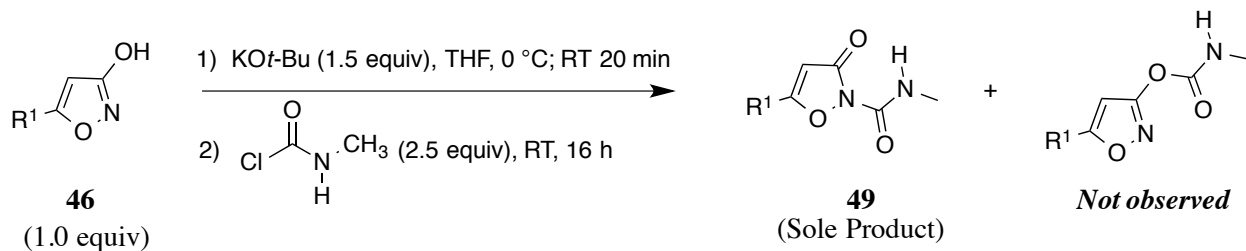


**Table 2.7:** Isolated yields of 5-substituted-*N*-methyl-3-oxoisoxazole-2(3*H*)-carboxamide **49**.

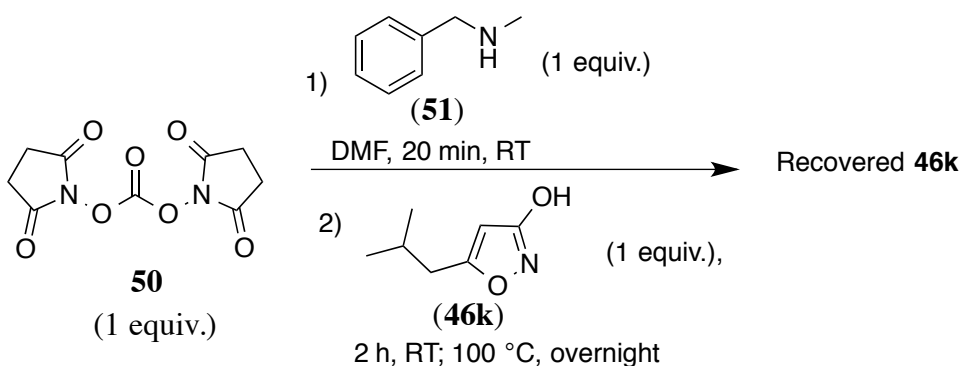
Entry	$\text{R}^1$	<sup>a</sup> Product Yield <b>49</b> (%)	Entry	$\text{R}^1$	<sup>a</sup> Product Yield <b>49</b> (%)
<b>49a</b>		76	<b>49i</b>		ND
<b>49b</b>		72	<b>49j</b>		66
<b>49c</b>		61	<b>49k</b>		90
<b>49d</b>		70	<b>49l</b>		90
<b>49e</b>		ND	<b>49m</b>		50
<b>49f</b>		97	<b>49n</b>		87
<b>49g</b>		90	<b>49o</b>		ND
<b>49h</b>		57			

<sup>a</sup> Isolated yields of the products.

To probe the effect of *N*-substituent on the mosquitocidal and enzyme inhibition activities, various *N*-substituted derivatives of 5-(pentan-2-yl)-*N,N*-dimethyl-3-oxoisoxazole-2(3*H*)-

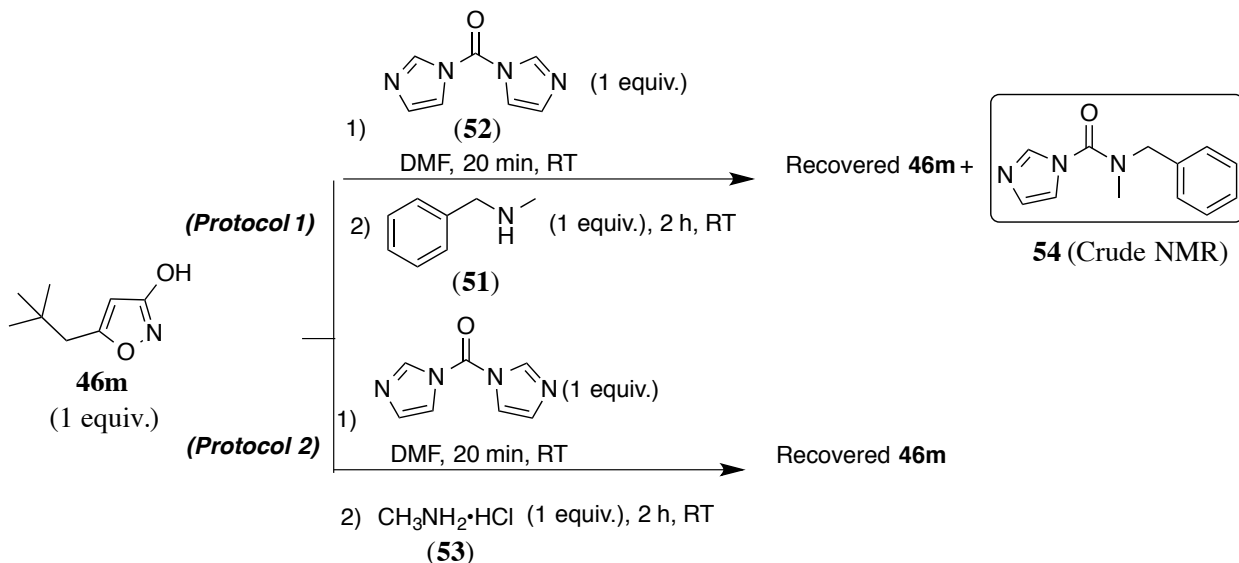
carboxamide and 5-(pentan-2-yl)isoxazol-3-yl dimethylcarbamates were synthesized. Earlier studies on substitution at carbamate nitrogen in aryl carbamates have suggested that the activity drops with the increase in the size of the *N*-substituent.<sup>8</sup> For example, precedents have demonstrated that the aryl methylcarbamates showed greater activity as compared to dimethyl version of the aryl carbamate.<sup>8, 39</sup> However, since these five membered heterocycles have a smaller core structure as compared to the aryl carbamates, and also the carboxamide structure represents a significant departure from the carbamate structure, we hoped that the extra bulk on the *N*-substituent could be tolerated in the active site of the mutated enzyme.

Due to limited commercial availability of the desired carbamoyl chlorides, we explored other routes to install the desired *N*-substituent. A quick search of the literature revealed that phosgene has been a popular choice for the synthesis of variety of carbamates, and ureas.<sup>40</sup> However, due to its high toxicity, and handling difficulties, we decided to use phosgene substitutes. We started a trial reaction with readily available 5-isobutylisoxazol-3-ol (**46k**), and disuccinimidyl carbonate (**50**). To 1 equiv. of disuccinimidyl carbonate (**50**) in DMF was added methyl benzyl amine (**51**) at RT, and the reaction mixture was allowed to stir for 20 minutes. To this reaction mixture was added **46k** in situ, and the reaction was monitored for 2 h. A TLC analysis after two hours showed the unconsumed **46k**. Heating the reaction mixture overnight at 100 °C did not help, and the starting material was recovered the next day (Scheme 2.8).



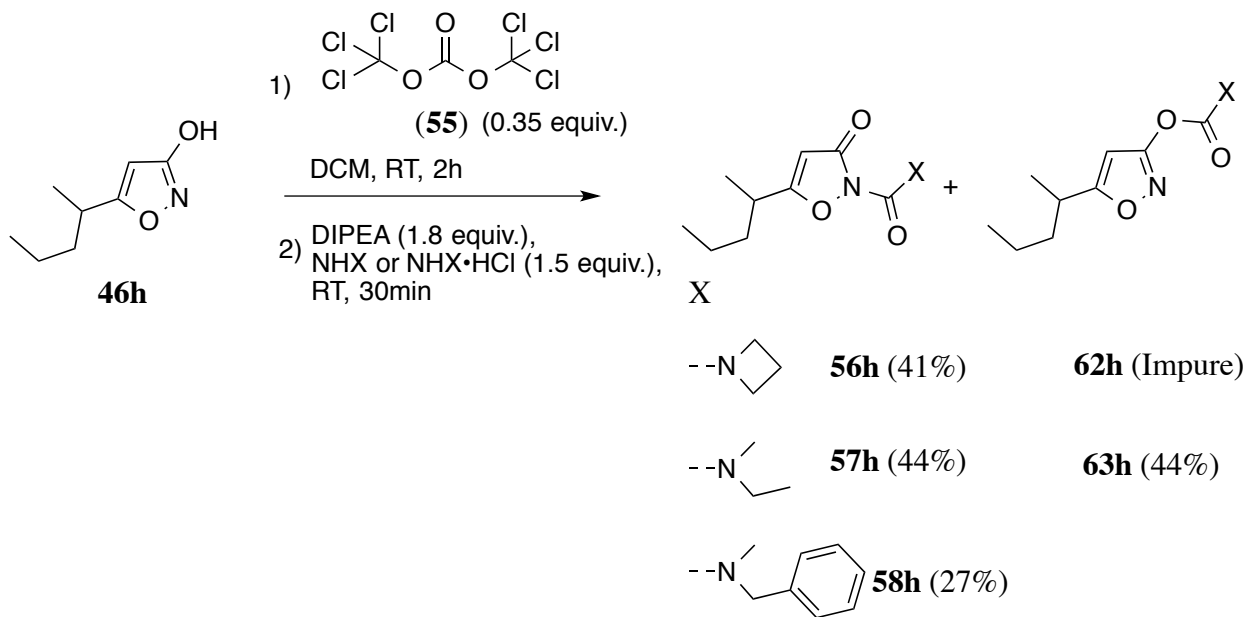
**Scheme 2.8:** Attempted synthesis of *N*-benzyl-*N*-methyl-3-oxo-5-(pentan-2-yl)isoxazole-2(3*H*)-carboxamide and 5-(pentan-2-yl)isoxazol-3-yl benzyl(methyl)carbamate using disuccinimidyl carbonate (**50**) as a carbonylating agent.

We have successfully exploited carbonyl diimidazole (CDI) as a carbonylating agent in the synthesis of pyrazol-4-yl methylcarbamates (Chapter 3). This prompted us to explore its potential in the synthesis of *N*-substituted 3-oxoisoxazole-2(3*H*)-carboxamide and isoxazol-3-yl carbamates; also considering the fact that it is a better carbonylating agent as compared to disuccinimidyl carbonate (**50**). Moreover, literature precedents have demonstrated that CDI reacts with amines to give amine adduct (*N*-substituted 1*H*-imidazole-1-carbonyl) that can undergo subsequent reaction with alcohols, and amines to yield carbamates, and ureas respectively.<sup>41</sup> However, as shown in Scheme 2.9 from both the trial reactions, we recovered the starting material **46m**. Further, a quick column of *Protocol 1* (Scheme 2.9) to remove **46m**, followed by NMR analysis of the remaining reaction mixture showed the presence of an adduct **54** (*N*-benzyl-*N*-methyl-1*H*-imidazole-1-carboxamide). It is possible that once **54** is formed, it does not react further. Substituting a secondary amine **51** by a primary amine salt **53** did not change the outcome of the reaction (Scheme 2.9).



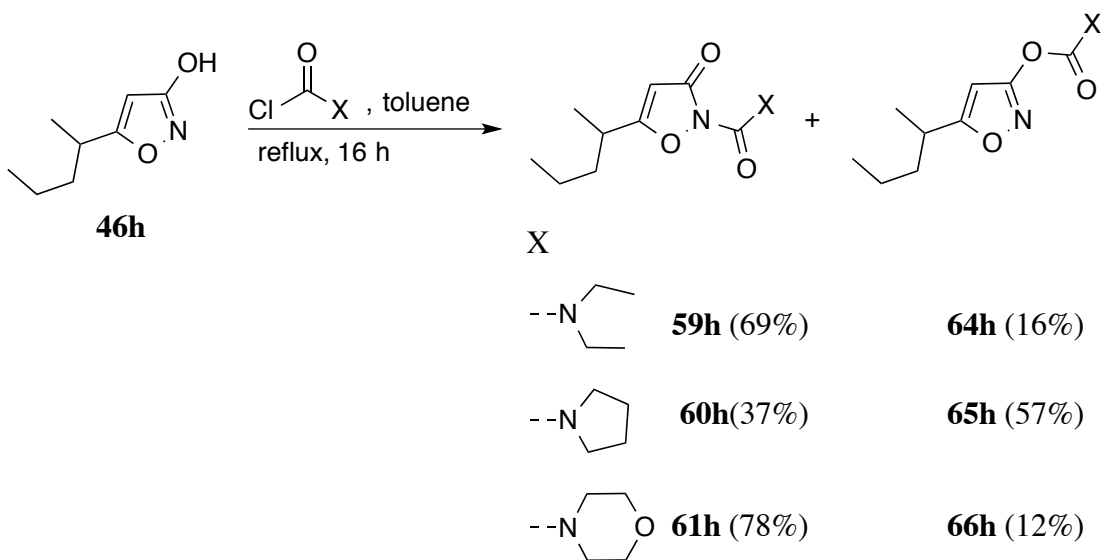
**Scheme 2.9:** Attempted synthesis of *N*-substituted-5-neopentyl-3-oxoisoxazole-2(3*H*)-carboxamide, and 5-neopentylisoxazol-3-yl-*N*-substituted carbamate using carbonyl diimidazole (**52**) as a carbonylating agent.

Finally, we were successful in synthesizing the desired compounds (**56h-58h**) in low to moderate yields by reacting isoxazol-3-ols with triphosgene (**55**) as the phosgene equivalent, and subsequent reaction of the intermediate with corresponding amine hydrogen chloride salt (in the presence of a tertiary amine) or amine. In the case of **56h**, the low yield is attributed to the low solubility of azetidine hydrogen chloride salt even in the presence of excess base (Scheme 2.10). Compound **62h** was obtained in low yield from the same reaction mixture but could not be purified and hence was not assayed.



**Scheme 2.10:** Synthesis of 5-(2-pentyl)-*N*-substituted-3-oxoisoxazole-2(3*H*)-carboxamide, and 5-(2-pentyl)-isoxazol-3-yl-*N*-substituted carbamate using triphosgene.

Compound **59h**, **60h**, and **61h** were synthesized by refluxing **46h** with corresponding carbamoyl chloride in toluene; the corresponding dimethylcarbamates **64h**, **65h**, and **66h**, were obtained in the same reactions (Scheme 2.11). As expected, carboxamides predominated under neutral conditions, except in the case of **60h** and **65h**, where the carbamate **65h** was obtained as the major product.



**Scheme 2.11:** Synthesis of 5-(2-pentyl)-*N*-substituted-3-oxoisoxazole-2(3*H*)-carboxamide and - (2-pentyl)-isoxazol-3-yl-*N*-substituted carbamate from commercially available carbamoyl chlorides.

## 2.5 Characterization of the 3-oxoisoxazole-2(3*H*)-carboxamide and isoxazol-3-yl carbamates

The final products were characterized and identified using  $^1\text{H}$  and  $^{13}\text{C}$  NMR, mass spectroscopy, and X-ray diffraction. Assignment of the carboxamide and carbamate structure was made in the following way. As illustrated in Figure 2.9, dimethylcarboxamides (e.g. **47a**) show a broad singlet for the *N*-Me protons in the  $^1\text{H}$  NMR spectrum, whereas dimethylcarbamates (e.g. **48a**) show two well-resolved singlets for these protons. The barrier to rotation of the C(O)-N bond in analogous urea-type dimethylcarboxamide analogues ranges from 8-13 kcal/mol, whereas in dimethylcarbamates it is higher, typically  $\sim$ 16 kcal/mol.<sup>42-43</sup> The lower barrier to rotation in urea-type carboxamides is due to reduced double bond character of the C(O)--N(CH<sub>3</sub>)<sub>2</sub> bond. Similar behavior is seen in the  $^{13}\text{C}$  NMR spectra of these compounds (Figure 2.9B), where the *N*-Me carbons of **47a** appear as broad signals, and the *N*-Me carbons of **48a** appear as two sharp resonances. Note as well that the  $^1\text{H}$  and  $^{13}\text{C}$  NMR behavior of the *N*-

methyl groups in isoxazol-3-yl carbamate **48a** corresponds well with the aryl dimethylcarbamate **67** previously synthesized and characterized in our group (Figure 2.9A, B).

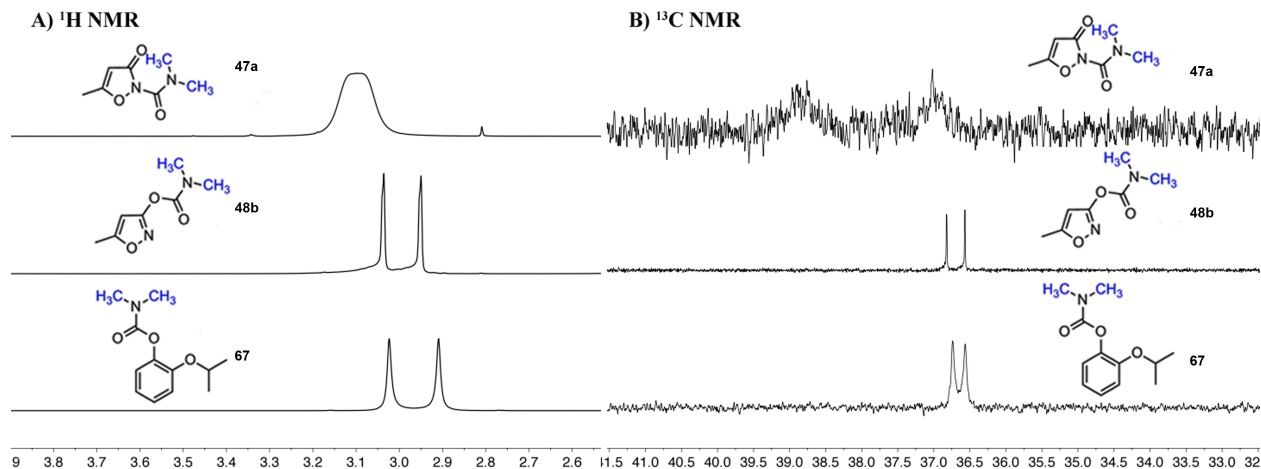


**Figure 2.9:** A) <sup>1</sup>H NMR of dimethylcarboxamide (**47a**), dimethylcarbamate (**48a**), and 2-isopropoxyphenyl dimethylcarbamate (**67**). B) <sup>13</sup>C NMR of dimethylcarboxamide (**47a**), dimethylcarbamate (**48a**), and 2-isopropoxyphenyl dimethylcarbamate (**67**).

Another characteristic difference between carboxamides (both methyl- and dimethyl), and dimethylcarbamates was seen in <sup>1</sup>H NMR chemical shifts of H-4. This proton appeared between 5.27 ppm and 5.58 ppm for carboxamides (both methyl- and dimethyl), whereas for isoxazol-3-yl dimethylcarbamates it appeared in the range 6.07 - 6.17 ppm (Figure 2.10). To correlate this chemical shift difference to structure we note that the H-4 chemical shift of dimethylcarboxamide **47k** is very similar to that of methylcarboxamide **49k**.

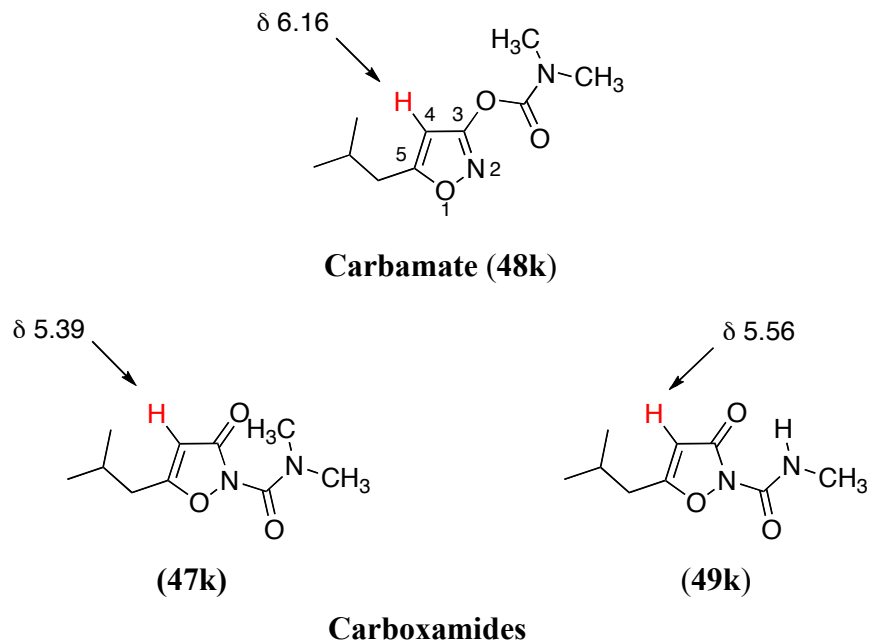


**Figure 2.10:** Characteristic chemical shift differences of H-4 in carboxamides and carbamates, as illustrated by **47k**, **49k**, and **48k**, respectively.

The identity of **49k** as a methylcarboxamide (and not a methylcarbamate), and **47e** as a dimethylcarboxamide (and not a dimethylcarbamate) was confirmed by X-ray crystallography (Figure 2.11 and 2.12, respectively).

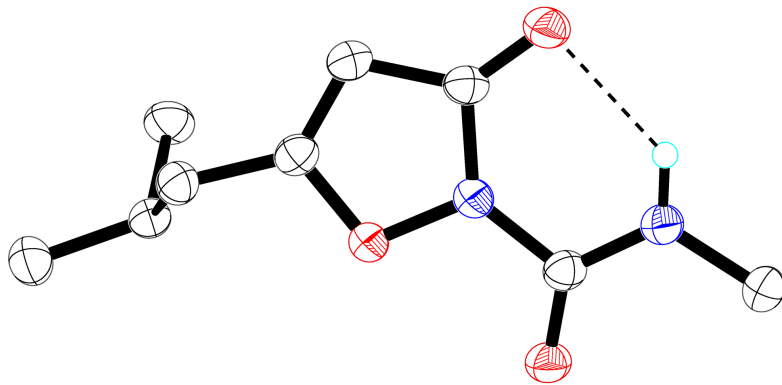


**Figure 2.11:** Anisotropic displacement ellipsoid drawings (50%) of X-ray structure of compound **49k**. Hydrogen atoms were omitted for clarity, except at the exocyclic *N*. Hydrogen bond is shown in dotted black line (H-bond distance 2.11 Å). X-ray structure provided by Dr. Carla Slebodnick (Department of Chemistry, Virginia Tech).

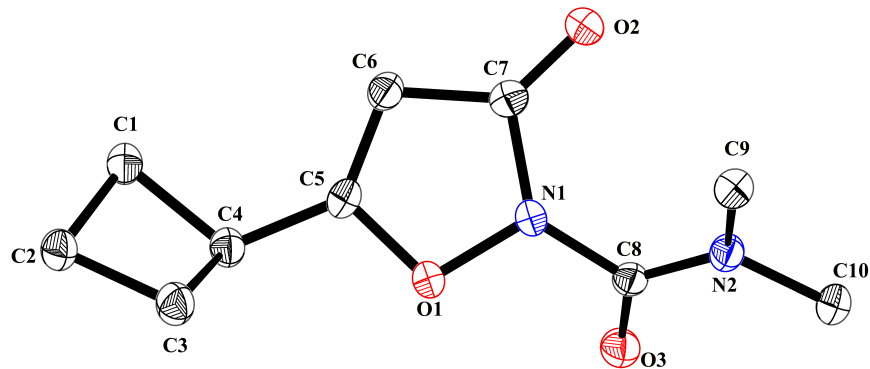


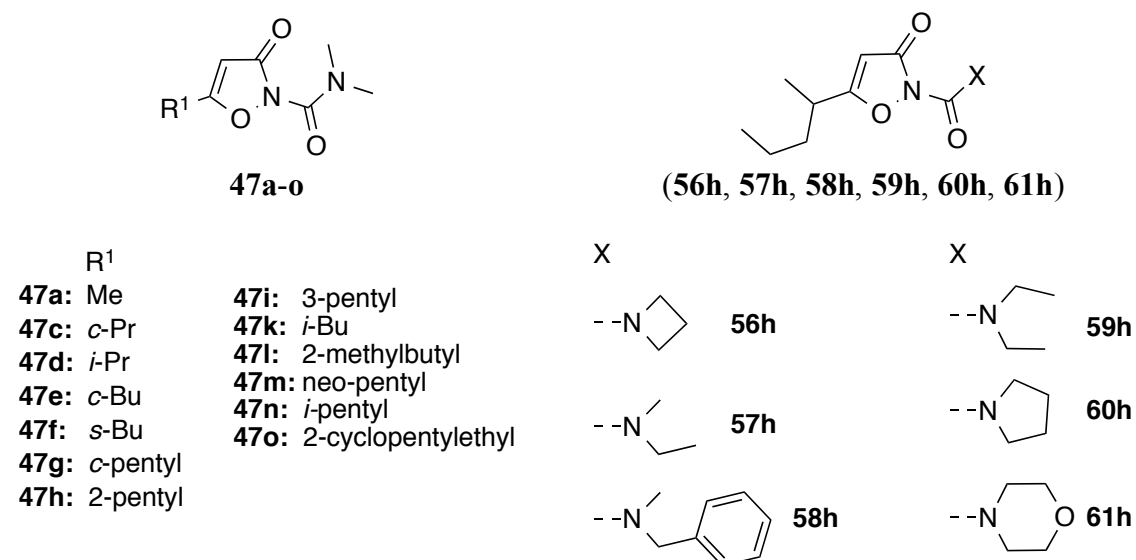
**Figure 2.12:** Anisotropic displacement ellipsoid drawings (50%) of X-ray structure of compound **47e**. Hydrogen atoms were omitted for clarity. The amide carbonyl group ( $\text{C}_8\text{-O}_3$ ) and  $\text{N}\text{-CH}_3$  ( $\text{N}_2\text{-C}_{10}$ ) are nearly planar with a dihedral angle of  $4.7^\circ$  ( $\text{C}_{10}\text{-N}_2\text{-C}_8\text{-O}_3$ ). However, the carbonyl (defined by the plane  $\text{N}_1\text{-C}_8\text{-O}_3$ ) is twisted out of the plane of the isoxazole ring (defined by  $\text{N}_1\text{-C}_7\text{-O}_2$ ), and forms a dihedral angle of  $52.4^\circ$ . X-ray structure provided by Dr. Carla Slebodnick (Department of Chemistry, Virginia Tech).

## 2.6 Tarsal contact toxicity of 3-oxoisoxazole-2(3H)-carboxamides and isoxazol-3-yl carbamates

Contact toxicity is a critical property for any insecticide that might be deployed on ITNs. Also, with the rising resistance against current anticholinesterase insecticides, there is an urgent need for an insecticide that is potent towards both susceptible and resistant strain mosquitoes. Tarsal contact toxicity was determined towards G3 (WT, susceptible) and Akron (G119S, carbamate-resistant) strain *An. gambiae*, using the standard WHO filter paper protocol (Section 2.2.1).<sup>1</sup> As reported previously, the LC<sub>50</sub> values for commercial carbamates **8**, **9**, **27**, **28** bearing a phenyl core fell between 16-42 µg/mL for the susceptible G3 strain of *An. gambiae*; however, these compounds were not toxic towards the resistant Akron strain even when treated at concentrations up to 5,000 µg/mL (Table 2.2). An important exception to the above-mentioned commercial insecticides was aldicarb, which showed high contact toxicity towards both G3 and Akron strain *An. gambiae*, and low toxicological cross-resistance (LC<sub>50</sub> = 70 and 32 µg/mL, respectively). We were thus interested to learn whether the isoxazole core could also confer high toxicity to Akron strain *An. gambiae*. As noted above, isoxazol-3-yl methylcarbamates could not be isolated, and methylcarboxamides **49** proved unstable in aqueous buffer. Therefore, our investigations focused on dimethylcarboxamides **47**, and dimethylcarbamates **48**. The carboxamide structure obviously represents a significant departure from the structure of aryl and pyrazole carbamates that we previously studied. Furthermore, the impact of dimethylcarbamate vs methylcarbamate structure on toxicity and enzyme inhibition was also unknown. But the nature of branching of the alkyl substituent is known to affect *An. gambiae* vs human AChE inhibition selectivity,<sup>6</sup> and mosquito toxicity<sup>6-7</sup>; thus we explored compounds bearing unbranched (**47a**, **48a**), α-branched (**47c-j**, **48c-j**), β-branched (**47k-m**, **48k-m**), and γ-branched

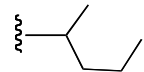
(**47n-o**, **48n-o**) substituents. Note that compounds that did not show appreciable toxicity to susceptible G3 strain (100 % at 1000 µg/mL) were not tested on the resistant Akron strain. Further, based on the LC<sub>50</sub>, the compounds were classified as having excellent toxicity (LC<sub>50</sub> < 100 µg/mL), good toxicity (LC<sub>50</sub> = 100-199 µg/mL), moderate toxicity (LC<sub>50</sub> = 200-399 µg/mL), and poor toxicity (LC<sub>50</sub> > 400 µg/mL).

**Table 2.8:** Tarsal contact toxicity of 5-substituted *N,N*-dialkyl-3-oxoisoxazole-2(3*H*)-carboxamides to G3 and Akron strain of *An. gambiae*.



R <sup>1</sup>	Compound	<i>An. gambiae</i> G3		<i>An. gambiae</i> Akron	<sup>b</sup> Resistance ratio (RR)
		<sup>a</sup> LC <sub>50</sub> µg/mL (95% CI)	<sup>a</sup> LC <sub>50</sub> µg/mL (95% CI)		
—	<b>47a</b>	0 % @ 1,000 µg/mL		ND	-
—>	<b>47c</b>	278 (225-345)		10 % @ 1,000 µg/mL	-

	<b>47d</b>	316 (22-428)	182 (138-253)	0.6
	<b>47e</b>	79 (57-116)	74 (55-105)	0.9
	<b>47f</b>	63 (49-81)	129 (91-196)	2.0
	<b>47g</b>	105 (78-157)	118 (89-171)	1.1
	<b>47h</b>	153 (109-211)	75 (53-111)	0.5
	<b>47i</b>	38 (28-53)	40 (31-54)	1.1
	<b>47k</b>	201 (145-284)	25 % @ 200 µg/mL	-
	<b>47l</b>	0 % @ 1,000 µg/mL	ND	-
	<b>47m</b>	80 % @ 1,000 µg/mL	ND	-
	<b>47n</b>	73 (58-93)	68 (54-87)	0.9
	<b>47o</b>	0 % @ 1,000 µg/mL	ND	-
COOCH <sub>3</sub>	<b>47p</b>	20 % @ 1,000 µg/mL	ND	-
<hr/>				
	<b>56g</b>	78 % @ 1,000 µg/mL	ND	-
	<b>57g</b>	400 (320-483)	614 (537-684)	1.5
	<b>58g</b>	0 % @ 1,000 µg/mL	ND	-
	<b>59g</b>	15 % @ 1,000 µg/mL	ND	-
	<b>60g</b>	77 % @ 1,000 µg/mL	ND	-

**61g**

45 % @ 1,000 µg/mL

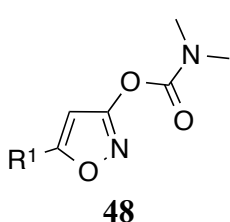
ND

-

<sup>a</sup>Mosquitoes were exposed (1 h) to dried filter papers previously treated with ethanolic solutions of carbamates; mortality was recorded after 24 h. LC<sub>50</sub> values derived from the concentrations of inhibitor used to treat the paper and were reported previously.<sup>6</sup> <sup>b</sup>Defined by LC<sub>50</sub> (Akron)/LC<sub>50</sub> (G3).

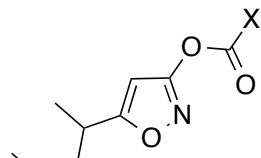
Compound **47a** did not show any contact toxicity at the highest concentration tested (1000 µg/mL, Table 2.8), perhaps as a consequence of low lipophilicity. However,  $\alpha$ -branched dimethylcarboxamides (**47c-i**) showed appreciable toxicities towards G3 and Akron strain (Table 2.8). Compound **47c** ( $R^1 = c\text{-Pr}$ ) showed moderate toxicity towards G3 strain, but was considerably less toxic against Akron strain. The open-chain analogs carboxamide **47d** ( $R^1 = i\text{-Pr}$ ), and **47h** ( $R^1 = 2\text{-pentyl}$ ) showed moderate and good G3 toxicity respectively, and were even more toxic to the Akron strain. The compounds with greatest G3 toxicity in the  $\alpha$ -branched series were **47f** ( $LC_{50} = 63 \mu\text{g/mL}$ ) and **47i** ( $LC_{50} = 38 \mu\text{g/mL}$ ), and they showed good and excellent Akron toxicity respectively. Amongst the  $\beta$ -branched dimethylcarboxamides explored (**47k-m**), only **47k** ( $R^1 = i\text{-Bu}$ ) showed moderate or better G3 toxicity, but Akron toxicity was lower. Among the  $\gamma$ -branched compounds explored (**47n-o**) carboxamide **47n** ( $R^1 = i\text{-pentyl}$ ) was the most toxic and showed almost equivalent LC<sub>50</sub> values towards G3 and Akron strain. Finally, a range of compounds (**56h-61h**) were examined to assess the effect of varying the substitution on the exocyclic nitrogen. Only **57h** (ethylmethylcarboxamide) showed appreciable toxicity to G3 strain, and it was 2-3 fold less toxic than the dimethylcarboxamide **47h**. These data may suggest that the *N*-substituent of **56h-61h** is too big to inhibit *AgAChE* well, and we address this point below. The low toxicity of azetidine carboxamide **56h** relative to dimethylcarboxamide **47h** may be due to instability of the azetidine ring.

**Table 2.9:** Tarsal contact toxicity of 5-substituted isoxazol-3-yl dialkylcarbamates to G3 and Akron strain of *An. gambiae*.



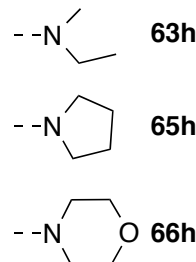
R<sup>1</sup>

- |                      |                                |
|----------------------|--------------------------------|
| <b>48a:</b> Me       | <b>48i:</b> 3-pentyl           |
| <b>48c:</b> c-Pr     | <b>48j:</b> 3-heptyl           |
| <b>48d:</b> i-Pr     | <b>48k:</b> i-Bu               |
| <b>48e:</b> c-Bu     | <b>48l:</b> 2-methylbutyl      |
| <b>48f:</b> s-Bu     | <b>48m:</b> neo-pentyl         |
| <b>48g:</b> c-pentyl | <b>48n:</b> i-pentyl           |
| <b>48h:</b> 2-pentyl | <b>48o:</b> 2-cyclopentylethyl |



(**63h, 65h, 66h**)

X



R <sup>1</sup>	Compound	An gambiae G3	An gambiae Akron	<sup>b</sup> Resistance ratio
		<sup>a</sup> LC <sub>50</sub> μg/mL (95% CI)	<sup>a</sup> LC <sub>50</sub> μg/mL (95% CI)	
—	<b>48a</b>	0 % @ 1000 μg/mL	ND	-
—Cyclopropyl	<b>48c</b>	0 % @ 1000 μg/mL	ND	-
—Isobutyl	<b>48d</b>	84 (30-124)	116 (79-151)	1.4
—Cyclobutyl	<b>48e</b>	349 (266-456)	392 (281-593)	1.1
—Isopentyl	<b>48f</b>	41 (28-58)	58 (42-92)	1.4
—Cyclopentyl	<b>48g</b>	60 % @ 1000 μg/mL	ND	-
—Isohexyl	<b>48h</b>	234 (163-307)	296 (210-381)	1.3

	<b>48i</b>	70 % @ 1000 µg/mL	ND	-
	<b>48j</b>	0 % @ 1000 µg/mL	ND	-
	<b>48k</b>	253 (184-367)	151 (112-211)	0.6
	<b>48l</b>	30 % @ 1,000 µg/mL	ND	-
	<b>48m</b>	0% @ 1,000 µg/mL	ND	-
	<b>48n</b>	415 (306-582)	429 (331-563)	1.0
	<b>48o</b>	674 (575-715)	ND	-
COOCH <sub>3</sub>	<b>48p</b>	50% @ 1,000 µg/mL	ND	-
	<b>63h</b>	410 (304-590)	574 (513-633)	1.4
	<b>65h</b>	0% @ 1,000 µg/mL	ND	-
	<b>66h</b>	10% @ 1,000 µg/mL	ND	-

<sup>a</sup>Mosquitoes were exposed (1 h) to dried filter papers previously treated with ethanolic solutions of carbamates; mortality was recorded after 24 h. LC<sub>50</sub> values derived from the concentrations of inhibitor used to treat the paper and were reported previously.<sup>6</sup> <sup>b</sup>Defined by LC<sub>50</sub> (Akron)/LC<sub>50</sub> (G3).

Turning to the corresponding dimethylcarbamates, **48a** bearing a C5-methyl group was not toxic to G3 strain at the highest concentration tested. In contrast,  $\alpha$ -branched analogs **48c-j** displayed G3 toxicities ranging from excellent (**48d, f**) to poor (**48c, g, i, j**, Table 2.9). Compounds **48d** ( $R^1 = i\text{-Pr}$ ) and **48f** ( $R^1 = s\text{-Bu}$ ) also demonstrated good and excellent toxicities

towards Akron strain *An. gambiae*, respectively. One interesting trend is that open-chain analogs typically show greater G3 toxicity than their cyclic analogs (cf. **48d** vs **48c**, **48f** vs **48e**, and **48h** vs **48g**). Finally **48j** ( $R^1 = 3$ -heptyl) was not toxic to G3 strain at the highest concentration tested (1000  $\mu$ g/mL).

Amongst the  $\beta$ -branched dimethylcarbamates examined (**48k-m**), only **48k** with an *i*-butyl side chain proved moderately toxic towards G3. Interestingly this compound proved even more toxic to Akron strain than it was to G3 (cf.  $LC_{50} = 151$  and 253  $\mu$ g/mL respectively). Amongst  $\gamma$ -branched compounds, **48n** and **48o** exhibited low toxicity towards both strains of *An. gambiae*. Finally, as was seen for the carboxamides, variation of the *N*-substituent reduced toxicity. Only **63h** (ethylmethylcarbamate) showed appreciable toxicity to G3 strain, but had reduced toxicity for Akron strain. Compound **65h** (pyrrolidinylcarbamate), and **66h** (morpholinocarbamate) did not show any toxicity to G3 strain *An. gambiae*.

Looking at both the series, three conclusions can be drawn. First, for a given C5-substituent, there is no general trend for dimethylcarboxamide vs dimethylcarbamate toxicity. In some cases, the dimethylcarboxamide is more toxic (**47 (c, e, g, h, i, k, m, n)**), and in others **48 (d, f, i, o)** the dimethylcarbamate is more toxic. Second, among the exocyclic *N*-substituents explored, dimethyl proved optimum, though ethylmethyl analogs **57h** and **63h** did show significant toxicity. Third, both in the  $\alpha$ - and  $\gamma$ -branched series, excellent G3 toxicity and low cross-resistance can be attained.

We have briefly touched on cross-resistance topic in Section 2.3. An insect population can be called resistant when it can tolerate doses of insecticide that can kill (98-100%) of the susceptible population.<sup>14, 44</sup> Further, cross-resistance arises when an insect population shows resistance towards another insecticide that it has never encountered before.<sup>13</sup> This can happen

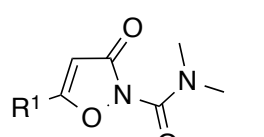
when the two insecticides share the same mode of action. Cross-resistance can be measured in terms of resistance ratio (RR), which defined as the ratio of the LC<sub>50</sub> of the resistant strain (Akron) to that of the LC<sub>50</sub> of the susceptible strain (G3).<sup>13</sup> Interestingly, unlike commercial aryl methylcarbamates that showed high (>130) toxicological cross-resistance ratio, the RR for dimethylcarboxamides and dimethylcarbamates was low. This was unexpected since they all belong to the same class of AChE inhibitors. However, this type of increased susceptibility of resistant population<sup>45</sup> is not unprecedented. Dunley et al. reported increased susceptibility of azinphosmethyl-resistant codling moth towards chlorpyrifos, and methyl-parathion, in spite of the fact that all these insecticide share the same mode of action i.e. AChE inhibition.<sup>46</sup> Moreover, for the toxic isoxazol-3-yl carboxamides and carbamates the RR was never greater than 2. According to Valles et al., an insect strain is resistant if the resistance ratio is >10.<sup>47</sup> However, based on the bioassays on German cockroaches (*Blattella germanica L.*), and house fly (*Musca domestica L.*) Scott and Wen suggested that an insect can be considered as cross-resistant if it exhibits resistance ratio >4.<sup>48</sup> However, there is no clear consensus on the exact RR needed to call a population resistant. Thus the low cross-resistance property of these isoxazole-3-yl AChE inhibitors would certainly be favorable for a new anticholinesterase-based mosquitocide.

## **2.7 Enzyme inhibition by 3-oxoisoxazole-2(3H)-carboxamides and isoxazol-3-yl carbamates**

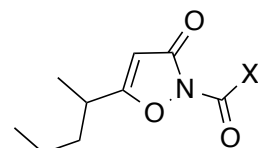
As expected from the high toxicological resistance ratios, the commercial aryl carbamates **8, 9, 27, 28** inhibited the susceptible enzyme (WT AChE) very rapidly as compared to the resistant enzyme (G119S AChE). The resistance ratio numbers were greater than 3800-fold. In contrast, the enzymatic resistance ratio for aldicarb (**29**) was only 4.2-fold, which correlates well with its low toxicological cross-resistance. On the basis of low toxicological cross-resistance seen for many dimethylcarbamates and dimethylcarboxamides (Tables 2.8 and 2.9), we predicted

low enzymatic resistance ratios. As will be seen below, this expectation was only partially realized. The  $k_i$  data for dimethylcarboxamides (**47a-i, k-o**), and derivatives of **47h** are summarized in Table 2.10.

**Table 2.10:** Inactivation rate constants  $k_i$  of 5-substituted *N,N*-dialkyl-3-oxoisoxazole-2(3*H*)-carboxamides for rAgAChE (WT and G119S), & rhAChE.



**47a-o**



(**56h, 57h, 58h, 59h, 60h, 61h**)

$R^1$	
<b>47a:</b> Me	<b>47i:</b> 3-pentyl
<b>47c:</b> <i>c</i> -Pr	<b>47k:</b> <i>i</i> -Bu
<b>47d:</b> <i>i</i> -Pr	<b>47l:</b> 2-methylbutyl
<b>47e:</b> <i>c</i> -Bu	<b>47m:</b> neo-pentyl
<b>47f:</b> <i>s</i> -Bu	<b>47n:</b> <i>i</i> -pentyl
<b>47g:</b> <i>c</i> -pentyl	<b>47o:</b> 2-cyclopentylethyl
<b>47h:</b> 2-pentyl	

**47i**

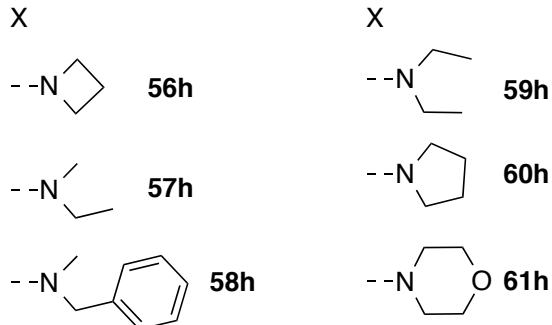
**47k**

**47l**

**47m**

**47n**

**47o**



Compound	<sup>a</sup> <i>Ag</i> AChE $k_i$ ( $\text{mM}^{-1} \text{min}^{-1}$ )	<sup>a</sup> G119S $k_i$ ( $\text{mM}^{-1} \text{min}^{-1}$ )	<sup>a</sup> hAChE $k_i$ ( $\text{mM}^{-1} \text{min}^{-1}$ )	<sup>b</sup> WT/G119S Resistance ratio	<sup>c</sup> <i>Ag/h</i> selectivity
<b>47a</b>	$0.46 \pm 0.04$	$0.098 \pm 0.029$	$1.22 \pm 0.04$	$4.7 \pm 1.4$	$0.37 \pm 0.03$
<b>47c</b>	$50.5 \pm 1.4$	$0.20 \pm 0.03$	$103 \pm 5$	$250 \pm 30$	$0.49 \pm 0.02$
<b>47d</b>	$500 \pm 10$	$1.85 \pm 0.09$	$561 \pm 21$	$270 \pm 10$	$0.90 \pm 0.04$
<b>47e</b>	$293 \pm 9$	$0.62 \pm 0.05$	$233 \pm 13$	$480 \pm 40$	$1.3 \pm 0.1$
<b>47f</b>	$2,290 \pm 80$	$10.6 \pm 0.5$	$2,170 \pm 40$	$220 \pm 10$	$1.1 \pm 0.1$

<b>47g</b>	$1,020 \pm 50$	$2.58 \pm 0.22$	$677 \pm 26$	$400 \pm 40$	$1.5 \pm 0.1$
<b>47h</b>	$5,240 \pm 140$	$14.7 \pm 0.3$	$3,110 \pm 120$	$360 \pm 10$	$1.7 \pm 0.1$
<b>47i</b>	$8,530 \pm 420$	$22.5 \pm 1.1$	$1,990 \pm 70$	$380 \pm 30$	$4.3 \pm 0.3$
<b>47k</b>	$252 \pm 4$	$0.55 \pm 0.02$	$30.9 \pm 2.6$	$450 \pm 20$	$8.2 \pm 0.7$
<b>47l</b>	$477 \pm 7$	$0.99 \pm 0.05$	$112 \pm 5$	$480 \pm 20$	$4.2 \pm 0.2$
<b>47m</b>	$161 \pm 12$	$0.37 \pm 0.06$	$26.2 \pm 1.1$	$440 \pm 80$	$6.2 \pm 0.5$
<b>47n</b>	$266 \pm 9$	$0.40 \pm 0.12$	$80.9 \pm 2.0$	$670 \pm 200$	$3.3 \pm 0.1$
<b>47o</b>	$24.3 \pm 0.1$	$0.41 \pm 0.27$	$92.0 \pm 4.0$	$60 \pm 4.1$	$0.26 \pm 0.01$
<b>56h</b>	$2,240 \pm 80$	$36.7 \pm 2.7$	$1,860 \pm 40$	$61 \pm 5$	$1.2 \pm 0.1$
<b>57h</b>	$156 \pm 6$	$3.84 \pm 0.20$	$1,080 \pm 50$	$41 \pm 3$	$0.14 \pm 0.01$
<b>58h</b>	$2.78 \pm 0.09^b$	$102 \pm 2$	$2,130 \pm 60$	$37 \pm 1$	$0.048 \pm 0.002$
<b>59h</b>	$7.30 \pm 0.09^d$	$1.24 \pm 0.05^d$	$180 \pm 3^d$	$5.9 \pm 0.3^d$	$0.041 \pm 0.001^d$
<b>60h</b>	$134 \pm 8$	$1.90 \pm 0.11$	$379 \pm 24$	$71 \pm 6$	$0.35 \pm 0.03$
<b>61h</b>	$39.0 \pm 2.1$	$2.15 \pm 0.27$	$26.0 \pm 0.3$	$18 \pm 3$	$1.5 \pm 0.1$

$k_i$  measurements were done by Dr. Dawn Wong in the Carlier group. <sup>a</sup>Measured at  $23 \pm 1^\circ\text{C}$ , pH 7.7, 0.1% (v/v) DMSO. Recombinant sources of AgAChE are rAgAChE-WT and rAgAChE-G119S. <sup>b</sup>Resistance ratio is calculated as  $k_i(\text{WT})/k_i(\text{G119S})$ . Standard error in the ratio is calculated according to a standard propagation of error formula. <sup>c</sup>Selectivity for inhibiting AgAChE (WT) vs hAChE, calculated as  $k_i(\text{AgAChE-WT})/k_i(\text{hAChE})$ , with standard error in the ratio calculated according to a standard propagation of error formula. <sup>d</sup> $k_i$  values extrapolated from single point incubation at various inhibitor concentration, e.g.  $t = 10$  min.

Compound **47a** ( $\text{R}^1 = \text{Me}$ ) showed very slow inactivation of AgAChE ( $0.46 \text{ mM}^{-1} \text{ min}^{-1}$ ), which could be a consequence of high desolvation penalty (low hydrophobicity). The rate of

inactivation of *AgAChE* by dimethylcarboxamides bearing larger C5-substituents was significantly larger, ranging from 24.3 to 8,530 mM<sup>-1</sup> min<sup>-1</sup> (**47o** and **47i**, respectively). In general, the largest *AgAChE* inactivation rate constants were realized with  $\alpha$ -substitution, in particular **47f-i**. These dimethylcarboxamides also exhibited the largest G119S inactivation constants (2.58 to 22.5 mM<sup>-1</sup> min<sup>-1</sup>), although the WT/G119S resistance ratios are still very large (220- to 400-fold), though at least 10-fold lower than that of **8**, **9**, **27**, and **28**. It is also instructive to compare cycloalkyl analogs **47c, e, g** with the corresponding open chain  $\alpha$ -branched analogs **47d, f, h, i**. In each case, the open chain compound offered significantly more rapid inactivation of WT or G119S *AgAChE* than the cycloalkyl analogs (cf **47d** vs **47c**, **47f** vs **47e**, and **47h** or **47i** vs **47g**). It is possible that the flexibility of the side chain gives **47d**, **47f**, **47h**, and **47i** a better fit in the active site of the enzyme as compared to **47c**, **47e**, and **47g**. With regard to *AgAChE/hAChE* enzymatic selectivity, the  $\alpha$ -branched carboxamides did not offer more than 4-fold selectivity. The three  $\beta$ -branched dimethylcarboxamides investigated (**47k-m**) exhibited reduced  $k_i$  values compared to those with  $\alpha$ -branching. However, compound **47k** possessed a WT *AgAChE*  $k_i$  value close to that of propoxur, but with a G119S  $k_i$  value at least 10-fold higher than that of propoxur. Selectivity for *AgAChE* over *hAChE* within this series remained lower than desired (8-fold for **47k**). Amongst the  $\gamma$ -branched dimethylcarboxamides (**47n-o**), the maximum *AgAChE* inactivation potency was achieved for compound **47n** ( $R^1 = i$ -pentyl). The  $\gamma$ -branched carboxamides did not offer more than 3-fold selectivity.

Variation of the exocyclic nitrogen substituents had a dramatic affect on WT *AgAChE*  $k_i$  values. The relatively conservative replacement of the dimethylamino group of **47h** with an azetidine moiety (**56h**) reduced WT *AgAChE*  $k_i$  value by 50%, but actually increased the G119S *AgAChE*  $k_i$  value. Replacement of one of the methyl groups of **47h** with an ethyl group (**59h**)

reduced the WT *AgAChE*  $k_i$  value 30-fold, and the G119S *AgAChE*  $k_i$  value nearly 4-fold, suggesting steric inhibition of binding or carbamoylation in the relatively crowded acyl pocket of *AgAChE*. Pyrrolino- and morpholino-carboxamides **60h** and **61h**, respectively, offered more rapid inactivation than the diethylcarboxamide **59h**, but were much slower than dimethyl carboxamide **47h**. In closing we note that three of the carboxamides featuring larger exocyclic *N*-substituents exhibited inverse inhibition selectivity. This phenomenon is likely due to the more spacious oxyanion hole in *hAChE* relative to *AgAChE*.<sup>10</sup>

**Table 2.11:** Inactivation rate constants  $k_i$  of 5-substituted isoxazol-3-yl dialkylcarbamates for r*AgAChE* (WT and G119S), & r*hAChE*.

**48**

(**63h**, **65h**, **66h**)

R<sup>1</sup>

<b>48a:</b> Me	<b>48i:</b> 3-pentyl	
<b>48c:</b> <i>c</i> -Pr	<b>48j:</b> 3-heptyl	
<b>48d:</b> <i>i</i> -Pr	<b>48k:</b> <i>i</i> -Bu	
<b>48e:</b> <i>c</i> -Bu	<b>48l:</b> 2-methylbutyl	
<b>48f:</b> <i>s</i> -Bu	<b>48m:</b> neo-pentyl	
<b>48g:</b> <i>c</i> -pentyl	<b>48n:</b> <i>i</i> -pentyl	
<b>48h:</b> 2-pentyl	<b>48o:</b> 2-cyclopentylethyl	

Compound	<sup>a</sup> <i>AgAChE</i> $k_i$ (mM <sup>-1</sup> min <sup>-1</sup> )	<sup>a</sup> <i>G119S</i> $k_i$ (mM <sup>-1</sup> min <sup>-1</sup> )	<sup>a</sup> <i>hAChE</i> $k_i$ (mM <sup>-1</sup> min <sup>-1</sup> )	WT/G119S <sup>b</sup> Resistance ratio	<sup>c</sup> <i>Ag/h</i> selectivity
<b>48a</b>	0.0323 ± 0.0082 <sup>d</sup>	0.0224 ± 0.0125	0.118 ± 0.019	1.4 ± 0.9	0.27 ± 0.08
<b>48c</b>	3.02 ± 0.13	0.30 ± 0.03	2.02 ± 0.27	10 ± 1	1.5 ± 0.2

<b>48d</b>	$7.71 \pm 0.20$	$0.50 \pm 0.04$	$4.46 \pm 0.12$	$15 \pm 1$	$1.7 \pm 0.1$
<b>48e</b>	$6.84 \pm 0.20$	$0.44 \pm 0.04$	$1.86 \pm 0.10$	$16 \pm 2$	$3.7 \pm 0.2$
<b>48f</b>	$323 \pm 6$	$20.4 \pm 0.6$	$60.1 \pm 1.8$	$16 \pm 1$	$5.4 \pm 0.2$
<b>48g</b>	$64.7 \pm 2.7$	$1.94 \pm 0.04$	$4.62 \pm 0.07$	$33 \pm 2$	$14 \pm 1$
<b>48h</b>	$416 \pm 7$	$30.6 \pm 0.5$	$50.9 \pm 1.0$	$14 \pm 1$	$8 \pm 1$
<b>48i</b>	$221 \pm 7$	$10.5 \pm 0.7$	$9.04 \pm 0.31$	$21 \pm 2$	$24 \pm 1$
<b>48j</b>	$2.85 \pm 0.11$	$0.26 \pm 0.01$	$2.13 \pm 0.09$	$11 \pm 1$	$1.3 \pm 0.1$
<b>48k</b>	$10.6 \pm 0.5$	$0.87 \pm 0.06$	$1.59 \pm 0.08$	$12 \pm 1$	$6.7 \pm 0.5$
<b>48l</b>	$7.64 \pm 0.21$	$0.50 \pm 0.05$	$1.70 \pm 0.09$	$15 \pm 2$	$4.5 \pm 0.3$
<b>48m</b>	$0.12 \pm 0.03$	$0.05 \pm 0.01$	$0.44 \pm 0.04$	$2.4 \pm 0.7$	$0.28 \pm 0.07$
<b>48n</b>	$3.12 \pm 0.16$	$0.37 \pm 0.03$	$1.91 \pm 0.04$	$8.3 \pm 0.8$	$1.6 \pm 0.1$
<b>48o</b>	$0.60 \pm 0.05$	$0.12 \pm 0.03$	$13.1 \pm 0.4$	$5.2 \pm 1.2$	$0.046 \pm 0.04$
<b>63h</b>	$24.5 \pm 0.5$	$3.37 \pm 0.20$	$9.14 \pm 1.97$	$7.3 \pm 0.5$	$2.7 \pm 0.6$
<b>65h</b>	$12.4 \pm 0.1^d$	$2.24 \pm 0.08^d$	$1.62 \pm 0.07^d$	$5.5 \pm 0.2^d$	$7.6 \pm 0.3^d$
<b>66h</b>	$18.6 \pm 0.3^d$	$2.30 \pm 0.10^d$	$2.68 \pm 0.06^d$	$8.1 \pm 0.4^d$	$6.9 \pm 0.2^d$

$k_i$  measurements were done by Dr. Dawn Wong in the Carlier group. <sup>a</sup>Measured at  $23 \pm 1^\circ\text{C}$ , pH 7.7, 0.1% (v/v) DMSO. Recombinant sources of AgAChE are rAgAChE-WT and rAgAChE-G119S. <sup>b</sup>Resistance ratio is calculated as  $k_i(\text{WT})/k_i(\text{G119S})$ . Standard error in the ratio is calculated according to a standard propagation of error formula. <sup>c</sup>Selectivity for inhibiting AgAChE (WT) vs hAChE, calculated as  $k_i(\text{AgAChE-WT})/k_i(\text{hAChE})$ , with standard error in the ratio calculated according to a standard propagation of error formula. <sup>d</sup> $k_i$  values extrapolated from single point incubation at various inhibitor concentration, e.g.  $t = 10$  min.

Turning to the  $k_i$  values of the dimethylcarbamates, compound **48a** (like its carboxamide counterpart **47a**) exhibited extremely slow inactivation of all three enzymes; again poor hydrophobicity is attributed as the cause (Table 2.11). Among  $\alpha$ -,  $\beta$ -, and  $\gamma$ -branched dimethylcarbamates, the highest WT and G119S *AgAChE* values were seen for the  $\alpha$ -branched compounds (e.g. **48f-i**), as was the case for dimethylcarboxamides. These  $\alpha$ -branched dimethylcarbamates **48f-i** however exhibited at least 10-fold slower inactivation than the corresponding dimethylcarboxamides **47f-i**. Nevertheless, as was seen for dimethylcarboxamides, *AgAChE*  $k_i$  values for open chain  $\alpha$ -branched dimethylcarbamates were higher than those of their cycloalkyl homologs (cf. **48d** vs **48c**, **48f** vs **48e**, **48i**, **48h** vs **48g**). Among the  $\beta$ -branched dimethylcarbamates, the bulky neopentyl compound **48m** was much less inhibitory at all three enzymes than the *i*-butyl (**48k**) and 2-methylbutyl (**48l**) compounds. The  $\gamma$ -branched dimethylcarbamates exhibited a trend similar to that observed for  $\gamma$ -branched dimethylcarboxamides. Compound **48n** displayed 5- and 3-fold increased *AgAChE* and G119S enzyme potency, respectively as compared to **48o** with a more bulky side chain. As mentioned before, the corresponding dimethylcarboxamide displayed similar low RR. Finally, with regard to variation of the exocyclic *N*-substituents, increasing steric bulk reduced  $k_i$  values at all three enzymes (cf **63h**, **65h**, **66h** vs **48h**).

It would seem obvious to expect that G3 toxicity and WT *AgAChE*  $k_i$  values would be highly correlated. However, as we have shown for aryl methylcarbamates, ADME is very influential, and there is no general correlation between G3 or Akron LC<sub>50</sub> and *AgAChE*  $k_i$  values (WT or G119S). For example, the  $\alpha$ -branched compounds **47i** and **48f** have almost equal toxicities towards G3 *An. gambiae* (38 and 41  $\mu\text{g}/\text{mL}$  respectively). Despite the similar toxicities, **48f** is 26-fold less inhibitory than **47i** ( $323$  and  $8,530 \text{ mM}^{-1} \text{ min}^{-1}$ , respectively). Similarly, **47k**

and **47n** have similar *AgAChE* (WT)  $k_i$  values (252 and 266 mM<sup>-1</sup> min<sup>-1</sup>, respectively), but the G3 LC<sub>50</sub> value of **47k** is 2.4 fold higher than of **47n** (201 and 73 µg/mL, respectively). Further, despite the fact that these two compounds have similar G119S *AgAChE*  $k_i$  values, **47n** is considerably more toxic to Akron strain than **47k**. Clearly in all these cases, pharmacokinetics and metabolism may be dominant factors in the in vivo toxicity. Since Akron *An. gambiae* exhibits increased expression of CYP6P450,<sup>49-50</sup> one possible reason for the high toxicity of these compounds could be bio-activation of these dimethyl compounds to more reactive monomethyl compounds by oxidative dealkylation.<sup>51</sup> Work is ongoing by our Molsoft LLC collaborators to develop a predictive toxicity model that includes physicochemical parameters (relevant to ADME) as well as the measured  $k_i$  values. This approach was quite successful for a series of aryl methylcarbamates.<sup>7</sup>

Nevertheless, we can offer the following observations. C5-methyl dimethylcarboxamide **47a** and dimethylcarbamate **48a** had very poor toxicity and very slow enzyme inactivation rates, likely as a consequence of low hydrophobicity. As previously mentioned, open chain  $\alpha$ -branched dimethylcarboxamides were more toxic to G3 and Akron strain than the corresponding cycloalkyl analogs (cf **47d** vs **47c**, **47f** vs **47e**, and **47h** or **47i** vs **47g**), and this trend correlates reasonably well with changes enzyme inactivation rates. Increasing the size of the exocyclic *N*-substituent reduced toxicity in both dimethylcarboxamides (**47h** vs **56-61h**) and dimethylcarbamate (**48h** vs **63h**, **65h**, **66h**) series, and decreased enzyme inactivation rates accompany these decreased toxicities. It is possible that the bulkier *N*-substituent might decrease the binding affinity of the carbamate or carboxamide. Also, it is highly possible that a bulkier *N*-substituent hinders the attack of active site Serine-OH on the carbamate or the urea carbonyl. In order to gain an insight into what factors play role in decreasing  $k_i$ , we would need to look into

$K_a$  (affinity constant, Scheme 2.2), and  $k_2$  (carbamylation constant, Scheme 2.2) of these individual compounds.<sup>52</sup>

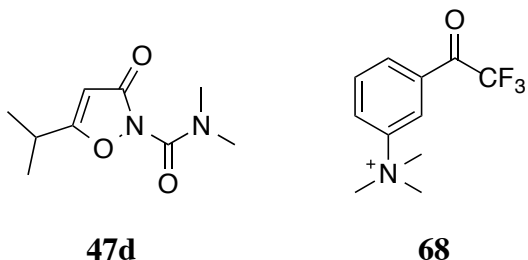


**Figure 2.13:** Structure of the synthesized dimethylcarboxamide **47d**, and **68**, a known potent AChE trifluoromethylketone inhibitor (TFK).

To gain insight into the unusually high inactivation rates ( $k_i$ ) of these dimethylcarboxamides, our Molsoft LLC collaborator Dr. Max Totrov modeled inhibitor **47d** in the active site of mouse AChE, and compared it to the covalently bound X-ray structure of **68**, a known potent inhibitor of AChE, in mouse AChE (PDB ID 2H9Y).<sup>53</sup> The choice of mouse AChE was motivated by three factors: 1) availability of a high-resolution crystal structure; 2) high sequence identity of mouse and human AChE; and 3) our observation of fast inactivation of *h*AChE by the dimethylcarboxamides. Figure 2.14 shows the tetrahedral adduct formed after the attack of active site serine (S203) on the carbonyl of **47d** and TFK **68**. A comparative analysis of the Figure 2.14A and 2.14B show similar interactions stabilizing the two tetrahedral intermediates; the oxyanion formed is stabilized through hydrogen bonding with the oxyanionic hole residues G121, G122 and A204. The TFK is additionally stabilized by a cation-π interaction with W86 at the choline biding site. Further, the overlay of the two structures in Figure 2.14C highlights the similar positioning of the two molecules in the active site of AChE. It is noteworthy that the  $\text{NMe}_2$  group in **47d** occupies a position in the hydrophobic acyl pocket,

composed of residues W236, F295 and F297, similar to that occupied by trifluoromethyl group in **68**, and the side chain of the dimethylcarboxamides inhibitor superimposed closely with the quaternary ammonium group of **68**. It is also worth noting that the CF<sub>3</sub> group is larger than expected, and is close in volume to an isopropyl group<sup>54</sup>; the CF<sub>3</sub> group is thus similar in size to NMe<sub>2</sub>. The overlay structure sheds some light on the fast inactivation of AChE by these dimethylcarboxamide inhibitors. Further, we turned towards <sup>13</sup>C NMR to investigate if it is the increased electrophilicity of the carbonyl carbon in dimethylcarboxamides that contributes to the high  $k_i$  values observed for dimethylcarboxamides in comparison to dimethylcarbamates. Interestingly, the carbonyl carbons in the synthesized dimethylcarbamates (~151 ppm) and dimethylcarboxamides (~150 ppm) inhibitors appear in the same region in <sup>13</sup>C NMR, which hints towards similar electrophilicities of the carbonyl carbon. Looking at the similar electrophilicity of carbonyl group in-spite of different leaving groups, it is highly possible that these carboxamides are benefiting from a favorable orientation and interaction in the active site of the enzyme as seen from the X-ray structure and computer modeling as depicted in Figure 2.14. Note that the residues W86, S203, G121, G122, A204, W236, F295 and F297 in mouse AChE are equivalent to W84, S199, G118, G119, A200, W232, C286 and F288 in *Ag*AChE.

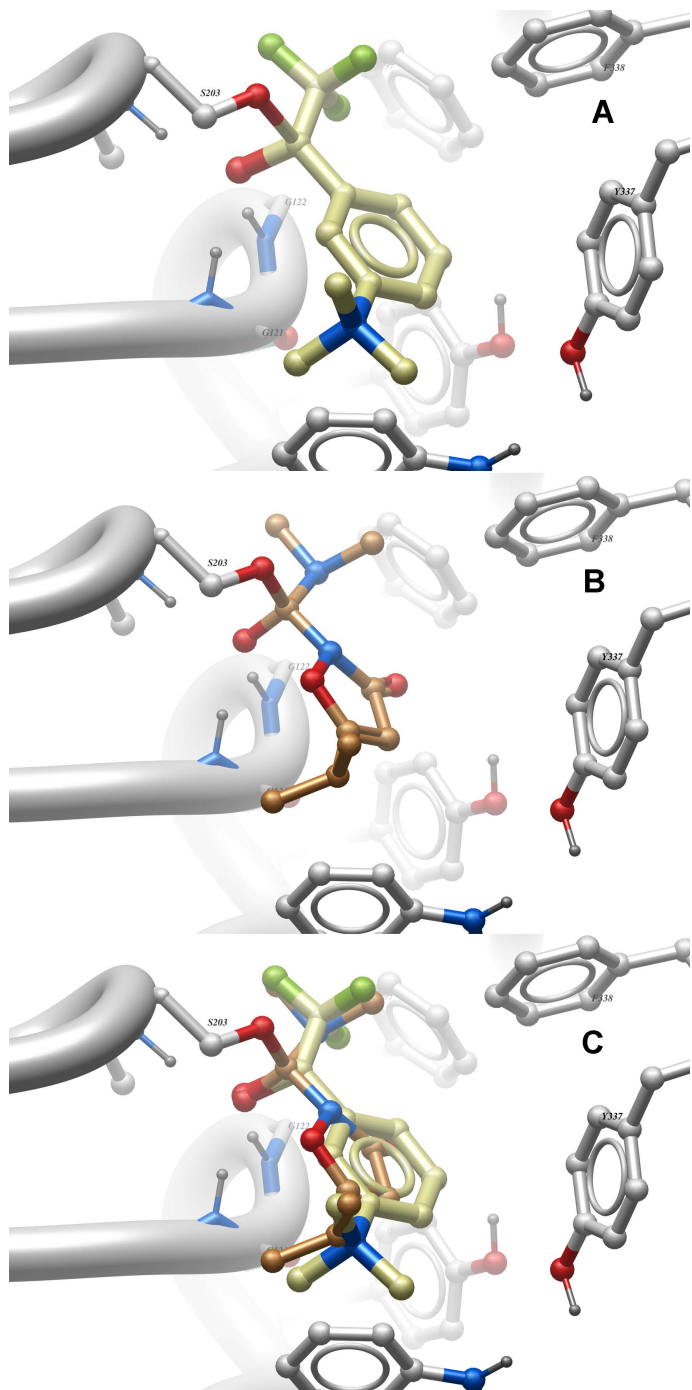


**Figure 2.14:** Tetrahedral adduct formed after the attack of AChE (mouse) active site serine S203 on carbonyl carbon of **68** and **47d**. (A) X-ray structure of the tetrahedral adduct of TFK **68** with S203 (**PDB ID 2H9Y**).<sup>53</sup> (B) Computational modelling of the tetrahedral adduct of dimethylcarboxamide **47d** with S203. (C) Overlay of tetrahedral adduct of TFK **68**, and dimethylcarboxamide **47d** with S203. Note that hydrogen bonding interactions between the

tetrahedral oxyanion for each inhibitor and the oxyanion hole residues G121, G122 and A204 in mouse AChE are not shown or highlighted in the figure.

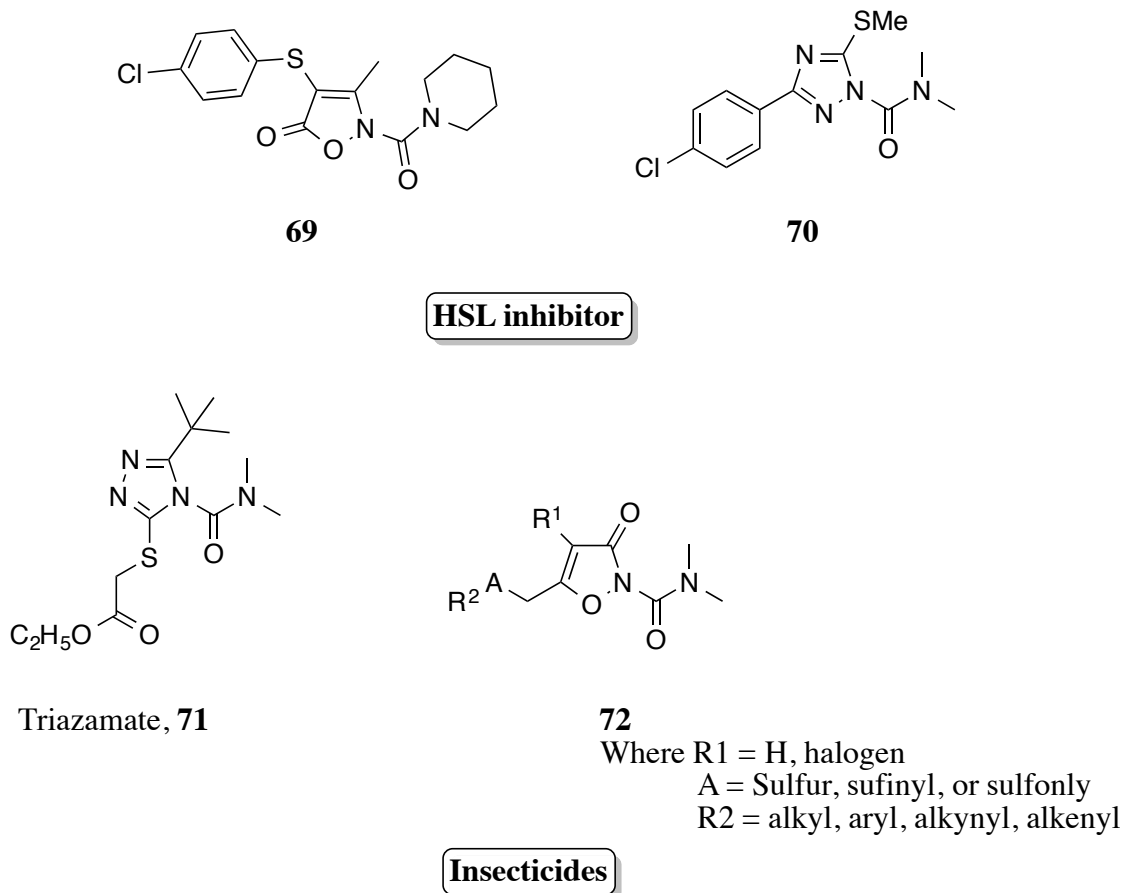


**Figure 2.15:** Chemical structures of previously reported serine hydrolase inhibitors.<sup>55-57</sup>

A literature search provided insight for the high AChE potency observed for the isoxazol-3-yl carboxamides. Close analogues of these carboxamides have also been cited in the literature as potent serine hydrolases. Isoxazolonyl carboxamide<sup>55</sup> **69** and 1,2,4-triazole carboxamide<sup>56</sup> **70** inhibitors are potent hormone-sensitive lipases (HSL) inhibitors. Like vertebrate AChE, HSL belongs to the family of serine hydrolases with a  $\alpha/\beta$  hydrolase fold.<sup>58</sup> Since they originated from the same ancestor, the catalytic residues are preserved in these enzymes. Triazamate **71**, a

carbamoyl triazole AChE inhibitor aphicide, has been approved for plant protection in many European countries.<sup>59</sup> Furthermore, derivatives of **72** have been described in a patent literature as having good insecticidal and/or acaricidal with concomitant low toxicity towards warm-blooded animals.<sup>57</sup> However, the exact mode of action has not been discussed.

## 2.8 Conclusion

In conclusion, 3-oxoisoxazole-2(3*H*)-carboxamide and isoxazol-3-yl carbamates demonstrated excellent toxicity towards susceptible (G3), and resistant strain (Akron) *An. gambiae*. On the contrary, commercial aryl methylcarbamates although effective against G3, showed no potency against Akron. Compound **48f**, ( $LC_{50}$  G3 = 41  $\mu\text{g}/\text{mL}$ ,  $LC_{50}$  Akron = 58  $\mu\text{g}/\text{mL}$ ) and **47i** ( $LC_{50}$  G3 = 38  $\mu\text{g}/\text{mL}$ ,  $LC_{50}$  Akron = 40  $\mu\text{g}/\text{mL}$ ) were effective against both strains of *An. gambiae*. Further, we have identified novel compound which were more susceptible towards Akron mosquitoes; for example compound **47h** ( $LC_{50}$  G3 = 153  $\mu\text{g}/\text{mL}$ ,  $LC_{50}$  Akron = 75  $\mu\text{g}/\text{mL}$ ), and **47n** ( $LC_{50}$  G3 = 73  $\mu\text{g}/\text{mL}$ ,  $LC_{50}$  Akron = 68  $\mu\text{g}/\text{mL}$ ). Apart from being toxic to both strains of *An. gambiae*, these compounds showed no toxicological cross-resistance. Although these compounds did not show greater than 24-fold (**48i**) selectivity for *AgAChE* vs *hAChE*, they appreciably inhibited the G119S enzyme in comparison to commercial aryl carbamates, which showed no inhibition at all. Aldicarb was the only commercial carbamate that exhibited significant G119S AChE inhibition, and was toxic to Akron at the same time ( $G119S k_i = 3.15 \text{ mM}^{-1}\text{min}^{-1}$ ,  $LC_{50}$  Akron = 32  $\mu\text{g}/\text{mL}$ , selectivity  $Ag/h = 2\text{-fold}$ ). We have identified compound **47i** with enzyme inhibition potency 7-fold greater as compared to aldicarb, and at the same time showing excellent toxicity towards Akron ( $G119S k_i = 30.6 \text{ mM}^{-1}\text{min}^{-1}$ ,  $LC_{50}$  Akron = 40  $\mu\text{g}/\text{mL}$ , selectivity  $Ag/h = 4.4\text{-fold}$ ). Further, we demonstrated that modification of the *N*-substituent on the urea, and the carbamate moiety leads to loss in toxicity against *An. gambiae*,

and also in *AgAChE* inhibition. To the best of our knowledge this is the first report where any heterocyclic dimethylcarbamate or dimethylcarboxamide has shown significant contact toxicity towards the malaria vector *An. gambiae*. Whether these compounds have potential to be further developed into commercial insecticides depends on other factors (like mouse toxicities), which remain to be seen.

## 2.9 Bibliography

1. WHO. *Guidelines for testing mosquito adulticides for indoor residual spraying and treatment of mosquito nets*. Geneva: World Health Organization, Who/cds/ntd/whopes/gcdpp/2006.3.
2. Ellman, G. L.; Courtney, K. D.; Andres, V., Jr.; Feather-Stone, R. M., A new and rapid colorimetric determination of acetylcholinesterase activity. *Biochem. Pharmacol.* **1961**, *7*, 88-95.
3. Colletier, J.-P., Structural insights into substrate traffic and inhibition in acetylcholinesterase *EMBO J.* **2006**, *25*, 2746-2756.
4. Bar-On, P.; Millard, C. B.; Harel, M.; Dvir, H.; Enz, A.; Sussman, J. L.; Silman, I., Kinetic and structural studies on the interaction of cholinesterases with the anti-Alzheimer drug rivastigmine. *Biochemistry* **2002**, *41*, 3555-3564.
5. Reiner, E.; Aldridge, W. N., Effect of pH on inhibition and spontaneous reactivation of acetylcholinesterase treated with esters of phosphorus acids and of carbamic acids. *Biochem. J.* **1967**, *105*, 171-179.
6. Hartsel, J. A.; Wong, D. M.; Mutunga, J. M.; Ma, M.; Anderson, T. D.; Wysinski, A.; Islam, R.; Wong, E. A.; Paulson, S. L.; Li, J.; Lam, P. C. H.; Totrov, M. M.; Bloomquist, J. R.; Carlier, P. R., Re-engineering aryl methylcarbamates to confer high selectivity for

- inhibition of *Anopheles gambiae* versus human acetylcholinesterase. *Bioorg. Med. Chem. Lett.* **2012**, *22*, 4593-4598.
7. Wong, D. M.; Li, J.; Lam, P. C. H.; Hartsel, J. A.; Mutunga, J. M.; Totrov, M.; Bloomquist, J. R.; Carlier, P. R., Aryl methylcarbamates: Potency and selectivity towards wild-type and carbamate-insensitive (G119S) *Anopheles gambiae* acetylcholinesterase, and toxicity to G3 strain *An. gambiae*. *Chem. Biol. Interact.* **2013**, *203*, 314-318.
  8. Metcalf, R. L., Structure-activity relationships for insecticidal carbamates. *Bull. World Health Organ.* **1971**, *44*, 43-78.
  9. Andraos, J., On the propagation of statistical errors for a function of several variables. *J. Chem. Educ.* **1996**, *73*, 150.
  10. Carlier, P. R.; Anderson, T. D.; Wong, D. M.; Hsu, D. C.; Hartsel, J.; Ma, M.; Wong, E. A.; Choudhury, R.; Lam, P. C.; Totrov, M. M.; Bloomquist, J. R., Towards a species-selective acetylcholinesterase inhibitor to control the mosquito vector of malaria, *Anopheles gambiae*. *Chem. Biol. Interact.* **2008**, *175*, 368-375.
  11. Weill, M.; Lutfalla, G.; Mogensen, K.; Chandre, F.; Berthomieu, A.; Berticat, C.; Pasteur, N.; Philips, A.; Fort, P.; Raymond, M., Comparative genomics: Insecticide resistance in mosquito vectors. *Nature* **2003**, *423*, 136-137.
  12. Weill, M.; Malcolm, C.; Chandre, F.; Mogensen, K.; Berthomieu, A.; Marquine, M.; Raymond, M., The unique mutation in ace-1 giving high insecticide resistance is easily detectable in mosquito vectors. *Insect Mol. Biol.* **2004**, *13*, 1-7.
  13. Hidayati, H.; Nazni, W. A.; Lee, H. L.; Sofian-Azirun, M., Insecticide resistance development in *Aedes aegypti* upon selection pressure with malathion. *Trop. Biomed.* **2011**, *28*, 425-437.

14. WHO, *Test procedures for insecticide resistance monitoring in malaria vector mosquitoes.* World health organization. 2013  
[http://apps.Who.Int/iris/bitstream/10665/80139/1/9789241505154\\_eng.Pdf](http://apps.Who.Int/iris/bitstream/10665/80139/1/9789241505154_eng.Pdf).
15. Pittendrigh, B. R.; Gaffney, P.; Murdock, L. L., Deterministic modeling of negative cross-resistance strategies for use in transgenic host-plant resistance. *J. Theor. Biol.* **2000**, *204*, 135-150.
16. Bull, D. L.; Lindquist, D. A.; Coppedge, J. R., Metabolism of 2-methyl-2-(methylthio)propionaldehyde o-methylcarbamoyl)oxime (temik, uc-21149) in insects. *J. Agric. Food Chem.* **1967**, *15*, 610-616.
17. Frølund, B.; Tagmose, L.; Liljefors, T.; Stensbøl, T. B.; Engblom, C.; Kristiansen, U.; Krogsgaard-Larsen, P., A novel class of potent 3-isoxazolol GABA<sub>A</sub> antagonists: Design, synthesis, and pharmacology. *J. Med. Chem.* **2000**, *43*, 4930-4933.
18. Frølund, B.; Jensen, L. S.; Guandalini, L.; Canillo, C.; Vestergaard, H. T.; Kristiansen, U.; Nielsen, B.; Stensbøl, T. B.; Madsen, C.; Krogsgaard-Larsen, P.; Liljefors, T., Potent 4-aryl- or 4-arylalkyl-substituted 3-isoxazolol GABA<sub>A</sub> antagonists: Synthesis, pharmacology, and molecular modeling. *J. Med. Chem.* **2004**, *48*, 427-439.
19. Krogsgaard-Larsen, P.; Johnston, G. A. R.; Lodge, D.; Curtis, D. R., A new class of GABA agonist. *Nature* **1977**, *268*, 53-55.
20. Sato, K., Synthesis of 3-hydroxyisoxazoles from  $\beta$ -ketoesters and hydroxylamine. *Agric. Biol. Chem.* **1986**, *50* 1831-1837.
21. Onda, M.; Fukushima, H.; Akagawa, M., A flycidal constituent of *Amanita pantherina* (DC) FR. *Chem. Pharm. Bull.* **1964**, *12*, 751-751.

22. Krogsgaard-Larsen, P.; Ebert, B.; Lund, T. M.; Bräuner-Osborne, H.; Sløk, F. A.; Johansen, T. N.; Brehm, L.; Madsen, U., Design of excitatory amino acid receptor agonists, partial agonists and antagonists: Ibotenic acid as a key lead structure. *Eur. J. Med. Chem.* **1996**, *31*, 515-537.
23. Jacobsen, N., Synthesis of 3-isoxazolols revisited. Diketene and  $\beta$ -ketoesters as starting materials. *Can. J. Chem.* **1984**, *62*, 1940-1944.
24. Katritzky, A. R.; Barczynski, P.; Ostercamp, D. L.; Yousaf, T. I., Mechanisms of heterocyclic ring formations. 4. A carbon-13 NMR study of the reaction of  $\beta$ -keto esters with hydroxylamine. *J. Org. Chem.* **1986**, *51*, 4037-4042.
25. Sorensen, U. S.; Falch, E.; Krogsgaard-Larsen, P., A novel route to 5-substituted 3-isoxazolols. Cyclization of *N,O*-diboc  $\beta$ -keto hydroxamic acids synthesized via acyl Meldrum's acids. *J. Org. Chem.* **2000**, *65*, 1003-1007.
26. Meldrum, A. N., LIV.-A  $\beta$ -lactonic acid from acetone and malonic acid. *J. Chem. Soc., Trans.* **1908**, *93*, 598-601.
27. Davidson, D.; Bernhard, S. A., The structure of Meldrum's supposed  $\beta$ -lactonic acid. *J. Am. Chem. Soc.* **1948**, *70*, 3426-3428.
28. Oikawa, Y.; Sugano, K.; Yonemitsu, O., Meldrum's acid in organic synthesis. 2. A general and versatile synthesis of  $\beta$ -keto esters. *J. Org. Chem.* **1978**, *43*, 2087-2088.
29. Rosowsky, A.; Forsch, R.; Uren, J.; Wick, M.; Kumar, A. A.; Freisheim, J. H., Methotrexate analogs. 20. Replacement of glutamate by longer-chain amino diacids: Effects on dihydrofolate reductase inhibition, cytotoxicity, and in vivo antitumor activity. *J. Med. Chem.* **1983**, *26*, 1719-1724.

30. Maibaum, J.; Rich, D. H., Synthesis of the novel  $\pi$ -(benzyloxymethyl)-protected histidine analog of statine. Inhibition of penicillopepsin by pepstatin-derived peptides containing different statine side-chain derivatives. *J. Med. Chem.* **1989**, *32*, 1571-1576.
31. Emténäs, H.; Alderin, L.; Almqvist, F., An enantioselective ketene-imine cycloaddition method for synthesis of substituted ring-fused 2-pyridinones. *J. Org. Chem.* **2001**, *66*, 6756-6761.
32. Staszak, M. A.; Doecke, C. W., A facile synthesis of *N,O*-bis(tert-butoxycarbonyl)-hydroxylamine. *Tetrahedron Lett.* **1993**, *34*, 7043-7044.
33. Xu, F.; Armstrong, J. D.; Zhou, G. X.; Simmons, B.; Hughes, D.; Ge, Z.; Grabowski, E. J., Mechanistic evidence for an  $\alpha$ -oxoketene pathway in the formation of  $\beta$ -ketoamides/esters via Meldrum's acid adducts. *J. Am. Chem. Soc.* **2004**, *126*, 13002-13009.
34. Emténäs, H.; Soto, G.; Hultgren, S. J.; Marshall, G. R.; Almqvist, F., Stereoselective synthesis of optically active  $\beta$ -lactams, potential inhibitors of pilus assembly in pathogenic bacteria. *Org. Lett.* **2000**, *2*, 2065-2067.
35. Yamamoto, Y.; Watanabe, Y.; Ohnishi, S., 1,3-oxazines and related compounds. XIII. Reaction of acyl Meldrum's acids with schiff bases giving 2,3-disubstituted 5-acyl-3,4,5,6-tetrahydro-2*H*-1,3-oxazine-4,6-diones and 2,3,6-trisubstituted 2,3-dihydro-1,3-oxazin-4-ones. *Chem. Pharm. Bull.* **1987**, *35*, 1860-1870.
36. Svetlik, J.; Goljer, I.; Turecek, F., Oxygen-bridged tetrahydropyridines, hexahydropyridines, and dihydropyridones via a hantzsch-like synthesis with 4-(2-hydroxyphenyl)but-3-en-2-one. *J. Chem. Soc., Perkin Trans. I* **1990**, 1315-1318.

37. Chan, A. W. K.; Crow, W. D.; Gosney, I., Isothiazole chemistry-X : Acylation, alkylation and tautomerism in 3-hydroxyisothiazole. *Tetrahedron* **1970**, *26*, 2497-2506.
38. Katritzky, A. R.; Øksne, S.; Boulton, A. J., The tautomerism of heteroaromatic compounds with five-membered rings--III : Further isoxazol-5-ones. *Tetrahedron* **1962**, *18*, 777-790.
39. Weiden, M. H., Toxicity of carbamates to insects. *Bull. World Health Organ.* **1971**.
40. Looker, A. R.; Littler, B. J.; Blythe, T. A.; Snoonian, J. R.; Ansell, G. K.; Jones, A. D.; Nyce, P.; Chen, M.; Neubert, B. J., Development and manufacture of the inosine monophosphate dehydrogenase inhibitor merimepodib, vx-497. *Org. Process Res. Dev.* **2008**, *12*, 666-673.
41. Padiya, K. J.; Gavade, S.; Kardile, B.; Tiwari, M.; Bajare, S.; Mane, M.; Gaware, V.; Varghese, S.; Harel, D.; Kurhade, S., Unprecedented "water" imidazole carbonylation: Paradigm shift for preparation of urea and carbamate. *Org. Lett.* **2012**, *14*, 2814-2817.
42. Deetz, M. J.; Forbes, C. C.; Jonas, M.; Malerich, J. P.; Smith, B. D.; Wiest, O., Unusually low barrier to carbamate C–N rotation. *J. Org. Chem.* **2002**, *67*, 3949-3952.
43. Zhao, Y. M.; Raymond, M. K.; Tsai, H.; Roberts, J. D., A proton NMR investigation of rotation about the C(O)-N bonds of urea. *J. Phys. Chem.* **1993**, *97*, 2910-2913.
44. Selvi, S.; Edah, M. A.; Nazni, W. A.; Lee, H. L.; Tyagi, B. K.; Sofian-Azirun, M.; Azahari, A. H., Insecticide susceptibility and resistance development in malathion selected *Aedes albopictus* (skuse). *Trop. Biomed.* **2010**, *27*, 534-550.
45. Kolaczinski, J. H.; Curtis, C. F., Investigation of negative cross-resistance as a resistance-management tool for insecticide-treated nets. *J Med Entomol* **2004**, *41*, 930-934.

46. Dunley, J. E.; Welter, S. C., Correlated insecticide cross-resistance in azinphosmethyl resistant codling moth (lepidoptera: Tortricidae). *J. Econ. Entomol.* **2000**, *93*, 955-962.
47. Valles, S. M.; Koehler, P. G.; Brenner, R. J., Antagonism of fipronil toxicity by piperonyl butoxide and S,S,S-tributyl phosphorotri thioate in the german cockroach (dictyoptera: Blattellidae). *J. Econ. Entomol.* **1997**, *90*, 1254-1258.
48. Scott, J. G.; Wen, Z., Toxicity of fipronil to susceptible and resistant strains of german cockroaches (dictyoptera: Blattellidae) and house flies (diptera: Muscidae). *J. Econ. Entomol.* **1997**, *90*, 1152-1156.
49. Djouaka, R. F.; Bakare, A. A.; Coulibaly, O. N.; Akogbeto, M. C.; Ranson, H.; Hemingway, J.; Strode, C., Expression of the cytochrome P450s, CYP6P3 and CYP6M2 are significantly elevated in multiple pyrethroid resistant populations of *Anopheles gambiae* s.s. From southern Benin and Nigeria. *BMC Genomics* **2008**, *9*, 538.
50. Oxborough, R. M.; Kitau, J.; Matowo, J.; Mndeme, R.; Feston, E.; Boko, P.; Odjo, A.; Metonnou, C. G.; Irish, S.; N'Guessan, R.; Mosha, F. W.; Rowland, M. W., Evaluation of indoor residual spraying with the pyrrole insecticide chlorgfenapyr against pyrethroid-susceptible *Anopheles arabiensis* and pyrethroid-resistant *Culex quinquefasciatus* mosquitoes. *Trans. R. Soc. Trop. Med. Hyg.* **2010**, *104*, 639-645.
51. Scharf, M. E.; Siegfried, B. D.; Meinke, L. J.; Wright, R. J.; Chandler, L. D., Cytochrome P450-mediated N-demethylation activity and induction in insecticide-resistant and susceptible western corn rootworm populations (coleoptera: Chrysomelidae). *Pestic. Biochem. Physiol.* **2000**, *67*, 137-143.

52. Groner, E.; Ashani, Y.; Schorer-Apelbaum, D.; Sterling, J.; Herzig, Y.; Weinstock, M., The kinetics of inhibition of human acetylcholinesterase and butyrylcholinesterase by two series of novel carbamates. *Mol. Pharmacol.* **2007**, *71*, 1610-1617.
53. Bourne, Y.; Radić, Z.; Sulzenbacher, G.; Kim, E.; Taylor, P.; Marchot, P., Substrate and product trafficking through the active center gorge of acetylcholinesterase analyzed by crystallography and equilibrium binding. *J. Biol. Chem.* **2006**, *281*, 29256-29267.
54. Meanwell, N. A., Synopsis of some recent tactical application of bioisosteres in drug design. *J. Med. Chem.* **2011**, *54*, 2529-2591.
55. Lowe, D. B.; Magnuson, S.; Qi, N.; Campbell, A.-M.; Cook, J.; Hong, Z.; Wang, M.; Rodriguez, M.; Achebe, F.; Kluender, H.; Wong, W. C.; Bullock, W. H.; Salhanick, A. I.; Witman-Jones, T.; Bowling, M. E.; Keiper, C.; Clairmont, K. B., In vitro SAR of (5-(2H)-isoxazolonyl) ureas, potent inhibitors of hormone-sensitive lipase. *Bioorg. Med. Chem. Lett.* **2004**, *14*, 3155-3159.
56. Ebdrup, S.; Sørensen, L. G.; Olsen, O. H.; Jacobsen, P., Synthesis and structure-activity relationship for a novel class of potent and selective carbamoyl-triazole based inhibitors of hormone sensitive lipase. *J. Med. Chem.* **2003**, *47*, 400-410.
57. Tomita, K.; Murakami, T.; Tsuji, H.; Matsumoto, K.; Fujita, K. Isoxazolinone derivatives, process for their preparation and insecticidal and acaricidal composition containing them. EP 94082 A1, Nov 16, 1983.
58. Harel, M.; Kryger, G.; Rosenberry, T. L.; Mallender, W. D.; Lewis, T.; Fletcher, R. J.; Guss, J. M.; Silman, I.; Sussman, J. L., Three-dimensional structures of *Drosophila melanogaster* acetylcholinesterase and of its complexes with two potent inhibitors. *Protein Sci.* **2000**, *9*, 1063-1072.

59. Hetmanski, M. T.; Fussell, R. J.; Sykes, M. D.; Vega, A. B.; Sharma, A., Determination of triazamate in apples, peas and brussels sprouts using high-performance liquid chromatography with tandem mass spectrometry. *Food Addit. Contam.* **2004**, *21*, 447-456.

## Chapter 3: Exploring pyrazol-5-yl and pyrazol-4-yl carbamates as mosquitocide.

### 3.1 Introduction

As seen in Chapter 2, five-membered heterocyclic 3-oxoisoxazole-2(3H)-carboxamide and isoxazol-3-yl dimethylcarbamates exhibited excellent toxicity towards susceptible G3 and resistant Akron strain *An. gambiae*, and demonstrated low cross-resistance. In addition, several of these dimethylcarboxamides and dimethylcarbamates showed potent inhibition of *AgAChE*, but the overall selectivity (*Ag* vs *h*) did not exceed 24-fold. Looking at the excellent toxicity of these five membered heterocyclic carbamates, and hoping to improve the enzyme inhibition selectivity, we decided to replace the isoxazole core with another small core heterocycle and evaluate the insecticidal properties. Pyrazole appeared to offer a reasonable alternative to the isoxazol-3-yl structure: pyrazoles and isoxazoles belong to the same class of 1,2-azoles, and are isomerically related to imidazoles that belong to 1,3-azole system. Pyrazole and its derivatives have been an interesting area of research owing to their promising pharmacological properties.<sup>1</sup> Some of the marketed drugs containing pyrazole include the selective COX-2 inhibitors like *deracoxib* (**73**),<sup>2</sup> and *celecoxib* (**74**).<sup>3</sup>

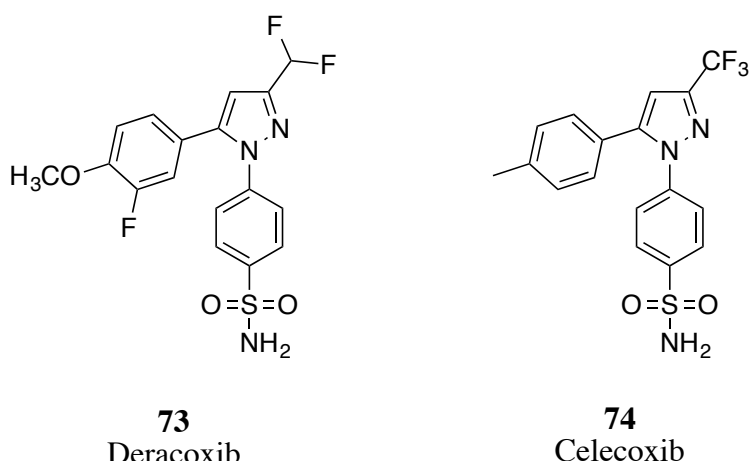


**Figure 3.1:** Marketed drugs containing pyrazole core as the basic moiety.

In addition, the pyrazole core has also shown promising results in the agrochemical industry. Looking at the literature precedents, we were further motivated to explore this core from an insecticidal perspective. A few of the successful and potent pyrazole-containing agrochemicals include the 1-phenylpyrazoles such as fipronil (**75**). Fipronil was the first successful phenyl pyrazole introduced for controlling agricultural pests for rice, corn, and cotton.<sup>4</sup> It is a GABA-gated chloride channel blocker, and offers selectivity for insects over mammalian channels.<sup>5</sup> On plants, fipronil photo-degrades to give the desulfinylfipronil (**76**), which is 10-fold more potent inhibitor of mammalian GABA-gated chloride channels vs insect chloride channels.<sup>4</sup> However, in animals fipronil is metabolized exclusively to its sulfone derivate, which has similar insecticidal potency as that of fipronil (**77**).

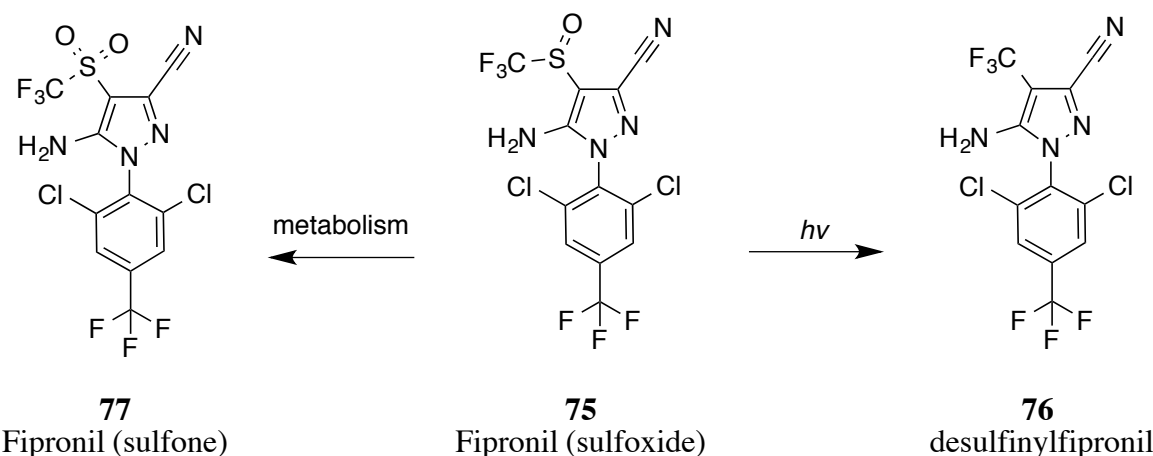


**Figure 3.2:** Degradation pathways of fipronil (**75**) in animals and plants.<sup>4</sup>

Further, pyrazole carboxamides such as tebufenpyrad (**78**), and tolfenpyrad (TFP) (**79**) belong to a class of mitochondrial respiration inhibitors.<sup>6</sup> Tebufenpyrad, discovered in 1987 by Mitsubishi Kasei Co. Ltd, showed excellent acaricidal activity.<sup>7</sup> Tolfenpyrad, is an important insecticide to control pests that have shown resistance to various other insecticides, and has shown contact toxicity towards various stages (eggs, larva, nymph, and adult stages) of targeted pests.<sup>7-8</sup> It has been approved for use in several countries including the United

States.<sup>8</sup> Many 5-hydroxypyrazoles such as **80** demonstrated herbicidal activity (weed control) through inhibition of 4-hydroxyphenylpyruvate dioxygenase (HPPD).<sup>9</sup> There are two prerequisites for HPPD inhibitors to show herbicidal activity. Firstly, the presence of an acidic enolic hydrogen next to the keto group, and secondly, an electron deficient aromatic ring system with an ortho-substituent.<sup>9</sup> Therefore, compounds like **81** are actually pro-drugs, and metabolically generate the active compound 5-hydroxypyrazole.<sup>9</sup> Interesting, pyrazol-5-yl carbamates such as Pyrolan (**82a**), and Isolan (**82b**) have been reported in the literature as commercial cholinesterase inhibitor insecticides. These compounds have shown good contact toxicity towards housefly, *Musca domestica*.<sup>10</sup> However, not much is known regarding their mosquitocidal properties. Their interesting insecticidal properties prompted us to explore them as potent mosquitocides.

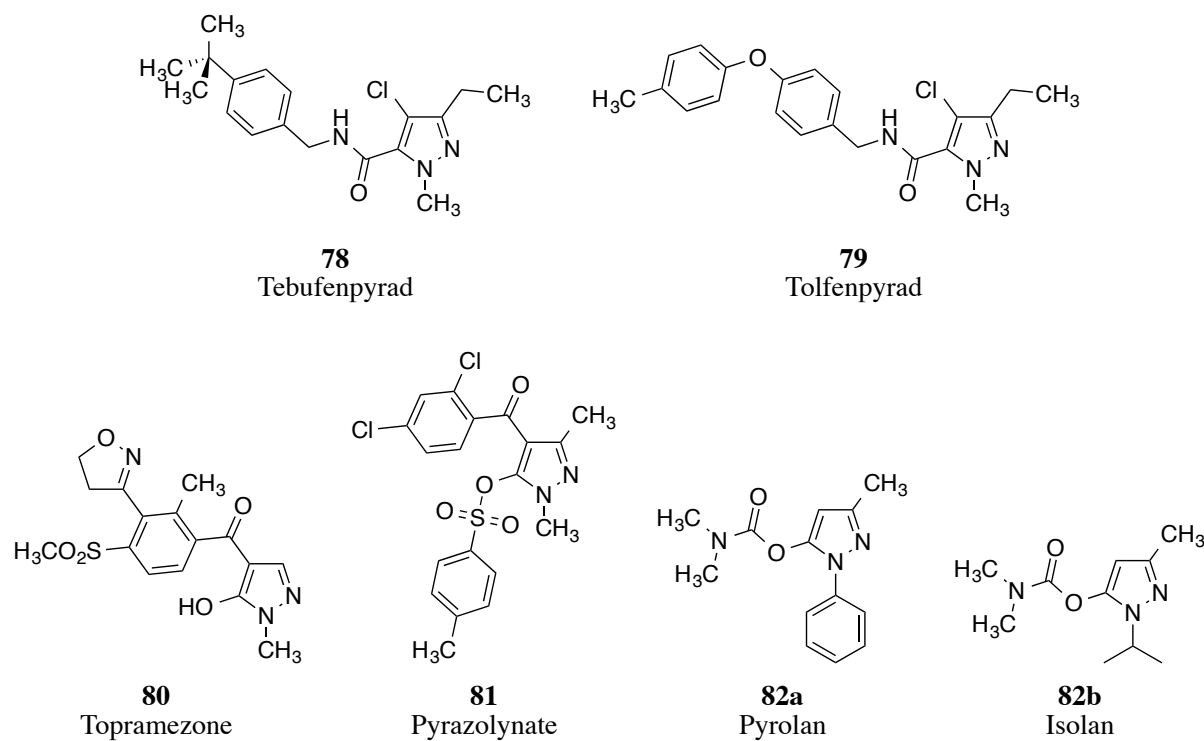


**Figure 3.3:** Commercially available agrochemicals containing pyrazole as the basic moiety.

In the present chapter, we will report the synthesis, toxicology, and enzyme inhibition studies of two classes of pyrazole carbamates (Figure 3.4); 1) pyrazol-5-yl carbamates, where

the carbamate is attached to position 5 on the ring, and 2) pyrazol-4-yl carbamates, where the carbamate is attached to position 4 on the ring. In Section 3.6, we will discuss a newly developed efficient synthesis of pyrazol-4-yl carbamates utilizing a protecting group strategy.

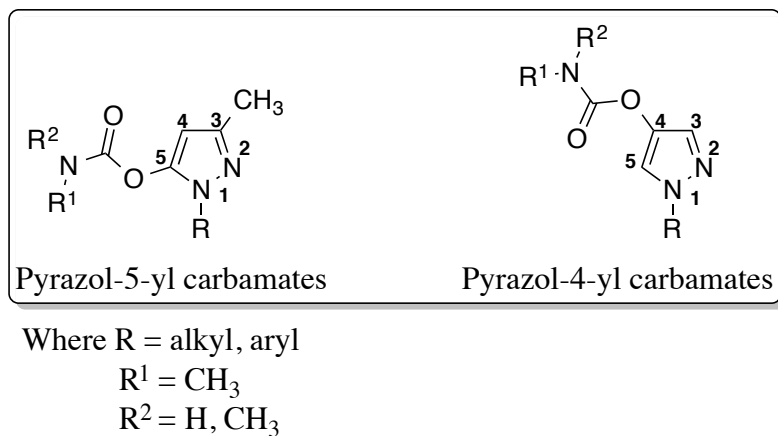
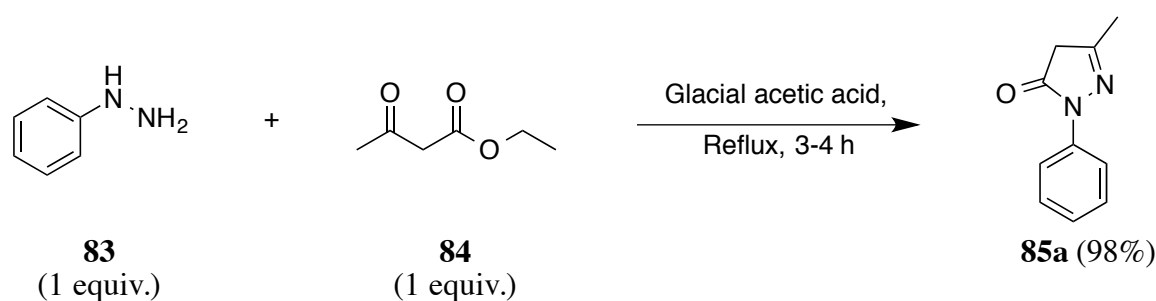


**Figure 3.4:** Structures of pyrazol-5-yl and pyrazol-4-yl carbamates.

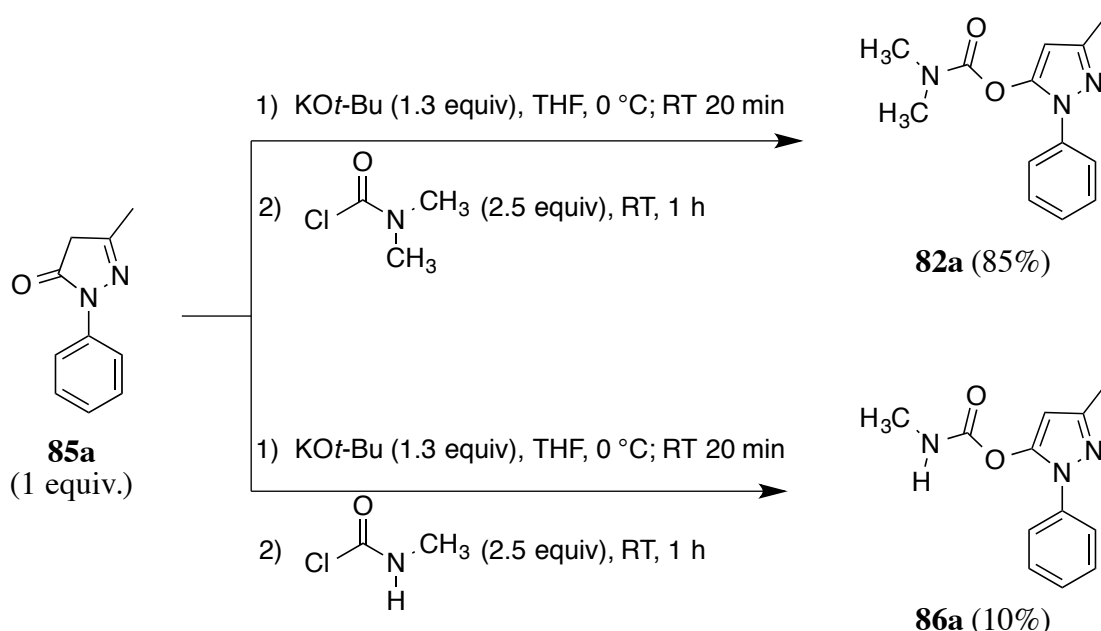
### 3.2 Synthesis of pyrazol-5-yl carbamates

In order to test the mosquitocidal activity of pyrazol-5-yl carbamates, a few analogues were synthesized and tested. We started with the synthesis of a commercially available insecticide, pyrolan (**82a**). The intermediate 3-methyl-1-phenylpyrazol-5-one (**85a**) was obtained in 98% by the condensation of phenylhydrazine (**83**, commercially available) with acetoacetate (**84**) in acetic acid (Scheme 3.1).<sup>11</sup>



**Scheme 3.1:** Synthesis of 3-methyl-1-phenylpyrazol-5-one.<sup>11</sup>

The desired final product, pyrolan (**82a**), was obtained in 85% yield by deprotonating **85a** with KO*t*-Bu as the base at 0 °C, and subsequently treating it with dimethylcarbamoyl chloride for 1 h. However, substituting dimethylcarbamoyl chloride with methylcarbamoyl chloride yielded the corresponding pyrazol-5-yl methylcarbamate (**86a**) in substantially lower yield (10%), and the starting material **85a** was recovered in 67% yield. Attempts to purify **86a** from starting material through silica-gel column chromatography were unsuccessful. Through a careful analysis of the reaction mixture, it was noticed that the product (**86a**) was actually decomposing into starting material at room temperature after isolation.

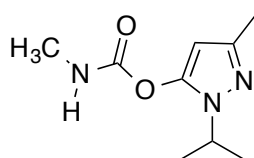


**Scheme 3.2:** Synthesis of 3-methyl-1-phenylpyrazol-5-yl dimethylcarbamate (**82a**) and methylcarbamate (**86a**).

A search through the literature revealed similar observations reported by Gubler et al., where they noticed a decline in the insecticidal activity of methylcarbamates, when the assay was performed with an aqueous suspension of the compound.<sup>10</sup> This was attributed to the hydrolytic instability of these compounds. These authors have determined the half-life of 1-

isopropyl-3-methyl-1*H*-pyrazol-5-yl methylcarbamates (**86b**) through titrimetric measurements at various pH values (Table 3.1).<sup>10</sup> From Table 3.1, it is evident that the hydrolysis is faster in neutral and alkaline ranges in comparison to the acidic range. Metcalf et al. have published similar differences in the hydrolytic instability of methylcarbamates of various phenols and the corresponding dimethylcarbamate analogues.<sup>12</sup> For instance, *N*-methyl-3-isopropylphenyl carbamate showed half-life of 94 min at pH 9.6, whereas the dimethyl analogue showed no signs of hydrolysis even after 24 h.<sup>12</sup>

**Table 3.1:** Half-life of 1-isopropyl-3-methyl-1*H*-pyrazol-5-yl methylcarbamate (**86b**) at various pH values as reported by Gubler et al.<sup>10</sup>



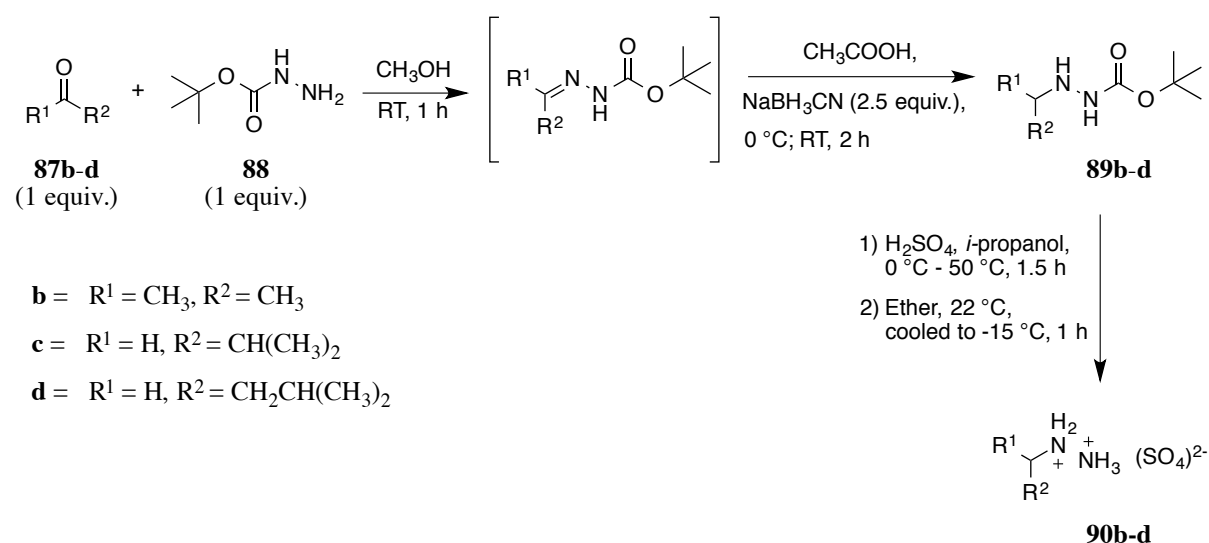
**86b**  
1-isopropyl-3-methyl-1*H*-pyrazol-5-yl methylcarbamate

Medium	pH	Half life
0.1 N HCl	1.1	9 h
Acetate buffer 1:1	4.7	1 h
Succinic acid buffer 1:1	5.6	40 min
Phosphate buffer 1:1	7.1	36 min
Tris-ethanolamine buffer 1:1	7.8	~0.5 min
Borax buffer	9.2	Not measurable

Looking at the instability of the pyrazol-5-yl methylcarbamates at room temperature, we did not consider them a suitable option to explore. Hence, further investigation was restricted to pyrazol-5-yl dimethylcarbamates. A quick literature search for commercially available hydrazines for the synthesis of *N*-alkyl pyrazol-5-yl dimethylcarbamates revealed that not many alkyl hydrazines were commercially available. The desired alkyl hydrazines were synthesized according to the reported literature protocol as shown in Table 3.2.<sup>13-14</sup> The

Schiff base formation proceeded smoothly in various solvents like *i*-propanol, and even in refluxing hexane. Surprisingly, the reduction of hydrazones formed in situ by Pt/H<sub>2</sub> took 2 days to finish. In an attempt to shorten the reaction time, we utilized a protocol reported by Dragovich et al. for the reduction of their benzyl carbamate hydrazone using sodium cyanoborohydride in glacial acetic acid.<sup>14</sup> Interestingly, the reduction of *tert*-butyl carbamate hydrazone completed within 1 h to give monosubstituted carbamate (**89**) in comparison to 23 h as observed for benzyl carbamate hydrazone. In the following step, the cleavage of BOC protecting group was accomplished by treating **90** with sulfuric acid.<sup>13</sup>

**Table 3.2:** Isolated yields of alkyl hydrazine sulfate salt **90b-d**.<sup>13-14</sup>



Entry	R <sup>1</sup>	R <sup>2</sup>	<b>89b-d</b> <sup>a</sup> Isolated Yield (%)	<b>90b-d</b> <sup>a</sup> Isolated Yield (%)
<b>b</b>	CH <sub>3</sub>	CH <sub>3</sub>	100	61
<b>c</b>	<i>i</i> -propyl	H	94	49
<b>d</b>	<i>i</i> -butyl	H	67	62

<sup>a</sup>Isolated yield after filtration.

The alkyl hydrazine sulfate salts (**90b-d**) obtained were condensed with ethyl acetoacetate (**84**) to yield *N*-alkyl pyrazol-5-one (**85b-d**).<sup>15</sup> Although, we could obtain the desired products, the reactions were not clean, and the yield was quite low.

**Table 3.3:** Isolated yields of *N*-alkyl pyrazol-5-one **85b-d**.

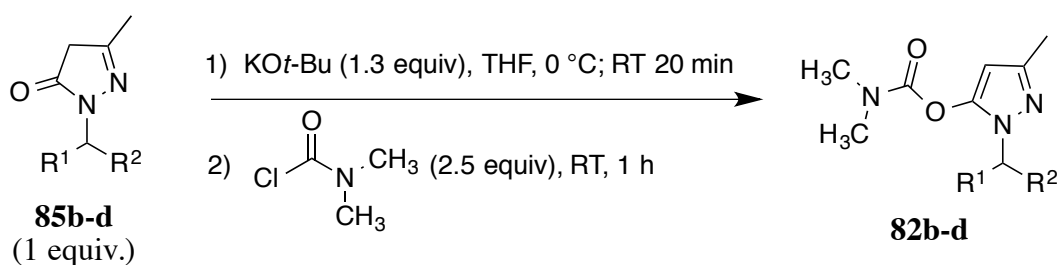
The reaction scheme shows the condensation of an alkyl hydrazine sulfate salt (**90**) with ethyl acetoacetate (**84**) to form *N*-alkyl pyrazol-5-one (**85b-d**). The reagents are **90** (1 equiv.) and **84** (1 equiv.). The reaction conditions are NaOH (CH<sub>3</sub>OH:H<sub>2</sub>O) at 50 °C for 18 h. The product is **85b-d**, which has the structure of a pyrazol-5-one ring with an *N*-alkyl group (R<sup>1</sup> and R<sup>2</sup>).

Entry	Compound No.	R <sup>1</sup>	R <sup>2</sup>	<b>85b-d</b>	
				<sup>a</sup> Isolated Yield (%)	
1	<b>85b</b>	CH <sub>3</sub>	CH <sub>3</sub>	19%	
2	<b>85c</b>	<i>i</i> -propyl	H	47%	
3	<b>85d</b>	<i>i</i> -butyl	H	24%	

<sup>a</sup>Isolated yield after column chromatography.

Finally, the *N*-alkyl pyrazol-5-yl dimethylcarbamates (**82b-d**) were obtained in good yield according to the previously described procedure in Scheme 3.2.

**Table 3.4:** Isolated yields of *N*-alkyl pyrazol-5-yl dimethylcarbamate **82b-d**.



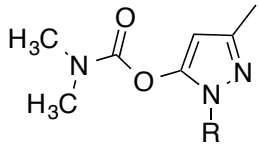
Entry	Compound No.	R <sup>1</sup>	R <sup>2</sup>	<b>82b-d</b> Isolated Yield (%)
1	<b>82b</b>	CH <sub>3</sub>	CH <sub>3</sub>	77
2	<b>82c</b>	<i>i</i> -propyl	H	79
3	<b>82d</b>	<i>i</i> -butyl	H	61

<sup>a</sup>Isolated yield after column chromatography.

The final compounds (**82a-d**) obtained were evaluated for their insecticidal activity as detailed in the next section.

### 3.3 Toxicity and enzyme inhibition studies on pyrazol-5-yl dimethylcarbamates

The pyrazol-5-yl dimethylcarbamates were tested against both susceptible G3 strain and resistant Akron strain *An. gambiae* using the WHO tarsal contact toxicity protocol described in Chapter 2 Section 2.2.1. Compounds that did not show appreciable toxicity to susceptible G3 strain (100% at 1000 µg/mL) were not tested on the resistant Akron strain. The toxicity results are summarized in Table 3.5. As noted above, the pyrazol-5-yl methyl carbamates were unstable. Hence, our investigation focused on pyrazol-5-yl dimethylcarbamates.



**82a-d**

**Table 3.5:** Tarsal contact toxicity pyrazol-5-yl dimethylcarbamates to G3 and Akron strain of *An. gambiae*.

R	<sup>a</sup> <i>An. gambiae</i> G3 % Mortality at highest conc. tested	<sup>a</sup> <i>An. gambiae</i> Akron % Mortality at the highest conc. tested
Phenyl ( <b>82a</b> )	0% @1000 µg/mL	ND
<i>i</i> -propyl ( <b>82b</b> )	100% @500 µg/mL	50% @1000 µg/mL
<i>i</i> -butyl ( <b>82c</b> )	100% @500 µg/mL	0% @1000 µg/mL
<i>i</i> -pentyl ( <b>82d</b> )	0% @500 µg/mL	ND

Toxicity assays were performed by members of the Bloomquist group. <sup>a</sup>Mosquitoes were exposed (1 h) to dried filter papers previously treated with ethanolic solutions of carbamates; mortality was recorded after 24 h.<sup>16</sup>

Compound **82a** (Pyrolan), a commercial insecticide did not show contact toxicity towards *An. gambiae* at the highest concentration tested (1000 µg/mL). Isolan (**82b**), a commercial insecticide, has previously shown appreciable and excellent contact toxicity towards housefly, *Musca domestica* (100% at 1000 µg/petri dish), and mosquito, *Aedes aegypti* (100% at 100 µg/petri dish), respectively in a petri dish contact toxicity assay.<sup>10</sup> Interestingly, it maintained its toxicity towards G3 strain *An. gambiae*. However, the toxicity was lower when tested against resistant Akron strain *An. gambiae*. Similar results were seen for β-branched pyrazol-5-yl dimethylcarbamate (**82c**), which demonstrated moderate toxicity towards G3 but were not toxic towards Akron at the highest concentration tested. The toxicity dropped further as we went to γ-branched compound (**82d**), which showed low toxicity against G3 strain *An. gambiae*; hence, was not tested against Akron.

As expected from the poor toxicological results, these compounds also exhibited slow inactivation of *AgAChE* (Table 3.6). Pyrolan (**82a**), which did not show toxicity towards G3, also showed extremely slow inactivation of *AgAChE* enzyme. Isolan (**82b**) inactivated the *hAChE* faster as compared to *AgAChE*. As we moved from  $\alpha$ - to  $\beta$ -branched compound (**82b** and **82c**, respectively) the  $k_i$  value dropped further for *AgAChE*. The largest *AgAChE* inactivation rate was seen for  $\gamma$ -branched compound **82d** amongst the pyrazol-5-yl dimethylcarbamates tested. However, as seen in Table 3.5, this insecticide showed poor contact toxicity towards G3 *An. gambiae*. This example reinforces the point that there is no general correlation between mosquito toxicity and *AgAChE*  $k_i$  values; a lot is dependent on the ADME properties of these compounds. Overall, pyrazol-5-yl dimethylcarbamates were more selective towards inactivation of *hAChE* vs *AgAChE*. The faster inactivation of *hAChE* might result from the more spacious oxyanion hole in *hAChE* relative to *AgAChE*.<sup>17</sup>

**Table 3.6:** Inactivation rate constants  $k_i$  ( $\text{mM}^{-1} \text{ min}^{-1}$ ) for *AgAChE* (WT and G119S), and *rhAChE*.

<b>R<sup>1</sup></b>	<sup>a</sup> <i>AgAChE hmg k<sub>i</sub></i> ( $\text{mM}^{-1} \text{ min}^{-1}$ )	<sup>a</sup> G119S $k_i$ ( $\text{mM}^{-1} \text{ min}^{-1}$ )	<sup>a</sup> <i>hAChE k<sub>i</sub></i> ( $\text{mM}^{-1} \text{ min}^{-1}$ )	<sup>b</sup> <i>Ag vs h</i> Selectivity
Phenyl ( <b>82a</b> )	$4.98 \pm 0.62$	ND	$114 \pm 16$	0.04
<i>i</i> -propyl ( <b>82b</b> )	<sup>c</sup> $13.8 \pm 0.3$	$0.21 \pm 0.03$	$172 \pm 6$	0.08
<i>i</i> -butyl ( <b>82c</b> )	$8.94 \pm 0.29$	ND	ND	ND
<i>i</i> -pentyl ( <b>82d</b> )	$121 \pm 11$	ND	$682 \pm 21$	0.17

$k_i$  measurements were done by Dr. Dawn Wong in the Carlier group. <sup>a</sup>Measured at  $23 \pm 1^\circ\text{C}$ , pH 7.7, 0.1% (v/v) DMSO. Standard error in the ratio is calculated according to a standard propagation of error formula. <sup>b</sup>Selectivity for inhibiting *AgAChE* (WT) vs *hAChE*, calculated as  $k_i(\text{AgAChE-WT})/k_i(\text{hAChE})$ , with standard error in the ratio calculated according to a standard propagation of error formula.<sup>18-19</sup> <sup>c</sup> $k_i$  measured against *rAgAChE*.

To summarize, although compound **82b** and **82c** showed appreciable toxicity towards susceptible G3 strain *An. gambiae*, none of the evaluated compounds showed good contact

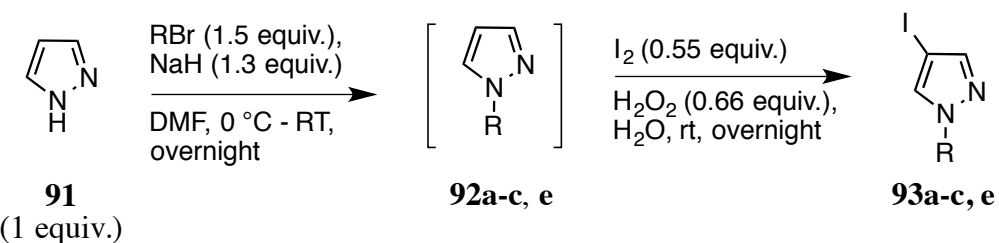
toxicity towards resistant Akron strain. Further, these compounds demonstrated slow inactivation of wild-type *AgAChE*, and showed reversed selectivity, featuring faster inactivation of *hAChE* than *AgAChE*. Based on these preliminary results on pyrazol-5-yl dimethylcarbamates, any further investigation on these compounds was discontinued.

### 3.4 Synthesis of pyrazol-4-yl carbamates

Looking at the poor pharmacological outcome of pyrazol-5-yl dimethylcarbamates, we shifted our focus to developing pyrazol-4-yl methylcarbamates. Pyrazol-4-yl carbamates are isomers of pyrazol-5-yl carbamates. Prior to work in the Carlier lab, these compounds had not yet been explored in literature as potential mosquitocides. Dr. Qiao-Hong Chen from Carlier's group did the groundwork on exploring this pharmacophore before I got involved with this project. Through her work it became clear that pyrazol-4-yl methylcarbamates were chemically stable, and were more potent inhibitors of *AgAChE* than pyrazol-4-yl dimethylcarbamates. In addition, pyrazol-4-yl methylcarbamates also exhibited significantly more toxicity towards *An. gambiae* as compared to the pyrazol-4-yl dimethylcarbamates. Hence, our investigation in later stages of this project focused exclusively on the pyrazol-4-yl methylcarbamates.

The preparation of pyrazol-4-yl methylcarbamates required the synthesis of the precursor pyrazol-4-ols. Synthesis began with *N*-alkylation of pyrazole **91**, which was achieved by deprotonation with sodium hydride and subsequent treatment with the desired alkyl bromide. Due to the high volatility of alkyl pyrazoles **92a-c**, following the work-up, the solvent (ether) was evaporated at no greater than 30 °C. Succeeding this, the iodination of the crude alkyl pyrazoles **92a-c**, e was performed utilizing a literature procedure reported by Kim et al.<sup>20</sup> The *N*-alkyl 4-iodopyrazoles **93a-c**, e were obtained in moderate yield over two steps.

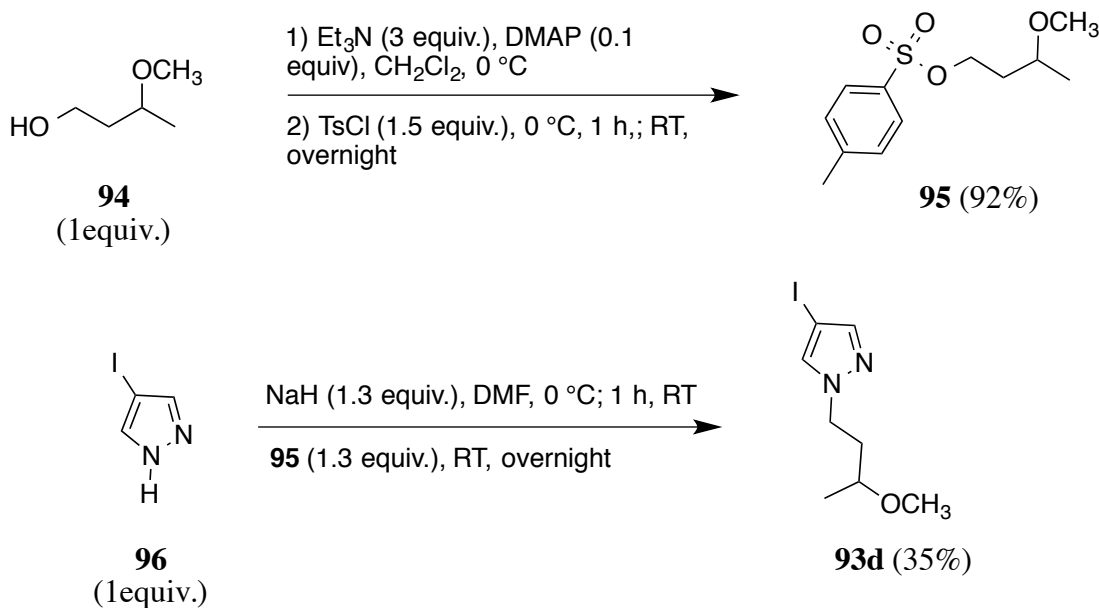
**Table 3.7:** Synthesis of *N*-substituted 4-iodopyrazole **93a-c,e**.



Entry	Compound No.	$R^1$	<b>93a-c,d</b>	
			<sup>a</sup> Isolated Yield (%)	
1	<b>93a</b>	2-pentyl	56%	
2	<b>93b</b>	3-pentyl	57%	
3	<b>93c</b>	<i>c</i> -pentyl	63%	
4	<b>93e</b>	3-phenylpropyl	68%	

<sup>a</sup>Isolated after column chromatography.

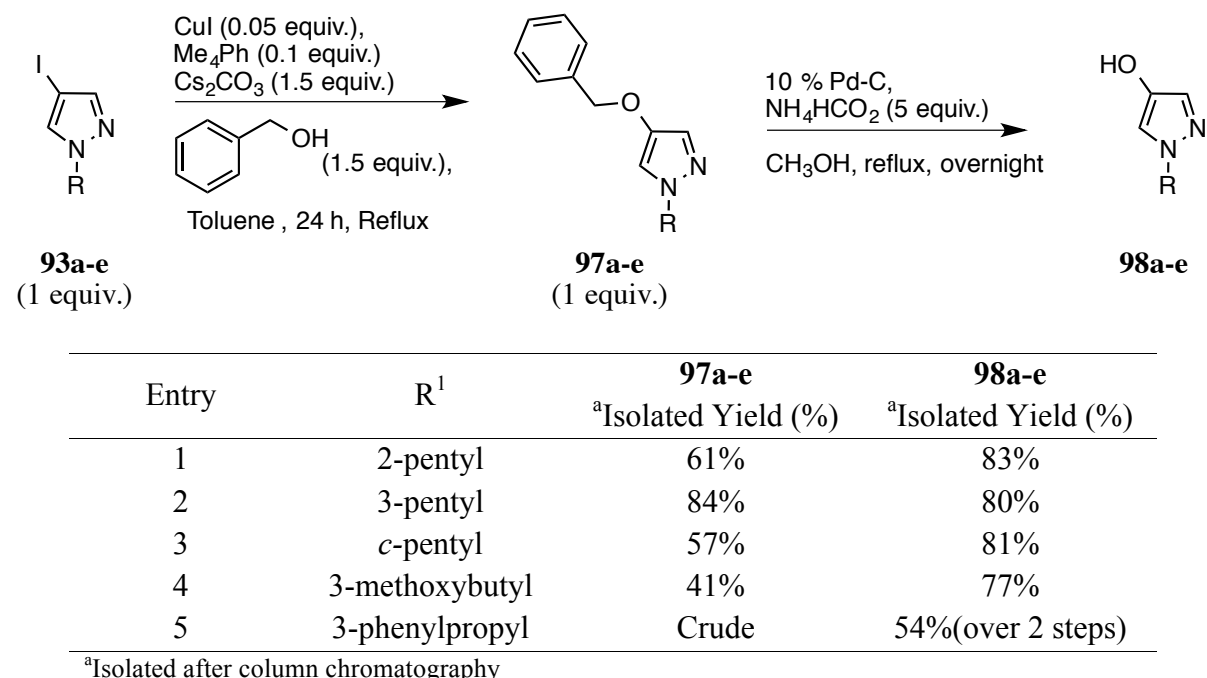
For the synthesis of **93d**, the corresponding 3-methoxybutyl tosylate (**95**) was synthesized from the reaction of 3-methoxybutan-1-ol **94** with 4-toluenesulfonyl to yield the corresponding tosylate **95** in 92% yield. Compound **95** was reacted with 4-iodo-1*H*-pyrazole **96** and afforded **93d** in rather low yield.



**Scheme 3.3:** Synthesis of 4-iodo-1-(3-methoxybutyl)-1*H*-pyrazole (**93d**).

The subsequent copper-catalyzed benzyloxylation of **93a-e** gave the corresponding products in moderate yields Table 3.8.<sup>21</sup> This was followed by hydrogenolysis of **97a-e** to afford *N*-substituted pyrazol-4-ols (**98a-e**) in good yields.

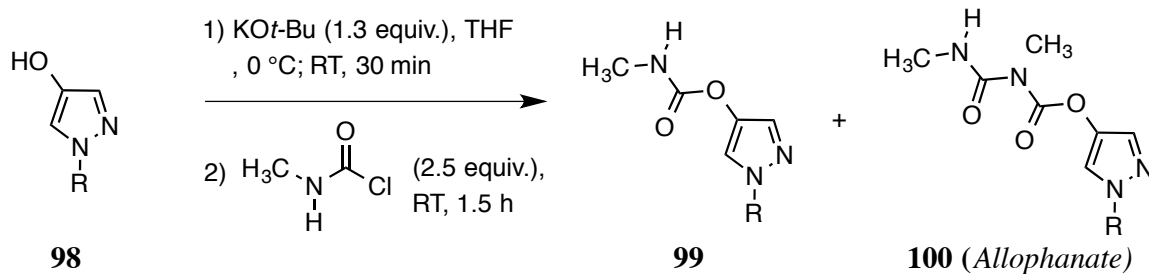
**Table 3.8:** Synthesis of *N*-substituted 4-benzyloxypyrazole **97a-e**, and *N*-substituted pyrazol-4-ols **98a-e**.



The final step in the reaction sequence is always the carbamoylation of the synthesized alcohol. Seemingly the easiest and most straightforward reaction of the sequence, for heterocyclic enols it has turned out to be the most unpredictable and challenging step. Recall from Chapter 2 Section 2.4, during the synthesis of isoxazol-3-yl dimethylcarbamates under basic conditions, we obtained dimethylcarboxamides as a minor product in the same reaction mixture. In contrast, the attempted synthesis of isoxazol-3-yl methylcarbamates under basic conditions gave methylcarboxamides exclusively. We have also noted that isolation of the desired product can be difficult due to reduced stability. For instance, in case of pyrazol-5-yl carbamates the dimethylcarbamate analogues could be conveniently isolated,

whereas the methylcarbamate analogues could not. A different sort of challenge was faced during the synthesis of pyrazol-4-yl methylcarbamates. Since Dr. Qiao-Hong Chen initially worked on this project, her efforts to optimize the reaction conditions of the final carbamoylation step deserves a mention.

In the past, the synthesis of pyrazol-4-yl methylcarbamates was performed utilizing technical grade *N*-methylcarbamoyl chloride (Scheme 3.4). Using this procedure, the desired pyrazol-4-yl methylcarbamates **99** were obtained in moderate yield. In addition to the desired product, the reaction also afforded undesired by-products called allophanates **100**. Interestingly, these allophanates had not been encountered by previous Carlier group members in numerous reactions of *N*-methylcarbamoyl chloride with substituted phenols. Allophanates derived from phenol and isocyanate have been previously reported by other workers, however, no reports of their insecticidal properties were described.<sup>22-23</sup> A few of the allophanates prepared by Dr. Chen showed appreciable toxicity towards G3 strain *An. gambiae* but were not toxic against Akron strain. It is speculated that these compounds might act as pro-insecticides, and generate the active compound “methylcarbamate” in vivo by hydrolysis, or through oxidative demethylation by the action of cytochrome P-450 monooxygenases.

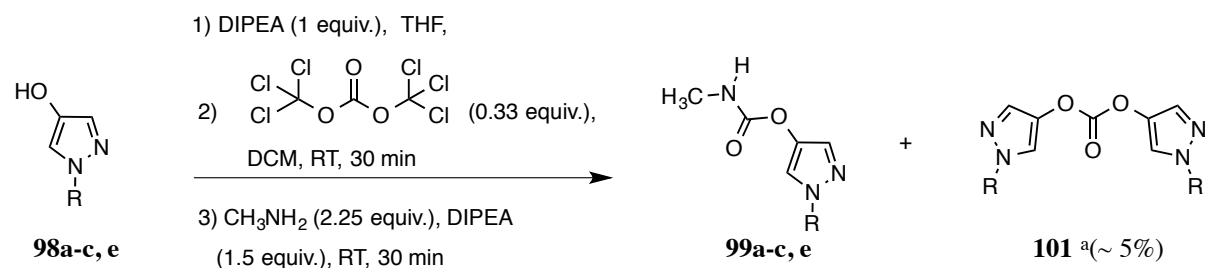


Where R = alkyl

**Scheme 3.4:** Synthesis of pyrazol-4-yl methylcarbamate using *N*-methylcarbamoyl chloride.

Furthermore, allophanates and the desired product had similar R<sub>f</sub> on TLC, which made the isolation of the **99** through column chromatography laborious and time-consuming. The formation of by-product **100** was overcome by employing a new protocol, where triphosgene served as the carbonylating agent and *N*-methylamine in THF was used as the amine source.<sup>16</sup> I have successfully used this method for the synthesis of series of pyrazol-4-yl methylcarbamates shown in Table 3.9.<sup>16</sup>

**Table 3.9:** Synthesis and isolated yields of pyrazol-4-yl methylcarbamates **99a-c,e** using triphosgene and *N*-methylamine.

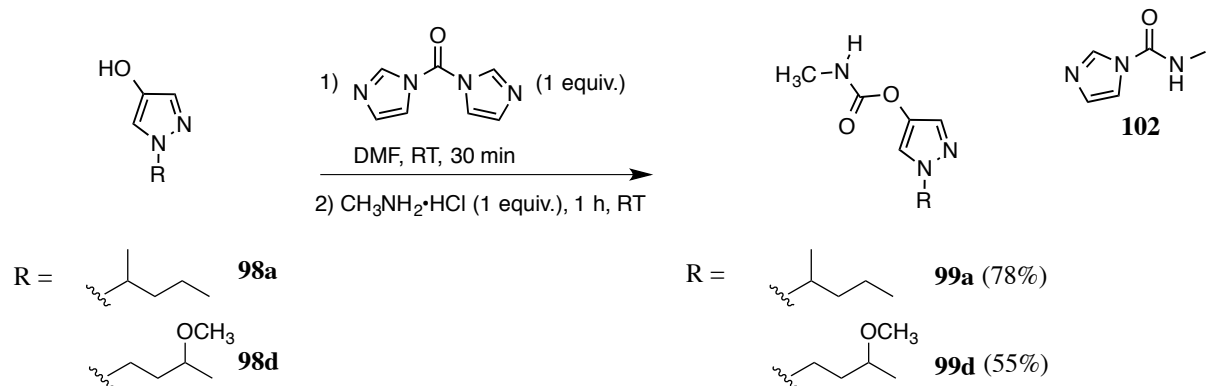


Entry	Compound No.	R <sup>1</sup>	<b>99a-c,e</b> <sup>b</sup> Isolated Yield (%)
1	<b>99a</b>	2-pentyl	73%
2	<b>99b</b>	3-pentyl	69%
3	<b>99c</b>	c-pentyl	73%
4	<b>99e</b>	3-phenylpropyl	76%

<sup>a</sup>With a new bottle of  $\text{CH}_3\text{NH}_2$  the by-product **101** was obtained in ~ 5%, which otherwise with an old bottle was formed in ~40-50% yield. <sup>b</sup>Isolated after column chromatography.

Though this procedure was convenient and gave the desired products in good yields, two shortcomings were noticed. First, triphosgene although a much safer choice than phosgene, is still toxic.<sup>24-25</sup> Secondly, this method is highly dependent on the shelf life of *N*-methylamine solution in THF. *N*-methylamine is a highly volatile compound (-6.6 °C-6.0 °C) and thus the THF solution has a very short shelf life. Further, we have observed a noticeable

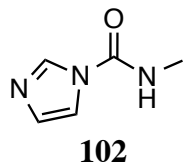
drop in product yield, and an increase in the formation of by-product **101** a symmetrical urea, when a month-old bottle of *N*-methylamine solution was used.



**Scheme 3.5:** Synthesis of pyrazol-4-yl methylcarbamate using CDI, and *N*-methyamine hydrogenchloride salt.

In an attempt to develop another procedure for the synthesis of pyrazol-4-yl carbamates safely, we decided to explore the potential of 1,1-carbonyldiimidazole (CDI, **58**). Recall from Chapter 2 that the synthesis of 3-oxoisoxazole-2(3*H*)-carboxamide and isoxazol-3-yl carbamates was unsuccessful when CDI was used as the potential carbonylating agent. However, gratifyingly, a one-pot protocol utilizing CDI, and *N*-methylamine hydrogen chloride salt afforded **99a** (78%), and **99d** (55%) in good to moderate yield. Further, no base was used as the liberated imidazole acts as a base. Although this protocol needs to be further explored, we did not observe the formation of by-products (**100**, **101**) in the two reactions described in Scheme 3.5. While we were working independently on exploring the protocol employing CDI for the synthesis of **99**, we came across a similar procedure reported by Duspara et al.<sup>26</sup> However, the authors have first synthesized the intermediate *N*-methyl carbonyldiimidazole (**102**) from CDI (**58**) and *N*-methylamine hydrogen chloride salt (**60**), which was subsequently reacted with various nucleophiles in the presence of a base to give the corresponding desired product. The authors have proposed the formation of a protonated

CDI through a proton transfer from the amine salt, which further reacts with the liberated free *N*-methylamine to give the intermediate **102**.

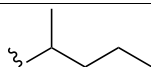
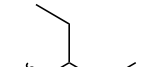
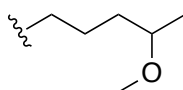
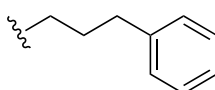


### 3.5 Toxicity and enzyme inhibition studies on pyrazole-4-yl methylcarbamates

As mentioned before, Dr. Qiao-Hong Chen made a major contribution to the pyrazol-4-yl methylcarbamate project. Apart from the pyrazol-4-yl carbamates mentioned in this thesis, a series of 1-substituted pyrazol-4-yl methyl and dimethyl carbamates have been developed with her help. Gratifyingly, these molecules have proved toxic to both susceptible and resistant strain of *An. gambiae*.<sup>16</sup> The toxicity data for the pyrazol-4-yl methylcarbamates I prepared (**99a-e**) are summarized in Table 3.10. As was seen for 3-oxoisoxazole-2(3H)-carboxamide and isoxazol-3-yl carbamates in Chapter 2, pyrazol-4-yl methylcarbamate (**99a**, **99b**) exhibited similar low toxicological resistance ratios (RR = 1.7). Compound **99a** and **99b** are structural isomers and demonstrated similar good toxicities towards G3 strain *An. gambiae*. Interestingly, they also exhibited moderate toxicities towards Akron strain *An. gambiae*. Recall from Chapter 2, in contrast, commercial aryl methylcarbamates (**8**, **9**, **27**, **28**) although toxic towards G3 strain did not show any toxicity towards resistant strain *An. gambiae* ( $LC_{50} = >5000 \mu\text{g/mL}$ ). In addition, the toxicological resistance ratios were greater than 130-fold. Moving on, compound **99c** a cyclic analog of **99b** showed excellent toxicity towards G3 ( $LC_{50} = 29 \mu\text{g/mL}$ ). It was 2-fold more potent than aldicarb (**29**,  $LC_{50} = 70 \mu\text{g/mL}$ ), and exhibited contact toxicity identical to propoxur (**9**,  $LC_{50} = 39$  (32-45)  $\mu\text{g/mL}$ ). Disappointingly, it showed only moderate contact toxicity towards Akron. Also, unlike other pyrazol-4-yl methylcarbamates the high toxicological resistance ratio (RR = 12.6) for this

compound confirmed the cross-resistance exhibited by compound towards the two strain of *An. gambiae*. Finally, compounds **99d** and **99e** were not toxic towards the susceptible G3 strain, and hence were not tested against the resistant Akron strain.

**Table 3.10:** Tarsal contact toxicity of pyrazol-4-yl methylcarbamates (**99a-e**) towards G3 and Akron strain of *An. gambiae*.

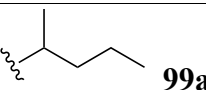
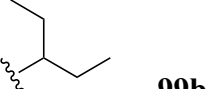
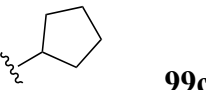
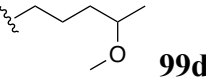
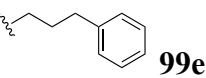
R <sup>1</sup>	Compound No.	<sup>a</sup> <i>An. gambiae</i> G3 LC <sub>50</sub> µg/mL (95% CI)	<sup>a</sup> <i>An. gambiae</i> Akron LC <sub>50</sub> µg/mL (95% CI)	<sup>b</sup> Resistance ratio (RR)
	<b>99a</b>	154 (140-167)	267 (241-289)	1.7
	<b>99b</b>	138 (125-151)	231 (217-245)	1.7
	<b>99c</b>	29 (26-32)	365(344-384)	12.6
	<b>99d</b>	45% @1000 µg/mL	ND	-
	<b>99e</b>	10% @1000 µg/mL	ND	-

Toxicity assays were performed by members of the Bloomquist group.<sup>a</sup> Mosquitoes were exposed (1 h) to dried filter papers previously treated with ethanolic solutions of carbamates; mortality was recorded after 24 h. LC<sub>50</sub> values derived from the concentrations of inhibitor used to treat the paper and were reported previously.  
<sup>b</sup>Defined by LC<sub>50</sub> (Akron)/LC<sub>50</sub> (G3).

As expected from the low toxicological resistance ratios, we expected low enzymatic cross-resistance for these compounds. As seen in Table 3.11, the enzymatic cross-resistance ratio, although high, did not exceed 65-fold. In contrast, for commercial aryl methylcarbamates, the enzymatic cross-resistance ratio ranged between 2,600- to 60,000-fold. Further, compound **99a**, **99b**, and **99c** showed potent inhibition of *AgAChE* vs *hAChE*. Interestingly, these compounds also exhibited rapid inactivation of mutant G119S enzyme. The G119S inactivation rate constants for **99a**, and **99b** are far greater than that observed for

commercial aryl methylcarbamates ( $k_i = < 0.0037 \pm 0.007 \text{ mM}^{-1} \text{ min}^{-1}$ ). Compound **99d**, and **99e** showed slow inactivation of the *AgAChE* (WT and G119S), which correlates well with the low toxicity of these compounds towards G3.

**Table 3.11:** Pyrazol-4-yl methylcarbamates (**99a-e**) inactivation rate constants  $k_i$  for r*AgAChE* (WT and G119S), and r*hAChE*.

<b>R<sup>1</sup></b>	<sup>a</sup> <i>AgAChE k<sub>i</sub></i> (mM <sup>-1</sup> min <sup>-1</sup> )	<sup>a</sup> <i>G119S k<sub>i</sub></i> (mM <sup>-1</sup> min <sup>-1</sup> )	<sup>a</sup> <i>hAChE k<sub>i</sub></i> (mM <sup>-1</sup> min <sup>-1</sup> )	<sup>b</sup> WT/G119S Resistance ratio	<sup>c</sup> <i>Ag/h</i> selectivity
 <b>99a</b>	9,140 ± 260	290 ± 7	805 ± 36	32 ± 1	11 ± 1
 <b>99b</b>	2,220 ± 80	125 ± 3	168 ± 8	18 ± 1	13 ± 1
 <b>99c</b>	2,380 ± 50	36.5 ± 0.8	174 ± 7	65 ± 2	13 ± 1
 <b>99d</b>	8.12 ± 0.18	0.52 ± 0.06	0.60 ± 0.04	16 ± 2	14 ± 1
 <b>99e</b>	18.8 ± 0.6	1.80 ± 0.12	3.40 ± 0.01	10 ± 1	5.5 ± 0.2

$k_i$  measurements were done by Dr. Dawn Wong in the Carlier group. <sup>a</sup>Measured at 23 ± 1°C, pH 7.7, 0.1% (v/v) DMSO. Values at r*AgAChE* (WT and G119S), and r*hAChE* were reported previously. <sup>b</sup>Resistance ratio is calculated as  $k_i(\text{WT})/k_i(\text{G119S})$ . Standard error in the ratio is calculated according to a standard propagation of error formula.<sup>16, 18</sup> <sup>c</sup>Selectivity for inhibiting *AgAChE* (WT) vs *hAChE*, calculated as  $k_i(\text{AgAChE-WT})/k_i(\text{hAChE})$ , with standard error in the ratio calculated according to a standard propagation of error formula

Furthermore, in an effort to understand the low enzymatic resistance ratios exhibited by some of the pyrazol-4-yl carbamates in comparison to the commercial aryl methylcarbamates, our Molsoft LLC collaborators computationally modeled the tetrahedral adduct formed after the attack of active site serine on *S*-enantiomer of **99a** (the best fitting enantiomer was chosen), and terbam **28**. As can be seen in Figure 3.5, the six membered aromatic ring of terbam (**28**) is well accommodated in the active site of the susceptible

enzyme (Figure 3.5 A); however, it encounters a steric clash with the hydroxyl group of S119 (a mutated glycine to a serine at position 119) in the mutant enzyme (Figure 3.5 B). In contrast to this, *S*-enantiomer of pyrazol-4-yl methylcarbamate **99a** due to its smaller size could fit well in both the WT, and the mutant enzyme, and encounters no clash with the hydroxyl of S119 (Figure 3.5 C).

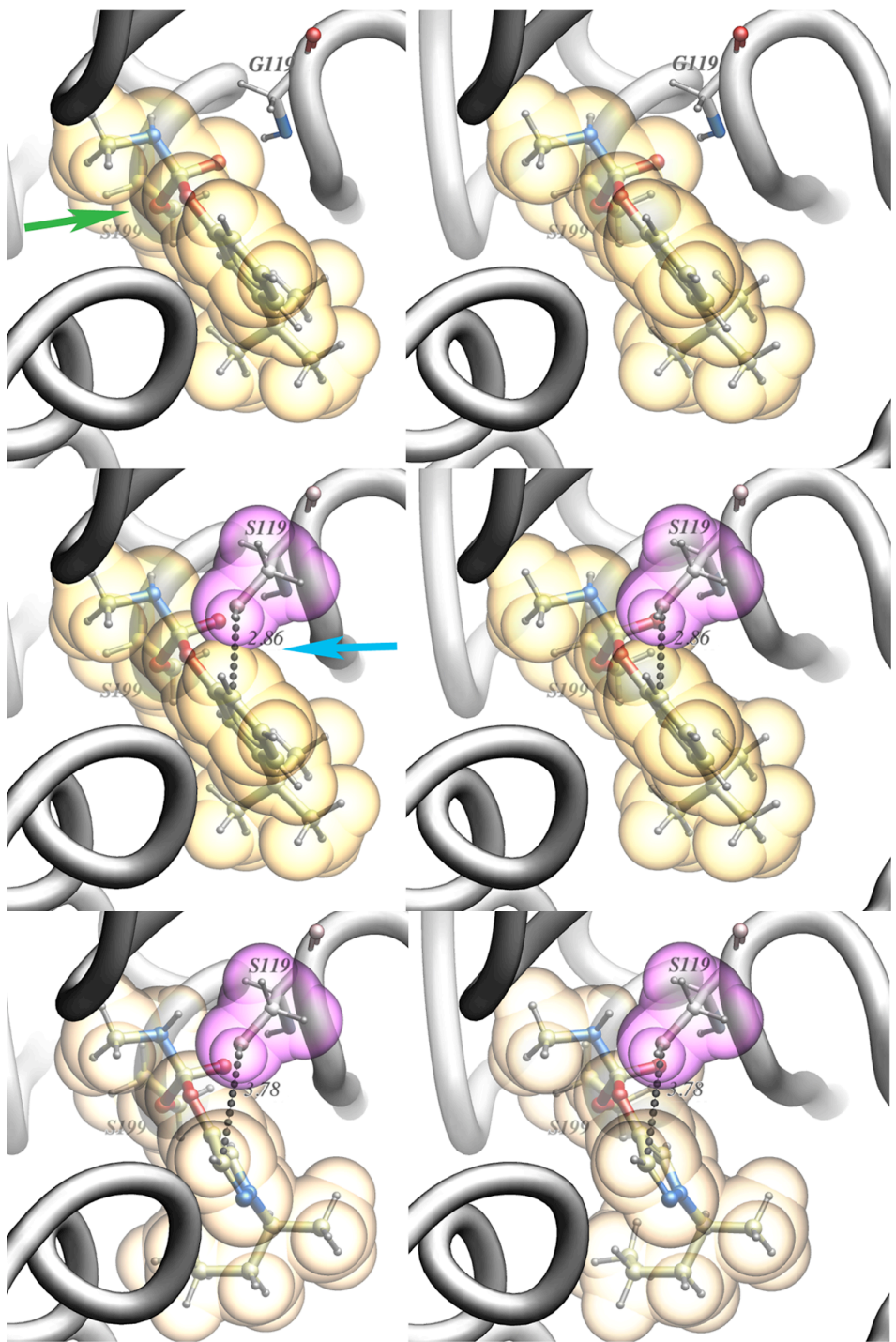
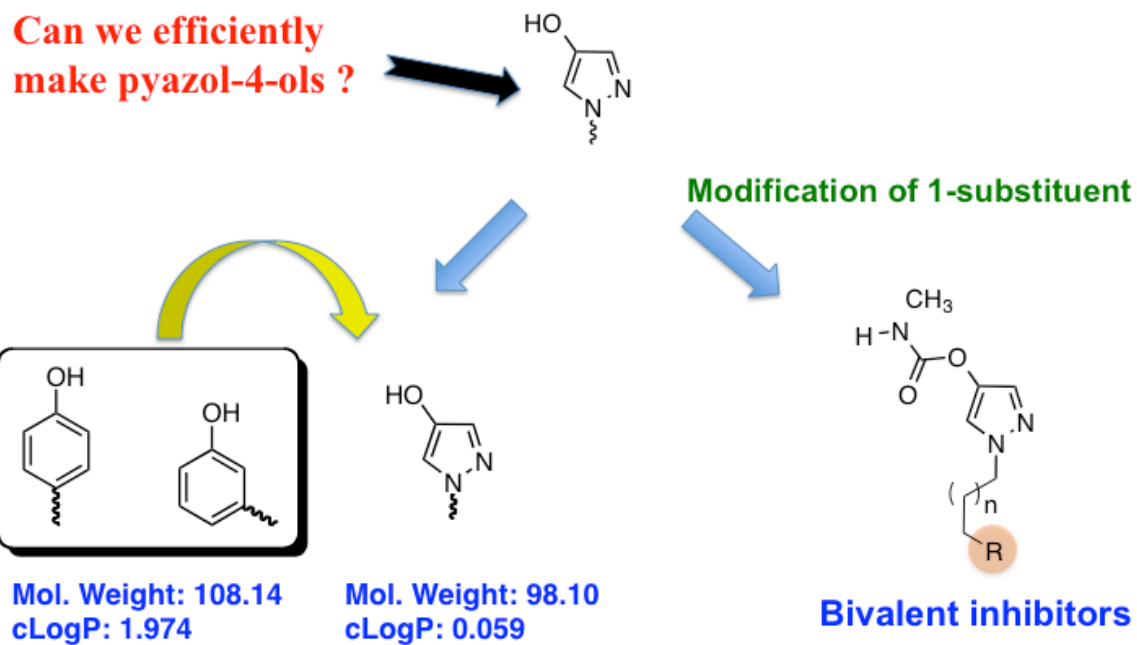


**Figure 3.5:** Computational modeling of (A) terbam (**28**) in the active site of susceptible enzyme. (B) terbam (**28**) in the active site of G119S enzyme. (C) *S*-enantiomer of pyrazol-4-yl methylcarbamate (**99a**) in the active site of G119S enzyme

### 3.6 An efficient protecting group protocol for the synthesis of pyrazol-4-yl carbamates

Pyrazol-4-yl carbamates have shown excellent toxicity towards susceptible and resistant strain of *An. gambiae*. Interestingly, these compounds have also exhibited excellent

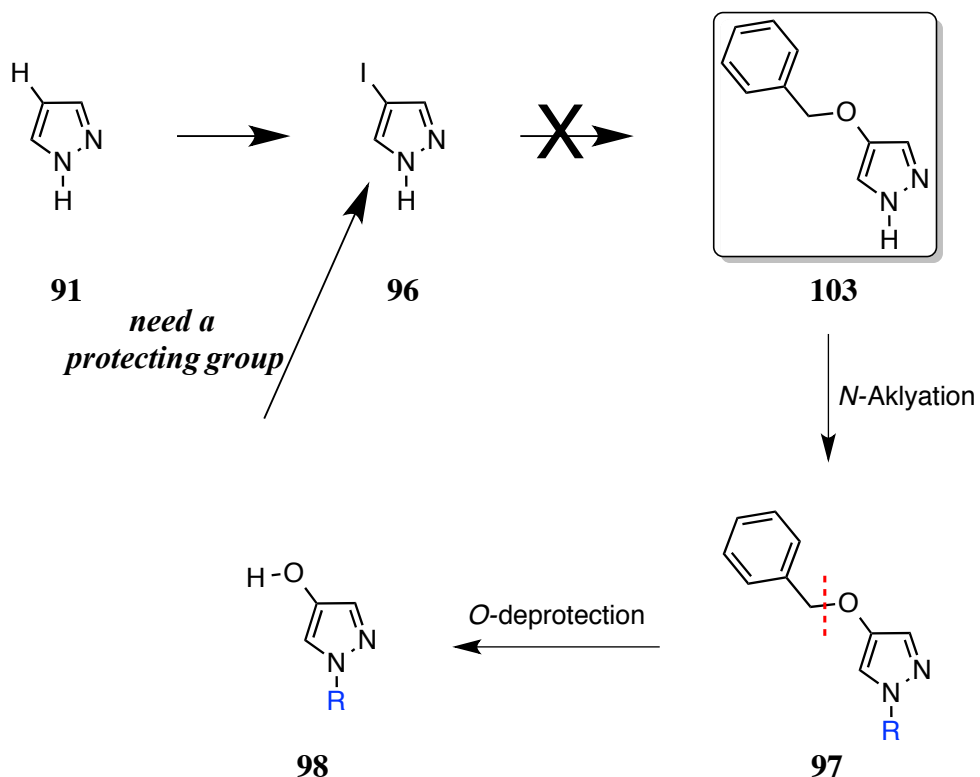
*AgAChE* vs *hAChE* selectivity (*Ag* vs *h* >100-fold, compound not shown in this thesis). Looking at the interesting mosquitocidal properties of pyrazol-4-yl carbamates, we were highly motivated to develop and test a library of these compounds against *An. gambiae*. However, a major roadblock in the way was the lengthy reaction sequence for the synthesis of *N*-substituted pyrazol-4-yl carbamates, and purification required *via* silica-gel column chromatography at every stage. An efficient synthesis for the development of precursor pyrazol-4-ols was highly desirable, which will give easy access to the *N*-substituted pyrazol-4-yl carbamates. Moreover, the pyrazol-4-ol motif is found in medicinal chemistry, such as in glucagon receptor antagonists.<sup>27-28</sup> We believe that pyrazol-4-ols can serve as a potential useful replacement for 4- and 3-hydroxy phenols in fragment based drug design. Further, an efficient synthesis of pyrazol-4-ols could later be utilized in the synthesis of a novel class of pyrazol-4-yl bivalent inhibitors. Bivalent inhibitors maintain their potency incase of single-site point mutation through multiple point of contact within the enzyme.<sup>17, 29</sup> In the proposed smaller core pyrazol-4-yl carbamates bivalent inhibitors, the heterocyclic carbamate core interacts with the catalytic active site, whereas, the R group simultaneously interacts with the anionic peripheral site of the enzyme. Since, they exert their potency through multiple-point of contact within the enzyme, we propose that any single-site resistance mutation may not dramatically affect the potency of these compounds.



**Useful for fragment-based drug design?**

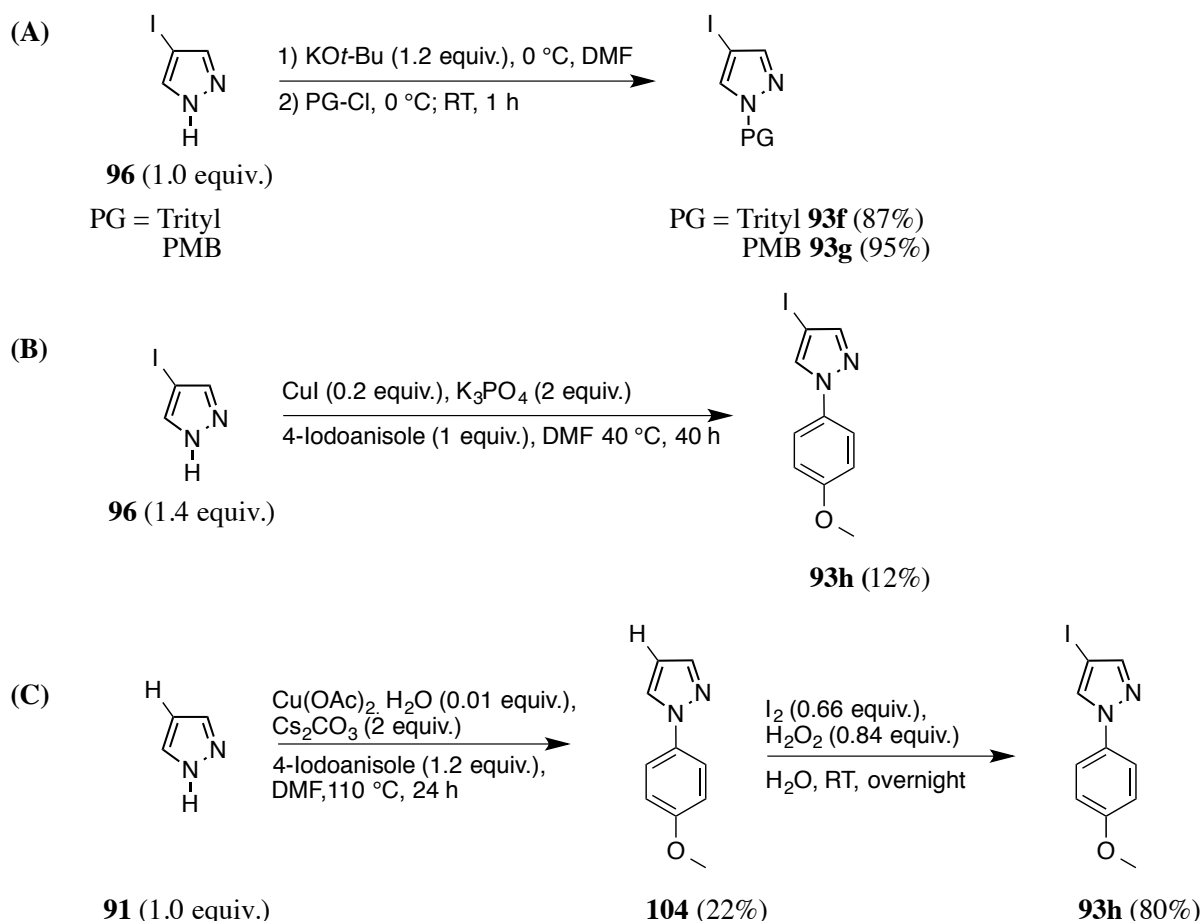
**Figure 3.6:** Proposed applicability of an efficient synthesis of pyrazol-4-ol.

Considering the objectives mentioned above, our aim is to develop an inexpensive and operationally simple protocol (eliminating the need for column-chromatography), which could be easily scaled-up if required. We envisioned that the intermediate **103** can act as a precursor to access a diverse series of *N*-substituted of pyrazol-4-yl carbamates in two steps; alkylation followed by debenzylation (Scheme 3.6). From our past work on pyrazole heterocycle, we were aware that the Cu-catalyzed *O*-benzyloxylation does not proceed with an *N*-unsubstituted pyrazole **96**. So our first step was to explore potential *N*-protecting groups, which could be easily introduced and cleaved to give us the desired intermediate (Scheme 3.6).



**Scheme 3.6:** Proposed scheme for the synthesis of pyrazol-4-ols.

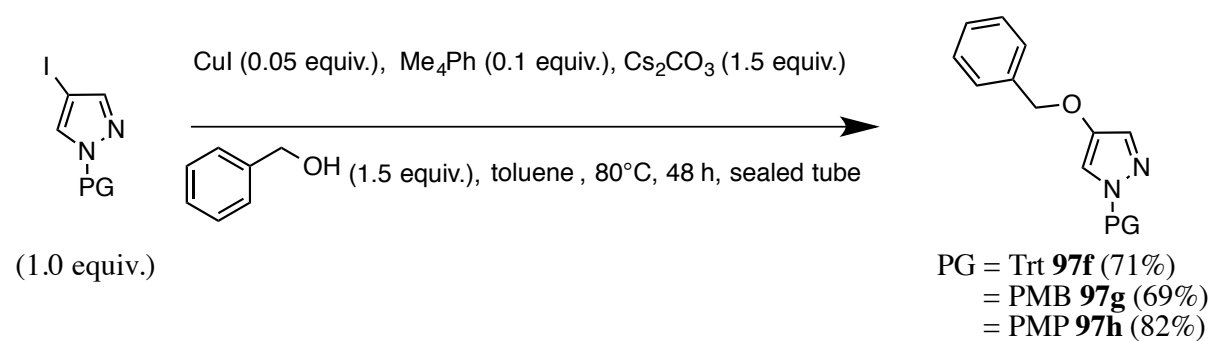
The protection of azole heterocycles (including pyrazole) has been widely explored in literature.<sup>30</sup> Few of the successfully explored protecting groups for pyrazole nitrogen include benzyl (Bz),<sup>31</sup> *p*-methoxybenzyl (PMB),<sup>32</sup> *p*-methoxyphenyl (PMP),<sup>33-35</sup> trityl (Trt),<sup>36</sup> and tosyl<sup>37</sup> group. Considering the requirement for stability of the protecting group during the basic conditions employed in our reaction sequence, we decided to explore Trt, PMB, and PMP group for the protection of pyrazole nitrogen.



**Scheme 3.7:** (A) Protection of 4-iodopyrazole using trityl, and PMB protecting group.<sup>38</sup> (B) Attempted protection of 4-iodopyrazole using PMP group.<sup>33</sup> (C) Protection of pyrazole using PMP group.<sup>35</sup>

We started the initial screening with 4-iodopyrazole (**96**) (Scheme 3.7). Various conditions to introduce the desired protecting group were explored. Trt, and PMB group could be easily introduced by treating 4-iodopyrazole with the base  $Kt\text{-OBu}$  followed by the addition of the respective chlorides.<sup>38</sup> The corresponding protected pyrazoles were obtained in high yield (87% and 95%, respectively). In contrast, the protection of pyrazole nitrogen using PMP did not proceed smoothly. *N*-protection in the presence of  $CuI$ ,  $K_3PO_4$ , and 4-iodoanisole (Scheme 3.7 B) gave the desired *N*-protected pyrazole (**93h**) in only 12% yield.<sup>33</sup> It is likely that the presence of iodo substituent in the heterocycle is not well tolerated and self-coupling occurs in addition to the desired coupling with 4-iodoanisole. In order to

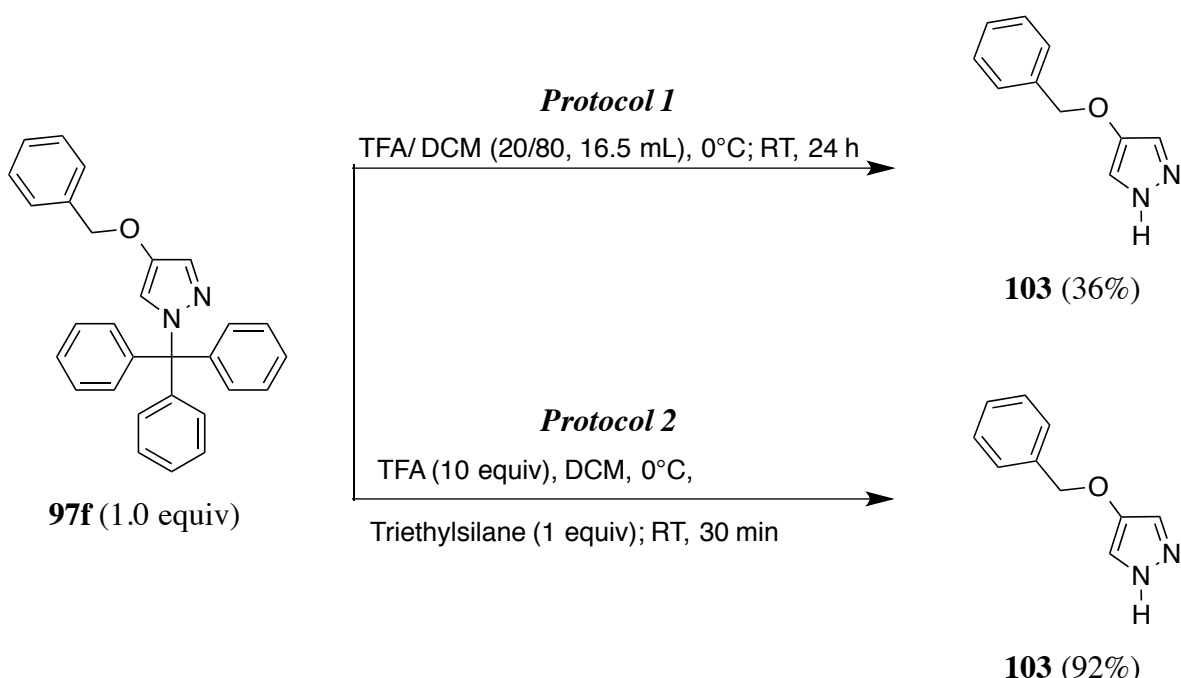
overcome this problem, the reaction was carried out with pyrazole and 4-iodoanisole in the presence of  $\text{Cu}(\text{OAc})_2 \cdot \text{H}_2\text{O}$  and  $\text{Cs}_2\text{CO}_3$  as the catalyst at  $110^\circ\text{C}$ .<sup>35</sup> Surprisingly, in-spite of a clean TLC, the desired intermediate **104** was obtained in a meager 22% yield. The following iodination of **104** proceeded smoothly to afford **93h** in high yield (80%). Next, the *O*-benzyloxylation of the *N*-protected pyrazoles proceeded smoothly and the corresponding compounds were obtained in good yields (Scheme 3.8).<sup>21</sup>



**Scheme 3.8:** Cu-catalyzed benzyloxylation of **97f**, **97g**, **97h**.<sup>21</sup>

The final step presented the challenging task of selectively cleaving the protecting group in the presence of an *O*-benzyl group. We were quite confident about selective cleavage of the trityl group (**97f**), we anticipated difficulty in the preferential cleavage of PMB (**97g**), and PMP (**97h**) group in the presence of *O*-benzyl substituent. Although, the initial attempt to cleave the trityl group using TFA in  $\text{CH}_2\text{Cl}_2$  yielded the desired de-protected product **103** in surprisingly low yield (36%) with the recovery of most of the starting material (Scheme 3.9, *Protocol 1*).<sup>39</sup> During the reaction, the color of the reaction mixture changed from colorless to yellow on addition of TFA, implying the successful formation of trityl cation. However, the color did not disappear during the course of the reaction. We speculated that the unconsumed trityl cation might be re-attaching to the pyrazole under the employed reaction conditions. In an attempt to drive the reaction to completion, triethylsilane was

added to the reaction as a trityl cation scavenger (Scheme 3.9, *Protocol 2*). Interestingly, the color of the reaction disappeared immediately on addition of triethylsilane, signifying the trapping of the trityl cation. Although, the reaction completed within 10 minutes, we let it stir for additional 30 minutes to ensure completion of reaction and the desired product was obtained in 92% yield following the *in vacuo* evaporation of the solvent, and washing the crude solid **103** with hexane and diethyl ether to remove the non-polar triphenylmethane impurity.

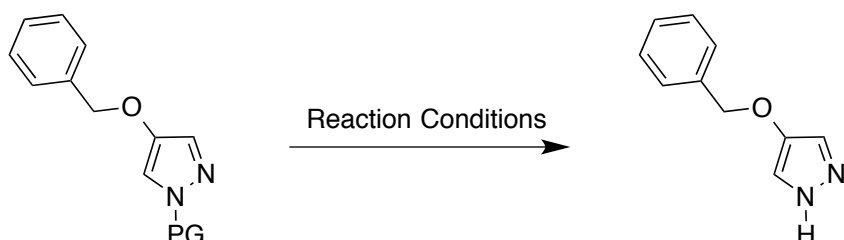


**Scheme 3.9:** De-protection of **97f** using TFA.

Next, we focused our attention on the challenging task of cleavage of PMB, and PMP group in the presence of *O*-benzyl group. To accomplish this task different reaction conditions were evaluated as shown in Table 3.12. Andersen et al. have successfully utilized TFA in the presence of anisole as the PMB cation scavenger for the de-protection of PMB-protected indoles.<sup>38</sup> Employing the above mentioned conditions to our substrate lead to the recovery of starting material in 94% yield after 24 h. Addition of catalytic amount of H<sub>2</sub>SO<sub>4</sub>,

and increasing the equivalents of TFA lead to complete conversion of starting material.<sup>40</sup> However, the <sup>1</sup>H NMR spectrum of the crude product confirmed the formation of un-desired *O*-debenzylated product. Further efforts for the selective removal of *N*-PMB over *O*-benzyl repeatedly lead to the undesired debenzylated product leaving the PMB intact (Table 3.12).<sup>41</sup>  
<sup>42</sup> In case of the PMP-protected pyrazole intermediate **97h**, the attempted deprotection reactions were messy, with no indication of formation of the desired product.

**Table 3.12:** Attempted deprotection of PMB, and PMP protected 4-(benzyloxy)-1*H*-pyrazole.



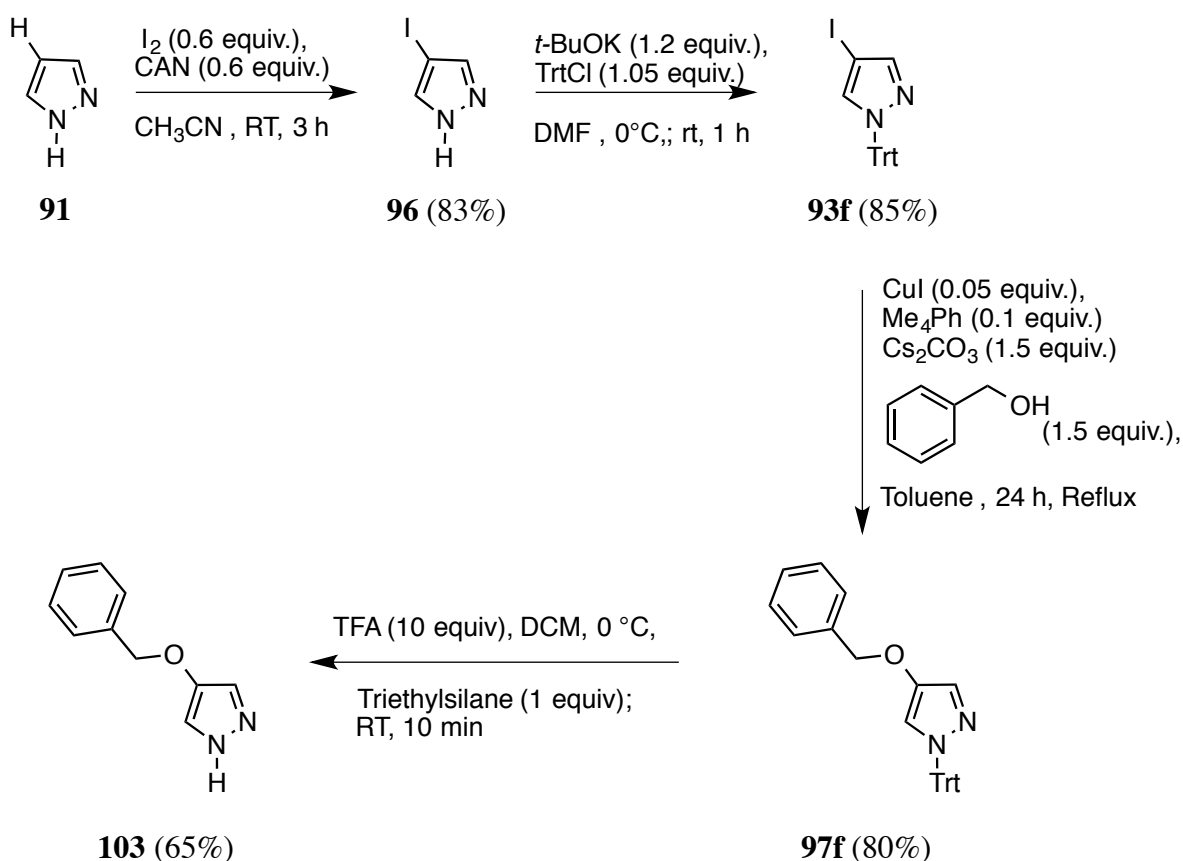
PG	Reaction Conditions	Reaction Outcome
 <b>97g</b>	1) TFA (33 equiv.), Anisole (0.5 equiv.), 60 °C, 24 h 2) TFA (41.5 equiv.), Anisole (2.9 equiv.), H <sub>2</sub> SO <sub>4</sub> (cat.), RT, 2 h 3) DDQ (1.2 equiv.), CH <sub>2</sub> Cl <sub>2</sub> :H <sub>2</sub> O (18 :1), RT, 24 h	1) 94% (starting material recovered <b>97g</b> ) 2) <i>O</i> -debenzylation ( <b>105</b> ) 3) TLC analysis indicated starting material and <i>O</i> -debenzylation after 24 h
 <b>97h</b>	(NH <sub>4</sub> ) <sub>2</sub> Ce(NO <sub>3</sub> ) <sub>6</sub> (4.8 equiv.), CH <sub>3</sub> CN:H <sub>2</sub> O (1.5:1), 0°C, 1.5 h	Messy Reaction (No indication of desired product)

One of the major goals in devising the pyrazole protecting group protocol was to demonstrate the scalability of this procedure by eliminating the need for column chromatography. Interestingly, for the trityl series, the intermediates leading up to the synthesis

of **103** were all solids. So next, we focused on further optimization of the reaction procedures and work-up to employ minimal extractions, and no chromatography.

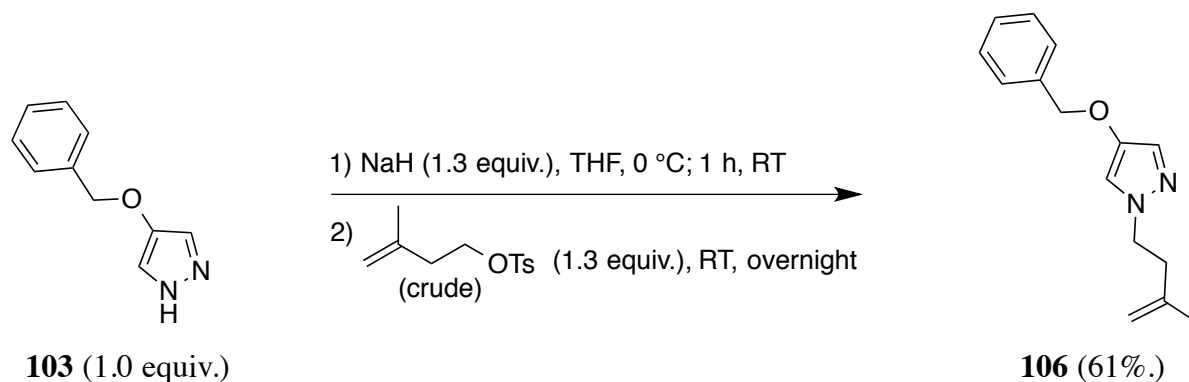
The iodination of pyrazole **91** was performed using iodine and ceric ammonium nitrate (CAN,  $\text{NH}_4\text{Ce}(\text{NO}_3)_6$ ) at room temperature for 3 h. After completion of the reaction, the reaction was filtered, followed by the *in vacuo* evaporation of the solvent ( $\text{CH}_3\text{CN}$ ). Any residual iodine was quenched using a cold saturated thiosulfate solution, which was followed by an extraction in DCM. At this point, any starting material left will be removed during aqueous work-up owing to the solubility of **91** in water. The concentration of the organic layer yielded **96** as a crude yellow solid, which was purified further by trituration in hot hexane, followed by a quick filtration yielding **96** as an off white crystalline solid in 83% yield. The *N*-protection was done in DMF utilizing *t*-BuOK, and trityl chloride. The amount of trityl chloride used was reduced to 1.05 equiv. to ensure easy removal of residual trityl chloride. The work-up was modified to meet our specified goals. Instead of an aqueous extraction, the reaction mixture was poured into cold water, stirred, and a quick filtration afforded crude trityl-protected 4-iodopyrazole (**93f**). Subsequently, the crude product obtained was recrystallized from hot hexane and THF. The recrystallized product was obtained as white crystalline solid in 85% yield (in two crops). The copper catalyzed benzyloxylation of 4-iodopyrazole was originally performed in a sealed tube as described before. We soon realized that sealed tube reactions could be a major safety issue during scale-up. So, in an attempt to simplify the protocol and improve safety, the reaction was refluxed for 24 h at atmospheric pressure. Upon cooling to room temperature the reaction mixture was passed through a plug of silica to remove any residual catalyst. *In vacuo* removal of the solvent, followed by water bath sonication of the contents, lead to precipitation of the crude product (**97f**) in the flask. We observed that the only impurities present in the crude product were the benzyl alcohol, and a second impurity, albeit in small amount, which has an

*R*f higher than the desired product. These impurities were removed by washing the crude solid with hexane and methanol (50:1) solvent mixture. Compound **97f** was obtained as an off white-solid in 80% yield, which was pure by  $^1\text{H}$  NMR and  $^{13}\text{C}$  NMR. Finally, the de-protection was performed using the previously described procedure in Scheme 3.9 (*Protocol B*). The crude solid obtained was co-evaporated in *vacuo* several times with toluene to remove any traces of TFA. The non-polar triphenylmethane impurity could be easily removed by trituration in hot hexane, followed by a quick filtration. A second trituration in hot ether followed by filtration afforded the first crop of pure product (Confirmed by  $^1\text{H}$  NMR spectroscopy). The de-protected **103** was obtained in 65% following two triturations. At this point this protocol has been successfully scaled up to 7 g.



**Scheme 3.10:** A no-column protocol for the synthesis of **103** using *N*-trityl-4-iodopyrazole.

The applicability of this protocol has been illustrated in Scheme 3.11. The synthesized product cleanly underwent reaction with crude 3-methylbut-3-en-1-yl 4-methylbenzenesulfonate to afford the desired product **106** in 61% yield after column chromatography.



**Scheme 3.11:** An illustrative example to demonstrate the applicability of synthesized **103** intermediate.

In summary, in Section 3.6, we have described a convenient, scalable, no-column approach for the synthesis of intermediate **103** from pyrazole. The trityl protecting group is stable under the Cu-catalyzed benzyloxylation reaction conditions, is easy to introduce, and can be easily cleaved. **103** can be a useful intermediate in the synthesis of pyrazol-4-yl carbamates, pyrazol-4-yl bivalent inhibitors and is worth exploring for any other modification at the pyrazole nitrogen, and at various positions on the azole ring. Currently employed methods are limited to the synthesis of pyrazol-4-ols possessing substituents at position 3- and 5- of the ring or have an *N*-aryl substituent.<sup>43</sup> The above-described method will be useful for the synthesis of 3- and 5- unsubstituted pyrazol-4-ols with varying *N*-substituents.

### 3.7 Conclusion

In conclusion, pyrazol-5-yl dimethylcarbamates and pyrazol-4-yl methylcarbamates were synthesized, and their mosquitocidal properties were evaluated against G3 and Akron

strain *An. gambiae* using WHO filter paper protocol. 1-substituted pyrazol-5-yl methylcarbamates were found to be not stable at room temperature and were not evaluated further. During preliminary investigation on these compounds, **82b** ( $R^1 = i$ -propyl) and **82c** ( $R^1 = i$ -butyl) proved toxic to susceptible G3 strain *An. gambiae*. However, they did show concomitant contact toxicity towards the resistant Akron strain *An. gambiae*. Furthermore, pyrazol-5-yl dimethylcarbamates demonstrated an undesirable inverse selectivity, that is, faster inactivation of the *hAChE* in comparison to *AgAChE*.

Among the pyrazol-4-yl methylcarbamates, compound **99a**, **99b**, and **99c** (all  $\alpha$ -branched compounds) showed good to excellent toxicity towards G3 strain. Excitingly, compound **99c** ( $R^1 = c$ -pentyl) was 2-fold more toxic than aldicarb. Although the toxicity dropped against resistant Akron strain for **99a**, **99b**, and **99c**, they were still moderately toxic. Compound **99a** and **99b** showed low cross-resistance ratios, a property, which we has seen for other class of 5-membered heterocycles explored in Chapter 2, namely 3-oxoisoxazole-2(*3H*)-carboxamide and isoxazol-3-yl carbamates. Pyrazol-4-yl methylcarbamates with longer chains were not toxic towards G3 strain. Further, the high toxicity of pyrazol-4-yl methylcarbamates (**99a**, **99b**, and **99c**) correlates well with the faster inactivation of *AgAChE* by these compounds. In-spite of this, the selectivity (*Ag* vs *h*) did not exceed 13-fold for these compounds. Due to our continued interest in pyrazol-4-yl carbamates, we have devised a convenient, scalable, no-column approach for the synthesis an intermediate **103** that can be utilized to synthesize these compounds more efficiently.

### 3.8 Bibliography

1. Kumar, H.; Saini, D.; Jain, S.; Jain, N., Pyrazole scaffold: A remarkable tool in the development of anticancer agents. *Eur. J. Med. Chem.* **2013**, *70*, 248-258.
2. Sakya, S. M.; Cheng, H.; Lundy DeMello, K. M.; Shavnya, A.; Minich, M. L.; Rast, B.; Dutra, J.; Li, C.; Rafka, R. J.; Koss, D. A.; Li, J.; Jaynes, B. H.; Ziegler, C. B.;

- Mann, D. W.; Petras, C. F.; Seibel, S. B.; Silvia, A. M.; George, D. M.; Hickman, A.; Haven, M. L.; Lynch, M. P., 5-heteroatom-substituted pyrazoles as canine cox-2 inhibitors: Part 2. Structure–activity relationship studies of 5-alkylethers and 5-thioethers. *Bioorg. Med. Chem. Lett.* **2006**, *16*, 1202-1206.
3. Ranatunge, R. R.; Garvey, D. S.; Janero, D. R.; Letts, L. G.; Martino, A. M.; Murty, M. G.; Richardson, S. K.; Young, D. V.; Zemetseva, I. S., Synthesis and selective cyclooxygenase-2 (COX-2) inhibitory activity of a series of novel bicyclic pyrazoles. *Bioorg. Med. Chem.* **2004**, *12*, 1357-1366.
4. Hainzl, D.; Casida, J. E., Fipronil insecticide: Novel photochemical desulfinylation with retention of neurotoxicity. *Proc. Natl. Acad. Sci.* **1996**, *93*, 12764-12767.
5. Cole, L. M.; Nicholson, R. A.; Casida, J. E., Action of phenylpyrazole insecticides at the GABA-gated chloride channel. *Pestic. Biochem. Physiol.* **1993**, *46*, 47-54.
6. Song, H.; Liu, Y.; Xiong, L.; Li, Y.; Yang, N.; Wang, Q., Design, synthesis, and insecticidal evaluation of new pyrazole derivatives containing imine, oxime ether, oxime ester, and dihydroisoxazoline groups based on the inhibitor binding pocket of respiratory complex I. *J. Agric. Food Chem.* **2013**, *61*, 8730-8736.
7. Song, H.; Liu, Y.; Xiong, L.; Li, Y.; Yang, N.; Wang, Q., Design, synthesis, and insecticidal activity of novel pyrazole derivatives containing  $\alpha$ -hydroxymethyl-*N*-benzyl carboxamide,  $\alpha$ -chloromethyl-*N*-benzyl carboxamide, and 4,5-dihydrooxazole moieties. *J. Agric. Food Chem.* **2012**, *60*, 1470-1479.
8. Hikiji, W.; Yamaguchi, K.; Saka, K.; Hayashida, M.; Ohno, Y.; Fukunaga, T., Acute fatal poisoning with tolfenpyrad. *J. Forensic Leg. Med.* **2013**, *20*, 962-964.
9. Lamberth, C., Pyrazole chemistry in crop protection. *Heterocycles* **2007**, *71*, 1467.
10. Gubler, K.; Margot, A.; Gysin, H., Alicyclic and heterocyclic carbamates. *J. Sci. Food Agric.* **1968**, *19*, 13-18.

11. Moreau, F.; Desroy, N.; Genevard, J. M.; Vongsouthi, V.; Gerusz, V.; Le Fralliec, G.; Oliveira, C.; Floquet, S.; Denis, A.; Escaich, S.; Wolf, K.; Busemann, M.; Aschenbrenner, A., Discovery of new gram-negative antivirulence drugs: Structure and properties of novel *E. Coli* WaaC inhibitors. *Bioorg. Med. Chem. Lett.* **2008**, *18*, 4022-4026.
12. Metcalf, R. L.; Fukuto, T. R.; Winton, M. Y., Insecticidal carbamates: Comparison of the activities of *N*-methyl and *N,N*-dimethylcarbamates of various phenols. *J. Econ. Entomol.* **1962**, *55*, 345-347.
13. Hilpert, H., Practical approaches to the matrix metalloproteinase inhibitor trocade<sup>®</sup> (Ro 32-3555) and to the TNF- $\alpha$  converting enzyme inhibitor Ro 32-7315. *Tetrahedron* **2001**, *57*, 7675-7683.
14. Dragovich, P. S.; Bertolini, T. M.; Ayida, B. K.; Li, L.-S.; Murphy, D. E.; Ruebsam, F.; Sun, Z.; Zhou, Y., Regiospecific synthesis of 1,5-disubstituted-1*H*-pyrazoles containing differentiated 3,4-dicarboxylic acid esters via suzuki coupling of the corresponding 5-trifluoromethane sulfonates. *Tetrahedron* **2007**, *63*, 1154-1166.
15. Chemistry of Heterocyclic Compounds (New York, N., United States)(Translation of Khimiya Geterotsiklicheskikh Soedinenii) Nam, N.; Grandberg, I., Condensation of *N*-3-substituted 5-pyrazolones with esters of  $\beta$ -keto acids. Synthesis of pyrano[2,3-c]pyrazol-6-ones. *Chem. Heterocycl. Compd.* **2006**, *42*, 326-330.
16. Wong, D. M.; Li, J.; Chen, Q.-H.; Han, Q.; Mutunga, J. M.; Wysinski, A.; Anderson, T. D.; Ding, H.; Carpenetti, T. L.; Verma, A.; Islam, R.; Paulson, S. L.; Lam, P. C. H.; Totrov, M.; Bloomquist, J. R.; Carlier, P. R., Select small core structure carbamates exhibit high contact toxicity to "carbamate-resistant" strain malaria mosquitoes, *Anopheles gambiae* (Akon). *PLoS One* **2012**, *7*, e46712.

17. Carlier, P. R.; Anderson, T. D.; Wong, D. M.; Hsu, D. C.; Hartsel, J.; Ma, M.; Wong, E. A.; Choudhury, R.; Lam, P. C.; Totrov, M. M.; Bloomquist, J. R., Towards a species-selective acetylcholinesterase inhibitor to control the mosquito vector of malaria, *Anopheles gambiae*. *Chem. Biol. Interact.* **2008**, *175*, 368-375.
18. Andraos, J., On the propagation of statistical errors for a function of several variables. *J. Chem. Educ.* **1996**, *73*, 150-154.
19. Hartsel, J. A.; Wong, D. M.; Mutunga, J. M.; Ma, M.; Anderson, T. D.; Wysinski, A.; Islam, R.; Wong, E. A.; Paulson, S. L.; Li, J.; Lam, P. C. H.; Totrov, M. M.; Bloomquist, J. R.; Carlier, P. R., Re-engineering aryl methylcarbamates to confer high selectivity for inhibition of *Anopheles gambiae* versus human acetylcholinesterase. *Bioorg. Med. Chem. Lett.* **2012**, *22*, 4593-4598.
20. Kim, M. M.; Ruck, R. T.; Zhao, D.; Huffman, M. A., Green iodination of pyrazoles with iodine/hydrogen peroxide in water. *Tetrahedron Lett.* **2008**, *49*, 4026-4028.
21. Altman, R. A.; Shafir, A.; Choi, A.; Lichtor, P. A.; Buchwald, S. L., An improved Cu-based catalyst system for the reactions of alcohols with aryl halides. *J. Org. Chem.* **2007**, *73*, 284-286.
22. Kogon, I., Notes- chemistry of aryl isocyanates. The influence of metal carboxylates on the aryl isocyanate-ethyl carbanilate reaction. *J. Org. Chem.* **1961**, *26*, 3004-3005.
23. Ulrich, H.; Tucker, B.; Sayigh, A. A. R., Base-catalyzed reactions of isocyanates. Synthesis of 2,4-dialkylallophanates. *J. Org. Chem.* **1967**, *32*, 3938-3941.
24. Hollingsworth, M. D.; TerBeek, K. J., Triphosgene warning. *Chem. Eng. News* 13 July, 1992, p 4.
25. Damle, S. B., Safe handling of diphosgene, triphosgene. *Chem. Eng. News* 8 Feb, 1993, p 4.

26. Duspara, P. A.; Islam, M. S.; Lough, A. J.; Batey, R. A., Synthesis and reactivity of *N*-alkyl carbamoylimidazoles: Development of *N*-methyl carbamoylimidazole as a methyl isocyanate equivalent. *J. Org. Chem.* **2012**.
27. Filipski, K. J.; Bian, J.; Ebner, D. C.; Lee, E. C. Y.; Li, J.-C.; Sammons, M. F.; Wright, S. W.; Stevens, B. D.; Didiuk, M. T.; Tu, M.; Perreault, C.; Brown, J.; Atkinson, K.; Tan, B.; Salatto, C. T.; Litchfield, J.; Pfefferkorn, J. A.; Guzman-Perez, A., A novel series of glucagon receptor antagonists with reduced molecular weight and lipophilicity. *Bioorg. Med. Chem. Lett.* **2012**, *22*, 415-420.
28. Shen, H. C.; Ding, F.-X.; Luell, S.; Forrest, M. J.; Carballo-Jane, E.; Wu, K. K.; Wu, T.-J.; Cheng, K.; Wilsie, L. C.; Krsmanovic, M. L.; Taggart, A. K.; Ren, N.; Cai, T.-Q.; Deng, Q.; Chen, Q.; Wang, J.; Wolff, M. S.; Tong, X.; Holt, T. G.; Waters, M. G.; Hammond, M. L.; Tata, J. R.; Colletti, S. L., Discovery of biaryl anthranilides as full agonists for the high affinity niacin receptor. *J. Med. Chem.* **2007**, *50*, 6303-6306.
29. Ren, J.; Nichols, C. E.; Chamberlain, P. P.; Weaver, K. L.; Short, S. A.; Chan, J. H.; Kleim, J. P.; Stammers, D. K., Relationship of potency and resilience to drug resistant mutations for GW420867X revealed by crystal structures of inhibitor complexes for wild-type, Leu100Ile, Lys101Glu, and Tyr188Cys mutant HIV-1 reverse transcriptases. *J. Med. Chem.* **2007**, *50*, 2301-2309.
30. Iddon, B.; Tønder, J. E.; Hosseini, M.; Begtrup, M., The *N*-vinyl group as a protection group of the preparation of 3(5)-substituted pyrazoles via bromine–lithium exchange. *Tetrahedron* **2007**, *63*, 56-61.
31. Katritzky, A. R.; Jayaram, C.; Socrates, V. N., Alpha-lithiation of *N*-alkyl groups in pyrazoles. *Tetrahedron* **1983**, *39*, 2023-2029.
32. Subramanyam, C.; Mallamo, J. P.; Dority, J. A.; Earley, W. G.; Kumar, V.; Aimone, L. D.; Ault, B.; Miller, M. S.; Luttinger, D. A.; DeHaven-Hudkins, D. L., Discovery

- of 6,11-ethano-12,12-diaryl-6,11-dihydrobenzo[b]quinolizinium cations, a novel class of *N*-methyl-D-aspartate antagonists. *J. Med. Chem.* **1995**, *38*, 21-27.
33. Zhu, L.; Li, G.; Luo, L.; Guo, P.; Lan, J.; You, J., Highly functional group tolerance in copper-catalyzed *N*-arylation of nitrogen-containing heterocycles under mild conditions. *J. Org. Chem.* **2009**, *74*, 2200-2202.
34. Cano, R.; Ramón, D. J.; Yus, M., Transition-metal-free O-, S-, and N-arylation of alcohols, thiols, amides, amines, and related heterocycles. *J. Org. Chem.* **2011**, *76*, 654-660.
35. Xu, Z.-L.; Li, H.-X.; Ren, Z.-G.; Du, W.-Y.; Xu, W.-C.; Lang, J.-P., Cu(OAc)<sub>2</sub>.H<sub>2</sub>O-catalyzed *N*-arylation of nitrogen-containing heterocycles. *Tetrahedron* **2011**, *67*, 5282-5288.
36. Aslanian, R.; Mutahi, M. W.; Shih, N.-Y.; McCormick, K. D.; Piwinski, J. J.; Ting, P. C.; Albanese, M. M.; Berlin, M. Y.; Zhu, X.; Wong, S.-C.; Rosenblum, S. B.; Jiang, Y.; West, R.; She, S.; Williams, S. M.; Bryant, M.; Hey, J. A., Identification of a novel, orally bioavailable histamine H3 receptor antagonist based on the 4-benzyl-(1*H*-imidazol-4-yl) template. *Bioorg. Med. Chem. Lett.* **2002**, *12*, 937-941.
37. Booker-Milburn, K. I., A convenient method for the synthesis of C-5 substituted 1-tosylpyrazoles. *Synlett* **1992**, *1992*, 327-328.
38. Anderson, E. D.; Boger, D. L., Inverse electron demand diels-alder reactions of 1,2,3-triazines: Pronounced substituent effects on reactivity and cycloaddition scope. *J. Am. Chem. Soc.* **2011**, *133*, 12285-12292.
39. Gellibert, F.; de Gouville, A.-C.; Woolven, J.; Mathews, N.; Nguyen, V.-L.; Bertho-Ruault, C.; Patikis, A.; Grygielko, E. T.; Laping, N. J.; Huet, S., Discovery of 4-[4-[3-(pyridin-2-yl)-1*H*-pyrazol-4-yl]pyridin-2-yl]-*N*-(tetrahydro-2*H*-pyran-4-yl)

- benzamide (GW788388): A potent, selective, and orally active transforming growth factor- $\beta$  type I receptor inhibitor. *J. Med. Chem.* **2006**, *49*, 2210-2221.
40. Forbes, I. T.; Johnson, C. N.; Thompson, M., Syntheses of functionalised pyrido[2,3-b]indoles. *J. Chem. Soc., Perkin Trans. 1* **1992**, 275-281.
41. Cappa, A.; Marcantoni, E.; Torregiani, E.; Bartoli, G.; Bellucci, M. C.; Bosco, M.; Sambri, L., A simple method for the selective deprotection of *p*-methoxybenzyl ethers by cerium(III) chloride heptahydrate and sodium iodide. *J. Org. Chem.* **1999**, *64*, 5696-5699.
42. Wright, J. A.; Yu, J.; Spencer, J. B., Sequential removal of the benzyl-type protecting groups PMB and NAP by oxidative cleavage using CAN and DDQ. *Tetrahedron Lett.* **2001**, *42*, 4033-4036.
43. Lamberth, C., An improved procedure for the preparation of 1-aryl-4-hydroxy-1*H*-pyrazoles *Org. Prep. Proced. Int.* **2002**, *34*, 98-102.

## Chapter 4: Future research project ideas

Acetylcholinesterase (AChE) is a member of one of the largest classes of enzymes called serine hydrolases (SH). In mammals, this class is further equally sub-divided into two subgroups; a) approximately 125 serine proteases, majorly belonging to the trypsin and chymotrypsin classes, and b) another approximately 110 metabolic serine hydrolases mostly from  $\alpha/\beta$  hydrolase class (these hydrolases are characterized by an  $\alpha/\beta$  hydrolase fold).<sup>1</sup> The later subgroup includes esterases (*e.g.* AChE), thioesterases, lipases (*e.g.* HSL), peptidases, and amidases (*e.g.* FAAH).<sup>2</sup> The catalytic mechanism is common to all serine hydrolases irrespective of the subgroups, where a conserved serine nucleophile attacks the substrate to be hydrolyzed to form an acylated enzyme.<sup>1</sup> This intermediate subsequently undergoes attack by  $H_2O$  to generate the free enzyme. Most of the serine hydrolases utilize a serine-histidine-aspartate catalytic triad, however, there are a few subgroups that employ a different catalytic triad (Serine-Serine-Lysine) or a catalytic dyad (Serine-Aspartate).<sup>3-5</sup> Nonetheless, the overall reaction remains the same. Due to this many of these serine hydrolases share a common broad-spectrum inhibitor such as carbamates and fluorophosphonates.<sup>1</sup> A wealth of information can be obtained by studying the potent inhibitors of closely related serine hydrolases. This can in turn provide the lead to new, alternate class of inhibitors that can be modified and made more individual serine hydrolase selective.

1,2,3- and 1,2,4-Triazole ureas have shown promising results as serine hydrolase inhibitors.<sup>1, 6-7</sup> Figure 4.1 shows a few of the potent triazole urea inhibitors of serine hydrolase described in literature. Particularly interesting are compound **71**, which is a potent AChE-inhibiting insecticide, and **70**, a known hormone sensitive lipase inhibitor (HSL).<sup>8</sup> HSL hydrolyses triglycerides to monoglycerides and fatty acid.<sup>8</sup> The inhibition of HSL plays a vital

role in controlling diabetes 2, where a decrease in levels of fatty acids is desired. Although HSL does not share a similar amino acid sequence homology with AChE, it does share structural similarities with the latter.<sup>9</sup> The above statement is justified by the off-target inhibition of AChE by compound **70**.<sup>8</sup> Therefore, inhibitors of HSL can provide a lead for identifying potent and selective inhibitors for AChE. Further, a few of the novel 1,2,3-triazole urea serine hydrolase (mammalian) inhibitors explored by Adibekian et al. have demonstrated better potency than aryl *N,N*-dialkylcarbamate inhibitors due to better electrophilicity imparted to the target carbonyl carbon by the leaving group. These precedents and also our own observations, where 3-oxoisoxazole-2(3*H*)-carboxamide (urea like) have exhibited faster inactivation of AChE than the isomeric carbamates make them worth exploring as *Ag*AChE inhibitors.

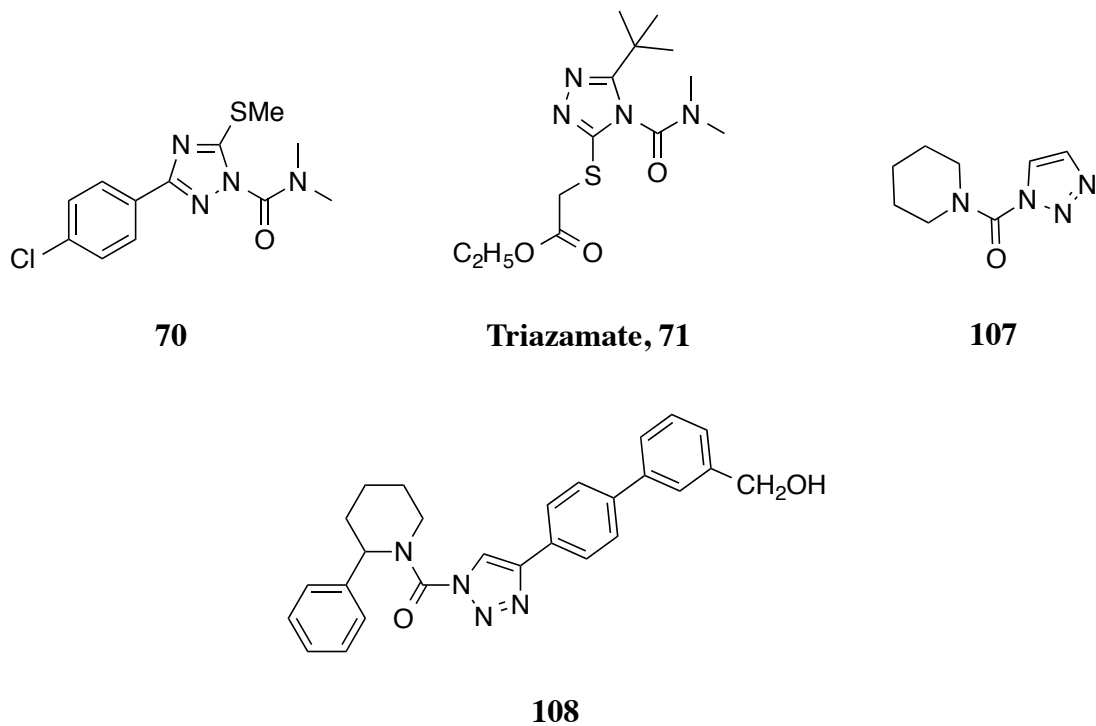
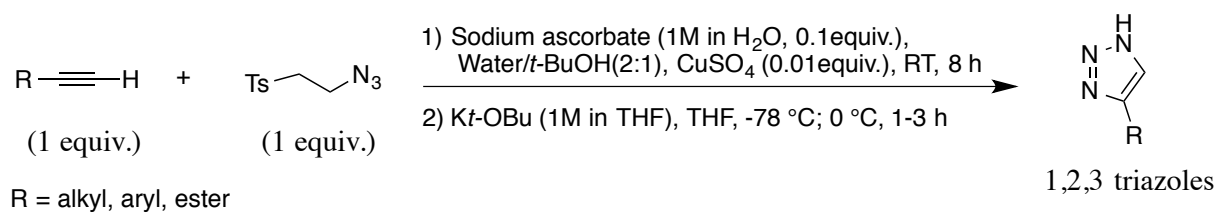


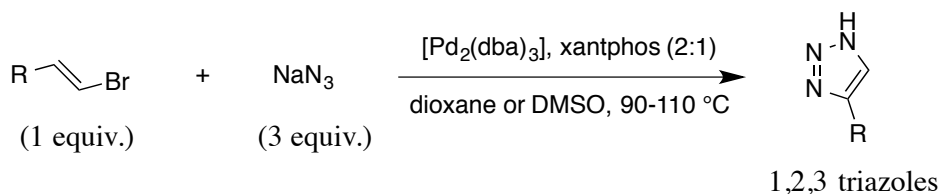
**Figure 4.1:** Potent serine hydrolase inhibitors.<sup>1, 6, 8</sup>

A 1-unsubstituted triazole would be required for the synthesis of 1,2,3- and 1,2,4-triazole ureas.  $1H$ -1,2,3-Triazoles could be prepared using the procedures given in Figure 4.2.<sup>10-11</sup> The subsequent reaction of  $1H$ -1,2,3-triazoles with the desired carbamoyl chloride can yield the desired *N*-substituted-1,2,3-triazole ureas.<sup>1</sup>

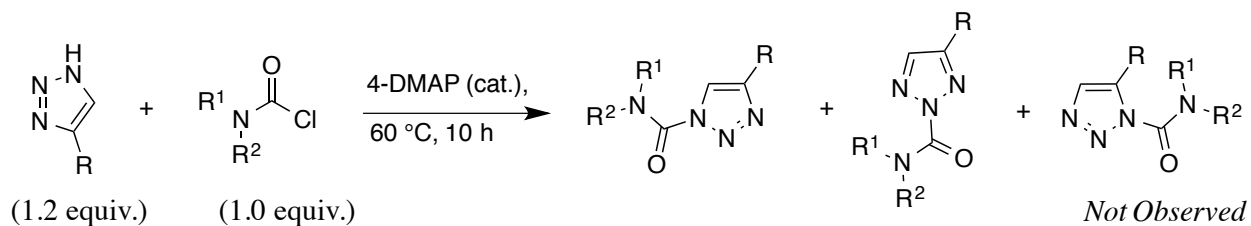
**A) Synthesis of 1*H*-1,2,3-triazoles by Cu-catalyzed cycloaddition reaction**



**B) Synthesis of 1*H*-1,2,3-triazoles by Pd-catalyzed cycloaddition reaction**



**C) Synthesis of 1*H*-1,2,3-triazole ureas**



**D) Synthesis of carbamoyl chlorides using triphosgene**

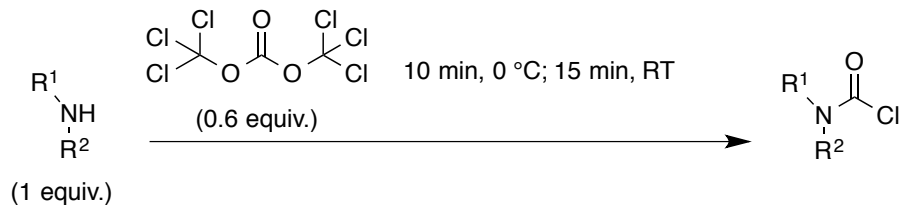
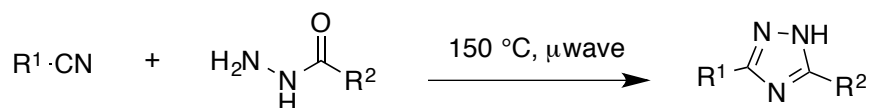


**Figure 4.2:** Schemes depicting the synthesis of desired 1*H*-1,2,3 triazole ureas.<sup>1, 10-11</sup>

Further, substituted 1*H*-1,2,4-triazoles could be synthesized using a procedure reported by Yeung et al.<sup>12</sup> (Figure 4.3) However, when aliphatic nitriles were used the reaction gave the

product in low yield. Further, the reaction to obtain the desired  $1H$ -1,2,4-triazole ureas will yield two regioisomers as shown in Figure 4.3.

**A) Synthesis of 3,5-disubstituted- $1H$ -1,2,4-triazole using hydrazides and nitriles.**



**B) Synthesis of  $1H$ -1,2,4-triazole ureas**

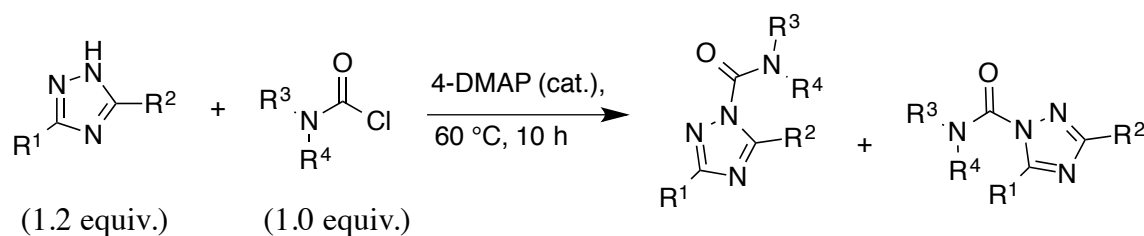


**Figure 4.3:** Synthesis of 3,5-disubstituted- $1H$ -1,2,4-triazole <sup>12</sup>

## Bibliography

1. Adibekian, A.; Martin, B. R.; Wang, C.; Hsu, K. L.; Bachovchin, D. A.; Niessen, S.; Hoover, H.; Cravatt, B. F., Click-generated triazole ureas as ultrapotent in vivo-active serine hydrolase inhibitors. *Nat. Chem. Biol.* **2011**, *7*, 469-478.
2. Simon, G. M.; Cravatt, B. F., Activity-based proteomics of enzyme superfamilies: Serine hydrolases as a case study. *J. Biol. Chem.* **2010**, *285*, 11051-11055.
3. Holmquist, M., Alpha beta-hydrolase fold enzymes structures, functions and mechanisms. *Curr. Protein Pept. Sci.* **2000**, *1*, 209-235.
4. Otrubova, K.; Ezzili, C.; Boger, D. L., The discovery and development of inhibitors of fatty acid amide hydrolase (FAAH). *Bioorg. Med. Chem. Lett.* **2011**, *21*, 4674-4685.

5. Kienesberger, P. C.; Oberer, M.; Lass, A.; Zechner, R., Mammalian patatin domain containing proteins: A family with diverse lipolytic activities involved in multiple biological functions. *J. Lipid Res.* **2009**, *50*, S63-S68.
6. Hsu, K.-L.; Tsuboi, K.; Chang, J. W.; Whitby, L. R.; Speers, A. E.; Pugh, H.; Cravatt, B. F., Discovery and optimization of piperidyl-1,2,3-triazole ureas as potent, selective, and in vivo-active inhibitors of  $\alpha/\beta$ -hydrolase domain containing 6 (ABHD6). *J. Med. Chem.* **2013**, *56*, 8270-8279.
7. Aaltonen, N.; Savinainen, Juha R.; Ribas, Casandra R.; Rönkkö, J.; Kuusisto, A.; Korhonen, J.; Navia-Paldanius, D.; Häyrynen, J.; Takabe, P.; Käsnänen, H.; Pantsar, T.; Laitinen, T.; Lehtonen, M.; Pasonen-Seppänen, S.; Poso, A.; Nevalainen, T.; Laitinen, Jarmo T., Piperazine and piperidine triazole ureas as ultrapotent and highly selective inhibitors of monoacylglycerol lipase. *Chem. Biol.* **2013**, *20*, 379-390.
8. Ebdrup, S.; Sørensen, L. G.; Olsen, O. H.; Jacobsen, P., Synthesis and structure–activity relationship for a novel class of potent and selective carbamoyl-triazole based inhibitors of hormone sensitive lipase. *J. Med. Chem.* **2003**, *47*, 400-410.
9. Contreras, J. A.; Karlsson, M.; Østerlund, T.; Laurell, H.; Svensson, A.; Holm, C., Hormone-sensitive lipase is structurally related to acetylcholinesterase, bile salt-stimulated lipase, and several fungal lipases: Building of a three-dimentional model for the catalytic domain of harmone-sensitive lipase. *J. Biol. Chem.* **1996**, *271*, 31426-31430.
10. Yap, A. H.; Weinreb, S. M., B-tosylethylazide: A useful synthon for preparation of n-protected 1,2,3-triazoles via click chemistry. *Tetrahedron Lett.* **2006**, *47*, 3035-3038.

11. Barluenga, J.; Valdés, C.; Beltrán, G.; Escribano, M.; Aznar, F., Developments in Pd catalysis: Synthesis of 1*H*-1,2,3-triazoles from sodium azide and alkenyl bromides. *Angew. Chem. Int. Ed.* **2006**, *45*, 6893-6896.
12. Yeung, K.-S.; Farkas, M. E.; Kadow, J. F.; Meanwell, N. A., A base-catalyzed, direct synthesis of 3,5-disubstituted 1,2,4-triazoles from nitriles and hydrazides. *Tetrahedron Lett.* **2005**, *46*, 3429-3432.

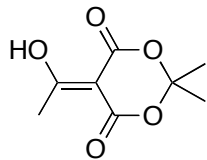
## **Chapter 5: Experimental procedures and analytical data for Chapter 2**

### **5.1 Materials**

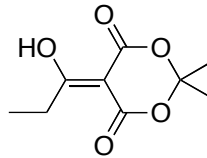
NMR spectra were obtained on JEOL Eclipse-plus 500 MHz MHz spectrometer at 500 ( $^1\text{H}$ ) and 126 ( $^{13}\text{C}$ ) MHz or Unity-plus 400 at 400 ( $^1\text{H}$ ) and 101 ( $^{13}\text{C}$ ) MHz. The chemical shifts are reported in  $\delta$  (ppm), and coupling constants are given in Hz. High-resolution ESI mass spectra were obtained on an Agilent 6220 accurate mass TOF LC/MS. X-ray data collection routine, unit cell refinement, and data processing were carried out with the program CrysAlisPro. The structure was solved using SHELXS-2013 and refined using SHELXL-2013 via OLEX2. THF for moisture sensitive reactions was distilled from sodium-benzophenone. Other dry solvents were purchased from EMD Millipore and were used without any further purification. Column chromatography was performed using Silica gel (ZEOPrep 60 ECO 40-63  $\mu$ ) was purchased from AIC. Reagents were purchased mainly from Sigma Aldrich and were used as received.

### **5.2 General procedure for the synthesis of acyl Meldrum's acids 44a-f, k, m, o using acid chlorides**

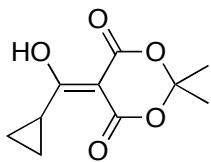
**Method A.** *Adapted from the procedure of Sorensen et al.<sup>1</sup>:* To a solution of Meldrum's acid in dichloromethane at 0 °C was added pyridine drop wise, and the resulting solution was stirred for 15 minutes. The corresponding acid chloride was added to this reaction mixture. Thereafter, the reaction was stirred for 1.5 h at 0 °C, and for an additional 1.5 h at room temperature. The reaction was quenched with 2 M hydrochloric acid, and extracted with dichloromethane. The combined organic layers were dried over sodium sulfate, filtered, and concentrated in vacuo. The residue was purified by silica gel chromatography using a gradient from 5-10% ethyl acetate in hexane, 1% acetic acid to yield acyl Meldrum's acids (**44a-f, k, m, o**).



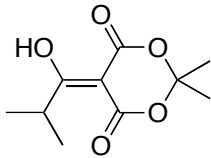
5-(1-hydroxyethylidene)-2,2-dimethyl-1,3-dioxane-4,6-dione (44a): Prepared using the general procedure above (*Method A*) from Meldrum's acid (500 mg, 3.47 mmol), acetyl chloride (0.25 mL, 3.47 mmol), pyridine (0.71 mL, 6.94 mmol), and CH<sub>2</sub>Cl<sub>2</sub> (4.2 mL). Aqueous workup, and silica gel chromatography (5-10% ethyl acetate in hexane, 1% acetic acid) afforded **44a** as a white solid (536 mg, 83%). <sup>1</sup>H NMR (500 MHz, Chloroform-*d*) δ 15.12 (s, 1H), 2.67 (s, 3H), 1.73 (s, 6H). <sup>13</sup>C NMR (126 MHz, Chloroform-*d*) δ 194.77, 170.34, 160.62, 105.07, 91.98, 27.00, 23.68. The <sup>1</sup>H NMR and <sup>13</sup>C NMR for this compound matches the reported literature.<sup>1</sup> (**AA-IV-90**)



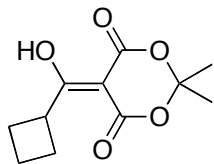
5-(1-hydroxypropylidene)-2,2-dimethyl-1,3-dioxane-4,6-dione (44b): Prepared using the general procedure above (*Method A*) above from Meldrum's acid (1.00 g, 6.94 mmol), propionyl chloride (0.60 mL, 6.94 mmol), pyridine (1.12 mL, 13.8 mmol), and CH<sub>2</sub>Cl<sub>2</sub> (10.0 mL). Aqueous workup, and silica gel chromatography (5-10% ethyl acetate in hexane, 1% acetic acid) afforded **44b** as a white solid (891 mg, 65%). <sup>1</sup>H NMR (500 MHz, Chloroform-*d*) δ 15.38 (s, 1H), 3.11 (q, *J* = 7.6 Hz, 2H), 1.73 (s, 6H), 1.25 (t, *J* = 7.6 Hz, 3H). <sup>13</sup>C NMR (126 MHz, Chloroform-*d*) δ 199.12, 170.77, 160.33, 104.98, 91.04, 29.63, 26.94, 9.85. The <sup>1</sup>H NMR and <sup>13</sup>C NMR for this compound matches the reported literature.<sup>1</sup> (**AA-I-177**)



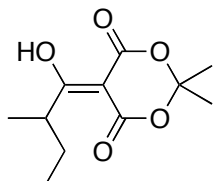
5-(cyclopropyl(hydroxy)methylene)-2,2-dimethyl-1,3-dioxane-4,6-dione (44c): Prepared using the general procedure above (*Method A*) from Meldrum's acid (500 mg, 3.46 mmol), cyclopropyl chloride (0.32 mL, 3.46 mmol), pyridine (0.56 mL, 6.93 mmol), and CH<sub>2</sub>Cl<sub>2</sub> (5.0 mL). Aqueous work up, and silica gel chromatography (5-10% ethyl acetate in hexane, 1% acetic acid) afforded **44c** as a yellowish oil (462 mg, 63%). <sup>1</sup>H NMR (500 MHz, Chloroform-*d*) δ 15.41 (s, 1H), 3.54-3.44 (m, 1H), 1.74 (s, 6H), 1.49-1.41 (m, 2H), 1.32-1.20 (m, 2H). <sup>13</sup>C NMR (126 MHz, Chloroform-*d*) δ 198.05, 170.73, 161.36, 104.76, 91.18, 26.86, 15.74, 14.34. The <sup>1</sup>H NMR and <sup>13</sup>C NMR for this compound matches the reported literature.<sup>1</sup> (**AA-I-159**)



5-(1-hydroxy-2-methylpropylidene)-2,2-dimethyl-1,3-dioxane-4,6-dione (44d): Prepared using the general procedure above (*Method A*) from Meldrum's acid (2.00 g, 13.9 mmol), isobutyryl chloride (1.46 mL, 13.9 mmol), pyridine (2.24 mL, 27.7 mmol), and CH<sub>2</sub>Cl<sub>2</sub> (17.0 mL). Aqueous workup, and silica gel chromatography (5-10% ethyl acetate in hexane, 1% acetic acid) afforded **44d** as a yellowish oil (1.77 g, 60%). <sup>1</sup>H NMR (500 MHz, Chloroform-*d*) δ 15.53 (s, 1H), 4.08 (hept, *J* = 6.8 Hz, 1H), 1.73 (s, 6H), 1.23 (d, *J* = 6.8 Hz, 6H). <sup>13</sup>C NMR (126 MHz, Chloroform-*d*) δ 202.56, 171.07, 160.15, 104.83, 90.28, 33.15, 26.91, 19.23. The <sup>1</sup>H NMR and <sup>13</sup>C NMR for this compound matches the reported literature.<sup>1</sup> (**AA-III-48**)

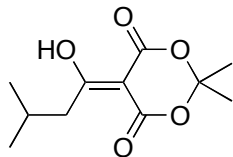


5-(cyclobutyl(hydroxy)methylene)-2,2-dimethyl-1,3-dioxane-4,6-dione (44e): Prepared using the general procedure above (*Method A*) from Meldrum's acid (500 mg, 3.47 mmol), cyclobutane carbonyl chloride (0.40 mL, 3.47 mmol), pyridine (0.71 mL, 6.94 mmol), and CH<sub>2</sub>Cl<sub>2</sub> (4.2 mL). Aqueous work up and silica gel chromatography (5-10% ethyl acetate in hexane, 1% acetic acid) afforded **44e** as a yellowish oil (604 mg, 77%). <sup>1</sup>H NMR (500 MHz, Chloroform-*d*) δ 15.53 (s, 1H), 4.47 (quintet, *J* = 8.5 Hz, 1H), 2.42-2.27 (m, 4H), 2.12-2.01 (m, 1H), 1.96-1.86 (m, 1H), 1.72 (s, 6H). <sup>13</sup>C NMR (126 MHz, Chloroform-*d*) δ 198.27, 170.85, 159.95, 104.82, 89.78, 39.29, 26.77, 25.35, 17.95. HRMS (ESI) calcd for C<sub>11</sub>H<sub>14</sub>O<sub>5</sub> [M-H]<sup>-</sup> 225.0768, found 225.0759. (AA-IV-69)

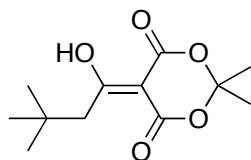


5-(1-hydroxy-2-methylbutylidene)-2,2-dimethyl-1,3-dioxane-4,6-dione (44f): Prepared using the general procedure above (*Method A*) from Meldrum's acid (3.00 g, 20.8 mmol), 2-methyl butyryl chloride (2.58 mL, 20.8 mmol), pyridine (3.36 mL, 41.6 mmol), and CH<sub>2</sub>Cl<sub>2</sub> (25.0 mL). Aqueous work up, and silica gel chromatography (5-10% ethyl acetate in hexane, 1% acetic acid) afforded **44f** as a yellowish oil (2.44 g, 52%). <sup>1</sup>H NMR (500 MHz, Chloroform-*d*) δ 15.48 (s, 1H), 3.97 (heptet, *J* = 6.9 Hz, 1H), 1.81-1.74 (m, 1H), 1.73 (s, 6H), 1.54 (doublet of quintet, *J* = 14.6, 7.3 Hz, 1H), 1.21 (d, *J* = 6.8 Hz, 3H), 0.93 (t, *J* = 7.3 Hz, 3H). <sup>13</sup>C NMR (126 MHz, Chloroform-*d*) δ

202.15, 170.95, 160.30, 104.77, 91.28, 39.53, 27.27, 26.97, 26.78, 17.09, 11.85. HRMS (ESI) calcd for C<sub>11</sub>H<sub>16</sub>O<sub>5</sub> [M+Na]<sup>+</sup> 251.0895, found 251.1618. (**AA-III-26**)

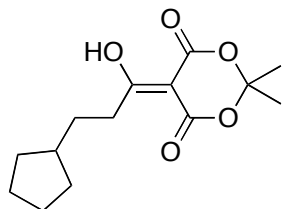


**5-(1-hydroxy-3-methylbutylidene)-2,2-dimethyl-1,3-dioxane-4,6-dione (44k):** Prepared using the general procedure above (*Method A*) from Meldrum's acid (300 mg, 2.08 mmol), isovaleryl chloride (0.25 mL, 2.08 mmol), pyridine (0.34 mL, 4.16 mmol), and CH<sub>2</sub>Cl<sub>2</sub> (2.5 mL). Aqueous work up, and silica gel chromatography (5-10% ethyl acetate in hexane, 1% acetic acid) afforded **44k** as a yellowish oil (274 mg, 58%). <sup>1</sup>H NMR (500 MHz, Chloroform-*d*) δ 15.30 (s, 1H), 2.98 (d, *J* = 7.1 Hz, 2H), 2.26-2.14 (m, 1H), 1.73 (s, 6H), 1.01 (d, *J* = 6.7 Hz, 6H). <sup>13</sup>C NMR (126 MHz, Chloroform-*d*) δ 197.72, 170.71, 160.42, 104.84, 92.04, 43.98, 27.54, 26.95, 22.67. HRMS (ESI) calcd for C<sub>11</sub>H<sub>16</sub>O<sub>5</sub> [M-H]<sup>-</sup> 227.0925, found 227.0939. (**AA-IV-72**)



**5-(1-hydroxy-3,3-dimethylbutylidene)-2,2-dimethyl-1,3-dioxane-4,6-dione (44m):** Prepared using the general procedure above (*Method A*) from Meldrum's acid (500 mg, 3.47 mmol), cyclopentane propionyl chloride (0.49 mL, 3.47 mmol), pyridine (0.71 mL, 6.94 mmol), and CH<sub>2</sub>Cl<sub>2</sub> (4.0 mL). Aqueous work up, and silica gel chromatography (5-10% ethyl acetate in hexane, 1% acetic acid) afforded **44m** as an off white solid (377 mg, 45%). <sup>1</sup>H NMR (500 MHz, Chloroform-*d*) δ 15.38 (s, 1H), 3.12 (s, 2H), 1.73 (s, 6H), 1.07 (s, 9H). <sup>13</sup>C NMR (126 MHz,

Chloroform-*d*) δ 196.89, 170.58, 160.54, 104.44, 93.00, 46.38, 34.00, 30.02, 26.83. The <sup>1</sup>H NMR and <sup>13</sup>C NMR for this compound matches the reported literature.<sup>1</sup> (**AA-IV-122**)

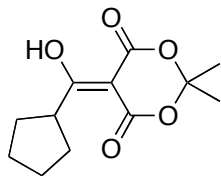


**5-(3-cyclopentyl-1-hydroxypropylidene)-2,2-dimethyl-1,3-dioxane-4,6-dione (44o):** Prepared using the general procedure above (*Method A*) from Meldrum's acid (1.50 g, 10.4 mmol), cyclopentane propionyl chloride (1.59 mL, 10.4 mmol), pyridine (2.12 mL, 20.8 mmol), and CH<sub>2</sub>Cl<sub>2</sub> (13.0 mL). However, the reaction was stirred at room temperature for 3.5 h instead of 1.5 h for this particular substrate. Aqueous workup and silica gel chromatography (5-10% ethyl acetate in hexane, 1% acetic acid) afforded **44o** as a yellowish oil (2.42 mg, 87%). <sup>1</sup>H NMR (500 MHz, Chloroform-*d*) δ 15.27 (s, 1H), 3.09-3.04 (m, 2H), 1.91-1.75 (m, 3H), 1.73 (s, 6H), 1.72-1.67 (m, 2H), 1.66-1.57 (m, 2H), 1.57-1.47 (m, 2H), 1.20-1.08 (m, 2H). <sup>13</sup>C NMR (126 MHz, Chloroform-*d*) δ 198.59, 170.73, 160.31, 104.89, 91.28, 40.13, 35.36, 32.56, 26.96, 25.31. HRMS (ESI) calcd for C<sub>14</sub>H<sub>20</sub>O<sub>5</sub> [M-H]<sup>-</sup> 267.1238, found 267.1228. (**AA-IV-57**)

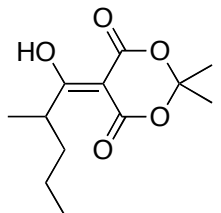
### 5.3 General procedure for the synthesis of acyl Meldrum's acids 44g-j, l, n using acids

**Method B.** *Adapted from the procedure of Sorensen et al.*<sup>1</sup>: Meldrum's acid and corresponding acid were dissolved in DMF, and cooled to 0 °C. To this solution was added diethyl cyanophosphonate and triethylamine drop wise. The mixture was allowed to stir at 0 °C for 30 minutes followed by 16 h at room temperature. The reaction was quenched with 2 M hydrochloric acid and extracted twice with ethyl acetate. The combined organic extracts were washed with brine, and dried over sodium sulfate. The solution was filtered, and concentrated in

vacuo. The residue was purified by silica gel chromatography using a gradient from 5-10% ethyl acetate in hexane, 1% acetic acid to yield acyl Meldrum's acids (**44g-j, l, n**).

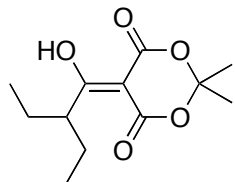


5-(cyclopentyl(hydroxy)methylene)-2,2-dimethyl-1,3-dioxane-4,6-dione (44g): Prepared using the general procedure above (*Method B*) from Meldrum's acid (500 mg, 3.47 mmol), cyclopentanoic acid (0.38 mL, 3.47 mmol), diethyl cyanophosphonate (0.58 mL, 3.82 mmol), triethylamine (1.52 mL, 10.7 mmol), and DMF (7.2 mL). Aqueous work up, and silica gel chromatography (5-10% ethyl acetate in hexane, 1% acetic acid) afforded **44g** as an off white solid (721 mg, 86 %); mp 68.8-70.7 °C. <sup>1</sup>H NMR (500 MHz, Chloroform-*d*) δ 15.51 (s, 1H), 4.24-4.17 (m, 1H), 2.08-1.98 (m, 2H), 1.88-1.75 (m, 5H), 1.73 (s, 7H), 1.71-1.66 (m, 1H). <sup>13</sup>C NMR (126 MHz, Chloroform-*d*) δ 201.61, 171.00, 160.38, 104.77, 90.83, 43.90, 31.11, 26.91, 26.63. HRMS (ESI) calcd for C<sub>12</sub>H<sub>16</sub>O<sub>5</sub> [M-H]<sup>-</sup> 239.0925, found 239.0935. (**AA-IV-75**)

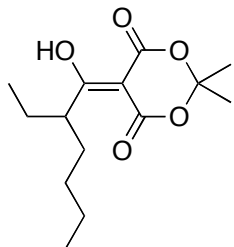


5-(1-hydroxy-2-methylpentylidene)-2,2-dimethyl-1,3-dioxane-4,6-dione (44h): Prepared using the general procedure above (*Method B*) from Meldrum's acid (3.00 g, 20.8 mmol), 2-methyl valeric acid (2.60 mL, 20.8 mmol), diethyl cyanophosphonate (3.47 mL, 22.9 mmol), triethylamine (8.99 mL, 64.6 mmol), and DMF (25.0 mL). Aqueous work up, and silica gel

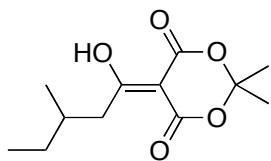
chromatography (5-10% ethyl acetate in hexane, 1% acetic acid) afforded **44h** as a yellowish oil (3.96 g, 79 %). <sup>1</sup>H NMR (500 MHz, Chloroform-*d*) δ 15.46 (s, 1H), 4.05 (heptet, *J* = 6.8 Hz, 1H), 1.71 (s, 6H), 1.50-1.24 (m, 4H), 1.20 (d, *J* = 6.8 Hz, 3H), 0.89 (t, *J* = 7.3 Hz, 3H). <sup>13</sup>C NMR (126 MHz, Chloroform-*d*) δ 202.18, 170.91, 160.23, 104.71, 91.11, 37.80, 36.23, 26.94, 26.73, 20.58, 17.47, 14.09. HRMS (ESI) calcd for C<sub>12</sub>H<sub>18</sub>O<sub>5</sub> [M-H]<sup>-</sup> 241.1081, found 241.1091. (**AA-IV-33**)



5-(2-ethyl-1-hydroxybutylidene)-2,2-dimethyl-1,3-dioxane-4,6-dione (44i): Prepared using the general procedure above (*Method B*) from Meldrum's acid (2.00 g, 13.9 mmol), 2-ethylbutyric acid (1.75 mL, 13.9 mmol), diethyl cyanophosphonate (2.32 mL, 15.3 mmol), triethylamine (5.99 mL, 43.0 mmol), and DMF (28.8 mL). Aqueous workup and silica gel chromatography (5-10% ethyl acetate in hexane, 1% acetic acid) afforded **44i** as a yellowish oil (1.65 g, 49 %). <sup>1</sup>H NMR (500 MHz, Chloroform-*d*) δ 15.43 (s, 1H), 4.02-3.93 (m, 1H), 1.73 (s, 6H), 1.77-1.68 (m, 2H), 1.68-1.58 (m, 2H), 0.92 (t, *J* = 7.5 Hz, 6H). <sup>13</sup>C NMR (126 MHz, Chloroform-*d*) δ 201.64, 170.75, 160.49, 104.70, 92.96, 46.15, 26.87, 25.86, 11.83. HRMS (ESI) calcd for C<sub>12</sub>H<sub>18</sub>O<sub>5</sub> [M-H]<sup>-</sup> 242.1116, found 242.1096. (**AA-IV-111**)

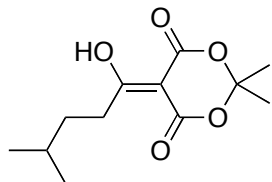


5-(2-ethyl-1-hydroxyhexylidene)-2,2-dimethyl-1,3-dioxane-4,6-dione (44j): Prepared using the general procedure above (*Method B*) from Meldrum's acid (2.00 g, 13.9 mmol), 2-ethylhexanoic acid (2.21 mL, 13.9 mmol), diethyl cyanophosphonate (2.32 mL, 15.3 mmol), triethylamine (5.99 mL, 43.0 mmol), and DMF (28.8 mL). Aqueous work up, and silica gel chromatography (5-10% ethyl acetate in hexane, 1% acetic acid) afforded **44j** as a yellowish oil (2.82 g, 75 %).  
<sup>1</sup>H NMR (500 MHz, Chloroform-*d*) δ 15.42 (s, 1H), 4.04 (tt, *J* = 8.7, 5.6 Hz, 1H), 1.73 (s, 6H), 1.72-1.52 (m, 4H), 1.34-1.18 (m, 4H), 0.91 (t, *J* = 7.5 Hz, 3H), 0.87 (t, *J* = 7.1 Hz, 3H). <sup>13</sup>C NMR (126 MHz, Chloroform-*d*) δ 201.77, 170.76, 160.48, 104.68, 92.85, 44.64, 32.50, 29.62, 26.89, 26.85, 26.37, 22.88, 14.05, 11.84. HRMS (ESI) calcd for C<sub>14</sub>H<sub>22</sub>O<sub>5</sub> [M-H]<sup>-</sup> 269.1394, found 269.1421. (**AA-II-140**)



5-(1-hydroxy-3-methylpentylidene)-2,2-dimethyl-1,3-dioxane-4,6-dione (44l): Prepared using the general procedure above (*Method B*) from Meldrum's acid (300 mg, 2.08 mmol), 3-methylvaleric acid (0.26 mL, 2.08 mmol), diethyl cyanophosphonate (0.35 mL, 2.29 mmol), triethylamine (0.86 mL, 6.45 mmol), and DMF (4.3 mL). Aqueous work up, and silica gel chromatography (5-10% ethyl acetate in hexane, 1% acetic acid) afforded **44l** as a yellowish oil (393 mg, 78 %). <sup>1</sup>H NMR (500 MHz, Chloroform-*d*) δ 15.31 (s, 1H), 3.08 (dd, *J* = 13.4, 7.2 Hz,

1H), 2.91 (dd,  $J$  = 13.4, 7.2 Hz, 1H), 2.04-1.93 (m, 1H), 1.72 (s, 6H), 1.44 (doublet of quintet,  $J$  = 14.8, 7.4, 1H), 1.30 (doublet of quintet,  $J$  = 14.8, 7.4 Hz, 1H), 0.96 (d,  $J$  = 6.7 Hz, 3H), 0.92 (t,  $J$  = 7.4 Hz, 3H).  $^{13}\text{C}$  NMR (126 MHz, Chloroform-*d*)  $\delta$  198.13, 170.70, 160.42, 104.82, 92.12, 42.21, 33.69, 29.79, 26.94, 19.22, 11.38. HRMS (ESI) calcd for  $\text{C}_{12}\text{H}_{18}\text{O}_5$  [M-H]<sup>-</sup> 241.1081, found 241.1093. (**AA-IV-71**)

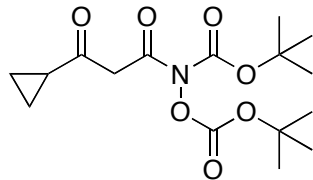


5-(1-hydroxy-4-methylpentylidene)-2,2-dimethyl-1,3-dioxane-4,6-dione (44n): Prepared using the general procedure above (*Method B*) from Meldrum's acid (500 mg, 3.47 mmol), 4-methylvaleric acid (0.44 mL, 3.47 mmol), diethyl cyanophosphonate (0.58 mL, 3.82 mmol), triethylamine (1.52 mL, 10.7 mmol), and DMF (7.2 mL). Aqueous work up, and silica gel chromatography (5-10% ethyl acetate in hexane, 1% acetic acid) afforded **44n** as a yellowish oil (646 mg, 77 %).  $^1\text{H}$  NMR (500 MHz, Chloroform-*d*)  $\delta$  15.29 (s, 1H), 3.11-3.03 (m, 2H), 1.74 (s, 6H), 1.72-1.62 (m, 1H), 1.61-1.55 (m, 2H), 0.95 (d,  $J$  = 6.5 Hz, 6H).  $^{13}\text{C}$  NMR (126 MHz, Chloroform-*d*)  $\delta$  198.79, 170.72, 160.31, 104.89, 91.29, 35.07, 34.09, 28.28, 26.94, 22.35. HRMS (ESI) calcd for  $\text{C}_{12}\text{H}_{18}\text{O}_5$  [M-H]<sup>-</sup> 241.1154, found 241.073. (**AA-IV-96**)

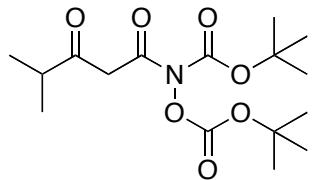
#### 5.4 General procedure for the synthesis of *N,O*-diBoc-protected $\beta$ -keto hydroxamic acids **45c, d, k, l, o**

**Method C.** *Adapted from the procedure of Sorensen et al.<sup>1</sup>:* To a solution of acyl Meldrum's acid (196 mg, 0.915 mmol) in toluene (8.5 mL) was added *N,O*-bis(*tert*-butoxycarbonyl)hydroxylamine (213 mg, 0.915 mmol). The resulting reaction mixture was

stirred at 65 °C for 16 h, and then cooled to room temperature. The solvent was concentrated in vacuo, and the residue was purified on silica gel chromatography using 5% ethyl acetate in hexane to yield the intermediate  $\beta$ -keto hydroxamic acid (**45c, d, k, l, o**) as colorless oil.

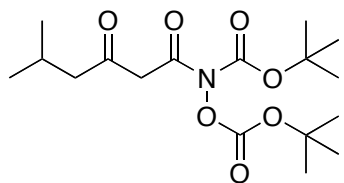


*tert*-butyl *tert*-butoxycarbonyloxy(3-cyclopropyl-3-oxopropanoyl)carbamate (**45c**): Prepared using the general procedure above (*Method C*) from acyl Meldrum's acid (**44c**) (600 mg, 2.82 mmol), *N,O*-bis(*tert*-butoxycarbonyl)hydroxylamine (659 mg, 2.82 mmol), and toluene (26.0 mL). Concentration of the reaction mixture in vacuo followed by silica gel flash chromatography (5 % ethyl acetate in hexane) yielded **45c** as a clear oil (503 mg, 52 %).  $^1\text{H}$  NMR (500 MHz, Chloroform-*d*)  $\delta$  4.27-3.98 (m, 2H), 2.02-1.96 (m, 1H), 1.53 (s, 9H), 1.50 (s, 9H), 1.15-1.06 (m, 2H), 0.98-0.90 (m, 2H).  $^{13}\text{C}$  NMR (126 MHz, Chloroform-*d*)  $\delta$  202.23, 163.55, 150.97, 149.47, 86.34, 85.93, 52.47, 27.89, 27.61, 20.78, 11.65. The  $^1\text{H}$  NMR for this compound matches the reported literature.<sup>1</sup> The *keto/enol* ratio for this compound was approximately 33:1. (**AA-I-181**)

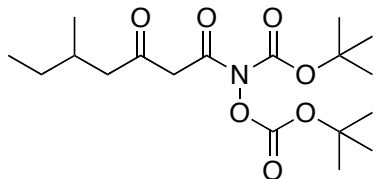


*tert*-butyl *tert*-butoxycarbonyloxy(4-methyl-3-oxopentanoyl)carbamate (**45d**). Prepared using the general procedure above (*Method C*) from acyl Meldrum's acid (**44d**) (196 mg, 0.92 mmol), *N,O*-bis(*tert*-butoxycarbonyl)hydroxylamine (213 mg, 0.92 mmol), and toluene (8.5 mL).

Concentration of the reaction mixture in vacuo followed by silica gel flash chromatography (5 % ethyl acetate in hexane) yielded **45d** as a clear oil (100 mg, 32%). <sup>1</sup>H NMR (500 MHz, Chloroform-*d*) of keto tautomer δ 4.23-3.89 (m, 2H), 2.73 (hept, *J* = 6.9 Hz, 1H), 1.54 (s, 9H), 1.49 (s, 9H), 1.13 (d, *J* = 6.9 Hz, 6H). <sup>13</sup>C NMR (126 MHz, Chloroform-*d*) for keto/enol tautomeric mixture δ 206.04, 187.80, 168.73, 163.76, 151.49, 150.96, 149.68, 87.63, 86.33, 86.19, 85.80, 85.34, 50.08, 41.11, 34.86, 28.04, 27.91, 27.67, 27.64, 19.90, 18.05. The <sup>1</sup>H NMR for this compound matches the reported literature.<sup>1</sup> The keto/enol ratio for this compound was approximately 4:1. (**AA-IV-40**)



tert-butyl tert-butoxycarbonyloxy(5-methyl-3-oxohexanoyl)carbamate (**45k**): Prepared using the general procedure above (*Method C*) from acyl Meldrum's acid (**44k**) (239 mg, 1.05 mmol), *N,O*-bis(*tert*-butoxycarbonyl)hydroxylamine (244 mg, 1.05 mmol), and toluene (9.7 mL). Concentration of the reaction mixture in vacuo followed by silica gel flash chromatography (5 % ethyl acetate in hexane) yielded **45k** as a clear oil (125 mg, 33 %). <sup>1</sup>H NMR (500 MHz, Chloroform-*d*) of keto tautomer δ 4.16-3.74 (m, 2H), 2.41 (d, *J* = 6.8 Hz, 2H), 2.22-2.11 (m, 1H), 1.54 (s, 9H), 1.49 (s, 9H), 0.93 (d, *J* = 6.7 Hz, 6H). <sup>13</sup>C NMR (126 MHz, Chloroform-*d*) for keto/enol tautomeric mixture δ 201.57, 182.35, 168.26, 163.34, 151.32, 150.83, 149.53, 149.23, 90.49, 86.22, 86.05, 85.74, 85.18, 52.18, 51.55, 45.16, 27.89, 27.78, 27.53, 27.50, 26.60, 24.06, 22.44. HRMS (ESI) calcd for C<sub>17</sub>H<sub>29</sub>NO<sub>7</sub> [M+Na]<sup>+</sup> 382.1836, found 382.869. The keto/enol ratio for this compound was approximately 4:1. (**AA-IV-74**)

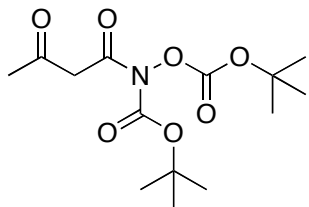


*tert*-butyl *tert*-butoxycarbonyloxy(5-methyl-3-oxoheptanoyl)carbamate (**45I**): Prepared using the general procedure above (*Method C*) from acyl Meldrum's acid (**44I**) (380 mg, 1.57 mmol), *N,O*-bis(*tert*-butoxycarbonyl)hydroxylamine (366 mg, 1.57 mmol), and toluene (14.5 mL). Concentration of the reaction mixture in vacuo followed by silica gel flash chromatography (5 % ethyl acetate in hexane) yielded **45I** as a clear oil (191 mg, 33 %). <sup>1</sup>H NMR (500 MHz, Chloroform-*d*) of keto tautomer δ 4.25-3.66 (m, 2H), 2.59-2.44 (m, 1H), 2.39-2.18 (m, 1H), 1.95 (m, *J* = 13.4, 6.7 Hz, 1H), 1.54 (s, 9H), 1.49 (s, 9H), 1.42 - 1.27 (m, 1H), 1.26 - 1.12 (m, 1H), 0.90 (d, *J* = 6.7 Hz, 3H), 0.87 (t, *J* = 7.4 Hz, 3H). <sup>13</sup>C NMR (126 MHz, Chloroform-*d*) for keto/enol tautomeric mixture δ 201.81, 182.62, 168.24, 163.37, 151.33, 150.84, 149.54, 149.23, 90.60, 86.23, 86.06, 85.75, 85.18, 52.23, 49.66, 43.27, 32.80, 30.23, 29.37, 29.30, 27.90, 27.79, 27.54, 27.51, 19.28, 19.03, 11.28, 11.25. HRMS (ESI) calcd for C<sub>18</sub>H<sub>31</sub>NO<sub>7</sub> [M+Na]<sup>+</sup> 396.1993, found 396.2007. The keto/enol ratio for this compound was approximately 4:1. (**AA-IV-73**)

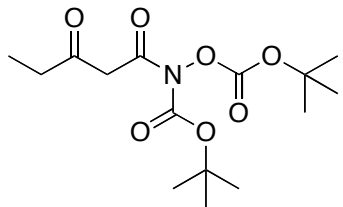
## 5.5 General procedure for the synthesis of *N,O*-diBoc-protected β-keto hydroxamic acids **45a, b, e, g-j, m**

**Method D.** To a solution of acyl meldrum's acid (314 mg, 1.69 mmol, 1.8 equiv) in dry toluene (4.5 mL) at room temperature was added *N,O*-bis(*tert*-butoxycarbonyl)hydroxylamine (219 mg, 0.938 mmol, 1.0 equiv), and the reaction mixture was immersed in an oil bath preheated to 90 °C. The reaction was monitored for the complete consumption of *N,O*-bis(*tert*-butoxycarbonyl)hydroxylamine. Leaving the reaction for longer time can lead to loss in yield and competing side reactions. After concentration in vacuo, the residue was purified on silica gel

chromatography using 5% ethyl acetate in hexane to yield  $\beta$ -keto hydroxamic acid (**45a, b, e, g-j, m**) as colorless oil.

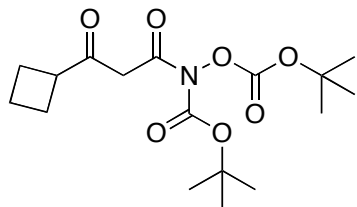


tert-butyl tert-butoxycarbonyloxy(3-oxobutanoyl)carbamate (**45a**): Prepared using the general procedure above (*Method D*) from acyl Meldrum's acid (**44a**) (314 mg, 1.69 mmol), *N,O*-bis(*tert*-butoxycarbonyl)hydroxylamine (219 mg, 0.94 mmol), and toluene (4.5 mL). Concentration of the reaction mixture in vacuo followed by silica gel flash chromatography (5 % ethyl acetate in hexane) yielded **45a** as a clear oil (212 mg, 72 %). <sup>1</sup>H NMR (500 MHz, Chloroform-*d*) of keto tautomer  $\delta$  4.11-3.85 (m, 2H), 2.26 (s, 3H), 1.54 (s, 9H), 1.50 (s, 9H). <sup>13</sup>C NMR (126 MHz, Chloroform-*d*) of keto tautomer  $\delta$  199.93, 163.35, 150.99, 149.71, 86.46, 86.07, 52.64, 30.06, 27.93, 27.65. The <sup>1</sup>H NMR for this compound matches the reported literature.<sup>1</sup> The *keto/enol* ratio for this compound was approximately 6:1. (**AA-IV-92**)

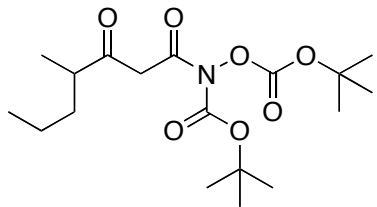


tert-butyl tert-butoxycarbonyloxy(3-oxopentanoyl)carbamate (**45b**): Prepared using the general procedure above (*Method D*) from acyl Meldrum's acid (**44b**) (144 mg, 0.72 mmol), *N,O*-bis(*tert*-butoxycarbonyl)hydroxylamine (93.2 mg, 0.40 mmol), and toluene (2.0 mL). Concentration of the reaction mixture in vacuo followed by silica gel flash chromatography (5 %

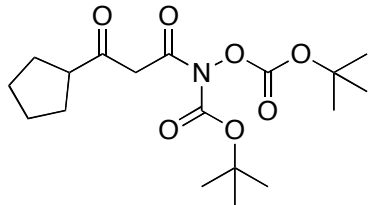
ethyl acetate in hexane) yielded crude **45b** (crude with residual *N,O*-bis(*tert*-butoxycarbonyl)hydroxylamine as the impurity) as a clear oil (104 mg, 79 % (Crude)). <sup>1</sup>H NMR (500 MHz, Chloroform-*d*) of keto tautomer δ 4.16-3.76 (m, 2H), 2.55 (qd, *J* = 7.3, 3.6 Hz, 2H), 1.54 (s, 9H), 1.49 (s, 9H), 1.08 (t, *J* = 7.3 Hz, 3H). <sup>13</sup>C NMR (126 MHz, Chloroform-*d*) of keto tautomer δ 202.71, 163.54, 150.98, 149.69, 86.42, 85.97, 51.66, 36.06, 27.92, 27.64, 7.62. The <sup>1</sup>H NMR and <sup>13</sup>C NMR for this compound matches the reported literature.<sup>1</sup> The *keto/enol* ratio for this compound was approximately 8:1. (**AA-IV-95**)



tert-butyl tert-butoxycarbonyloxy(3-cyclobutyl-3-oxopropanoyl)carbamate (45e): Prepared using the general procedure above (*Method D*) from acyl Meldrum's acid (**44d**) (522 mg, 2.30 mmol), *N,O*-bis(*tert*-butoxycarbonyl)hydroxylamine (298 mg, 1.28 mmol), and toluene (6.4 mL). Concentration of the reaction mixture in vacuo followed by silica gel flash chromatography (5 % ethyl acetate in hexane) yielded **45e** as a clear oil (crude) contaminated with residual *N,O*-bis(*tert*-butoxycarbonyl)hydroxylamine as the impurity (389 mg, 85 % (crude)). <sup>1</sup>H NMR (500 MHz, Chloroform-*d*) of keto tautomer δ 4.13-3.77 (m, 2H), 3.37 (p, *J* = 9.0 Hz, 1H), 2.37-2.22 (m, 2H), 2.21-2.10 (m, 2H), 2.01-1.90 (m, 1H), 1.88-1.77 (m, 1H), 1.54 (s, 9H), 1.49 (s, 9H). <sup>13</sup>C NMR (126 MHz, Chloroform-*d*) δ 203.23, 184.66, 168.56, 163.63, 151.48, 150.99, 149.61, 149.41, 88.18, 86.36, 86.19, 85.88, 85.34, 53.57, 49.64, 45.59, 40.14, 27.94, 27.65, 26.08, 24.52, 18.30, 17.87. HRMS (ESI) calcd for C<sub>17</sub>H<sub>27</sub>NO<sub>7</sub> [M+Na]<sup>+</sup> 380.1680, found 380.1706. The *keto/enol* ratio for this compound was approximately 5:1. (**AA-IV-118**)

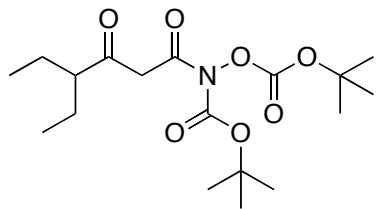


*tert*-butyl *tert*-butoxycarbonyloxy(4-methyl-3-oxoheptanoyl)carbamate (**45h**): Prepared using the general procedure above (*Method D*) from acyl Meldrum's acid (**44h**) (278 mg, 1.15 mmol), *N,O*-bis(*tert*-butoxycarbonyl)hydroxylamine (149 mg, 0.64 mmol), and toluene (3.1 mL). Concentration of the reaction mixture in vacuo followed by silica gel flash chromatography (5 % ethyl acetate in hexane) yielded **45h** as a clear oil (163 mg, 68 %). <sup>1</sup>H NMR (500 MHz, Chloroform-*d*) of keto tautomer δ 4.22-3.88 (m, 2H), 2.65 (h, *J* = 6.7 Hz, 1H), 1.73-1.62 (m, 2H), 1.54 (s, 9H), 1.49 (s, 9H), 1.40-1.26 (m, 2H), 1.11 (d, *J* = 7.0 Hz, 3H), 0.89 (t, *J* = 7.2 Hz, 3H). <sup>13</sup>C NMR (126 MHz, Chloroform-*d*) of keto/enol tautomer δ 205.94, 187.26, 168.63, 163.74, 151.50, 150.97, 149.65, 149.36, 88.68, 86.32, 86.18, 85.77, 85.30, 50.57, 46.24, 40.43, 36.55, 34.84, 28.05, 27.92, 27.68, 27.64, 20.59, 20.26, 18.17, 15.90, 14.19, 14.15. HRMS (ESI) calcd for C<sub>18</sub>H<sub>31</sub>NO<sub>7</sub> [M+H<sub>2</sub>O] 391.21, found 391.25. The *keto/enol* ratio for this compound was approximately 6:1. (**AA-IV-91**)

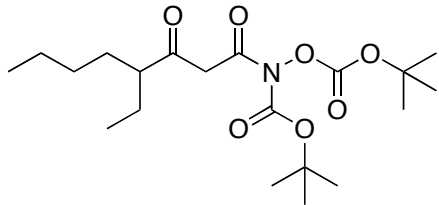


*tert*-butyl *tert*-butoxycarbonylox(3-cyclopentyl-3-oxopropanoyl)carbamate (**45g**): Prepared using the general procedure above (*Method D*) from acyl Meldrum's acid (**44g**) (93.3 mg, 0.39 mmol), *N,O*-bis(*tert*-butoxycarbonyl)hydroxylamine (50.0 mg, 0.22 mmol), and toluene (1.0 mL). Concentration of the reaction mixture in vacuo followed by silica gel flash chromatography (5 %

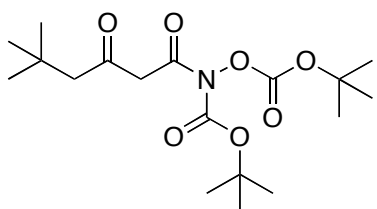
ethyl acetate in hexane) yielded **45g** as a clear oil (59.0 mg, 73 %). <sup>1</sup>H NMR (500 MHz, Chloroform-*d*) of keto tautomer δ 4.22-3.89 (m, 2H), 2.98 (p, *J* = 8.0 Hz, 1H), 1.91-1.76 (m, 4H), 1.70-1.63 (m, 2H), 1.62-1.56 (m, 2H), 1.54 (s, 9H), 1.49 (s, 9H). <sup>13</sup>C NMR (126 MHz, Chloroform-*d*) of keto/enol tautomeric mixture δ 204.70, 186.57, 168.54, 163.72, 151.50, 150.98, 149.63, 149.42, 88.45, 86.33, 86.18, 85.82, 85.29, 51.66, 51.18, 45.89, 30.94, 28.88, 28.04, 27.93, 27.68, 27.65, 26.00, 25.97. HRMS (ESI) calcd for C<sub>18</sub>H<sub>29</sub>NO<sub>7</sub> [M+Na]<sup>+</sup> 394.1836, found 394.1868. The *keto/enol* ratio for this compound was approximately 6:1. (**AA-IV-89**)



*tert*-butyl *tert*-butoxycarbonyloxy(4-ethyl-3-oxohexanoyl)carbamate (**45i**): Prepared using the general procedure above (*Method D*) from acyl Meldrum's acid (**44i**) (942 mg, 3.9 mmol), *N,O*-bis(*tert*-butoxycarbonyl)hydroxylamine (504 mg, 2.16 mmol), and toluene (11.0 mL). Concentration of the reaction mixture in vacuo followed by silica gel flash chromatography (5 % ethyl acetate in hexane) yielded **45i** as a clear oil (536 mg, 66 %). <sup>1</sup>H NMR of keto/enol tautomeric mixture (500 MHz, Chloroform-*d*) δ 13.13 (s, 1H), 6.14 (s, 1H), 4.29-3.80 (m, 2H), 2.49-2.42 (m, 1H), 2.00-1.92 (m, 1H), 1.75-1.55 (m, 4H), 1.55 (s, 9H), 1.54 (s, 9H), 1.53 (s, 9H), 1.49 (s, 9H), 0.91-0.84 (m, 6H). <sup>13</sup>C NMR of keto/enol tautomer (126 MHz, Chloroform-*d*) δ 205.40, 185.86, 168.43, 163.66, 151.49, 150.99, 149.60, 149.32, 90.40, 86.28, 86.17, 85.71, 85.28, 55.04, 51.28, 50.19, 28.05, 27.92, 27.68, 27.64, 25.74, 23.34, 12.06, 11.53. HRMS (ESI) calcd for C<sub>18</sub>H<sub>31</sub>NO<sub>7</sub> [M+Na]<sup>+</sup> 396.1993, found 396.197. The *keto/enol* ratio for this compound was approximately 2:1. (**AA-IV-112**)

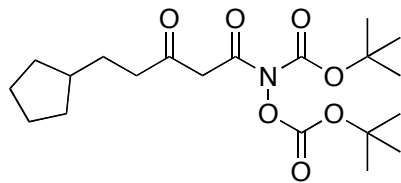


tert-butyl tert-butoxycarbonyloxy(4-ethyl-3-oxooctanoyl)carbamate (45j): Prepared using the general procedure above (*Method D*) from acyl Meldrum's acid (**44j**) (54.6 mg, 0.20 mmol), *N,O*-bis(*tert*-butoxycarbonyl)hydroxylamine (26.1 mg, 0.11 mmol), and toluene (0.9 mL). Concentration of the reaction mixture in vacuo followed by silica gel flash chromatography (5 % ethyl acetate in hexane) yielded **45j** as a clear oil (30.2 mg, 66 %). <sup>1</sup>H NMR of keto/enol tautomeric mixture (500 MHz, Chloroform-*d*) δ 13.14 (s, 0.5H), 6.13 (s, 0.5H), 4.41-3.63 (m, 2H), 2.50 (p, *J* = 6.5, 5.9 Hz, 1H), 2.07-2.00 (m, 0.5H), 1.80-1.57 (m, 4H), 1.55 (s, 4.5H), 1.54 (s, 9H), 1.53 (s, 4.5H), 1.49 (s, 9H), 1.48-1.35 (m, 2H), 1.34-1.15 (m, 7H), 0.91 - 0.84 (m, 9H). <sup>13</sup>C NMR of keto/enol tautomer (126 MHz, Chloroform-*d*) δ 205.53, 186.12, 168.46, 163.67, 151.50, 151.00, 149.62, 149.32, 90.28, 86.29, 86.19, 85.71, 85.28, 53.63, 51.26, 48.57, 32.50, 30.18, 29.72, 29.33, 28.07, 27.93, 27.69, 27.65, 26.12, 23.89, 22.98, 22.86, 14.10, 14.06, 12.10, 11.58. HRMS (ESI) calcd for C<sub>20</sub>H<sub>35</sub>NO<sub>7</sub> [M+Na]<sup>+</sup> 424.2306, found 424.2343. The *keto/enol* ratio for this compound was approximately 2:1. (**AA-IV-85**)



tert-butyl tert-butoxycarbonyloxy(5,5-dimethyl-3-oxohexanoyl)carbamate (45m): Prepared using the general procedure above (*Method D*) from acyl Meldrum's acid (**44m**) (362 mg, 1.49 mmol), *N,O*-bis(*tert*-butoxycarbonyl)hydroxylamine (194 mg, 0.83 mmol), and toluene (4.2 mL).

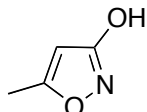
Concentration of the reaction mixture in vacuo followed by silica gel flash chromatography (5 % ethyl acetate in hexane) yielded **45m** as a clear oil (242 mg, 78 %). <sup>1</sup>H NMR (500 MHz, Chloroform-*d*) of keto tautomer δ 4.14-3.67 (m, 2H), 2.44 (s, 2H), 1.54 (s, 9H), 1.49 (s, 9H), 1.03 (s, 9H). <sup>13</sup>C NMR (126 MHz, Chloroform-*d*) of keto/enol tautomeric mixture δ 201.42, 182.02, 168.37, 163.49, 151.49, 150.99, 149.68, 149.33, 91.82, 86.35, 86.21, 85.84, 85.32, 54.91, 53.64, 49.93, 31.91, 30.94, 30.03, 29.62, 28.05, 27.93, 27.69, 27.65. The <sup>1</sup>H NMR for this compound matches the reported literature.<sup>1</sup> The keto/enol ratio for this compound was approximately 2:1. (AA-IV-126)



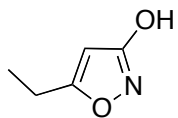
tert-butyl tert-butoxycarbonyloxy(5-cyclopentyl-3-oxopentanoyl)carbamate (45o): Prepared using the general procedure above (*Method D*) from acyl Meldrum's acid (**44o**) (2.32 g, 8.65 mmol), *N,O*-bis(*tert*-butoxycarbonyl)hydroxylamine (2.02 g, 8.65 mmol), and toluene (80.0 mL). Concentration of the reaction mixture in vacuo followed by silica gel flash chromatography (5 % ethyl acetate in hexane) yielded **45o** as a clear oil (1.50 g, 43 %). <sup>1</sup>H NMR (500 MHz, Chloroform-*d*) of keto tautomer δ 4.26-3.54 (m, 2H), 2.57-2.50 (m, 2H), 1.81-1.70 (m, 3H), 1.65-1.57 (m, 6H), 1.54 (s, 9H), 1.49 (s, 9H), 1.15-1.00 (m, 2H). <sup>13</sup>C NMR (126 MHz, Chloroform-*d*) δ of keto tautomer 202.23, 163.40, 150.83, 149.54, 86.23, 85.78, 51.78, 41.94, 39.40, 32.44, 29.41, 27.78, 27.50, 25.11. HRMS (ESI) calcd for  $\text{C}_{20}\text{H}_{33}\text{NO}_7$  [M+Na]<sup>+</sup> 422.2149, found 422.2172. The keto/enol ratio for this compound was approximately 6:1. (AA-IV-58)

## 5.6 General procedure for the synthesis of 5-substituted isoxazol-3-ols 46a-o

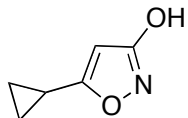
**Method E.** *Adapted from the procedure of Sorensen et al.<sup>1</sup>:*  $\beta$ -keto hydroxamic acid (496 mg, 1.33 mmol) was dissolved in methanol (3.0 mL), and added drop wise to concentrated HCl (5.0 mL) preheated to 50 °C. The reaction mixture was stirred for 2.5 h at 50 °C prior to being brought to room temperature. The reaction mixture was concentrated in vacuo. The residual reaction mixture was partitioned between water and dichloromethane. The aqueous layer was extracted twice with dichloromethane and the combined organic layers were dried with sodium sulfate. The solvent was evaporated, and the subsequent residue was purified on silica gel chromatography using a gradient from 5-10% ethyl acetate in hexane, 1% acetic acid to yield isoxazol-3-ols.



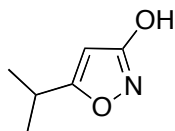
**5-methylisoxazol-3-ol (46a):** Prepared using the general procedure above (*Method E*) from  $\beta$ -keto hydroxamic acid (**45a**) (66.5 mg, 0.21 mmol), concentrated HCl (1.0 mL), and methanol (0.5 mL). Concentration of the reaction mixture in vacuo followed by an aqueous work up, and silica gel chromatography (5-10% ethyl acetate in hexane, 1% acetic acid) afforded **46a** as a white solid (15.5 mg, 75 %). <sup>1</sup>H NMR (500 MHz, Chloroform-d) δ, White crystalline solid. <sup>1</sup>H NMR (500 MHz, Chloroform-d) 11.57 (s, 1H), 5.67 (s, 1H), 2.33 (s, 3H). <sup>13</sup>C NMR (126 MHz, Chloroform-d) δ 171.43, 170.44, 94.00, 12.98. The <sup>1</sup>H NMR and <sup>13</sup>C NMR for this compound matches the reported literature.<sup>1</sup> (**AA-IV-124**)



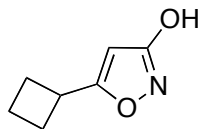
**5-ethylisoxazol-3-ol (46b):** Prepared using the general procedure above (*Method E*) from  $\beta$ -keto hydroxamic acid (**45b**) (287 mg, 0.87 mmol), concentrated HCl (3.0 mL), and methanol (2.0 mL). Concentration of the reaction mixture in vacuo followed by an aqueous work up, and silica gel chromatography (5-10% ethyl acetate in hexane, 1% acetic acid) afforded **46b** as a white solid (81.0 mg, 83 %).  $^1\text{H}$  NMR (500 MHz, Chloroform-*d*)  $\delta$  10.26 (s, 1H), 5.66 (s, 1H), 2.66 (q,  $J$  = 7.6 Hz, 2H), 1.26 (t,  $J$  = 7.6 Hz, 3H).  $^{13}\text{C}$  NMR (126 MHz, Chloroform-*d*)  $\delta$  175.83, 171.35, 92.60, 20.86, 11.45. The  $^1\text{H}$  NMR and  $^{13}\text{C}$  NMR for this compound matches the reported literature.<sup>1</sup> (**AA-I-184**)



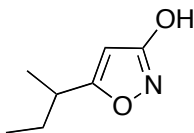
**5-cyclopropylisoxazol-3-ol (46c):** Prepared using the general procedure above (*Method E*) from  $\beta$ -keto hydroxamic acid (**45c**) (2.69 g, 7.83 mmol), concentrated HCl (25.0 mL), and methanol (16.0 mL). Concentration of the reaction mixture in vacuo followed by an aqueous work up, and silica gel chromatography (5-10% ethyl acetate in hexane, 1% acetic acid) afforded **46c** as an off white solid (464 mg, 47 %).  $^1\text{H}$  NMR (500 MHz, Chloroform-*d*)  $\delta$  10.94 (s, 1H), 5.57 (s, 1H), 1.95-1.86 (m, 1H), 1.08-1.00 (m, 2H), 0.97-0.91 (m, 2H).  $^{13}\text{C}$  NMR (126 MHz, Chloroform-*d*)  $\delta$  175.63, 171.45, 91.06, 8.61, 8.35. The  $^1\text{H}$  NMR and  $^{13}\text{C}$  NMR for this compound matches the reported literature.<sup>1</sup> (**AA-II-5, AA-II-6**)



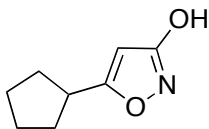
5-isopropylisoxazol-3-ol (46d): Prepared using the general procedure above (*Method E*) from  $\beta$ -keto hydroxamic acid (**45d**) (973 mg, 2.82 mmol), concentrated HCl (12.0 mL), and methanol (6.0 mL). Concentration of the reaction mixture in vacuo followed by an aqueous work up, and silica gel chromatography (5-10% ethyl acetate in hexane, 1% acetic acid) afforded **46d** as a white solid (276 mg, 77 %).  $^1\text{H}$  NMR (500 MHz, Chloroform-*d*)  $\delta$  10.17 (s, 1H), 5.64 (s, 1H), 2.94 (hept,  $J$  = 6.9 Hz, 1H), 1.27 (d,  $J$  = 7.0 Hz, 6H).  $^{13}\text{C}$  NMR (126 MHz, Chloroform-*d*)  $\delta$  179.66, 171.18, 91.47, 27.74, 20.62. The  $^1\text{H}$  NMR and  $^{13}\text{C}$  NMR for this compound matches the reported literature.<sup>1</sup> (**AA-III-50**)



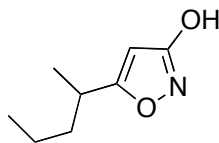
5-cyclobutylisoxazol-3-ol (46e): Prepared using the general procedure above (*Method E*) from  $\beta$ -keto hydroxamic acid (**45e**) (318 mg, 0.89 mmol), concentrated HCl (3.1 mL), and methanol (2.0 mL). Concentration of the reaction mixture in vacuo followed by an aqueous work up, and silica gel chromatography (5-10% ethyl acetate in hexane, 1% acetic acid) afforded **46e** as a semi-solid (75.0 mg, 61 %).  $^1\text{H}$  NMR (500 MHz, Chloroform-*d*)  $\delta$  5.68 (s, 1H), 3.50 (p,  $J$  = 8.5 Hz, 1H), 2.40-2.31 (m, 2H), 2.30-2.20 (m, 2H), 2.10-2.01 (m, 1H), 2.01-1.91 (m, 1H).  $^{13}\text{C}$  NMR (126 MHz, Chloroform-*d*)  $\delta$  177.38, 171.20, 91.95, 32.57, 27.76, 18.88. HRMS (ESI) calcd for C<sub>7</sub>H<sub>9</sub>NO<sub>2</sub> [M+H]<sup>+</sup> 140.0706, found 140.0693. (**AA-IV-120**)



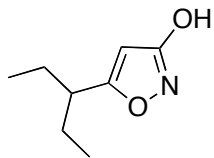
5-sec-butylisoxazol-3-ol (46f): Prepared using the general procedure above (*Method E*) from  $\beta$ -keto hydroxamic acid (**45f**) (1.96 g, 5.53 mmol), concentrated HCl (20.0 mL), and methanol (15.0 mL). Concentration of the reaction mixture in vacuo followed by an aqueous work up, and silica gel chromatography (5-10% ethyl acetate in hexane, 1% acetic acid) afforded **46f** as an off white solid (620 mg, 77 %); mp 37.0-38.0 °C.  $^1\text{H}$  NMR (500 MHz, Chloroform-*d*)  $\delta$  11.41 (s, 1H), 5.64 (s, 1H), 2.74 (h,  $J$  = 7.0 Hz, 1H), 1.74-1.64 (m, 1H), 1.58 (doublet of quintet,  $J$  = 14.1, 7.2 Hz, 1H), 1.24 (d,  $J$  = 7.0 Hz, 3H), 0.90 (t,  $J$  = 7.2 Hz, 3H).  $^{13}\text{C}$  NMR (126 MHz, Chloroform-*d*)  $\delta$  178.80, 171.19, 92.05, 34.49, 28.18, 18.12, 11.44. HRMS (ESI) calcd for  $\text{C}_7\text{H}_{11}\text{NO}_2$  [M+H]<sup>+</sup> 142.0863, found 142.086. (**AA-II-101**)



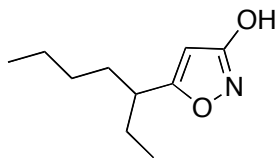
5-cyclopentylisoxazol-3-ol (46g): Prepared using the general procedure above (*Method E*) from  $\beta$ -keto hydroxamic acid (**45g**) (1.77 g, 4.76 mmol), concentrated HCl (25.0 mL), and methanol (10.0 mL). Concentration of the reaction mixture in vacuo followed by an aqueous work up, and silica gel chromatography (5-10% ethyl acetate in hexane, 1% acetic acid) afforded **46g** as a white solid (508 mg, 70 %); mp 71.3-73.4 °C.  $^1\text{H}$  NMR (500 MHz, Chloroform-*d*)  $\delta$  10.42 (s, 1H), 5.63 (s, 1H), 3.06 (quintet,  $J$  = 7.9 Hz, 1H), 2.09-1.96 (m, 2H), 1.80-1.61 (m, 6H).  $^{13}\text{C}$  NMR (126 MHz, Chloroform-*d*)  $\delta$  178.44, 171.20, 91.78, 37.99, 31.64, 25.36. HRMS (ESI) calcd for  $\text{C}_8\text{H}_{11}\text{NO}_2$  [M+H]<sup>+</sup> 154.0863, found 154.0855. (**AA-II-143**)



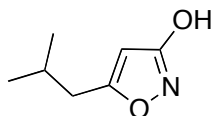
**5-(pentan-2-yl)isoxazol-3-ol (46h):** Prepared using the general procedure above (*Method E*) from  $\beta$ -keto hydroxamic acid (**45h**) (2.85 g, 7.63 mmol), concentrated HCl (15.0 mL), and methanol (16.0 mL). Concentration of the reaction mixture in vacuo followed by an aqueous work up, and silica gel chromatography (5-10% ethyl acetate in hexane, 1% acetic acid) afforded **46h** as a colorless oil (889 mg, 75 %).  $^1\text{H}$  NMR (500 MHz, Chloroform-*d*)  $\delta$  11.20 (s, 1H), 5.62 (s, 1H), 2.82 (h,  $J$  = 7.0 Hz, 1H), 1.64 (ddt,  $J$  = 13.5, 9.4, 6.6 Hz, 1H), 1.50 (ddt,  $J$  = 13.5, 9.4, 6.6 Hz, 1H), 1.38-1.26 (m, 2H), 1.23 (d,  $J$  = 7.1 Hz, 3H), 0.89 (t,  $J$  = 7.4 Hz, 3H).  $^{13}\text{C}$  NMR (126 MHz, Chloroform-*d*)  $\delta$  179.00, 171.15, 91.83, 37.39, 32.71, 20.16, 18.58, 13.92. HRMS (ESI) calcd for  $\text{C}_8\text{H}_{13}\text{NO}_2$  [M+H] $^+$  156.0946, found 156.1485. (**AA-IV-41**)



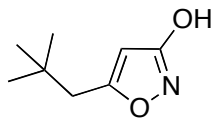
**5-(pentan-3-yl)isoxazol-3-ol (46i):** Prepared using the general procedure above (*Method E*) from  $\beta$ -keto hydroxamic acid (**45i**) (496 mg, 7.63 mmol), concentrated HCl (5.0 mL), and methanol (3.0 mL). Concentration of the reaction mixture in vacuo followed by an aqueous work up, and silica gel chromatography (5-10% ethyl acetate in hexane, 1% acetic acid) afforded **46i** an off white solid (115 mg, 81 %); mp 49.0-50.7 °C.  $^1\text{H}$  NMR (500 MHz, Chloroform-*d*)  $\delta$  10.00 (s, 1H), 5.65 (s, 1H), 2.55 (tt,  $J$  = 8.3, 5.8 Hz, 1H), 1.72-1.56 (m, 4H), 0.87 (t,  $J$  = 7.4 Hz, 6H).  $^{13}\text{C}$  NMR (126 MHz, Chloroform-*d*)  $\delta$  177.74, 171.13, 93.04, 42.18, 26.35, 11.70. HRMS (ESI) calcd for  $\text{C}_8\text{H}_{13}\text{NO}_2$  [M+H] $^+$  156.1019, found 156.1013. (**AA-IV-113**)



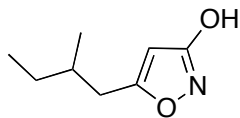
5-(heptan-3-yl)isoxazol-3-ol (46j): Prepared using the general procedure above (*Method E*) from  $\beta$ -keto hydroxamic acid (**45j**) (2.29 g, 5.70 mmol), concentrated HCl (22.0 mL), and methanol (12.0 mL). Concentration of the reaction mixture in vacuo followed by an aqueous work up, and silica gel chromatography (5-10% ethyl acetate in hexane, 1% acetic acid) afforded **46j** as a colorless oil (396 mg, 40 %).  $^1\text{H}$  NMR (500 MHz, Chloroform-*d*)  $\delta$  5.66 (s, 1H), 2.62 (quintet,  $J$  = 7.4 Hz, 1H), 1.74-1.53 (m, 4H), 1.39-1.12 (m, 6H), 0.95-0.81 (m, 6H).  $^{13}\text{C}$  NMR (126 MHz, Chloroform-*d*)  $\delta$  178.08, 171.21, 92.98, 40.60, 33.16, 29.43, 26.84, 22.72, 14.08, 11.73. HRMS (ESI) calcd for  $\text{C}_{10}\text{H}_{17}\text{NO}_2$  [ $\text{M}+\text{H}]^+$  184.1332, found 184.1339. (**AA-II-146**)



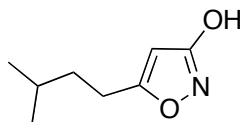
5-isobutylisoxazol-3-ol (46k): Prepared using the general procedure above (*Method E*) from  $\beta$ -keto hydroxamic acid (**45k**) (2.98 g, 8.67 mmol), concentrated HCl (25.0 mL), and methanol (18.0 mL). Concentration of the reaction mixture in vacuo followed by an aqueous work up, and silica gel chromatography (5-10% ethyl acetate in hexane, 1% acetic acid) afforded **46k** as an off white solid (804 mg, 66 %).  $^1\text{H}$  NMR (500 MHz, Chloroform-*d*)  $\delta$  11.80 (s, 1H), 5.66 (s, 1H), 2.50 (d,  $J$  = 7.1 Hz, 2H), 2.06-1.94 (m, 1H), 0.95 (d,  $J$  = 6.7 Hz, 6H).  $^{13}\text{C}$  NMR (126 MHz, Chloroform-*d*)  $\delta$  173.78, 171.26, 93.85, 36.30, 27.59. The  $^1\text{H}$  NMR and  $^{13}\text{C}$  NMR for this compound matches the reported literature.<sup>1</sup>



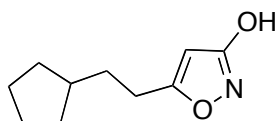
5-neopentylisoxazol-3-ol (46m): Prepared using the general procedure above (*Method E*) from  $\beta$ -keto hydroxamic acid (**45m**) (2.29 g, 6.40 mmol), concentrated HCl (20.0 mL), and methanol (14.0 mL). Concentration of the reaction mixture in vacuo followed by an aqueous work up, and silica gel chromatography (5-10% ethyl acetate in hexane, 1% acetic acid) afforded **46m** as an off white solid (664 mg, 74 %).  $^1\text{H}$  NMR (500 MHz, Chloroform-*d*)  $\delta$  5.67 (s, 1H), 2.52 (s, 2H), 0.98 (s, 9H).  $^{13}\text{C}$  NMR (126 MHz, Chloroform-*d*)  $\delta$  173.12, 171.06, 94.90, 41.60, 31.71, 29.56. HRMS (ESI) calcd for  $\text{C}_8\text{H}_{13}\text{NO}_2$  [M+H] $^+$  156.1019, found 156.1021. The  $^1\text{H}$  NMR and  $^{13}\text{C}$  NMR for this compound matches the reported literature.<sup>1</sup> (**AA-IV-31**)



5-(2-methylbutyl)isoxazol-3-ol (46l): Prepared using the general procedure above (*Method E*) from  $\beta$ -keto hydroxamic acid (**45l**) (3.09 g, 8.27 mmol), concentrated HCl (30.0 mL), and methanol (17.0 mL). Concentration of the reaction mixture in vacuo followed by an aqueous work up, and silica gel chromatography (5-10% ethyl acetate in hexane, 1% acetic acid) afforded **46l** as an oil (871 mg, 68 %).  $^1\text{H}$  NMR (500 MHz, Chloroform-*d*)  $\delta$  10.87 (s, 1H), 5.66 (s, 1H), 2.62 (dd,  $J$  = 14.9, 6.1 Hz, 1H), 2.45 (dd,  $J$  = 14.9, 7.9 Hz, 1H), 1.84-1.71 (m,  $J$  = 6.6 Hz, 1H), 1.46-1.33 (m, 1H), 1.23 (dq,  $J$  = 21.1, 7.5 Hz, 2H), 0.92 (d,  $J$  = 6.7 Hz, 3H), 0.91 (t,  $J$  = 7.5 Hz, 3H).  $^{13}\text{C}$  NMR (126 MHz, Chloroform-*d*)  $\delta$  173.90, 171.27, 93.98, 34.36, 33.90, 29.24, 19.20, 11.42. HRMS (ESI) calcd for  $\text{C}_8\text{H}_{13}\text{NO}_2$  [M+H] $^+$  156.1019, found 156.1013. (**AA-II-160**)



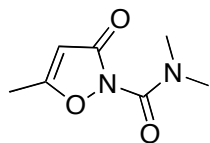
**5-isopentylisoxazol-3-ol (46n):** Prepared using the general procedure above (*Method E*) from  $\beta$ -keto hydroxamic acid (**45n**) (1.64 g, 4.39 mmol), concentrated HCl (11.0 mL), and methanol (9.0 mL). Concentration of the reaction mixture in vacuo followed by an aqueous work up, and silica gel chromatography (5-10% ethyl acetate in hexane, 1% acetic acid) afforded **46n** as a white solid (629 mg, 92 %); mp 53.0-54.8.  $^1\text{H}$  NMR (500 MHz, Chloroform-*d*)  $\delta$  9.64 (s, 1H), 5.65 (s, 1H), 2.65-2.61 (m, 2H), 1.66-1.49 (m, 3H), 0.93 (d,  $J$  = 6.5 Hz, 6H).  $^{13}\text{C}$  NMR (126 MHz, Chloroform-*d*)  $\delta$  174.96, 171.32, 93.02, 36.14, 27.65, 25.38, 22.34. HRMS (ESI) calcd for  $\text{C}_8\text{H}_{13}\text{NO}_2$  [M+H] $^+$  156.1019, found 156.1011. (AA-III-33)



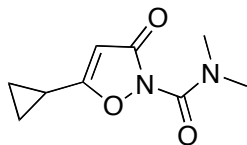
**5-(2-cyclopentylethyl)isoxazol-3-ol (46o):** Prepared using the general procedure above (*Method E*) from  $\beta$ -keto hydroxamic acid (**45o**) (1.50 g, 3.75 mmol), concentrated HCl (13.0 mL), and methanol (8.0 mL). Concentration of the reaction mixture in vacuo followed by an aqueous work up, and silica gel chromatography (5-10% ethyl acetate in hexane, 1% acetic acid) afforded **46o** as a white solid (521 mg, 77 %); mp 67.0-68.0 °C.  $^1\text{H}$  NMR (500 MHz, Chloroform-*d*)  $\delta$  5.65 (s, 1H), 2.67-2.59 (m, 2H), 1.84-1.75 (m, 3H), 1.70-1.64 (m, 2H), 1.64-1.49 (m, 4H), 1.17-1.01 (m, 2H).  $^{13}\text{C}$  NMR (126 MHz, Chloroform-*d*)  $\delta$  174.93, 171.30, 93.04, 39.60, 33.56, 32.55, 26.69, 25.28. HRMS (ESI) calcd for  $\text{C}_{10}\text{H}_{15}\text{NO}_2$  [M+H] $^+$  182.1176, found 182.1182. (AA-IV-60)

## 5.7 General procedure for the synthesis of *N,N*-dimethyl-3-oxoisoxazole-2(3*H*)-carboxamide 47a-p

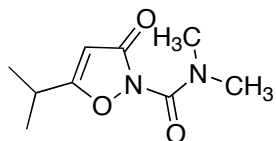
**Method F.** To solution of isoxazolol (62.0 mg, 0.40 mmol) in toluene (2.0 mL) was added *N,N*-dimethylcarbamoyl chloride (0.19 mL, 2.00 mmol) under nitrogen atmosphere. The resulting reaction mixture was refluxed overnight. The reaction mixture was cooled to room temperature and solvent was evaporated in vacuo. The resulting residue was purified by flash column chromatography on silica gel using a gradient of 20-30% ethyl acetate in hexane to yield carboxamide as the major product and carbamate as the minor product.



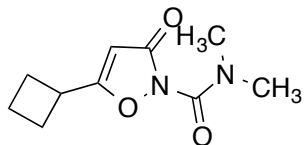
*N,N,5*-trimethyl-3-oxoisoxazole-2(3*H*)-carboxamide (47a): Prepared using the general procedure above (*Method F*) from 5-methylisoxazol-3-ol (**46a**) (45.7 mg, 0.46 mmol), *N,N*-dimethylcarbamoyl chloride (0.21 mL, 2.31 mmol), and toluene (2.5 mL). Concentration of the reaction mixture in vacuo followed by silica gel flash chromatography (20-30% ethyl acetate in hexane) yielded **47a** as an off white solid (66.3 mg, 84 %). <sup>1</sup>H NMR (500 MHz, Chloroform-*d*) δ 5.41 (s, 1H), 3.10 (bs, 6H), 2.31 (s, 3H). <sup>13</sup>C NMR (126 MHz, Chloroform-*d*) δ 174.53, 167.86, 150.22, 96.88, 38.76, 37.02, 13.88. HRMS (ESI) calcd for C<sub>7</sub>H<sub>10</sub>N<sub>2</sub>O<sub>3</sub> [M+H]<sup>+</sup> 171.0691, found 171.0525. (**AA-IV-105**)



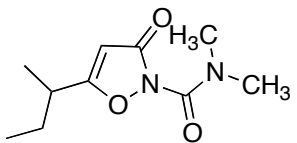
5-cyclopropyl-N,N-dimethyl-3-oxoisoxazole-2(3H)-carboxamide (47c): Prepared using the general procedure above (*Method F*) from 5-cyclopropylisoxazol-3-ol (**46c**) (20.5 mg, 0.16 mmol), *N,N*-dimethylcarbamoyl chloride (0.08 mL, 0.82 mmol), and toluene (1.0 mL). Concentration of the reaction mixture in vacuo followed by silica gel flash chromatography (20-30% ethyl acetate in hexane) yielded **47c** as a clear oil (4.60 mg, 14 %). <sup>1</sup>H NMR (500 MHz, Chloroform-*d*) δ 5.27 (s, 1H), 3.07 (bs, 6H), 1.91-1.81 (m, 1H), 1.19-1.00 (m, 4H). <sup>13</sup>C NMR (126 MHz, Chloroform-*d*) δ 179.99, 168.27, 150.41, 92.92, 38.81, 36.91, 9.32, 9.29. HRMS (ESI) calcd for C<sub>9</sub>H<sub>12</sub>N<sub>2</sub>O<sub>3</sub> [M+H]<sup>+</sup> 197.0921, found 197.0933. (**AA-IV-107**)



5-isopropyl-N,N-dimethyl-3-oxoisoxazole-2(3H)-carboxamide (47d): Prepared using the general procedure above (*Method F*) from 5-isopropylisoxazol-3-ol (**46d**) (136 mg, 1.07 mmol), *N,N*-dimethylcarbamoyl chloride (0.49 mL, 5.34 mmol), and toluene (6.0 mL). Concentration of the reaction mixture in vacuo followed by silica gel flash chromatography (20-30% ethyl acetate in hexane) yielded **47d** as a white solid (129 mg, 61 %); mp 94.0-95.5 °C. <sup>1</sup>H NMR (500 MHz, Chloroform-*d*) δ 5.37 (s, 1H), 3.10 (bs, 6H), 2.88 (hept, *J* = 6.7 Hz, 1H), 1.29 (d, *J* = 7.0 Hz, 6H). <sup>13</sup>C NMR (126 MHz, Chloroform-*d*) δ 183.12, 167.85, 150.14, 94.00, 38.68, 36.96, 28.09, 19.73. HRMS (ESI) calcd for C<sub>9</sub>H<sub>14</sub>N<sub>2</sub>O<sub>3</sub> [M+H]<sup>+</sup> 198.1004, found 199.1083. (**AA-III-51**)

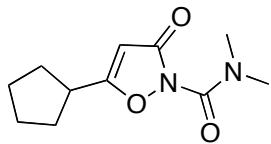


**5-cyclobutyl-*N,N*-dimethyl-3-oxoisoxazole-2(3*H*)-carboxamide (47e):** Prepared using the general procedure above (*Method F*) from 5-cyclobutylisoxazol-3-ol (**46e**) (63.0 mg, 0.45 mmol), *N,N*-dimethylcarbamoyl chloride (0.21 mL, 2.26 mmol), and toluene (2.2 mL). Concentration of the reaction mixture in vacuo followed by silica gel flash chromatography (20-30% ethyl acetate in hexane) yielded **47e** as a white solid (75.0 mg, 79 %); mp 62.5-64.3 °C.  $^1\text{H}$  NMR (500 MHz, Chloroform-*d*)  $\delta$  5.42 (s, 1H), 3.44 (quintet,  $J$  = 8.6 Hz, 1H), 3.10 (bs, 6H), 2.42-2.33 (m, 2H), 2.32-2.22 (m, 2H), 2.13-2.02 (m, 1H), 2.02-1.90 (m, 1H).  $^{13}\text{C}$  NMR (126 MHz, Chloroform-*d*)  $\delta$  180.87, 167.93, 150.29, 94.55, 38.83, 37.00, 32.76, 27.06, 18.90. HRMS (ESI) calcd for  $\text{C}_{10}\text{H}_{14}\text{N}_2\text{O}_3$  [ $\text{M}+\text{H}]^+$  211.1077, found 211.1068. (**AA-IV-121**)

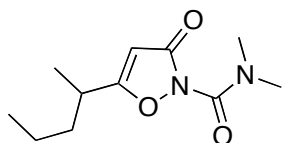


**5-sec-butyl-*N,N*-dimethyl-3-oxoisoxazole-2(3*H*)-carboxamide (47f):** Prepared using the general procedure above (*Method F*) from 5-sec-butylisoxazol-3-ol (**46f**) (96.0 mg, 0.68 mmol), *N,N*-dimethylcarbamoyl chloride (0.31 mL, 3.38 mmol), and toluene (3.0 mL). Concentration of the reaction mixture in vacuo followed by silica gel flash chromatography (20-30% ethyl acetate in hexane) yielded **47f** as clear oil (104 mg, 73 %).  $^1\text{H}$  NMR (500 MHz, Chloroform-*d*)  $\delta$  5.35 (s, 1H), 3.09 (bs, 6H), 2.67 (heptet,  $J$  = 6.9 Hz, 1H), 1.71 (doublet of quintets,  $J$  = 14.3, 7.3 Hz, 1H), 1.59 (doublet of quintets,  $J$  = 14.3, 7.3 Hz, 1H), 1.25 (d,  $J$  = 7.0 Hz, 8H), 0.95 (t,  $J$  = 7.3 Hz, 3H).  $^{13}\text{C}$  NMR (126 MHz, Chloroform-*d*)  $\delta$  179.39, 166.72, 152.01, 94.29, 37.00, 36.75, 34.72, 28.22,

18.09, 11.48. HRMS (ESI) calcd for  $C_{10}H_{16}N_2O_3$   $[M+H]^+$  213.1234, found 213.1238. (**AA-III-35**)

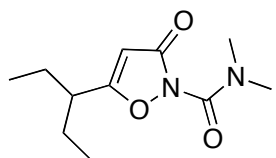


5-cyclopentyl-N,N-dimethyl-3-oxoisoazole-2(3H)-carboxamide (47g): Prepared using the general procedure above (*Method F*) from 5-cyclopentylisoxazol-3-ol (**46g**) (21.0 mg, 0.14 mmol), *N,N*-dimethylcarbamoyl chloride (0.06 mL, 0.69 mmol), and toluene (1.0 mL). Concentration of the reaction mixture in vacuo followed by silica gel flash chromatography (20-30% ethyl acetate in hexane) yielded **47g** as a white solid (21.0 mg, 67 %); mp 69.0-71.8 °C.  $^1H$  NMR (500 MHz, Chloroform-*d*)  $\delta$  5.36 (s, 1H), 3.10 (bs, 6H), 3.04-2.96 (m, 1H), 2.14-1.99 (m, 2H), 1.86-1.60 (m, 6H).  $^{13}C$  NMR (126 MHz, Chloroform-*d*)  $\delta$  182.30, 168.04, 150.34, 94.36, 38.37, 31.17, 25.49. HRMS (ESI) calcd for  $C_{11}H_{16}N_2O_3$   $[M+Na]^+$  225.1234, found 225.1212. Due to signal broadening (slow chemical exchange), the carboxamide methyls could not be detected by  $^{13}C$  NMR, though they were clearly visible in the  $^1H$  NMR spectrum (see Figure 2.9 Chapter 2 for explanation). (**AA-IV-106**)

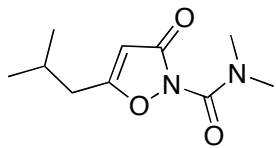


*N,N*-dimethyl-3-oxo-5-(pentan-2-yl)isoazole-2(3H)-carboxamide (47h): Prepared using the general procedure above (*Method F*) from 5-(pentan-2-yl)isoxazol-3-ol (**46h**) (98.0 mg, 0.63 mmol), *N,N*-dimethylcarbamoyl chloride (0.17 mL, 1.59 mmol), and toluene (3.0 mL). Concentration of the reaction mixture in vacuo followed by silica gel flash chromatography (20-

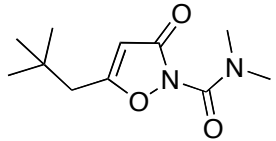
30% ethyl acetate in hexane) yielded **47h** as a clear oil (110 mg, 78 %).  $^1\text{H}$  NMR (500 MHz, Chloroform-*d*)  $\delta$  5.35 (s, 1H), 3.10 (bs, 6H), 2.75 (heptet,  $J$  = 6.9 Hz, 1H), 1.71-1.64 (m, 1H), 1.56-1.47 (m, 1H), 1.44-1.31 (m, 2H), 1.26 (d,  $J$  = 7.0 Hz, 3H), 0.92 (t,  $J$  = 7.3 Hz, 3H).  $^{13}\text{C}$  NMR (126 MHz, Chloroform-*d*)  $\delta$  182.92, 168.08, 150.33, 94.59, 36.69, 33.31, 20.16, 17.85, 13.98. HRMS (ESI) calcd for  $\text{C}_{11}\text{H}_{18}\text{N}_2\text{O}_3$   $[\text{M}+\text{H}]^+$  227.139, found 227.1385. Due to signal broadening (slow chemical exchange), the carboxamide methyls could not be detected by  $^{13}\text{C}$  NMR, though they were clearly visible in the  $^1\text{H}$  NMR spectrum (see Figure 2.9 Chapter 2 for explanation). (**AA-III-187**)



N,N-dimethyl-3-oxo-5-(pentan-3-yl)isoxazole-2(3H)-carboxamide (47i): Prepared using the general procedure above (*Method F*) from 5-(pentan-3-yl)isoxazol-3-ol (**46i**) (62.1 mg, 0.40 mmol), *N,N*-dimethylcarbamoyl chloride (0.18 mL, 2.00 mmol), and toluene (2.0 mL). Concentration of the reaction mixture in vacuo followed by silica gel flash chromatography (20 - 30% ethyl acetate in hexane) yielded **47i** as a clear oil (73.4 mg, 81 %).  $^1\text{H}$  NMR (500 MHz, Chloroform-*d*)  $\delta$  5.36 (s, 1H), 3.10 (bs, 6H), 2.52-2.44 (m, 1H), 1.74-1.57 (m, 4H), 0.94 (t,  $J$  = 7.4 Hz, 6H).  $^{13}\text{C}$  NMR (126 MHz, Chloroform-*d*)  $\delta$  181.77, 168.22, 150.34, 95.67, 42.56, 38.85, 36.98, 25.58, 11.57. HRMS (ESI) calcd for  $\text{C}_{11}\text{H}_{18}\text{N}_2\text{O}_3$   $[\text{M}+\text{Na}]^+$  249.121, found 249.1213. (**AA-IV-114**)

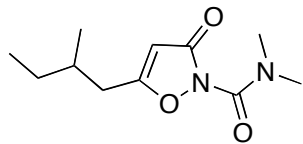


5-isobutyl-*N,N*-dimethyl-3-oxoisoxazole-2(3*H*)-carboxamide (**47k**): Prepared using the general procedure above (*Method F*) from 5-isobutylisoxazol-3-ol (**46k**) (49.0 mg, 0.35 mmol), *N,N*-dimethylcarbamoyl chloride (0.16 mL, 1.74 mmol), and toluene (1.7 mL). Concentration of the reaction mixture in vacuo followed by silica gel flash chromatography (20-30% ethyl acetate in hexane) yielded **47k** as a clear oil (40.0 mg, 54 %). <sup>1</sup>H NMR (500 MHz, Chloroform-*d*) δ 5.39 (s, 1H), 3.10 (bs, 6H), 2.47 (d, *J* = 7.1 Hz, 2H), 2.12-1.97 (m, 1H), 1.00 (d, *J* = 6.7 Hz, 6H). <sup>13</sup>C NMR (126 MHz, Chloroform-*d*) δ 177.75, 168.03, 150.28, 96.66, 36.90, 27.09, 22.41. Due to signal broadening (slow chemical exchange), the carboxamide methyls could not be detected by <sup>13</sup>C NMR, though they were clearly visible in the <sup>1</sup>H NMR spectrum (see Figure 2.9 Chapter 2 for explanation). HRMS (ESI) calcd for C<sub>10</sub>H<sub>16</sub>N<sub>2</sub>O<sub>3</sub> [M+H]<sup>+</sup> 213.1509, found 213.1261. (**AA-IV-108**)

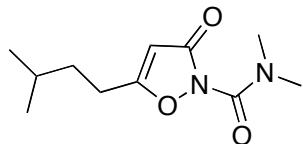


*N,N*-dimethyl-5-neopentyl-3-oxoisoxazole-2(3*H*)-carboxamide (**47m**): Prepared using the general procedure above (*Method F*) from 5-neopentylisoxazol-3-ol (**46m**) (40.0 mg, 0.28 mmol), *N,N*-dimethylcarbamoyl chloride (0.13 mL, 1.41 mmol), and toluene (1.4 mL). Concentration of the reaction mixture in vacuo followed by silica gel flash chromatography (20-30% ethyl acetate in hexane) yielded **47k** as a white solid (52.0 mg, 81 %); mp 70.7-72.0. <sup>1</sup>H NMR (500 MHz, Chloroform-*d*) δ 5.39 (s, 1H), 3.11 (bs, 6H), 2.48 (s, 2H), 1.03 (s, 9H). <sup>13</sup>C NMR (126 MHz,

Chloroform-*d*) δ 176.96, 168.17, 150.27, 97.67, 42.00, 38.81, 36.82, 31.83, 29.55. HRMS (ESI) calcd for C<sub>11</sub>H<sub>18</sub>N<sub>2</sub>O<sub>3</sub> [M+H]<sup>+</sup> 227.139, found 227.1383. (**AA-IV-131**)

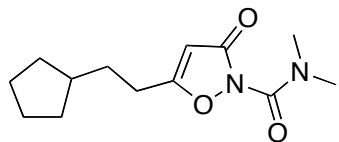


N,N-dimethyl-5-(2-methylbutyl)-3-oxoisoxazole-2(3H)-carboxamide (47l): Prepared using the general procedure above (*Method F*) from 5-(2-methylbutyl)isoxazol-3-ol (**46l**) (29.0 mg, 0.19 mmol), *N,N*-dimethylcarbamoyl chloride (0.09 mL, 0.94 mmol), and toluene (1.0 mL). Concentration of the reaction mixture in vacuo followed by silica gel flash chromatography (20-30% ethyl acetate in hexane) yielded **47l** as a clear oil (19.3 mg, 46 %). <sup>1</sup>H NMR (500 MHz, Chloroform-*d*) δ 5.38 (s, 1H), 3.10 (bs, 6H), 2.58 (dd, *J* = 15.0, 7.0 Hz, 1H), 2.39 (dd, *J* = 15.0, 7.0 Hz, 1H), 1.80 (doublet of quintets, *J* = 13.5, 6.7 Hz, 1H), 1.48-1.35 (m, 1H), 1.32-1.18 (m, 1H), 0.97 (d, *J* = 6.7 Hz, 3H), 0.91 (t, *J* = 7.4 Hz, 3H). <sup>13</sup>C NMR (126 MHz, Chloroform-*d*) δ 177.91, 168.04, 150.29, 96.71, 38.96, 37.08, 34.95, 33.28, 29.30, 19.18, 11.35. HRMS (ESI) calcd for C<sub>11</sub>H<sub>18</sub>N<sub>2</sub>O<sub>3</sub> [M+H]<sup>+</sup> 227.139, found 227.1403. (**AA-IV-109**)

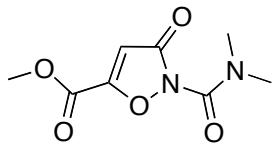


5-isopentyl-N,N-dimethyl-3-oxoisoxazole-2(3H)-carboxamide (47n): Prepared using the general procedure above (*Method F*) from 5-isopentylisoxazol-3-ol (**46n**) (100 mg, 0.64 mmol), *N,N*-dimethylcarbamoyl chloride (0.30 mL, 3.22 mmol), and toluene (3.0 mL). Concentration of the reaction mixture in vacuo followed by silica gel flash chromatography (20-30% ethyl acetate in

hexane) yielded **47n** as a clear oil (122 mg, 71 %).  $^1\text{H}$  NMR (500 MHz, Chloroform-*d*)  $\delta$  5.38 (s, 1H), 3.08 (bs, 6H), 2.57 (t,  $J$  = 7.9 Hz, 2H), 1.70-1.50 (m, 3H), 0.92 (d,  $J$  = 6.5 Hz, 6H).  $^{13}\text{C}$  NMR (126 MHz, Chloroform-*d*)  $\delta$  178.93, 167.98, 150.28, 95.73, 38.76, 36.96, 35.10, 27.71, 25.96, 22.23. HRMS (ESI) calcd for  $\text{C}_{11}\text{H}_{18}\text{N}_2\text{O}_3$  [M+H] $^+$  227.1390, found 227.1397. (**AA-III-41**)



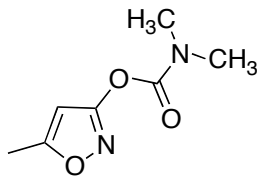
5-(2-cyclopentylethyl)-N,N-dimethyl-3-oxoisoxazole-2(3H)-carboxamide (47o): Prepared using the general procedure above (*Method F*) from 5-(2-cyclopentylethyl)isoxazol-3-ol (**46o**) (77.8 mg, 0.43 mmol), *N,N*-dimethylcarbamoyl chloride (0.20 mL, 2.15 mmol), and toluene (3.0 mL). Concentration of the reaction mixture in vacuo followed by silica gel flash chromatography (20 - 30% ethyl acetate in hexane) yielded **47o** as a white solid (85.0 mg, 79 %); mp 47.8-47.9 °C.  $^1\text{H}$  NMR (500 MHz, Chloroform-*d*)  $\delta$  5.39 (s, 1H), 3.11 (bs, 6H), 2.59 (t,  $J$  = 7.9 Hz, 2H), 1.87-1.74 (m, 3H), 1.71 - 1.65 (m, 2H), 1.65-1.61 (m, 2H), 1.58-1.49 (m, 2H), 1.18-1.01 (m, 2H).  $^{13}\text{C}$  NMR (126 MHz, Chloroform-*d*)  $\delta$  178.81, 167.92, 150.28, 95.75, 39.61, 38.84, 36.90, 32.57, 32.48, 27.29, 25.22. HRMS (ESI) calcd for  $\text{C}_{13}\text{H}_{20}\text{N}_2\text{O}_3$  [M+H] $^+$  253.1547, found 253.1547. (**AA-IV-63**)



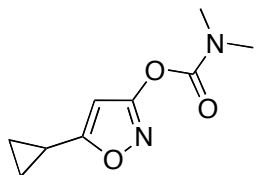
methyl 2-(dimethylcarbamoyl)-3-oxo-2,3-dihydroisoxazole-5-carboxylate (47p): Prepared using the general procedure above (*Method F*) from commercially available methyl 3-hydroxyisoxazole-5-carboxylate (100 mg, 0.70 mmol), *N,N*-dimethylcarbamoyl chloride (0.32 mL, 3.49 mmol), and toluene (3.0 mL). Aqueous work up followed by silica gel flash chromatography (20% ethyl acetate in hexane) of the residue yielded **48p** as a clear oil (86.0 mg, 58 %). <sup>1</sup>H NMR (500 MHz, Chloroform-*d*) δ 6.29 (s, 1H), 3.96 (s, 3H), 3.11 (s, 6H). <sup>13</sup>C NMR (126 MHz, Chloroform-*d*) δ 165.29, 160.97, 156.60, 148.82, 104.47, 53.63, 38.62, 37.15. HRMS (ESI) calcd for C<sub>8</sub>H<sub>10</sub>N<sub>2</sub>O<sub>5</sub> [M+Na]<sup>+</sup> 237.0482, found 237.0473. (AA-III-45)

### 5.8 General procedure for the synthesis of isoxazol-3-yl dimethylcarbamate

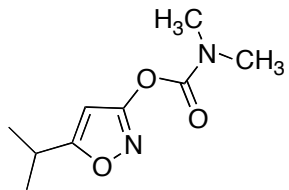
**Method G.** To a dry round bottom flask was added isoxazol-3-ol (73.5 mg, 0.47 mmol) and dry tetrahydrofuran (3.0 mL) prior to cooling it to 0 °C. To this solution was added potassium *tert*-butoxide (1M in THF, 0.71 mL, 0.71 mmol) at 0 °C and subsequently the reaction mixture was stirred for 20 min at RT. To this solution was added *N,N*-dimethyl carbamoyl chloride (0.11 mL, 1.18 mmol), and the resulting solution was stirred at room temperature for additional 16 h. The solvent was concentrated and the residue was taken up in dichloromethane and washed with 0.25 M HCl hydrochloric acid, and then brine, and dried over sodium sulfate. The solvent was evaporated and the residue was purified by silica gel column chromatography using 20% ethyl acetate in hexane to afford the dimethyl carbamate as the major product.



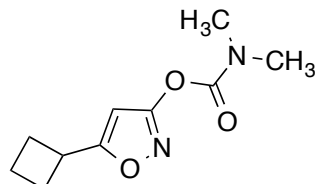
5-methylisoxazol-3-yl dimethylcarbamate (48a): Prepared using the general procedure above (*Method G*) from 5-methylisoxazol-3-ol (**46a**) (200 mg, 2.01 mmol), potassium *tert*-butoxide (2.62 mL, 2.62 mmol), *N,N*-dimethylcarbamoyl chloride (0.46 mL, 5.04 mmol), and THF (7.0 mL). Aqueous work up followed by silica gel flash chromatography (20% ethyl acetate in hexane) of the residue yielded **48a** as a clear oil (256 mg, 75 %). <sup>1</sup>H NMR (500 MHz, Chloroform-*d*) δ 6.09 (s, 1H), 3.04 (s, 3H), 2.95 (s, 3H), 2.34 (s, 3H). <sup>13</sup>C NMR (126 MHz, Chloroform-*d*) δ 170.88, 166.75, 151.81, 96.16, 36.82, 36.57, 13.05. HRMS (ESI) calcd for C<sub>7</sub>H<sub>10</sub>N<sub>2</sub>O<sub>3</sub> [M+H]<sup>+</sup> 171.0691, found 171.0771. (**AA-II-130**)



5-cyclopropylisoxazol-3-yl dimethylcarbamate (48c): Prepared using the general procedure above (*Method F*) from 5-cyclopropylisoxazol-3-ol (**46c**) (20.5 mg, 0.16 mmol), *N,N*-dimethylcarbamoyl chloride (0.08 mL, 0.82 mmol), and toluene (1.0 mL). Concentration of the reaction mixture in vacuo followed by silica gel flash chromatography (20-30% ethyl acetate in hexane) yielded **48c** as a clear oil (25.0 mg, 78 %). <sup>1</sup>H NMR (500 MHz, Chloroform-*d*) δ 6.07 (s, 1H), 3.08 (s, 3H), 3.00 (s, 3H), 1.98 (tt, *J* = 8.5, 5.1 Hz, 1H), 1.07-1.01 (m, 2H), 1.01-0.95 (m, 2H). <sup>13</sup>C NMR (126 MHz, Chloroform-*d*) δ 176.17, 166.85, 151.93, 93.34, 36.98, 36.73, 8.84, 8.35. HRMS (ESI) calcd for C<sub>9</sub>H<sub>12</sub>N<sub>2</sub>O<sub>3</sub> [M+H]<sup>+</sup> 197.0921, found 197.0921. (**AA-IV-107**)

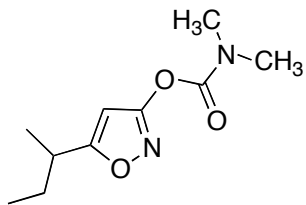


5-isopropylisoxazol-3-yl dimethylcarbamate (48d): Prepared using the general procedure above (*Method G*) from 5-isopropylisoxazol-3-ol (**46d**) (122 mg, 0.96 mmol), potassium *tert*-butoxide (1.24 mL, 1.25 mmol), *N,N*-dimethylcarbamoyl chloride (0.22 mL, 2.39 mmol), and THF (7.0 mL). Aqueous work up followed by silica gel flash chromatography (20% ethyl acetate in hexane) of the residue yielded **48d** as a clear oil (170 mg, 80 %). <sup>1</sup>H NMR (500 MHz, Chloroform-*d*) δ 6.12 (s, 1H), 3.09 (s, 3H), 3.06-2.96 (m, 1H), 3.00 (s, 3H), 1.29 (d, *J* = 7.0 Hz, 6H). <sup>13</sup>C NMR (126 MHz, Chloroform-*d*) δ 180.16, 166.71, 152.02, 93.70, 36.99, 36.74, 27.94, 20.59. HRMS (ESI) calcd for C<sub>9</sub>H<sub>14</sub>N<sub>2</sub>O<sub>3</sub> [M+H]<sup>+</sup> 198.1004, found 199.1079. (**AA-III-52**)

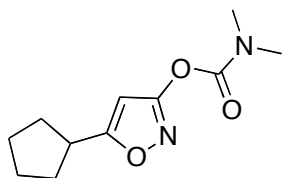


5-cyclobutylisoxazol-3-yl dimethylcarbamate (48e): Prepared using the general procedure above (*Method G*) from 5-cyclobutylisoxazol-3-ol (**46e**) (39.0 mg, 0.28 mmol), potassium *tert*-butoxide (0.42 mL, 0.42 mmol), *N,N*-dimethylcarbamoyl chloride (0.06 mL, 0.70 mmol), and THF (2.0 mL). Aqueous work up followed by silica gel flash chromatography (20% ethyl acetate in hexane) of the residue yielded **48e** as a clear oil (52.0 mg, 89 %). <sup>1</sup>H NMR (500 MHz, Chloroform-*d*) δ 6.17 (s, 1H), 3.57 (quintet, *J* = 8.5 Hz, 1H), 3.09 (s, 3H), 3.01 (s, 3H), 2.43-2.21 (m, 4H), 2.11-1.87 (m, 2H). <sup>13</sup>C NMR (126 MHz, Chloroform-*d*) δ 177.95, 166.75, 152.03,

94.25, 37.03, 36.77, 32.80, 27.85, 18.84. HRMS (ESI) calcd for C<sub>10</sub>H<sub>14</sub>N<sub>2</sub>O<sub>3</sub> [M+H]<sup>+</sup> 211.1077, found 211.1072. (**AA-IV-68**)

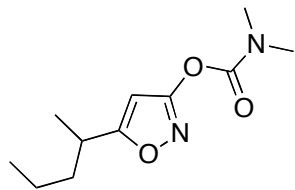


5-sec-butylisoxazol-3-yl dimethylcarbamate (48f): Prepared using the general procedure above (*Method G*) from 5-sec-butylisoxazol-3-ol (**46f**) (45.1 mg, 0.32 mmol), potassium *tert*-butoxide (0.48 mL, 0.48 mmol), *N,N*-dimethylcarbamoyl chloride (0.07 mL, 0.80 mmol), and THF (2.0 mL). Aqueous work up followed by silica gel flash chromatography (20% ethyl acetate in hexane) of the residue yielded **48f** as a clear oil (55.5 mg, 82 %). <sup>1</sup>H NMR (500 MHz, Chloroform-*d*) δ 6.14 (s, 1H), 3.09 (s, 3H), 3.01 (s, 3H), 2.82 (sextet, *J* = 7.0 Hz, 1H), 1.72 (doublet of quintet, *J* = 14.3, 7.2 Hz, 1H), 1.61 (doublet of quintet, *J* = 14.3, 7.2 Hz, 1H), 1.27 (d, *J* = 7.0 Hz, 3H), 0.91 (t, *J* = 7.2 Hz, 3H). <sup>13</sup>C NMR (126 MHz, Chloroform-*d*) δ 182.65, 168.08, 150.30, 94.74, 38.82, 34.96, 37.03, 27.54, 17.33, 11.34. HRMS (ESI) calcd for C<sub>10</sub>H<sub>16</sub>N<sub>2</sub>O<sub>3</sub> [M+H]<sup>+</sup> 213.1234, found 213.1243. (**AA-IV-70**)

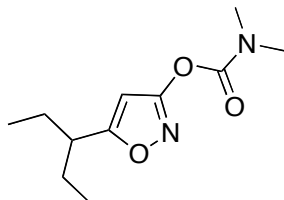


5-cyclopentylisoxazol-3-yl dimethylcarbamate (48g): Prepared using the general procedure above (*Method G*) from 5-cyclopentylisoxazol-3-ol (**46g**) (250 mg, 1.63 mmol), potassium *tert*-butoxide (2.12 mL, 2.12 mmol), *N,N*-dimethylcarbamoyl chloride (0.37 mL, 4.08 mmol), and THF (10.0 mL). Aqueous work up followed by silica gel flash chromatography (20% ethyl

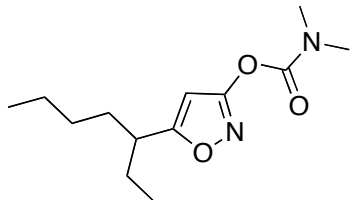
acetate in hexane) of the residue yielded **48g** as a clear oil (300 mg, 82 %). <sup>1</sup>H NMR (500 MHz, Chloroform-*d*) δ 6.13 (d, *J* = 0.8 Hz, 1H), 3.14 (quintet, *J* = 7.5 Hz, 1H), 3.09 (s, 3H), 3.01 (s, 3H), 2.12-1.97 (m, 2H), 1.80-1.70 (m, 4H), 1.70-1.60 (m, 2H). <sup>13</sup>C NMR (126 MHz, Chloroform-*d*) δ 178.91, 166.57, 151.92, 93.94, 38.13, 36.86, 36.62, 31.53, 25.24. HRMS (ESI) calcd for C<sub>11</sub>H<sub>16</sub>N<sub>2</sub>O<sub>3</sub> [M+Na]<sup>+</sup> 247.1053, found 247.1036. (**AA-II-147**)



5-(pentan-2-yl)isoxazol-3-yl dimethylcarbamate (48h): Prepared using the general procedure above (*Method G*) from 5-(pentan-2-yl)isoxazol-3-ol (**46h**) (170 mg, 1.09 mmol), potassium *tert*-butoxide (1.42 mL, 1.42 mmol), *N,N*-dimethylcarbamoyl chloride (0.25 mL, 2.74 mmol), and THF (7.0 mL). Aqueous work up followed by silica gel flash chromatography (20% ethyl acetate in hexane) of the residue yielded **48h** as a clear oil (207 mg, 84 %). <sup>1</sup>H NMR (500 MHz, Chloroform-*d*) δ 6.11 (s, 1H), 3.06 (s, 3H), 2.98 (s, 3H), 2.88 (sextet, *J* = 7.0 Hz, 1H), 1.66 (ddt, *J* = 13.4, 9.5, 6.5 Hz, 1H), 1.50 (ddt, *J* = 13.4, 9.5, 6.5 Hz, 1H), 1.38-1.26 (m, 2H), 1.24 (d, *J* = 7.0 Hz, 3H), 0.87 (t, *J* = 7.3 Hz, 3H). <sup>13</sup>C NMR (126 MHz, Chloroform-*d*) δ 179.53, 166.64, 151.93, 94.09, 37.37, 36.90, 36.66, 32.89, 20.13, 18.53, 13.93. HRMS (ESI) calcd for C<sub>11</sub>H<sub>18</sub>N<sub>2</sub>O<sub>3</sub> [M+H]<sup>+</sup> 227.1317, found 227.1677. (**AA-II-132**)

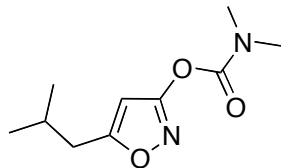


5-(pentan-3-yl)isoxazol-3-yl dimethylcarbamate (48i): Prepared using the general procedure above (*Method G*) from 5-(pentan-3-yl)isoxazol-3-ol (**46i**) (73.5 mg, 0.47 mmol), potassium *tert*-butoxide (0.71 mL, 0.71 mmol), *N,N*-dimethylcarbamoyl chloride (0.11 mL, 1.18 mmol), and THF (3.0 mL). Aqueous work up followed by silica gel flash chromatography (20% ethyl acetate in hexane) of the residue yielded **48i** as a clear oil (89.3 mg, 83 %). <sup>1</sup>H NMR (500 MHz, Chloroform-*d*) δ 6.17 (s, 1H), 3.10 (s, 3H), 3.01 (s, 3H), 2.67-2.59 (m, 1H), 1.78-1.50 (m, 4H), 0.87 (t, *J* = 7.4 Hz, 6H). <sup>13</sup>C NMR (126 MHz, Chloroform-*d*) δ 178.29, 166.74, 151.99, 95.14, 42.29, 37.00, 36.76, 26.27, 11.68. HRMS (ESI) calcd for C<sub>11</sub>H<sub>18</sub>N<sub>2</sub>O<sub>3</sub> [M+H]<sup>+</sup> 227.139, found 227.1392. (**AA-II-132**)

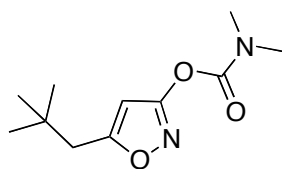


5-(heptan-3-yl)isoxazol-3-yl dimethylcarbamate (48j): Prepared using the general procedure above (*Method G*) from 5-(heptan-3-yl)isoxazol-3-ol (**46j**) (230 mg, 1.25 mmol), potassium *tert*-butoxide (1.63 mL, 1.63 mmol), *N,N*-dimethylcarbamoyl chloride (0.29 mL, 3.13 mmol), and THF (8.0 mL). Aqueous work up followed by silica gel flash chromatography (20% ethyl acetate in hexane) of the residue yielded **48j** as a clear oil (194 mg, 61 %). <sup>1</sup>H NMR (500 MHz, Chloroform-*d*) δ 6.15 (s, 1H), 3.08 (s, 3H), 2.99 (s, 3H), 2.68 (quintet, *J* = 7.2 Hz, 1H), 1.70-1.53 (m, 4H), 1.34-1.12 (m, 4H), 0.88-0.80 (m, 6H). <sup>13</sup>C NMR (126 MHz, Chloroform-*d*) δ 178.47,

166.70, 151.95, 94.98, 40.65, 36.94, 36.71, 33.02, 29.33, 26.72, 22.66, 14.00, 11.64. HRMS (ESI) calcd for  $C_{13}H_{22}N_2O_3$   $[M+H]^+$  255.1427, found 255.1630. (**AA-II-151**)



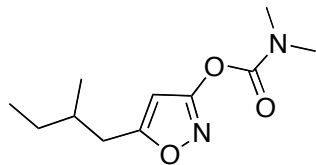
5-isobutylisoxazol-3-yl dimethylcarbamate (48k): Prepared using the general procedure above (*Method G*) from 5-isobutylisoxazol-3-ol (**46k**) (252 mg, 1.78 mmol), potassium *tert*-butoxide (2.32 mL, 2.32 mmol), *N,N*-dimethylcarbamoyl chloride (0.41 mL, 4.45 mmol), and THF (10.0 mL). Aqueous work up followed by silica gel flash chromatography (20% ethyl acetate in hexane) of the residue yielded **48k** as a clear oil (248 mg, 66 %).  $^1H$  NMR (500 MHz, Chloroform-*d*)  $\delta$  6.16 (s, 1H), 3.09 (s, 3H), 3.01 (s, 3H), 2.58 (d,  $J$  = 7.1 Hz, 2H), 2.09-1.97 (m, 1H), 0.96 (d,  $J$  = 6.7 Hz, 6H).  $^{13}C$  NMR (126 MHz, Chloroform-*d*)  $\delta$  174.38, 166.77, 151.98, 96.11, 37.01, 36.76, 36.60, 27.62, 22.41. HRMS (ESI) calcd for  $C_{10}H_{16}N_2O_3$   $[M+H]^+$  213.1509, found 213.1261. (**AA-II-116**)



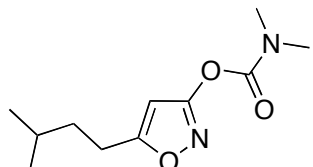
5-neopentylisoxazol-3-yl dimethylcarbamate (48m): Prepared using the general procedure above (*Method G*) from 5-neopentylisoxazol-3-ol (**46m**) (230 mg, 1.63 mmol), potassium *tert*-butoxide (2.12 mL, 2.12 mmol), *N,N*-dimethylcarbamoyl chloride (0.37 mL, 4.07 mmol), and THF (7.0 mL). Aqueous work up followed by silica gel flash chromatography (20% ethyl acetate in hexane) of the residue yielded **48m** as a clear oil (262 mg, 71 %).  $^1H$  NMR (500 MHz, Chloroform-*d*)  $\delta$  6.13 (s, 1H), 3.04 (s, 3H), 2.95 (s, 3H), 2.54 (s, 2H), 0.93 (s, 9H).  $^{13}C$  NMR

(126 MHz, Chloroform-*d*)  $\delta$  173.29, 166.51, 151.83, 97.01, 41.53, 36.83, 36.58, 31.58, 29.32.

HRMS (ESI) calcd for C<sub>11</sub>H<sub>18</sub>N<sub>2</sub>O<sub>3</sub> [M+NH<sub>4</sub>]<sup>+</sup> 244.1656, found 244.1668 (**AA-II-127**)

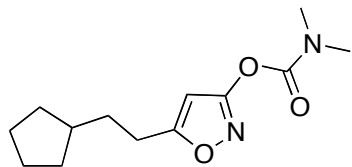


**5-(2-methylbutyl)isoxazol-3-yl dimethylcarbamate (48l):** Prepared using the general procedure above (*Method G*) from 5-(2-methylbutyl)isoxazol-3-ol (**46l**) (300 mg, 1.93 mmol), potassium *tert*-butoxide (2.5 mL, 2.5 mmol), *N,N*-dimethylcarbamoyl chloride (0.44 mL, 4.83 mmol), and THF (10 mL). Aqueous work up followed by silica gel flash chromatography (20% ethyl acetate in hexane) of the residue yielded **48l** as a clear oil (359 mg, 82 %). <sup>1</sup>H NMR (500 MHz, Chloroform-*d*)  $\delta$  6.15 (s, 1H), 3.09 (s, 3H), 3.00 (s, 3H), 2.69 (dd, *J* = 15.0, 7.0 Hz, 1H), 2.52 (dd, *J* = 15.0, 7.0 Hz, 1H), 1.79 (doublet of quintet, *J* = 13.5, 7.2 Hz, 1H), 1.47-1.32 (m, 1H), 1.27-1.16 (m, 1H), 0.92 (d, *J* = 6.7 Hz, 3H), 0.90 (t, *J* = 7.2 Hz, 3H). <sup>13</sup>C NMR (126 MHz, Chloroform-*d*)  $\delta$  174.45, 166.77, 151.98, 96.16, 36.98, 36.73, 34.56, 33.86, 29.18, 19.19, 11.38. HRMS (ESI) calcd for C<sub>11</sub>H<sub>18</sub>N<sub>2</sub>O<sub>3</sub> [M+Na]<sup>+</sup> 249.121, found 249.1201. (**AA-II-162**)

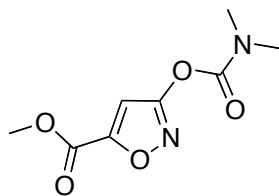


**5-isopentylisoxazol-3-yl dimethylcarbamate (48n):** Prepared using the general procedure above (*Method G*) from 5-isopentylisoxazol-3-ol (**46n**) (300 mg, 1.93 mmol), potassium *tert*-butoxide (2.5 mL, 2.5 mmol), *N,N*-dimethylcarbamoyl chloride (0.44 mL, 4.83 mmol), and THF (10.0 mL). Aqueous work up followed by silica gel flash chromatography (20% ethyl acetate in

hexane) of the residue yielded **48n** as a clear oil (342 mg, 80 %).  $^1\text{H}$  NMR (500 MHz, Chloroform-*d*)  $\delta$  6.15 (s, 1H), 3.10 (s, 3H), 3.01 (s, 3H), 2.71 (t, *J* = 8.0, 7.6 Hz, 2H), 1.68-1.54 (m, 3H), 0.93 (d, *J* = 6.3 Hz, 6H).  $^{13}\text{C}$  NMR (126 MHz, Chloroform-*d*)  $\delta$  175.37, 166.68, 151.87, 95.13, 36.86, 36.61, 35.94, 27.46, 25.44, 22.18. HRMS (ESI) calcd for  $\text{C}_{11}\text{H}_{18}\text{N}_2\text{O}_3$  [M+H] $^+$  227.139, found 227.1398. (**AA-II-164**)



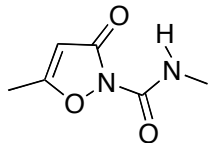
5-(2-cyclopentylethyl)isoxazol-3-yl dimethylcarbamate (48o): Prepared using the general procedure above (*Method G*) from 5-(2-cyclopentylethyl)isoxazol-3-ol (**46o**) (58.4 mg, 0.32 mmol), potassium *tert*-butoxide (0.48 mL, 0.48 mmol), *N,N*-dimethylcarbamoyl chloride (0.074 mL, 0.81 mmol), and THF (1.0 mL). Aqueous work up followed by silica gel flash chromatography (20% ethyl acetate in hexane) of the residue yielded **48o** as a clear oil (73.0 mg, 90 %).  $^1\text{H}$  NMR (500 MHz, Chloroform-*d*)  $\delta$  6.15 (s, 1H), 3.09 (s, 3H), 3.01 (s, 3H), 2.71 (t, *J* = 7.9 Hz, 2H), 1.86-1.73 (m, 3H), 1.69 (q, *J* = 7.2 Hz, 2H), 1.65-1.57 (m, 2H), 1.56-1.48 (m, 2H), 1.20-0.99 (m, 2H).  $^{13}\text{C}$  NMR (126 MHz, Chloroform-*d*)  $\delta$  175.50, 166.81, 152.01, 95.27, 39.57, 37.02, 36.77, 33.52, 32.55, 26.91, 25.26. HRMS (ESI) calcd for  $\text{C}_{13}\text{H}_{20}\text{N}_2\text{O}_3$  [M+H] $^+$  253.1547, found 253.1525. (**AA-IV-64**)



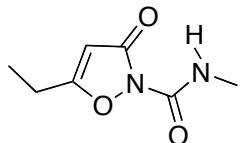
methyl 3-(dimethylcarbamoyloxy)isoxazole-5-carboxylate (48p): Prepared using the general procedure above (*Method F*) from commercially available methyl 3-hydroxyisoxazole-5-carboxylate (100 mg, 0.70 mmol), *N,N*-dimethylcarbamoyl chloride (0.32 mL, 3.49 mmol), and toluene (3.0 mL). Aqueous work up followed by silica gel flash chromatography (20% ethyl acetate in hexane) of the residue yielded **48p** as a clear oil (56.8 mg, 38 %). <sup>1</sup>H NMR (500 MHz, Chloroform-*d*) δ 7.12 (s, 1H), 3.96 (s, 1H), 3.11 (s, 1H), 3.03 (s, 1H). <sup>13</sup>C NMR (126 MHz, Chloroform-*d*) δ 166.71, 160.66, 156.88, 151.32, 104.04, 53.05, 37.14, 36.80. HRMS (ESI) calcd for C<sub>8</sub>H<sub>10</sub>N<sub>2</sub>O<sub>5</sub> [M+Na]<sup>+</sup> 237.0482, found 237.0473. (**AA-III-45**)

## 5.9 General procedure for the synthesis of *N*-methyl-3-oxoisoxazole-2(*3H*)-carboxamide

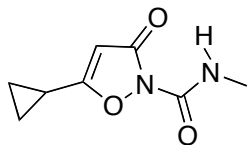
**Method H.** To a dry round bottom flask was added isoxazolol (150 mg, 0.979 mmol) and dry tetrahydrofuran (6.0 mL) prior to cooling it to 0 °C. To this solution was added potassium *tert*-butoxide (1M in THF, 1.27 mL, 1.27 mmol) at 0 °C and subsequently the reaction mixture was stirred for 20 min at RT. To this solution was added *N*-methylcarbamoyl chloride (228 mg, 2.44 mmol) and the resulting solution was stirred at room temperature for additional 16 h. The solvent was concentrated and the residue was taken up in dichloromethane and washed with 0.25 M HCl hydrochloric acid, and then brine, and dried over sodium sulfate. The solvent was evaporated and the residue was purified using silica gel column chromatography.



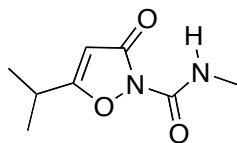
N,5-dimethyl-3-oxoisoxazole-2(3H)-carboxamide (49a): Prepared using the general procedure above (*Method H*) from 5-methylisoxazol-3-ol (**46a**) (100 mg, 1.00 mmol), potassium *tert*-butoxide (1.31 mL, 1.31 mmol), *N*-methylcarbamoyl chloride (0.24 mg, 2.53 mmol), and THF (6.0 mL). Aqueous work up followed by silica gel flash chromatography (20% ethyl acetate in hexane) of the residue yielded **49a** as a white semi-solid (120 mg, 76 %). <sup>1</sup>H NMR (500 MHz, Chloroform-*d*) δ 7.79 (s, 1H), 5.58 (s, 1H), 2.95 (d, *J* = 4.8 Hz, 3H), 2.34 (s, 3H). <sup>13</sup>C NMR (126 MHz, Chloroform-*d*) δ 171.32, 165.44, 148.41, 98.30, 26.47, 13.54. HRMS (ESI) calcd for C<sub>6</sub>H<sub>8</sub>N<sub>2</sub>O<sub>3</sub> [M+H]<sup>+</sup> 157.0608, found 157.0596. (**AA-I-127**)



5-ethyl-N-methyl-3-oxoisoxazole-2(3H)-carboxamide (49b): Prepared using the general procedure above (*Method H*) from 5-ethylisoxazol-3-ol (**46b**) (80.0 mg, 0.71 mmol), potassium *tert*-butoxide (0.92 mL, 0.92 mmol), *N*-methylcarbamoyl chloride (165 mg, 1.77 mmol), and THF (4.0 mL). Aqueous work up followed by silica gel flash chromatography (20% ethyl acetate in hexane) of the residue yielded **49b** as a white semi-solid (86.4 mg, 72 %). <sup>1</sup>H NMR (500 MHz, Chloroform-*d*) δ 7.82 (s, 1H), 5.57 (s, 1H), 2.96 (d, *J* = 4.8 Hz, 3H), 2.65 (q, *J* = 7.6 Hz, 3H), 1.29 (t, *J* = 7.6 Hz, 3H). <sup>13</sup>C NMR (126 MHz, Chloroform-*d*) δ 176.47, 165.52, 148.49, 96.81, 26.48, 21.15, 10.62. HRMS (ESI) calcd for C<sub>7</sub>H<sub>10</sub>N<sub>2</sub>O<sub>3</sub> [M+H]<sup>+</sup> 171.0691, found 171.0771. (**AA-I-188**)

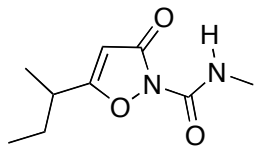


5-cyclopropyl-N-methyl-3-oxoisoxazole-2(3H)-carboxamide (49c): Prepared using the general procedure above (*Method H*) from 5-cyclopropylisoxazol-3-ol (**46c**) (114 mg, 0.92 mmol), potassium *tert*-butoxide (1.18 mL, 1.18 mmol), *N*-methylcarbamoyl chloride (212 mg, 2.28 mmol), and THF (4.0 mL). Aqueous work up followed by silica gel flash chromatography (20% ethyl acetate in hexane) of the residue yielded **49c** as a white semi-solid (100 mg, 61 %). <sup>1</sup>H NMR (500 MHz, Chloroform-*d*) δ 7.80 (s, 1H), 5.43 (s, 1H), 2.94 (d, *J* = 4.8 Hz, 3H), 1.93-1.86 (m, 1H), 1.19-1.13 (m, 2H), 1.12-1.05 (m, 2H). <sup>13</sup>C NMR (126 MHz, Chloroform-*d*) δ 176.71, 165.66, 148.49, 94.37, 26.45, 9.46, 9.00. HRMS (ESI) calcd for C<sub>8</sub>H<sub>10</sub>N<sub>2</sub>O<sub>3</sub> [M+H]<sup>+</sup> 183.0764, found 183.0766. (**AA-II-7**)

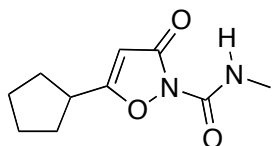


5-isopropyl-N-methyl-3-oxoisoxazole-2(3H)-carboxamide (49d): Prepared using the general procedure above (*Method H*) from 5-isopropylisoxazol-3-ol (**46d**) (155 mg, 1.22 mmol), potassium *tert*-butoxide (1.58 mL, 1.58 mmol), *N*-methylcarbamoyl chloride (285 mg, 3.05 mmol), and THF (7.5 mL). Aqueous work up followed by silica gel flash chromatography (20% ethyl acetate in hexane) of the residue yielded **49d** as a sticky off white solid (157 mg, 70 %). <sup>1</sup>H NMR (500 MHz, Chloroform-*d*) δ 7.80 (s, 1H), 5.50 (s, 1H), 2.93-2.90 (m, 3H), 2.90-2.81 (m, 1H), 1.26 (d, *J* = 7.2 Hz, 6H). <sup>13</sup>C NMR (126 MHz, Chloroform-*d*) δ 179.98, 165.45, 148.40,

95.48, 27.87, 26.38, 19.90. HRMS (ESI) calcd for  $C_8H_{12}N_2O_3$   $[M+H]^+$  184.0848, found 185.0928. (**AA-II-128**)

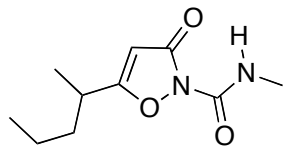


5-sec-butyl-N-methyl-3-oxoisoxazole-2(3H)-carboxamide (49f): Prepared using the general procedure above (*Method H*) from 5-sec-butylisoxazol-3-ol (**46f**) (170 mg, 1.20 mmol), potassium *tert*-butoxide (1.56 mL, 1.56 mmol), *N*-methylcarbamoyl chloride (282 mg, 3.01 mmol), and THF (7.0 mL). Aqueous work up followed by silica gel flash chromatography (20% ethyl acetate in hexane) of the residue yielded **49f** as a clear oil (231 mg, 97 %). <sup>1</sup>H NMR (500 MHz, Chloroform-*d*)  $\delta$  7.82 (s, 1H), 5.51 (s, 1H), 2.93 (d, *J* = 4.8 Hz, 3H), 2.69 (h, *J* = 7.0 Hz, 1H), 1.71 (doublet of quintet, *J* = 14.5, 7.3 Hz, 1H), 1.58 (doublet of quintet, *J* = 14.5, 7.3 Hz, 1H), 1.25 (d, *J* = 7.0 Hz, 3H), 0.92 (t, *J* = 7.3 Hz, 3H). <sup>13</sup>C NMR (126 MHz, Chloroform-*d*)  $\delta$  179.31, 165.44, 148.42, 96.14, 34.68, 27.53, 26.40, 17.46, 11.30. HRMS (ESI) calcd for  $C_9H_{14}N_2O_3$   $[M+H]^+$  199.1004, found 199.1083. (**AA-II-105**)

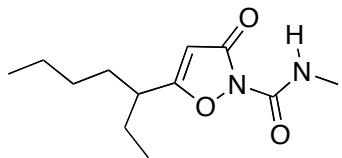


5-cyclopentyl-N-methyl-3-oxoisoxazole-2(3H)-carboxamide (49g): Prepared using the general procedure above (*Method H*) from 5-cyclopentylisoxazol-3-ol (**46g**) (150 mg, 0.98 mmol), potassium *tert*-butoxide (1.27 mL, 1.27 mmol), *N*-methylcarbamoyl chloride (228 mg, 2.44 mmol), and THF (6 mL). Aqueous work up followed by silica gel flash chromatography (20%

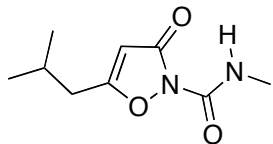
ethyl acetate in hexane) of the residue yielded **49g** as a clear oil (185 mg, 90 %). <sup>1</sup>H NMR (500 MHz, Chloroform-*d*) δ 7.82 (s, 1H), 5.52 (s, 1H), 3.01 (quintet, *J* = 7.6 Hz, 1H), 2.94 (d, *J* = 4.8 Hz, 3H), 2.13-2.02 (m, 2H), 1.79-1.62 (m, 6H). <sup>13</sup>C NMR (126 MHz, Chloroform-*d*) δ 179.08, 165.5, 148.50, 95.73, 38.03, 31.30, 26.44, 25.40. HRMS (ESI) calcd for C<sub>10</sub>H<sub>14</sub>N<sub>2</sub>O<sub>3</sub> [M+Na]<sup>+</sup> 233.0897, found 233.0886. (**AA-II-148**)



*N*-methyl-3-oxo-5-(pentan-2-yl)isoxazole-2(3*H*)-carboxamide (**49h**): Prepared using the general procedure above (*Method H*) from 5-(pentan-2-yl)isoxazol-3-ol (**46h**) (144 mg, 0.92 mmol), potassium *tert*-butoxide (1.20 mL, 1.20 mmol), *N*-methylcarbamoyl chloride (217 mg, 2.32 mmol), and THF (7.0 mL). Aqueous work up followed by silica gel flash chromatography (20% ethyl acetate in hexane) of the residue yielded **49h** as a clear oil (111 mg, 57 %). <sup>1</sup>H NMR (500 MHz, Chloroform-*d*) δ 7.81 (s, 1H), 5.50 (s, 1H), 2.92 (d, *J* = 7.4 Hz, 3H), 2.75 (sextet, *J* = 6.4 Hz, 1H), 1.70-1.57 (m, 1H), 1.54-1.45 (m, 1H), 1.38-1.25 (m, 2H), 1.24 (d, *J* = 6.8 Hz, 3H), 0.88 (t, *J* = 7.3 Hz, 3H). <sup>13</sup>C NMR (126 MHz, Chloroform-*d*) δ 179.56, 165.44, 148.41, 95.96, 36.57, 32.99, 26.39, 20.08, 17.90, 13.82. HRMS (ESI) calcd for C<sub>10</sub>H<sub>16</sub>N<sub>2</sub>O<sub>3</sub> [M+K]<sup>+</sup> 251.0793, found 251.0815. (**AA-II-131**)

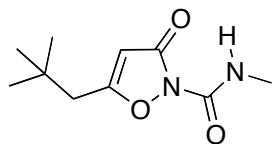


5-(heptan-3-yl)-N-methyl-3-oxoisoxazole-2(3H)-carboxamide (49j): Prepared using the general procedure above (*Method H*) from 5-(heptan-3-yl)isoxazol-3-ol (**46j**) (156 mg, 0.85 mmol), potassium *tert*-butoxide (1.11 mL, 1.11 mmol), *N*-methylcarbamoyl chloride (199 mg, 2.13 mmol), and THF (5.0 mL). Aqueous work up followed by silica gel flash chromatography (20% ethyl acetate in hexane) of the residue yielded **49j** as a clear oil (111 mg, 66 %). <sup>1</sup>H NMR (500 MHz, Chloroform-*d*) δ 7.84 (s, 1H), 5.52 (s, 1H), 2.95 (d, *J* = 4.8 Hz, 3H), 2.57 (quintet, *J* = 7.6 Hz, 1H), 1.74-1.55 (m, 4H), 1.36-1.20 (m, 4H), 0.90 (t, *J* = 7.6 Hz, 3H), 0.86 (t, *J* = 7.3 Hz, 3H). <sup>13</sup>C NMR (126 MHz, Chloroform-*d*) δ 178.68, 165.50, 148.48, 96.97, 40.85, 32.41, 29.29, 26.45, 26.18, 22.59, 13.97, 11.57. HRMS (ESI) calcd for C<sub>12</sub>H<sub>20</sub>N<sub>2</sub>O<sub>3</sub> [M+Na]<sup>+</sup> 263.1366, found 263.1357. (AA-II-152)

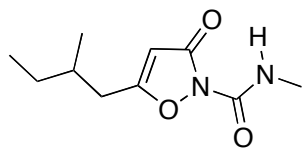


5-isobutyl-N-methyl-3-oxoisoxazole-2(3H)-carboxamide (49k): Prepared using the general procedure above (*Method H*) from 5-isobutylisoxazol-3-ol (**46k**) (165 mg, 1.17 mmol), potassium *tert*-butoxide (1.52 mL, 1.52 mmol), *N*-methylcarbamoyl chloride (273 mg, 2.92 mmol), and THF (7.0 mL). Aqueous work up followed by silica gel flash chromatography (20% ethyl acetate in hexane) of the residue yielded **49k** as a white semi-solid (207 mg, 90 %). <sup>1</sup>H NMR (500 MHz, Chloroform-*d*) δ 7.83 (s, 1H), 5.56 (s, 1H), 2.96 (d, *J* = 4.8 Hz, 3H), 2.49 (d, *J* = 7.2 Hz, 2H), 2.14-1.98 (m, 1H), 0.99 (d, *J* = 6.7 Hz, 6H). <sup>13</sup>C NMR (126 MHz, Chloroform-*d*)

$\delta$  174.44, 165.47, 148.45, 98.12, 36.55, 27.16, 26.48, 22.35. HRMS (ESI) calcd for C<sub>9</sub>H<sub>14</sub>N<sub>2</sub>O<sub>3</sub> [M+H]<sup>+</sup> 199.1077, found 199.1086. (**AA-II-110**)



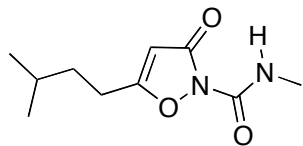
*N*-methyl-5-neopentyl-3-oxoisoxazole-2(3*H*)-carboxamide (**49m**): Prepared using the general procedure above (*Method H*) from 5-isobutylisoxazol-3-ol (**46m**) (183 mg, 1.29 mmol), potassium *tert*-butoxide (1.68 mL, 1.68 mmol), *N*-methylcarbamoyl chloride (303 mg, 3.24 mmol), and THF (7.0 mL). Aqueous work up followed by silica gel flash chromatography (20% ethyl acetate in hexane) of the residue yielded **49m** as an off white semi-solid (138 mg, 50 %); mp 70.7-74.0 °C. <sup>1</sup>H NMR (500 MHz, Chloroform-*d*)  $\delta$  7.83 (s, 1H), 5.56 (s, 1H), 2.95 (d, *J* = 4.8 Hz, 3H), 2.50 (s, 2H), 1.02 (s, 9H). <sup>13</sup>C NMR (126 MHz, Chloroform-*d*)  $\delta$  173.53, 165.42, 148.38, 99.10, 41.61, 31.93, 29.54, 26.47. HRMS (ESI) calcd for C<sub>10</sub>H<sub>16</sub>N<sub>2</sub>O<sub>3</sub> [M+H]<sup>+</sup> 213.1234, found 213.1225. (**AA-II-32**)



*N*-methyl-5-(2-methylbutyl)-3-oxoisoxazole-2(3*H*)-carboxamide (**49l**): Prepared using the general procedure above (*Method H*) from 5-(2-methylbutyl)isoxazol-3-ol (**46l**) (200 mg, 1.28 mmol), potassium *tert*-butoxide (1.67 mL, 1.67 mmol), *N*-methylcarbamoyl chloride (300 mg, 3.22 mmol), and THF (10.0 mL). Aqueous work up followed by silica gel flash chromatography (20% ethyl acetate in hexane) of the residue yielded **49l** as a white semi-solid (247 mg, 90 %). <sup>1</sup>H

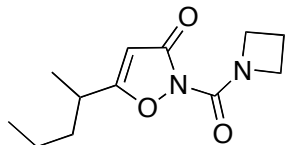
<sup>1</sup>H NMR (500 MHz, Chloroform-*d*) δ 7.82 (s, 1H), 5.55 (s, 1H), 2.95 (d, *J* = 4.8 Hz, 3H), 2.61 (dd, *J* = 15.1, 7.0 Hz, 1H), 2.41 (dd, *J* = 15.1, 7.0 Hz, 1H), 1.88-1.78 (m, *J* = 6.5 Hz, 1H), 1.46-1.36 (m, 1H), 1.25 (doublet of quintet, *J* = 14.7, 7.4 Hz, 1H), 0.95 (d, *J* = 6.6 Hz, 3H), 0.91 (t, *J* = 7.4 Hz, 3H). <sup>13</sup>C NMR (126 MHz, Chloroform-*d*) δ 174.63, 165.48, 148.45, 98.16, 34.67, 33.31, 29.29, 26.46, 19.07, 11.26. HRMS (ESI) calcd for C<sub>10</sub>H<sub>16</sub>N<sub>2</sub>O<sub>3</sub> [M+Na]<sup>+</sup> 235.1053, found 235.1049.

**(AA-II-161)**



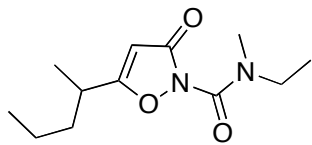
**5-isopentyl-N-methyl-3-oxoisoxazole-2(3H)-carboxamide (49n):** Prepared using the general procedure above (*Method H*) from 5-isopentylisoxazol-3-ol (**46n**) (200 mg, 1.28 mmol), potassium *tert*-butoxide (1.67 mL, 1.67 mmol), *N*-methylcarbamoyl chloride (300 mg, 3.22 mmol), and THF (10.0 mL). Aqueous work up followed by silica gel flash chromatography (20% ethyl acetate in hexane) of the residue yielded **49n** as a clear oil (238 mg, 87 %). <sup>1</sup>H NMR (500 MHz, Chloroform-*d*) δ 7.81 (s, 1H), 5.55 (s, 1H), 2.95 (d, *J* = 4.8 Hz, 3H), 2.64-2.53 (m, 2H), 1.67-1.48 (m, 3H), 0.92 (d, *J* = 6.4 Hz, 6H). <sup>13</sup>C NMR (126 MHz, Chloroform-*d*) δ 175.69, 165.51, 148.48, 97.20, 35.25, 27.73, 26.46, 25.67, 22.20. HRMS (ESI) calcd for C<sub>10</sub>H<sub>16</sub>N<sub>2</sub>O<sub>3</sub> [M+H]<sup>+</sup> 213.1234, found 213.1247. **(AA-II-163)**

## 5.10 Synthesis of *N*-substituted derivatives of **46h**

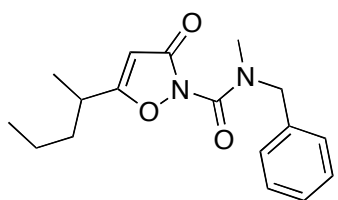


**2-(azetidine-1-carbonyl)-5-(pentan-2-yl)isoxazol-3(2*H*)-one (56h):** To a solution of triphosgene (63.5 mg, 0.21 mmol, 0.35 equiv.) in DCM (1.0 mL) was added a solution of 5-(pentan-2-yl)isoxazol-3-ol (**46h**) (94.0 mg, 0.61 mmol, 1 equiv.) in DCM (2.0 mL), and the resulting mixture was allowed to stir at room temperature for 5.3 h. To the reaction mixture, a solution of azetidine hydrochloride (85.0 mg, 0.91 mmol, 1.5 equiv) and diisopropylethylamine (0.35 mL, 1.99 mmol, 3.3 equiv.) in dichloromethane (3 mL) was added drop wise, and the reaction was stirred for an additional 30 min. The subsequent reaction mixture was washed with aqueous solution of ammonium chloride, and the organic phase was dried over sodium sulfate and concentrated. The residue was purified by silica gel chromatography eluting with 20% ethyl acetate in hexanes to yield the desired compound **56h** as clear oil (59.3 mg, 41% yield). Starting material recovered (18.0 mg).  $^1\text{H}$  NMR (500 MHz, Chloroform-d)  $\delta$  5.39 (s, 1H), 4.37 (s, 2H), 4.19 (s, 2H), 2.73 (sextet,  $J$  = 7.0 Hz, 1H), 2.36 (quintet,  $J$  = 7.8 Hz, 2H), 1.71-1.59 (m, 1H), 1.56-1.45 (m, 1H), 1.43-1.29 (m, 2H), 1.25 (d,  $J$  = 7.0 Hz, 3H), 0.92 (t,  $J$  = 7.3 Hz, 3H).  $^{13}\text{C}$  NMR (126 MHz, Chloroform-d)  $\delta$  181.06, 165.57, 148.98, 95.50, 53.01, 49.54, 36.63, 33.18, 20.14, 17.84, 16.57, 13.94. HRMS (ESI) calcd for  $\text{C}_{12}\text{H}_{18}\text{N}_2\text{O}_3$  [ $\text{M}+\text{H}$ ]<sup>+</sup> 239.139, found 239.1371.

(AA-IV-55)

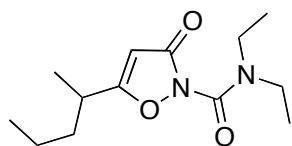


*N*-ethyl-*N*-methyl-3-oxo-5-(pentan-2-yl)isoxazole-2(3*H*)-carboxamide (**57h**): To a solution of triphosgene (66.2 mg, 0.22 mmol, 0.35 equiv.) in DCM (1.0 mL) was added a solution of 5-(pentan-2-yl)isoxazol-3-ol (**46h**) (98.0 mg, 0.63 mmol, 1 equiv.) in DCM (2.0 mL), and the resulting mixture was allowed to stir at room temperature for 2 h. To the reaction mixture, a solution of *N*-ethylmethyl amine (0.8 mL, 0.95 mmol, 1.5 equiv) and diisopropylethylamine (0.2 mL, 1.14 mmol, 1.8 equiv.) in dichloromethane (1.0 mL) was added drop wise, and the reaction was stirred for an additional 30 min. The subsequent reaction mixture was washed with aqueous solution of ammonium chloride, and the organic phase was dried over sodium sulfate and concentrated. The residue was purified by silica gel chromatography eluting with 20% ethyl acetate in hexanes to yield the desired compound **57h** as clear oil (66.1 mg, 44% yield). <sup>1</sup>H NMR (500 MHz, Chloroform-*d*) δ 5.35 (s, 1H), 3.47 (bs, 2H), 3.09 (bs, 3H), 2.75 (heptet, *J* = 7.0 Hz, 1H), 1.72 -1.61 (m, 1H), 1.56-1.47 (m, 1H), 1.45-1.31 (m, 2H), 1.26 (d, *J* = 7.0 Hz, 3H), 1.23 (t, *J* = 7.2 Hz, 3H), 0.92 (t, *J* = 7.3 Hz, 3H). <sup>13</sup>C NMR (126 MHz, Chloroform-*d*) δ 182.91, 168.23, 150.03, 94.58, 44.80, 36.68, 35.97, 33.31, 20.14, 17.84, 13.96, 12.24. HRMS (ESI) calcd for C<sub>12</sub>H<sub>20</sub>N<sub>2</sub>O<sub>3</sub> [M+H]<sup>+</sup> 241.1547, found 241.1527. (**AA-IV-53**)



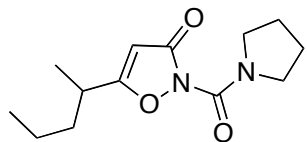
*N*-benzyl-*N*-methyl-3-oxo-5-(pentan-2-yl)isoxazole-2(3*H*)-carboxamide (**58h**): To a solution of triphosgene (67.6 mg, 0.23 mmol, 0.35 equiv) in DCM (1 mL) was added a solution of 5-

(pentan-2-yl)isoxazol-3-ol (**46h**) (100 mg, 0.64 mmol, 1 equiv) in DCM (2.0 mL), and the resulting mixture was allowed to stir at room temperature for 2 h. To the reaction mixture, a solution of methylbenzyl amine (0.13 mL, 0.97 mmol, 1.5 equiv) and diisopropylethylamine (0.2 mL, 1.16 mmol, 1.8 equiv) in dichloromethane (1.0 mL) was added drop wise, and the reaction was stirred for an additional 30 min. The subsequent reaction mixture was washed with aqueous solution of ammonium chloride, and the organic phase was dried over sodium sulfate and concentrated. The residue was purified by silica gel chromatography eluting with 20% ethyl acetate in hexanes to yield the desired compound **58h** as clear oil (42.0 mg, 27% yield). <sup>1</sup>H NMR (500 MHz, Chloroform-*d*)  $\delta$  7.39-7.27 (m, 5H), 5.38 (s, 1H), 4.65 (s, 2H), 3.05 (s, 3H), 2.77 (sextet, *J* = 7.0 Hz, 1H), 1.73-1.64 (m, 1H), 1.57-1.48 (m, 1H), 1.45-1.31 (m, 2H), 1.27 (d, *J* = 7.0 Hz, 3H), 0.93 (t, *J* = 7.3 Hz, 3H). <sup>13</sup>C NMR (126 MHz, CDCl<sub>3</sub>)  $\delta$  183.19, 168.24, 150.76, 135.95, 128.86, 128.10, 127.90, 94.57, 77.41, 77.16, 76.91, 53.06, 36.67, 36.04, 33.36, 20.15, 17.85, 13.97, 0.12. HRMS (ESI) calcd for C<sub>17</sub>H<sub>22</sub>N<sub>2</sub>O<sub>3</sub> [M+H]<sup>+</sup> 303.1703, found 303.1704. (**AA-IV-45**)

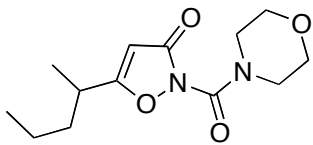


N,N-diethyl-3-oxo-5-(pentan-2-yl)isoxazole-2(3H)-carboxamide (**59h**): Prepared using the general procedure above (*Method F*) from 5-(pentan-2-yl)isoxazol-3-ol (**46h**) (85.0 mg, 0.55 mmol), *N,N*-diethylcarbamoyl chloride (0.35 mL, 2.74 mmol), and toluene (3.0 mL). Concentration of the reaction mixture in vacuo followed by silica gel flash chromatography (20 - 30% ethyl acetate in hexane) yielded **59h** as a clear oil (96.0 mg, 69 %). <sup>1</sup>H NMR (500 MHz, Chloroform-*d*)  $\delta$  5.34 (s, 1H), 3.49 (q, *J* = 6.5 Hz, 4H), 2.74 (heptet, *J* = 7.0 Hz, 1H), 1.74-1.61

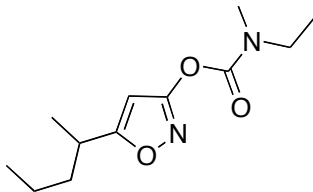
(m, 1H), 1.56-1.45 (m, 1H), 1.45-1.29 (m, 2H), 1.27-1.21 (m, 9H), 0.91 (t,  $J = 7.3$  Hz, 3H).  $^{13}\text{C}$  NMR (126 MHz, Chloroform-*d*)  $\delta$  182.81, 168.36, 149.62, 94.31, 42.47, 36.45, 33.07, 19.89, 17.59, 13.71, 13.30. Due to signal broadening (slow chemical exchange) in carboxamide the two CH<sub>2</sub> and two CH<sub>3</sub> of the *N,N*-diethyl overlap in  $^{13}\text{C}$  NMR. This is consistent with similar observations in seen  $^1\text{H}$  NMR. (see Figure 2.9 Chapter 2 for explanation). HRMS (ESI) calcd for C<sub>13</sub>H<sub>22</sub>N<sub>2</sub>O<sub>3</sub> [M+H]<sup>+</sup> 255.1703, found 255.1687. (**AA-IV-46**)



**5-(pentan-2-yl)-2-(pyrrolidine-1-carbonyl)isoxazol-3(2*H*)-one (60h):** Prepared using the general procedure above (*Method F*) from 5-(pentan-2-yl)isoxazol-3-ol (**46h**) (65.1 mg, 0.42 mmol), 1-pyrrolidinecarbonyl chloride (0.23 mL, 2.10 mmol), and toluene (2.0 mL). Concentration of the reaction mixture in vacuo followed by silica gel flash chromatography (20-30% ethyl acetate in hexane) yielded **60h** as a clear oil (38.7 mg, 37 %).  $^1\text{H}$  NMR (500 MHz, Chloroform-*d*)  $\delta$  5.36 (s, 1H), 3.73 (t,  $J = 6.3$  Hz, 2H), 3.57 (t,  $J = 6.4$  Hz, 2H), 2.75 (sextet,  $J = 7.0$  Hz, 1H), 1.94 (s, 4H), 1.72-1.61 (m, 1H), 1.56-1.47 (m, 1H), 1.45-1.31 (m, 2H), 1.26 (d,  $J = 7.0$  Hz, 3H), 0.92 (t,  $J = 7.3$  Hz, 3H).  $^{13}\text{C}$  NMR (126 MHz, Chloroform-*d*)  $\delta$  182.14, 167.78, 148.43, 94.91, 48.37, 47.31, 36.68, 33.24, 25.89, 24.48, 20.14, 17.83, 13.96. HRMS (ESI) calcd for C<sub>13</sub>H<sub>20</sub>N<sub>2</sub>O<sub>3</sub> [M+H]<sup>+</sup> 253.1547, found 253.1547. (**AA-IV-54**)



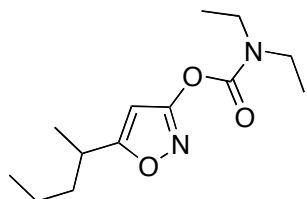
2-(morpholine-4-carbonyl)-5-(pentan-2-yl)isoxazol-3(2H)-one (61h): Prepared using the general procedure above (*Method F*) from 5-(pentan-2-yl)isoxazol-3-ol (**46h**) (99.4 mg, 0.64 mmol), 4-morpholinocarbamoyl chloride (0.37 mL, 3.20 mmol), and toluene (3.0 mL). Concentration of the reaction mixture in vacuo followed by silica gel flash chromatography (20-30% ethyl acetate in hexane) yielded **61h** as a clear oil (133 mg, 78 %). <sup>1</sup>H NMR (500 MHz, Chloroform-*d*) δ 5.36 (s, 1H), 3.80-3.75 (m, 4H), 3.64-3.56 (m, 4H), 2.77 (sextet, *J* = 7.0 Hz, 1H), 1.73-1.61 (m, 1H), 1.57-1.48 (m, 1H), 1.45-1.30 (m, 2H), 1.27 (d, *J* = 7.0 Hz, 3H), 0.93 (t, *J* = 7.3 Hz, 3H). <sup>13</sup>C NMR (126 MHz, Chloroform-*d*) δ 183.23, 167.55, 148.92, 94.29, 66.66, 47.73, 45.19, 36.53, 33.22, 20.00, 17.68, 13.80. HRMS (ESI) calcd for C<sub>13</sub>H<sub>20</sub>N<sub>2</sub>O<sub>4</sub> [M+H]<sup>+</sup> 269.1496, found 269.1476. (AA-IV-50)



5-(pentan-2-yl)isoxazol-3-yl ethyl(methyl)carbamate (63h): To a solution of triphosgene (66.2 mg, 0.22 mmol, 0.35 equiv.) in DCM (1.0 mL) was added a solution of 5-(pentan-2-yl)isoxazol-3-ol (**46h**) (98.0 mg, 0.63 mmol, 1 equiv.) in DCM (2.0 mL), and the resulting mixture was allowed to stir at room temperature for 2 h. To the reaction mixture, a solution of *N*-ethylmethyl amine (0.8 mL, 0.95 mmol, 1.5 equiv) and diisopropylethylamine (0.2 mL, 1.14 mmol, 1.8 equiv.) in dichloromethane (1.0 mL) was added drop wise, and the reaction was stirred for an additional 30 min. The subsequent reaction mixture was washed with aqueous solution of

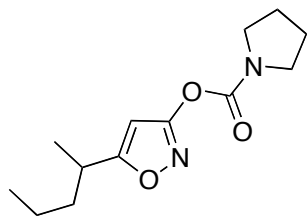
ammonium chloride, and the organic phase was dried over sodium sulfate and concentrated. The residue was purified by silica gel chromatography eluting with 20% ethyl acetate in hexanes to yield the desired compound **63h** as clear oil (30.0 mg, 20% yield). (*Observed (Z)- and (E)-amide rotamers in 1:1 ratio, the following integral ratios correspond to the 1:1 mixture*) <sup>1</sup>H NMR (500 MHz, Chloroform-d) δ 6.14 (s, 2H, both (Z)- and (E)-), 3.46 (q,  $J = 7.2$  Hz, 2H), 3.39 (q,  $J = 7.2$  Hz, 2H), 3.05 (s, 3H), 2.98 (s, 3H), 2.90 (sextet,  $J = 7.0$  Hz, 2H), 1.74-1.62 (m, 2H), 1.58-1.46 (m, 2H), 1.39-1.29 (m, 4H), 1.27 (d,  $J = 7.0$  Hz, 6H), 1.21 (t,  $J = 7.2$  Hz, 3H), 1.18 (t,  $J = 7.2$  Hz, 3H), 0.89 (t,  $J = 7.3$  Hz, 6H). <sup>13</sup>C NMR (126 MHz, Chloroform-d) δ 179.57, 166.75, 166.72, 151.71, 151.57, 94.21, 94.16, 44.59, 44.45, 37.47, 34.51, 34.18, 32.98, 20.21, 18.62, 14.02, 13.28, 12.37. HRMS (ESI) calcd for C<sub>12</sub>H<sub>20</sub>N<sub>2</sub>O<sub>3</sub> [M+H]<sup>+</sup> 241.1547, found 241.1532.

**(AA-IV-53)**

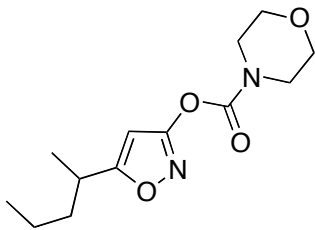


**5-(pentan-2-yl)isoxazol-3-yl diethylcarbamate (64h):** Prepared using the general procedure above (*Method F*) from 5-(pentan-2-yl)isoxazol-3-ol (**46h**) (85.0 mg, 0.55 mmol), *N,N*-diethylcarbamoyl chloride (0.35 mL, 2.74 mmol), and toluene (3.0 mL). Concentration of the reaction mixture in vacuo followed by silica gel flash chromatography (20-30% ethyl acetate in hexane) yielded **64h** as a clear oil (23.0 mg, 16%). <sup>1</sup>H NMR (500 MHz, Chloroform-d) δ 6.17 (s, 1H), 3.43 (q,  $J = 7.1$  Hz, 2H), 3.37 (q,  $J = 7.2$  Hz, 2H), 2.91 (sextet,  $J = 7.0$  Hz, 1H), 1.69 (ddt,  $J = 13.6, 9.2, 6.5$  Hz, 1H), 1.59-1.47 (m, 1H), 1.41-1.28 (m, 2H), 1.27 (d,  $J = 7.0$  Hz, 3H), 1.23 (t,  $J = 7.2$  Hz, 3H), 1.20 (t,  $J = 7.2$  Hz, 3H), 0.90 (t,  $J = 7.3$  Hz, 3H). <sup>13</sup>C NMR (126 MHz, Chloroform-d) δ 179.57, 166.75, 166.72, 151.71, 151.57, 94.21, 94.16, 44.59, 44.45, 37.47, 34.51, 34.18, 32.98, 20.21, 18.62, 14.02, 13.28, 12.37.

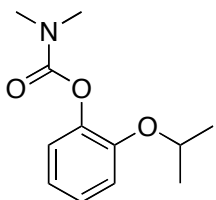
Chloroform-*d*) δ 179.52, 166.75, 151.39, 94.21, 42.70, 42.34, 37.48, 32.98, 20.22, 18.64, 14.24, 14.02, 13.24. HRMS (ESI) calcd for C<sub>13</sub>H<sub>22</sub>N<sub>2</sub>O<sub>3</sub> [M+H]<sup>+</sup> 255.1703, found 255.1687. (**AA-IV-46**)



5-(pentan-2-yl)isoxazol-3-yl pyrrolidine-1-carboxylate (65h): Prepared using the general procedure above (*Method F*) from 5-(pentan-2-yl)isoxazol-3-ol (**46h**) (65.1 mg, 0.42 mmol), 1-pyrrolidinecarbonyl chloride (0.23 mL, 2.10 mmol), and toluene (2.0 mL). Concentration of the reaction mixture in vacuo followed by silica gel flash chromatography (20-30% ethyl acetate in hexane) yielded **65h** as a clear oil (60.4 mg, 57 %). <sup>1</sup>H NMR (500 MHz, Chloroform-*d*) δ 6.17 (s, 1H), 3.56 (t, *J*= 6.6 Hz, 2H), 3.46 (t, *J*= 6.6 Hz, 2H), 2.90 (sextet, *J*= 7.0 Hz, 1H), 2.01-1.84 (m, 4H), 1.74-1.63 (m, 1H), 1.58-1.47 (m, 1H), 1.41-1.28 (m, 2H), 1.26 (d, *J*= 7.0 Hz, 3H), 0.89 (t, *J*= 7.3 Hz, 3H). <sup>13</sup>C NMR (126 MHz, Chloroform-*d*) δ 179.51, 166.67, 150.20, 94.11, 46.80, 46.71, 37.46, 32.97, 25.84, 25.01, 20.21, 18.62, 14.02. HRMS (ESI) calcd for C<sub>13</sub>H<sub>20</sub>N<sub>2</sub>O<sub>3</sub> [M+H]<sup>+</sup> 253.1547, found 253.1528. (**AA-IV-54**)



5-(pentan-2-yl)isoxazol-3-yl morpholine-4-carboxylate (66h): Prepared using the general procedure above (*Method F*) from 5-(pentan-2-yl)isoxazol-3-ol (**46h**) (99.4 mg, 0.64 mmol), 4-morpholinocarbamoyl chloride (0.37 mL, 3.20 mmol), and toluene (3.0 mL). Concentration of the reaction mixture in vacuo followed by silica gel flash chromatography (20-30% ethyl acetate in hexane) yielded **66h** as a clear oil (20.0 mg, 12 %). <sup>1</sup>H NMR (500 MHz, Chloroform-*d*) δ 6.14 (s, 1H), 3.77-3.69 (m, 4H), 3.68-3.64 (m, 2H), 3.59-3.51 (m, 2H), 2.91 (t, *J* = 7.0 Hz, 1H), 1.74-1.64 (m, 1H), 1.58-1.48 (m, 1H), 1.39-1.29 (m, 2H), 1.28 (d, *J* = 7.0 Hz, 3H), 0.90 (t, *J* = 7.3 Hz, 3H). <sup>13</sup>C NMR (126 MHz, Chloroform-*d*) δ 179.86, 166.47, 150.75, 94.11, 66.59, 66.48, 45.20, 44.42, 37.46, 33.01, 20.22, 18.61, 14.03. HRMS (ESI) calcd for C<sub>13</sub>H<sub>20</sub>N<sub>2</sub>O<sub>4</sub> [M+H]<sup>+</sup> 269.1496, found 269.1478. (AA-IV-50)



2-isopropoxyphenyl dimethylcarbamate (67): To a dry round bottom flask was added 2-isopropoxy phenol (500 mg, 12.8 mmol) and dry tetrahydrofuran (9.0 mL) prior to cooling it to 0 °C. To this solution was added potassium *tert*-butoxide (1M in THF, 19.2 mL, 19.2 mmol) at 0 °C and subsequently the reaction mixture was stirred for 20 min at RT. To this solution was added *N,N*-dimethyl carbamoyl chloride (2.94 mL, 32.1 mmol), and the resulting solution was stirred at room temperature for additional 16 h. The solvent was concentrated and the residue

was taken up in dichloromethane and washed with 0.25 M HCl hydrochloric acid, and then brine, and dried over sodium sulfate. The solvent was evaporated and the residue was purified by silica gel column chromatography using 20% ethyl acetate in hexane to afford the **67** as a clear oil (734 mg, 99%). <sup>1</sup>H NMR (500 MHz, Chloroform-*d*) δ 7.14-7.06 (m, 2H), 6.97-6.89 (m, 2H), 4.47 (hept, *J* = 6.1 Hz, 1H), 3.12 (s, 3H), 3.01 (s, 3H), 1.31 (d, *J* = 6.1 Hz, 6H). <sup>13</sup>C NMR (126 MHz, Chloroform-*d*) δ 154.99, 150.05, 142.31, 126.06, 123.56, 121.03, 116.09, 71.78, 36.86, 36.68, 22.34. HRMS (ESI) calcd for C<sub>12</sub>H<sub>17</sub>NO<sub>3</sub> [M+H]<sup>+</sup> 224.1281, found 224.1300.

### 5.11 X-ray crystallographic analysis

X-ray data and structure refinement for compound 46m:

Empirical formula	C <sub>8</sub> H <sub>13</sub> NO <sub>2</sub>	
Formula weight	155.19	
Temperature	100.0 K	
Wavelength	1.54178 Å	
Crystal system	monoclinic	
Space group	<i>P</i> 1 2 <sub>1</sub> / <i>n</i> 1	
Unit cell dimensions	a = 7.5252(2) Å	a= 90°.
	b = 13.0868(4) Å	b= 102.931(3)°.
	c = 9.4783(3) Å	g = 90°.
Volume	909.76(5) Å <sup>3</sup>	
Z	4	
Density (calculated)	1.133 Mg/m <sup>3</sup>	
Absorption coefficient	0.663 mm <sup>-1</sup>	
F(000)	336	
Crystal size	0.269 x 0.115 x 0.047 mm <sup>3</sup>	
Theta range for data collection	5.86 to 76.19°.	
Index ranges	-9<=h<=9, -16<=k<=16, -11<=l<=10	
Reflections collected	7061	
Independent reflections	1891 [R(int) = 0.0186]	
Completeness to theta = 76.19°	99.4 %	
Absorption correction	Gaussian	

Max. and min. transmission	0.971 and 0.919
Refinement method	Full-matrix least-squares on $F^2$
Data / restraints / parameters	1891 / 0 / 106
Goodness-of-fit on $F^2$	1.040
Final R indices [ $I > 2\sigma(I)$ ]	$R_1 = 0.0366, wR_2 = 0.0968$
R indices (all data)	$R_1 = 0.0392, wR_2 = 0.0992$
Largest diff. peak and hole	0.213 and -0.156 e. $\text{\AA}^{-3}$

X-ray data and structure refinement for compound 49k:

Empirical formula	$C_9H_{14}N_2O_3$
Formula weight	198.22
Temperature	100.5 K
Wavelength	1.54178 $\text{\AA}$
Crystal system	monoclinic
Space group	$P\bar{1}\ 2_1/c\ \bar{1}$
Unit cell dimensions	$a = 5.11746(18) \text{\AA}$ $a = 90^\circ$ . $b = 9.3660(3) \text{\AA}$ $b = 91.787(4)^\circ$ . $c = 20.8721(9) \text{\AA}$ $g = 90^\circ$ .
Volume	999.92(6) $\text{\AA}^3$
Z	4
Density (calculated)	1.317 Mg/m <sup>3</sup>
Absorption coefficient	0.831 mm <sup>-1</sup>
F(000)	424
Crystal size	0.2382 x 0.1393 x 0.0307 mm <sup>3</sup>
Theta range for data collection	4.24 to 74.70°.
Index ranges	-5≤h≤6, -11≤k≤11, -25≤l≤25
Reflections collected	8518
Independent reflections	2054 [R(int) = 0.0313]
Completeness to theta = 74.70°	99.5 %
Absorption correction	Gaussian
Max. and min. transmission	0.974 and 0.903
Refinement method	Full-matrix least-squares on $F^2$
Data / restraints / parameters	2054 / 0 / 130
Goodness-of-fit on $F^2$	1.028

Final R indices [ $I > 2\sigma(I)$ ]	$R_1 = 0.0365$ , $wR_2 = 0.0969$
R indices (all data)	$R_1 = 0.0419$ , $wR_2 = 0.1016$
Largest diff. peak and hole	0.183 and -0.240 e. $\text{\AA}^{-3}$

X-ray data and structure refinement for compound 47e:

Empirical formula	$C_{10}H_{14}N_2O_3$
Formula weight	210.23
Temperature	99.95(10) K
Wavelength	1.54184 $\text{\AA}$
Crystal system	Triclinic
Space group	P -1
Unit cell dimensions	$a = 7.9449(6) \text{\AA}$ $a = 64.790(7)^\circ$ . $b = 8.1997(5) \text{\AA}$ $b = 68.251(7)^\circ$ . $c = 9.5467(6) \text{\AA}$ $g = 70.562(6)^\circ$ .
Volume	511.18(7) $\text{\AA}^3$
Z	2
Density (calculated)	1.366 Mg/m <sup>3</sup>
Absorption coefficient	0.848 mm <sup>-1</sup>
F(000)	224
Crystal size	0.2751 x 0.1604 x 0.0677 mm <sup>3</sup>
Theta range for data collection	5.316 to 74.822°.
Index ranges	-8≤h≤9, -10≤k≤10, -11≤l≤11
Reflections collected	4498
Independent reflections	2068 [R(int) = 0.0307]
Completeness to theta = 67.684°	99.6 %
Absorption correction	Gaussian
Max. and min. transmission	0.960 and 0.877
Refinement method	Full-matrix least-squares on $F^2$
Data / restraints / parameters	2068 / 0 / 138
Goodness-of-fit on $F^2$	1.060
Final R indices [ $I > 2\sigma(I)$ ]	$R_1 = 0.0416$ , $wR_2 = 0.1124$
R indices (all data)	$R_1 = 0.0455$ , $wR_2 = 0.1163$
Extinction coefficient	n/a
Largest diff. peak and hole	0.254 and -0.240 e. $\text{\AA}^{-3}$

## **5.12 Bibliography**

1. Sorensen, U. S.; Falch, E.; Krogsgaard-Larsen, P., A novel route to 5-substituted 3-isoxazolols. Cyclization of *N,O*-diboc  $\beta$ -keto hydroxamic acids synthesized via acyl meldrum's acids. *J. Org. Chem.* **2000**, *65*, 1003-1007.

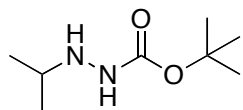
## Chapter 6: Experimental procedures and analytical data for Chapter 3

### 6.1 Materials

NMR spectra were obtained on JEOL Eclipse-plus 500 MHz MHz spectrometer at 500 ( $^1\text{H}$ ) and 126 ( $^{13}\text{C}$ ) MHz or Unity-plus 400 at 400 ( $^1\text{H}$ ) and 101 ( $^{13}\text{C}$ ) MHz. The chemical shifts are reported in  $\delta$  (ppm), and coupling constants are given in Hz. High-resolution ESI Mass spectra were obtained on an Agilent 6220 Accurate Mass TOF LC/MS. THF for moisture-sensitive reactions was distilled from sodium-benzophenone. Other dry solvents were purchased from EMD Millipore and were used without any further purification. Column chromatography was performed using Silica gel (ZEOprep 60 ECO 40-63  $\mu$ ) was purchased from AIC. Reagents were purchased mainly from Sigma Aldrich and were used as received.

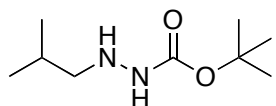
### 6.2 Experimental section for chapter 3 section 3.2

Synthesis and characterization of *N*-alkyl-*t*-butoxycarbonyl hydrazine (**89b-d**): Adapted from the procedure of Dragowich et al.<sup>1</sup>

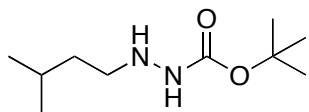


*t*-butyl 2-isopropylhydrazinecarboxylate (**89b**): To a solution of acetone (1.12 mL, 15.1 mmol) in methanol (10.0 mL) was added *t*-butyl carbazate (2.00 g, 15.1 mmol) at room temperature. The resulting reaction mixture was stirred at room temperature for 1 h and then cooled to 0 °C. To this solution was added glacial acetic acid (1.64 mL) and sodium cyanoborohydride (2.37 g, 37.8 mmol) sequentially, and the reaction was stirred for additional 1 h at room temperature. On completion of the reaction, the solvent was concentrated in vacuo and the residue was taken up

in dichloromethane. The organic layer was washed with sodium bicarbonate, and then brine, and dried over sodium sulfate. The solvent was evaporated affording **89b** as a clear oil in quantitative yield (2.6 g). <sup>1</sup>H NMR (500 MHz, Chloroform-*d*) δ 6.13 (s, 1H), 3.52 (s, 1H), 3.18-3.07 (m, 1H), 1.45 (s, 9H), 1.01 (d, *J* = 6.3 Hz, 6H). <sup>13</sup>C NMR (126 MHz, Chloroform-*d*) δ 156.99, 80.52, 50.89, 28.50, 20.75. HRMS (ESI) calcd for C<sub>8</sub>H<sub>18</sub>N<sub>2</sub>O<sub>2</sub> [M+Na]<sup>+</sup> 197.126, found 197.128. (**AA-I-130**)

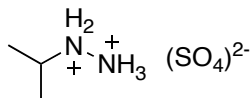


*t*-butyl 2-isobutylhydrazinecarboxylate (**89c**): To a solution of *i*-butyraldehyde (1.38 mL, 15.1 mmol) in methanol (10.0 mL) was added *t*-butyl carbazate (2.00 g, 15.1 mmol) at room temperature. The resulting reaction mixture was stirred at room temperature for 1 h and then cooled to 0 °C. To this solution was added glacial acetic acid (1.64 mL) and sodium cyanoborohydride (2.37 g, 37.8 mmol) sequentially, and the reaction was stirred for additional 1 h at room temperature. On completion of the reaction, the solvent was concentrated in vacuo and the residue was taken up in dichloromethane. The organic layer was washed with sodium bicarbonate, and then brine, and dried over sodium sulfate. The solvent was evaporated affording **89c** as a clear oil (2.69 g, 94%). <sup>1</sup>H NMR (500 MHz, Chloroform-*d*) δ 6.06 (s, 1H), 3.92 (s, 1H), 2.65 (d, *J* = 6.9 Hz, 2H), 1.78-1.66 (m, 1H), 1.45 (s, 9H), 0.92 (d, *J* = 6.7 Hz, 6H). <sup>13</sup>C NMR (126 MHz, Chloroform-*d*) δ 156.92, 80.49, 60.10, 28.52, 27.02, 20.71. HRMS (ESI) calcd for C<sub>9</sub>H<sub>20</sub>N<sub>2</sub>O<sub>2</sub> [M+H]<sup>+</sup> 189.1598, found 133.0928. (**AA-I-120**)



t-butyl 2-isopentylhydrazinecarboxylate (89d): To a solution of isovaleraldehyde (100 mg, 0.76 mmol) in methanol (2.0 mL) was added *t*-butyl carbazate (0.082 mL, 0.76 mmol) at room temperature. The resulting reaction mixture was stirred at room temperature for 1 h and then cooled to 0 °C. To this solution was added glacial acetic acid (0.1 mL) and sodium cyanoborohydride (120 mg, 1.89 mmol) sequentially, and the reaction was stirred for additional 1 h at room temperature. On completion of the reaction, the solvent was concentrated in vacuo and the residue was taken up in dichloromethane. The organic layer was washed with sodium bicarbonate, and then brine, and dried over sodium sulfate. The solvent was evaporated affording **89d** as a clear oil, which was taken to the next step as crude (102 mg crude, 67%). (AA-I-34)

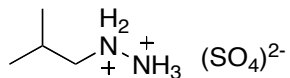
Synthesis and characterization of N-alkyl hydrazine salt (90b-d): Adapted from the procedure of Hilpert et al.<sup>2</sup>



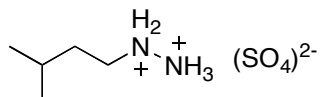
i-propyl hydrazine sulfate (90b): To a solution of **89b** (2.84 g, 16.3 mmol) in *i*-propanol (15.0 mL) was added H<sub>2</sub>SO<sub>4</sub> (1.0 mL) drop wise, and the resulting reaction mixture was stirred at 50 °C for 2 h. Following this, the reaction mixture was brought to room temperature and diluted with diethyl ether. The resulting solution was cooled to -15 °C and stirred for additional 2 hour. Filtration followed by washing with cold (-10 °C) *i*-propanol/diethyl ether afforded the desired compound **90b** as a white crystalline solid (1.70 g, 61%). <sup>1</sup>H NMR (500 MHz, Methanol-*d*<sub>4</sub>) δ

3.31-3.25 (m, 1H), 1.26 (d,  $J = 6.6$  Hz, 6H).  $^{13}\text{C}$  NMR (126 MHz, Methanol- $d_4$ )  $\delta$  54.85, 17.82.

This compound has been reported previously in literature.<sup>3</sup> (**AA-I-131**)



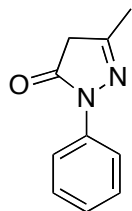
*i*-butylhydrazine sulfate (**90c**): To a solution of **89c** (470 mg, 2.51 mmol) in *i*-propanol (2.6 mL) was added H<sub>2</sub>SO<sub>4</sub> (0.22 mL) drop wise, and the resulting reaction mixture was stirred at 50 °C for 2 h. Following this, the reaction mixture was brought to room temperature and diluted with diethyl ether. The resulting solution was cooled to -15 °C and stirred for additional 1 hour. Filtration followed by washing with cold (-10 °C) *i*-propanol/diethyl ether afforded the desired compound **90c** as a white crystalline solid (230 mg, 49%) white crystalline salt.  $^1\text{H}$  NMR (500 MHz, Methanol- $d_4$ )  $\delta$  2.82 (d,  $J = 7.1$  Hz, 2H), 1.99-1.86 (m, 1H), 0.96 (d,  $J = 6.7$  Hz, 6H).  $^{13}\text{C}$  NMR (126 MHz, Methanol- $d_4$ )  $\delta$  59.89, 26.42, 20.41. The  $^1\text{H}$  NMR and  $^{13}\text{C}$  NMR for this compound matches the reported literature data.<sup>2</sup> (**AA-I-121**)



*i*-pentylhydrazine sulfate (**90d**): To a solution of **89d** (104 mg, 0.51 mmol) in *i*-propanol was added H<sub>2</sub>SO<sub>4</sub> (0.07 mL) drop wise, and the resulting reaction mixture was stirred at 50 °C for 30 minutes. Following this, the reaction mixture was brought to room temperature and diluted with diethyl ether. The resulting solution was cooled to -15 °C and stirred for additional 1 h. Filtration followed by washing with cold (-10 °C) *i*-propanol/diethyl ether afforded the desired compound **90d** as a white crystalline solid (65 mg, 62%).  $^1\text{H}$  NMR (500 MHz, Methanol- $d_4$ )  $\delta$  3.05-2.98 (m, 2H), 1.68-1.57 (m, 1H), 1.53-1.44 (m, 2H), 0.91 (d,  $J = 6.6$  Hz, 6H).  $^{13}\text{C}$  NMR (126 MHz,

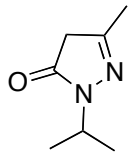
Methanol-*d*<sub>4</sub>) δ 51.27, 34.62, 27.03, 22.60. This compound has been reported previously in literature.<sup>4</sup> (**AA-I-34**)

Synthesis and characterization of 3-methyl-*N*-alkyl pyrazol-5-one (**85a-d**):



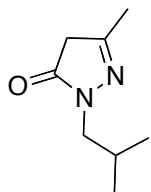
3-methyl-1-phenyl-1*H*-pyrazol-5(4*H*)-one (**85a**): Adapted from the procedure of Moreau et al.<sup>5</sup>

To a solution of phenyl hydrazine (1.50 g, 13.9 mmol) in glacial acetic acid (7.5 mL) was added ethyl acetoacetate (1.75 mL, 13.9 mmol). The resulting reaction mixture was refluxed for 4 hours, and then the reaction was cooled to room temperature. The solvent was concentrated in vacuo, and the residue was purified on silica gel chromatography using 30% ethyl acetate in hexane to yield the intermediate **85a** as white solid (2.36 g, 98%). <sup>1</sup>H NMR (500 MHz, Chloroform-*d*) δ 7.85 (d, *J* = 8.0 Hz, 2H), 7.39 (t, *J* = 7.9 Hz, 2H), 7.18 (t, *J* = 7.4 Hz, 1H), 3.44 (s, 2H), 2.20 (s, 3H). <sup>13</sup>C NMR (126 MHz, Chloroform-*d*) δ 170.70, 156.40, 138.18, 128.98, 125.20, 119.04, 43.26, 17.19. HRMS (ESI) calcd for C<sub>10</sub>H<sub>10</sub>N<sub>2</sub>O [M+H]<sup>+</sup> 175.0866, found 175.0865. The <sup>1</sup>H NMR and <sup>13</sup>C NMR for this compound matches the reported literature data. The <sup>1</sup>H NMR and <sup>13</sup>C NMR for this compound matches the reported literature data.<sup>6</sup> (**AA-I-22**)



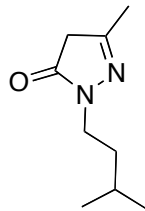
1-isopropyl-3-methyl-1*H*-pyrazol-5(4*H*)-one (85b): Adapted from the procedure of Nam et al.<sup>7</sup>

To a solution of sodium hydroxide (232 mg, 0.24 mmol) in methanol/water (8 mL/2mL) was added **90b** (1.00 g, 5.81 mmol). To the resulting reaction mixture was added ethyl acetoacetate (0.74 mL, 5.81 mmol) drop wise. The reaction mixture was allowed to stir overnight at 50 °C before in vacuo concentration of the solvent. The residue was taken up in dichloromethane and washed with water, and then brine, and dried over sodium sulfate. The organic layer was evaporated and the residue was purified by silica gel column chromatography using 4-6% methanol/dichloromethane to afford **85b** as an off white solid (151 mg, 19%). <sup>1</sup>H NMR (500 MHz, Chloroform-*d*) δ 4.41 (heptet, *J* = 6.6 Hz, 1H), 3.19 (s, 2H), 2.10 (s, 3H), 1.28 (d, *J* = 6.6 Hz, 6H). Due to limited amount of the sample full characterization was done in the next step. The <sup>1</sup>H NMR for this compound matches the reported literature data.<sup>8</sup> (**AA-I-132**)



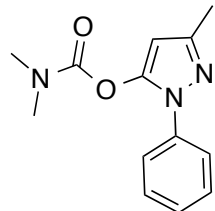
1-isobutyl-3-methyl-1*H*-pyrazol-5(4*H*)-one (85c): Adapted from the procedure of Nam et al.<sup>7</sup> To a solution of sodium hydroxide (236 mg, 5.91 mmol) in methanol/water (6 mL/0.6 mL) was added **90c** (1.10 g, 5.91 mmol). To the resulting reaction mixture was added ethyl acetoacetate (0.75 mL, 5.91 mmol) drop wise. The reaction mixture was allowed to stir overnight at 50 °C before in vacuo concentration of the solvent. The residue was taken up in dichloromethane and washed with water, and then brine, and dried over sodium sulfate. The organic layer was

evaporated and the residue was purified by silica gel column chromatography using 4-6% methanol/dichloromethane to afford **85c** as an off white solid (426 mg, 47%). <sup>1</sup>H NMR (500 MHz, Chloroform-*d*) δ 3.43 (d, *J* = 7.2 Hz, 2H), 3.21 (s, 2H), 2.10 (s, 3H), 2.16-2.02 (m, 1H), 0.92 (d, *J* = 6.7 Hz, 6H). <sup>13</sup>C NMR (126 MHz, Chloroform-*d*) δ 172.45, 155.30, 51.48, 41.79, 27.94, 20.08, 17.10. HRMS (ESI) calcd for C<sub>8</sub>H<sub>14</sub>N<sub>2</sub>O [M+H]<sup>+</sup> 155.1179, found 155.1171. The <sup>1</sup>H NMR and <sup>13</sup>C NMR for this compound matches the reported literature data.<sup>9</sup> (**AA-I-123**)

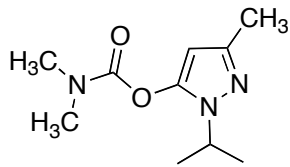


**1-isopentyl-3-methyl-1*H*-pyrazol-5(4*H*)-one (85d):** Adapted from the procedure of Nam et al.<sup>7</sup> To a solution of sodium hydroxide (20.0 mg, 0.50 mmol) in methanol/water (4 mL/0.4 mL) was added **90d** (100 mg, 0.50 mmol). To the resulting reaction mixture was added ethyl acetoacetate (0.06 mL, 0.50 mmol) drop wise. The reaction mixture was allowed to stir overnight at 50 °C before in vacuo concentration of the solvent. The residue was taken up in dichloromethane and washed with water, and then brine, and dried over sodium sulfate. The organic layer was evaporated and the residue was purified by silica gel column chromatography using 4-6% methanol/dichloromethane to afford **85d** as an off white solid (20.0 mg, 24%). <sup>1</sup>H NMR (500 MHz, Chloroform-*d*) δ 3.63 (t, *J* = 7.5 Hz, 2H), 3.18 (s, 2H), 2.09 (s, 3H), 1.65-1.48 (m, 3H), 0.93 (d, *J* = 6.2 Hz, 6H). <sup>13</sup>C NMR (126 MHz, Chloroform-*d*) δ 172.05, 155.48, 42.52, 41.91, 37.18, 25.90, 22.53, 17.11. HRMS (ESI) calcd for C<sub>9</sub>H<sub>16</sub>N<sub>2</sub>O [M+H]<sup>+</sup> 169.1335, found 169.1341. The <sup>1</sup>H NMR and <sup>13</sup>C NMR for this compound matches the reported literature data on Scifinder. (**AA-I-62**)

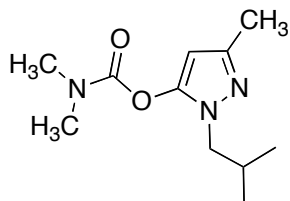
Synthesis and characterization of 3-methyl-N-alkylpyrazol-5-yl dimethylcarbamates (**82a-d**):



3-methyl-1-phenyl-1*H*-pyrazol-5-yl dimethylcarbamates (**82a**): To a dry round bottom flask was added **85a** (900 mg, 5.10 mmol) and dry tetrahydrofuran (7.0 mL) prior to cooling it to 0 °C. To this solution was added potassium *tert*-butoxide (1 M in THF, 6.72 mL, 6.72 mmol) at 0 °C and subsequently the reaction mixture was stirred for 20 min at room temperature. To this solution was added *N,N*-dimethyl carbamoyl chloride (1.19 mL, 12.9 mmol), and the resulting solution was stirred at room temperature for additional 1 h. The solvent was concentrated and the residue was taken up in dichloromethane and washed with 0.25 M HCl hydrochloric acid, and then brine, and dried over sodium sulfate. The organic layer was evaporated and the residue was purified by silica gel column chromatography using 40% ethyl acetate in hexane to afford the **82a** as clear oil (1.07g, 85%). <sup>1</sup>H NMR (500 MHz, Chloroform-*d*) δ 7.53 (d, *J* = 8.1 Hz, 2H), 7.45-7.37 (m, 2H), 7.30 (t, *J* = 7.4 Hz, 1H), 6.05 (s, 1H), 3.00 (s, 3H), 2.97 (s, 3H), 2.31 (s, 3H). <sup>13</sup>C NMR (126 MHz, Chloroform-*d*) δ 151.91, 149.07, 145.38, 138.34, 129.07, 127.14, 95.69, 37.20, 36.67, 14.69. HRMS (ESI) calcd for C<sub>13</sub>H<sub>15</sub>N<sub>3</sub>O<sub>2</sub> [M+H]<sup>+</sup> 246.1237, found 246.1245. (**AA-I-30**)

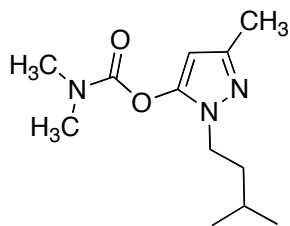


1-isopropyl-3-methyl-1*H*-pyrazol-5-yl dimethylcarbamates (82b): To a dry round bottom flask was added **85b** (151 mg, 1.08 mmol) and dry tetrahydrofuran (2.0 mL) prior to cooling it to 0 °C. To this solution was added potassium *tert*- butoxide (1 M in THF, 1.40 mL, 1.40 mmol) at 0 °C and subsequently the reaction mixture was stirred for 20 min at room temperature. To this solution was added *N,N*-dimethyl carbamoyl chloride (0.25 mL, 2.69 mmol), and the resulting solution was stirred at room temperature for additional 3 h. The solvent was concentrated and the residue was taken up in dichloromethane and washed with 0.25 M HCl hydrochloric acid, and then brine, and dried over sodium sulfate. The organic layer was evaporated and the residue was purified by silica gel column chromatography using 30% ethyl acetate in hexane to afford the **82b** as clear oil (177 mg, 77%). <sup>1</sup>H NMR (500 MHz, Chloroform-*d*) δ 5.76 (s, 1H), 4.37-4.27 (m, 1H), 3.09 (s, 3H), 3.01 (s, 3H), 2.22 (s, 3H), 1.43 (d, *J* = 6.7 Hz, 6H). <sup>13</sup>C NMR (126 MHz, Chloroform-*d*) δ 152.30, 146.86, 144.43, 93.61, 48.75, 37.11, 36.64, 22.13, 14.66. HRMS (ESI) calcd for C<sub>10</sub>H<sub>17</sub>N<sub>3</sub>O<sub>2</sub> [M+H]<sup>+</sup> 212.1394, found 212.1389. (**AA-I-133**)



1-isobutyl-3-methyl-1*H*-pyrazol-5-yl dimethylcarbamates (82c): To a dry round bottom flask was added **85c** (300 mg, 1.95 mmol) and dry tetrahydrofuran (3.0 mL) prior to cooling it to 0 °C. To this solution was added potassium *tert*- butoxide (1 M in THF, 2.53 mL, 2.53 mmol) at 0 °C

and subsequently the reaction mixture was stirred for 20 min at room temperature. To this solution was added *N,N*-dimethyl carbamoyl chloride (0.45 mL, 4.90 mmol), and the resulting solution was stirred at room temperature for additional 1 h. The solvent was concentrated and the residue was taken up in dichloromethane and washed with 0.25 M HCl hydrochloric acid, and then brine, and dried over sodium sulfate. The organic layer was evaporated and the residue was purified by silica gel column chromatography using 30% ethyl acetate in hexane to afford the **82c** as clear oil (349 mg, 79%). <sup>1</sup>H NMR (500 MHz, Chloroform-*d*) δ 5.78 (s, 1H), 3.65 (d, *J* = 7.4 Hz, 2H), 3.05 (s, 3H), 2.98 (s, 3H), 2.18 (s, 3H), 2.14 (m, 1H), 0.86 (d, *J* = 6.7 Hz, 6H). <sup>13</sup>C NMR (126 MHz, Chloroform-*d*) δ 152.00, 147.05, 145.62, 93.12, 54.82, 37.10, 36.60, 29.33, 20.11, 14.56. HRMS (ESI) calcd for C<sub>11</sub>H<sub>19</sub>N<sub>3</sub>O<sub>2</sub> [M+H]<sup>+</sup> 226.155, found 226.1557. (**AA-I-124**)

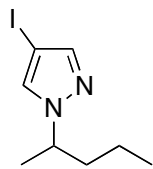


1-isopentyl-3-methyl-1*H*-pyrazol-5-yl dimethylcarbamates (82d): To a dry round bottom flask was added **85d** (142 mg, 0.84 mmol) and dry tetrahydrofuran (2.0 mL) prior to cooling it to 0 °C. To this solution was added potassium *tert*- butoxide (1 M in THF, 1.1 mL, 1.1 mmol) at 0 °C and subsequently the reaction mixture was stirred for 20 min at room temperature. To this solution was added *N,N*-dimethyl carbamoyl chloride (0.23 mL, 2.11 mmol), and the resulting solution was stirred at room temperature for additional 1 h. The solvent was concentrated and the residue was taken up in dichloromethane and washed with 0.25 M HCl hydrochloric acid, and then brine, and dried over sodium sulfate. The organic layer was evaporated and the residue was purified by silica gel column chromatography using 30% ethyl acetate in hexane to afford the **82d** as clear

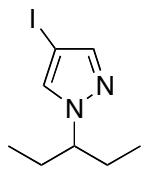
oil (124 mg, 61%).  $^1\text{H}$  NMR (500 MHz, Methanol-*d*<sub>4</sub>)  $\delta$  5.81 (s, 1H), 3.91 (t, *J* = 7.4 Hz, 2H), 3.11 (s, 3H), 3.00 (s, 3H), 2.18 (s, 3H), 1.64 (q, *J* = 7.1 Hz, 2H), 1.58-1.46 (m, 1H), 0.92 (d, *J* = 6.6 Hz, 6H).  $^{13}\text{C}$  NMR (126 MHz, Methanol-*d*<sub>4</sub>)  $\delta$  152.24, 147.11, 145.68, 93.65, 45.16, 38.25, 35.86, 35.51, 25.26, 21.34, 12.77. HRMS (ESI) calcd for C<sub>12</sub>H<sub>21</sub>N<sub>3</sub>O<sub>2</sub> [M+H]<sup>+</sup> 240.1707, found 240.1702. (**AA-I-129**)

### 6.3 Experimental section for chapter 3 section 3.4

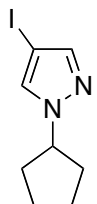
Synthesis and characterization of 4-iodo-N-alkyl pyrazoles (93a-e): *Partly adapted from the procedure of Kim et al.*<sup>10</sup>



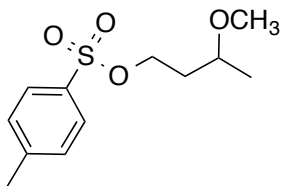
4-iodo-1-(pentan-2-yl)-1*H*-pyrazole (93a): To a mixture of crude mixture of **92a** (1.38 g, 10.0 mmol) in water (7.0 mL) was sequentially added iodine (1.40 g, 5.50 mmol) and 35% hydrogen peroxide (0.56 mL, 6.60 mmol), and the mixture was kept stirring for 24 h at room temperature. The reaction was quenched by the addition of a cold solution of saturated sodium thiosulfate and the subsequent mixture was extracted with ethyl acetate. The combined extracts were dried over anhydrous sodium sulfate and concentrated in vacuo. The residue obtained was chromatographed over silica gel eluting with 5% ethyl acetate in hexanes to furnish **93a** as a colorless oil (1.48 g, 56%).  $^1\text{H}$  NMR (500 MHz, Chloroform-*d*)  $\delta$  7.48 (s, 1H), 7.41 (s, 1H), 4.27-4.33 (m, 1H), 1.81-1.88 (m, 1H), 1.63-1.70 (m, 1H), 1.45 (d, *J* = 6.8 Hz, 3H), 1.10-1.25 (m, 2H), 0.87 (t, *J* = 7.4 Hz, 3H).  $^{13}\text{C}$  NMR (126 MHz, Chloroform-*d*)  $\delta$  143.65, 131.66, 58.78, 55.29, 39.14, 21.30, 19.29, 13.71. HRMS (ESI) calcd for C<sub>8</sub>H<sub>13</sub>N<sub>2</sub>I [M+H]<sup>+</sup> 265.0116, found 265.0189. (**AA-III-77**)



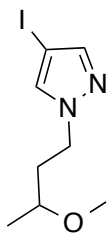
**4-iodo-1-(pentan-3-yl)-1*H*-pyrazole (**93b**):** To a mixture of sodium hydride (60% dispersion in mineral oil, 770 mg, 19.1 mmol) in DMF (5.8 mL) at 0 °C was added drop wise a solution of pyrazole (1.00 g, 14.7 mmol) in DMF (1.5 mL), and the subsequent mixture was kept stirring at room temperature for 1 h. To this mixture was added 3-bromopentane (2.74 mL, 22.0 mmol), and the reaction was allowed to proceed at room temperature (25 °C) for 16 h. The reaction mixture was diluted with diethyl ether, which was rinsed with brine. After removing the diethyl ether, the crude product **92b** was directly used for the next step reaction without further purification. To a mixture of **92b** (2.03 g, 14.6 mmol) in water (10.0 mL) was sequentially added iodine (2.05 g, 8.08 mmol) and 35% hydrogen peroxide (0.83 mL, 9.69 mmol), and the mixture was kept stirring for 24 h at room temperature. The reaction was quenched by the addition of a cold solution of saturated sodium thiosulfate and the subsequent mixture was extracted with ethyl acetate. The combined extracts were dried over anhydrous sodium sulfate and concentrated in vacuo. The residue obtained was chromatographed over silica gel eluting with 5% ethyl acetate in hexanes to furnish **93b** as a colorless oil (2.22 g, 57%). <sup>1</sup>H NMR (500 MHz, Chloroform-*d*) δ 7.51 (s, 1H), 7.40 (s, 1H), 3.94-3.85 (m, 1H), 1.91-1.73 (m, 4H), 0.76 (t, *J* = 7.4 Hz, 6H). <sup>13</sup>C NMR (126 MHz, Chloroform-*d*) δ 144.03, 132.85, 67.30, 55.21, 28.51, 10.77. HRMS (ESI) calcd for C<sub>8</sub>H<sub>13</sub>N<sub>2</sub>I [M+H]<sup>+</sup> 265.0126, found 265.0199. (**AA-III-85**)



**1-cyclopentyl-4-iodo-1*H*-pyrazole (93c):** To a mixture of sodium hydride (60% dispersion in mineral oil, 763 mg, 19.1 mmol) in DMF (5.8 mL) at 0 °C was added drop wise a solution of pyrazole (1.00 g, 14.7 mmol) in DMF (1.5 mL), and the subsequent mixture was kept stirring at room temperature for 1 h. To this mixture was added bromocyclopentane (2.36 mL, 22.0 mmol), and the reaction was allowed to proceed at room temperature (25 °C) for 16 h. The reaction mixture was diluted with diethyl ether, which was rinsed with brine. After removing the diethyl ether, the crude product **92c** was directly used for the next step reaction without further purification. To a mixture of **92c** (1.98 g, 14.6 mmol) in water (10.0 mL) was sequentially added iodine (2.04 g, 8.03 mmol) and 35% hydrogen peroxide (0.83 mL, 9.64 mmol), and the mixture was kept stirring for 24 h at room temperature. The reaction was quenched by the addition of a cold solution of saturated sodium thiosulfate and the subsequent mixture was extracted with ethyl acetate. The combined extracts were dried over anhydrous sodium sulfate and concentrated in vacuo. The residue obtained was chromatographed over silica gel eluting with 5% ethyl acetate in hexanes to furnish **93c** as a colorless oil (2.42 g, 63%). <sup>1</sup>H NMR (500 MHz, Chloroform-*d*) δ 7.46 (s, 1H), 7.42 (s, 1H), 4.61 (quintet, *J* = 7.1 Hz, 1H), 2.16-2.01 (m, 2H), 1.99-1.90 (m, 2H), 1.87-1.75 (m, 2H), 1.72-1.60 (m, 2H). <sup>13</sup>C NMR (126 MHz, Chloroform-*d*) δ 143.82, 132.00, 63.51, 55.39, 33.02, 24.12. This compound is described by Chemical Abstracts Service as Registry Number 1194377-14-4. (**AA-IV-78**)

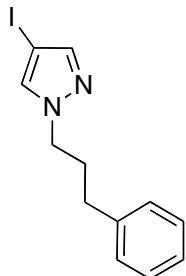


3-methoxybutyl 4-methylbenzenesulfonate (95): To a solution of 3-methoxy-*t*-butanol (1.10 mL, 9.60 mmol) in DCM (38 mL) at 0 °C was added triethylamine (4.0 mL, 28.8 mmol), and *N,N*-dimethylaminopyridine (117 mg, 0.96 mmol). The reaction mixture was brought to room temperature and stirred for 30 minutes. The above solution was brought to 0 °C and tosylchloride (2.75 g, 14.4 mmol) dissolved in DCM was added drop wise. The subsequent reaction mixture was allowed to stir at room temperature overnight. The resulting solution was allowed to stir at room temperature for 24 hours followed by a work-up in water, and brine. The combined organic layers were dried over anhydrous sodium sulfate, and a column purification in 20% ethyl acetate in hexane yielded the desired compound **95** as a clear oil (2.28 g, 92%). <sup>1</sup>H NMR (400 MHz, Chloroform-*d*) δ 7.76 (d, *J* = 7.3 Hz, 1H), 7.32 (d, *J* = 7.3 Hz, 1H), 4.17-4.09 (m, 1H), 4.10-4.01 (m, 1H), 3.40-3.29 (m, 1H), 3.17 (s, 3H), 2.41 (s, 3H), 1.87-1.67 (m, 2H), 1.06 (d, *J* = 5.9 Hz, 3H). <sup>13</sup>C NMR (101 MHz, Chloroform-*d*) δ 144.69, 132.97, 129.79, 127.84, 72.56, 67.58, 56.04, 35.90, 21.57, 18.77. HRMS (ESI) calcd for C<sub>12</sub>H<sub>18</sub>O<sub>4</sub>S [M+H]<sup>+</sup> 259.0999, found 259.0986. (**AA-III-182**)



4-iodo-1-(3-methoxybutyl)-1*H*-pyrazole (93d): To a mixture of sodium hydride (60% dispersion in mineral oil, 134 mg, 3.35 mmol) in DMF (1.3 mL) at 0 °C was added drop wise a solution of

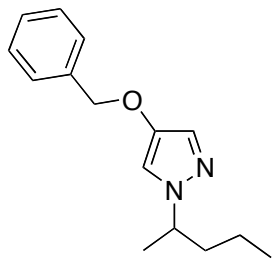
4-iodopyrazole (500 mg, 2.58 mmol) in DMF (2.6 mL), and the subsequent mixture was kept stirring at room temperature for 1 h. To this mixture was added **95** (866 mg, 3.35 mmol) in DMF (1.3 mL), and the reaction was allowed to proceed at room temperature (25 °C) for 16 h. The reaction mixture was diluted with diethyl ether, which was rinsed with brine. After removing the diethyl ether, the residue obtained was chromatographed over silica gel eluting with 5% ethyl acetate in chloroform to furnish **93d** as a clear oil (507 mg, 35%). <sup>1</sup>H NMR (500 MHz, Chloroform-*d*) δ 7.49 (s, 1H), 7.41 (s, 1H), 4.27-4.15 (m, 2H), 3.29 (s, 3H), 3.22-3.13 (m, 1H), 2.02 (dtd, *J* = 14.9, 8.0, 4.1 Hz, 1H), 1.89 (dtd, *J* = 14.9, 8.0, 4.1 Hz, 1H), 1.12 (d, *J* = 5.8 Hz, 3H). <sup>13</sup>C NMR (126 MHz, Chloroform-*d*) δ 144.45, 133.90, 73.46, 56.15, 55.54, 49.15, 37.22, 18.85. HRMS (ESI) calcd for C<sub>8</sub>H<sub>13</sub>IN<sub>2</sub>O [M+H]<sup>+</sup> 280.0073, found 281.0122. (**AA-III-183**)



4-iodo-1-(3-phenylpropyl)-1*H*-pyrazole (93e): To a mixture of sodium hydride (60% dispersion in mineral oil, 1.15 g, 28.6 mmol) in DMF (8.8 mL) at 0 °C was added drop wise a solution of pyrazole (1.50 g, 22.1 mmol) in DMF (2.2 mL), and the subsequent mixture was kept stirring at room temperature for 1 h. To this mixture was added 3-bromo-3-phenylpentane (3.40 mL, 22.3 mmol), and the reaction was allowed to proceed at room temperature (25 °C) for 16 h. The reaction mixture was diluted with diethyl ether, which was rinsed with brine. After removing the diethyl ether, the crude product **92e** was directly used for the next step reaction without further purification. To a mixture of **92e** (4.10 g, 22.0 mmol) in water (16 mL) was sequentially added

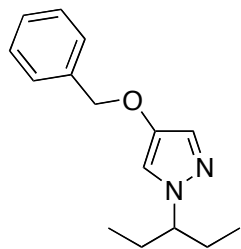
iodine (3.07 g, 12.1 mmol) and 35% hydrogen peroxide (1.24 mL, 14.5 mmol), and the mixture was kept stirring for 24 h at room temperature. The reaction was quenched by the addition of a cold solution of saturated sodium thiosulfate and the subsequent mixture was extracted with ethyl acetate. The combined extracts were dried over anhydrous sodium sulfate and concentrated in vacuo. The residue obtained was chromatographed over silica gel eluting with 5% ethyl acetate in hexanes to furnish **93e** as a clear oil (4.68 g, 68%). <sup>1</sup>H NMR (500 MHz, Chloroform-*d*) δ 7.52 (s, 1H), 7.39 (s, 1H), 7.29 (t, *J* = 7.5 Hz, 2H), 7.21 (t, *J* = 7.4 Hz, 1H), 7.16 (d, *J* = 7.3 Hz, 2H), 4.12 (t, *J* = 7.0 Hz, 2H), 2.61 (t, *J* = 7.6 Hz, 2H), 2.19 (quintet, *J* = 7.3 Hz, 2H). <sup>13</sup>C NMR (126 MHz, Chloroform-*d*) δ 144.46, 140.70, 133.67, 128.69, 128.56, 126.36, 55.77, 51.94, 32.67, 31.74. HRMS (ESI) calcd for C<sub>12</sub>H<sub>13</sub>IN<sub>2</sub> [M+H]<sup>+</sup> 313.0196, found 313.0173. (**AA-III-114**)

Synthesis and characterization of N-alkyl-4-benzyloxypyrazole (**97a-e**): Adapted from the procedure of Altman et al.<sup>11</sup>



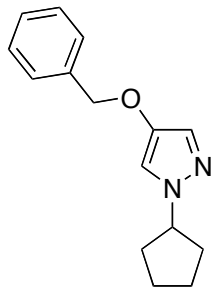
4-(benzyloxy)-1-(pentan-2-yl)-1H-pyrazole (**97a**): A thick-walled sealable reaction tube was charged with CuI (12.2 mg, 0.06 mmol), 3,4,7,8-tetramethyl-1,10-phenanthroline (30.2 mg, 0.13 mmol), Cs<sub>2</sub>CO<sub>3</sub> (625 mg, 1.92 mmol), **93a** (338 mg, 1.28 mmol), benzyl alcohol (0.20 mL, 1.92 mmol), toluene (0.6 mL), and a magnetic stir bar. The reaction was purged with dry nitrogen and then quickly sealed with a teflon screwcap. The vessel was immersed in a 80 °C oil bath and stirred vigorously for 18 h. The reaction mixture was allowed to cool to room temperature,

diluted with ethyl acetate, filtered through a plug of silica gel. The filtrate was concentrated and the resulting residue was purified by column chromatography over silica gel (10% ethyl acetate in hexanes) to provide the desired **97a** as a clear oil (170 mg, 61%). <sup>1</sup>H NMR (500 MHz, Chloroform-*d*) δ 7.41-7.28 (m, 5H), 7.25 (s, 1H), 7.06 (s, 1H), 4.91 (s, 2H), 4.22-4.09 (m, 1H), 1.87-1.75 (m, 1H), 1.70-1.56 (m, 1H), 1.42 (d, *J* = 6.8 Hz, 3H), 1.29-1.00 (m, 2H), 0.87 (t, *J* = 7.4 Hz, 3H). <sup>13</sup>C NMR (126 MHz, Chloroform-*d*) δ 145.10, 137.10, 128.59, 128.14, 127.78, 126.57, 113.43, 73.91, 58.67, 39.36, 21.27, 19.43, 13.82. HRMS (ESI) calcd for C<sub>15</sub>H<sub>20</sub>N<sub>2</sub>O [M+H]<sup>+</sup> 245.1648, found 245.1639. (**AA-III-83**).

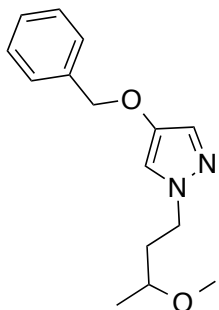


4-(benzyloxy)-1-(pentan-3-yl)-1*H*-pyrazole (97b): A thick-walled sealable reaction tube was charged with CuI (7.80 mg, 0.041 mmol), 3,4,7,8-tetramethyl-1,10- phenantholine (19.3 mg, 0.08 mmol), Cs<sub>2</sub>CO<sub>3</sub> (399 mg, 1.22 mmol), **93b** (215 mg, 0.82 mmol), benzyl alcohol (0.13 mL, 1.22 mmol), toluene (0.4 mL), and a magnetic stir bar. The reaction was purged with dry nitrogen and then quickly sealed with a teflon screwcap. The vessel was immersed in a 80 °C oil bath and stirred vigorously for 18 h. The reaction mixture was allowed to cool to room temperature, diluted with ethyl acetate, filtered through a plug of silica gel. The filtrate was concentrated and the resulting residue was purified by column chromatography over silica gel (10% ethyl acetate in hexanes) to provide the desired **90b** as a clear oil (166 mg, 84%). <sup>1</sup>H NMR (500 MHz, Chloroform-*d*) δ 7.42-7.35 (m, 4H), 7.32 (t, *J* = 7.0 Hz, 1H), 7.27 (s, 1H), 7.05 (s, 1H), 4.92 (s, 2H), 3.81-3.70 (m, 1H), 1.87-1.69 (m, 4H), 0.76 (t, *J* = 7.4 Hz, 6H). <sup>13</sup>C NMR (126

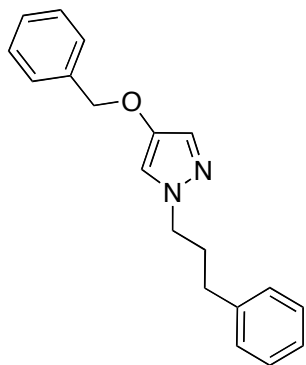
MHz, Chloroform-*d*) δ 144.99, 137.12, 128.63, 128.19, 127.87, 126.80, 114.51, 74.00, 67.06, 28.59, 10.81. HRMS (ESI) calcd for C<sub>15</sub>H<sub>20</sub>N<sub>2</sub>O [M+H]<sup>+</sup> 245.1648, found 245.1639. (**AA-III-86**).



**4-(benzyloxy)-1-cyclopentyl-1*H*-pyrazole (97c):** A thick-walled sealable reaction tube was charged with CuI (6.50 mg, 0.03 mmol), 3,4,7,8-tetramethyl-1,10-phenanthroline (16.3 mg, 0.07 mmol), Cs<sub>2</sub>CO<sub>3</sub> (336 mg, 1.03 mmol), **93c** (180 mg, 0.69 mmol), benzyl alcohol (0.11 mL, 1.03 mmol), toluene (0.3 mL), and a magnetic stir bar. The reaction was purged with dry nitrogen and then quickly sealed with a teflon screwcap. The vessel was immersed in a 80 °C oil bath and stirred vigorously for 18 h. The reaction mixture was allowed to cool to room temperature, diluted with ethyl acetate, filtered through a plug of silica gel. The filtrate was concentrated and the resulting residue was purified by column chromatography over silica gel (10% ethyl acetate in hexanes) to provide the desired **97c** as a colorless oil (94.7 mg, 57%). <sup>1</sup>H NMR (500 MHz, Chloroform-*d*) δ 7.41-7.35 (m, 4H), 7.33-7.29 (m, 1H), 7.10 (s, 1H), 4.91 (s, 2H), 4.52 (quintet, *J* = 7.1 Hz, 1H), 2.16-2.06 (m, 2H), 2.01-1.90 (m, 2H), 1.88-1.76 (m, 2H), 1.72-1.59 (m, 2H). <sup>13</sup>C NMR (126 MHz, Chloroform-*d*) δ 145.18, 137.03, 128.53, 128.07, 127.65, 126.72, 113.74, 73.81, 63.42, 32.83, 24.13. HRMS (ESI) calcd for C<sub>15</sub>H<sub>18</sub>N<sub>2</sub>O [M+H]<sup>+</sup> 243.1492, found 243.148. (**AA-IV-91**).

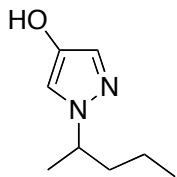


**4-(benzyloxy)-1-(3-methoxybutyl)-1*H*-pyrazole (97d):** A thick-walled sealable reaction tube was charged with CuI (13.8 mg, 0.07 mmol), 3,4,7,8-tetramethyl-1,10- phenantholine (35.0 mg, 0.15 mmol), Cs<sub>2</sub>CO<sub>3</sub> (712 mg, 2.19 mmol), **93d** (408 mg, 1.46 mmol), benzyl alcohol (0.23 mL, 2.19 mmol), toluene (0.7 mL), and a magnetic stir bar. The reaction was purged with dry nitrogen and then quickly sealed with a teflon screwcap. The vessel was immersed in a 80 °C oil bath and stirred vigorously for 18 h. Surprisingly, the reaction mixture turned black the following day. Nonetheless, the reaction mixture was allowed to cool to room temperature, diluted with ethyl acetate, filtered through a plug of silica gel. The filtrate was concentrated and the resulting residue was purified by column chromatography over silica gel (10% ethyl acetate in hexanes) to provide the desired **97d** as a colorless clear oil (154 mg, 41%). <sup>1</sup>H NMR (500 MHz, Chloroform-*d*) δ 7.42-7.28 (m, 5H), 7.26 (s, 1H), 7.05 (s, 1H), 4.92 (s, 2H), 4.11-4.07 (m, 2H), 3.27 (s, 3H), 3.22-3.11 (m, 1H), 1.99 (dtd, *J* = 14.1, 7.9, 4.0 Hz, 1H), 1.92-1.83 (m, 1H), 1.12 (d, *J* = 6.1 Hz, 3H). <sup>13</sup>C NMR (126 MHz, Chloroform-*d*) δ 145.18, 137.01, 128.64, 128.19, 127.72, 127.41, 115.73, 73.92, 73.63, 56.11, 49.18, 37.24, 18.85. HRMS (ESI) calcd for C<sub>15</sub>H<sub>20</sub>N<sub>2</sub>O<sub>2</sub> [M+H]<sup>+</sup> 261.1598, found 261.1578. (**AA-IV-4**)



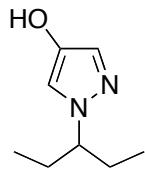
4-(benzyloxy)-1-(3-phenylpropyl)-1H-pyrazole (97e): A thick-walled sealable reaction tube was charged with CuI (57.0 mg, 0.30 mmol), 3,4,7,8-tetramethyl-1,10-phenanthroline (142 mg, 0.60 mmol), Cs<sub>2</sub>CO<sub>3</sub> (2.93 g, 9.02 mmol), **93e** (1.88 g, 6.01 mmol), benzyl alcohol (0.93 mL, 9.02 mmol), toluene (3.0 mL), and a magnetic stir bar. The reaction was purged with dry nitrogen and then quickly sealed with a teflon screwcap. The vessel was immersed in a 80 °C oil bath and stirred vigorously for 18 h. The reaction mixture was allowed to cool to room temperature, diluted with ethyl acetate, filtered through a plug of silica gel. The filtrate was concentrated and the resulting crude **97e** was taken to the next step without further purification (1.66 g, *crude contaminated with residual benzyl alcohol, 94%*). (**AA-III-115**)

Synthesis and characterization of N-alkyl-4-hydroxypyrazoles (98a-e):

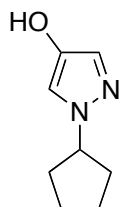


1-(pentan-2-yl)-1H-pyrazol-4-ol (98a): Compound **97a** (407 mg, 1.67 mmol) was dissolved in methanol (11.6 mL), to which was added 10% Pd-C (50% wet, 382 mg) and ammonium formate (525 mg, 8.33 mmol) sequentially, and the reaction was allowed to proceed under reflux for 16 h. After cooling to room temperature, the reaction was filtered through a silica gel pad, which was

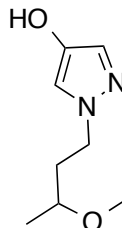
then rinsed with ethyl acetate to ensure the complete recovery of product. The filtrate was evaporated under reduced pressure and the resulting residue was purified by column chromatography over silica gel (40% ethyl acetate in hexanes) to afford the desired products **98a** as a pale yellow oil (212 mg, 83%). <sup>1</sup>H NMR (500 MHz, Chloroform-*d*) δ 8.45 (s, 1H), 7.11 (s, 1H), 7.06 (s, 1H), 4.20-4.10 (m, 1H), 1.82-1.71 (m, 1H), 1.67-1.54 (m, 1H), 1.40 (d, *J* = 6.8 Hz, 3H), 1.29-0.99 (m, 2H), 0.84 (t, *J* = 7.4 Hz, 3H). <sup>13</sup>C NMR (126 MHz, Chloroform-*d*) δ 141.50, 127.11, 114.69, 58.64, 39.32, 21.35, 19.44, 13.78. HRMS (ESI) calcd for C<sub>8</sub>H<sub>14</sub>N<sub>2</sub>O [M+H]<sup>+</sup> 155.1113, found 155.1186. (**AA-III-81**)



**1-(pentan-3-yl)-1*H*-pyrazol-4-ol (98b):** Compound **97a** (408 mg, 1.67 mmol) was dissolved in methanol (11.7 mL), to which was added 10% Pd-C (50% wet, 382 mg) and ammonium formate (526 mg, 8.35 mmol) sequentially, and the reaction was allowed to proceed under reflux for 16 h. After cooling to room temperature, the reaction was filtered through a silica gel pad, which was then rinsed with ethyl acetate to ensure the complete recovery of product. The filtrate was evaporated under reduced pressure to afford the desired products **98a** as a pale yellow oil (206 mg, 80%). <sup>1</sup>H NMR (500 MHz, Chloroform-*d*) δ 7.82 (s, 1H), 7.15 (s, 1H), 7.05 (s, 1H), 3.80-3.71 (m, 1H), 1.83-1.68 (m, 4H), 0.75 (t, *J* = 7.4 Hz, 6H). <sup>13</sup>C NMR (126 MHz, Chloroform-*d*) δ 141.33, 127.40, 115.63, 67.00, 28.60, 10.79. HRMS (ESI) calcd for C<sub>8</sub>H<sub>14</sub>N<sub>2</sub>O [M+H]<sup>+</sup> 155.1104, found 155.1177. (**AA-III-89**)



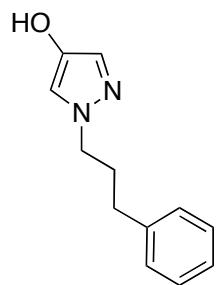
**1-cyclopentyl-1*H*-pyrazol-4-ol (98c):** Compound **91c** (361 mg, 1.49 mmol) was dissolved in methanol (10.0 mL), to which was added 10% Pd-C (50% wet, 342.5 mg) and ammonium formate (469 mg, 7.45 mmol) sequentially, and the reaction was allowed to proceed under reflux for 16 h. After cooling to room temperature, the reaction was filtered through a silica gel pad, which was then rinsed with ethyl acetate to ensure the complete recovery of product. The filtrate was evaporated under reduced pressure to afford the desired products **98c** as an off-white solid (184 mg, 81%). <sup>1</sup>H NMR (500 MHz, Chloroform-*d*) δ 7.13 (d, *J* = 0.7 Hz, 1H), 7.11 (d, *J* = 0.7 Hz, 1H), 6.61 (s, 1H), 4.52 (quintet, *J* = 7.2 Hz, 1H), 2.18-2.08 (m, 2H), 1.95-1.87 (m, 2H), 1.87-1.77 (m, 2H), 1.72-1.62 (m, 2H). <sup>13</sup>C NMR (126 MHz, Chloroform-*d*) δ 141.23, 127.75, 115.16, 63.50, 32.98, 24.18. This compound has been reported previously in literature.<sup>12</sup> (**AA-III-97**)



**1-(3-methoxybutyl)-1*H*-pyrazol-4-ol (98d):** Compound **97d** (154 mg, 0.59 mmol) was dissolved in methanol (4.0 mL), to which was added 10% Pd-C (50% wet, 136 mg) and ammonium formate (186 mg, 2.95 mmol) sequentially, and the reaction was allowed to proceed under reflux for 16 h. After cooling to room temperature, the reaction was filtered through a silica gel pad, which was then rinsed with ethyl acetate to ensure the complete recovery of product. The filtrate

was evaporated under reduced pressure and the resulting residue was purified by column chromatography over silica gel (2-3% methanol in dichloromethane) to afford the desired products **98d** as a clear oil (77.4 mg, 77%). <sup>1</sup>H NMR (500 MHz, Chloroform-*d*) δ 7.76 (s, 1H), 7.13 (s, 1H), 7.04 (s, 1H), 4.07 (t, *J* = 6.9 Hz, 2H), 3.29 (s, 3H), 3.23-3.13 (m, 1H), 2.01-1.92 (m, 1H), 1.91-1.81 (m, 1H), 1.11 (d, *J* = 6.0 Hz, 3H). <sup>13</sup>C NMR (126 MHz, Chloroform-*d*) δ 141.36, 127.92, 116.86, 73.60, 56.00, 48.88, 37.14, 18.70. We do not have HRMS for compound **98d**. However, the experimental HRMS (ESI) for **97d** and **99d** matches with the calculated value.

**(AA-IV-6)**

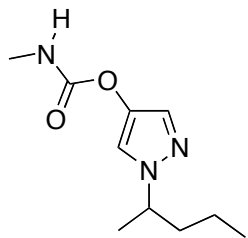


**1-(3-phenylpropyl)-1*H*-pyrazol-4-ol (98e):** Compound **97e** (1.66 g, 1.49 mmol) was dissolved in methanol (10.0 mL), to which was added 10% Pd-C (50% wet, 1.30 g) and ammonium formate (1.78 mg, 28.3 mmol) sequentially, and the reaction was allowed to proceed under reflux for 16 h. After cooling to room temperature, the reaction was filtered through a silica gel pad, which was then rinsed with ethyl acetate to ensure the complete recovery of product. The filtrate was evaporated under reduced pressure and the resulting residue was purified by column chromatography over silica gel (40% ethyl acetate in hexanes) to afford the desired products **98e** as an off white solid (699 mg, 54% over two steps); mp 105-107 °C. <sup>1</sup>H NMR (500 MHz, Chloroform-*d*) δ 7.31-7.24 (m, 2H), 7.21-7.17 (m, 2H), 7.15 (d, *J* = 6.9 Hz, 2H), 7.06 (s, 1H), 6.02 (s, 1H), 4.00 (t, *J* = 7.0 Hz, 2H), 2.62-2.55 (t, *J* = 7.5 Hz, 2H), 2.14 (quintet, *J* = 7.2 Hz, 2H).

<sup>13</sup>C NMR (126 MHz, Chloroform-*d*) δ 141.14, 140.94, 128.63, 128.55, 128.38, 126.26, 116.80, 51.95, 32.73, 31.82. HRMS (ESI) calcd for C<sub>19</sub>H<sub>20</sub>N<sub>2</sub>O [M+H]<sup>+</sup> 203.1179, found 203.1161.

(AA-III-116)

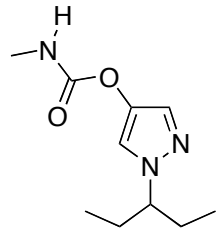
Synthesis and characterization of 1-alkylpyrazol-4-yl methylcarbamates (99a-e): The procedure for synthesis of 93a-c,e is loosely based on the 7-hydroxycoumarin alanine methyl ester carbamate protocol of Xue et al.<sup>13</sup>



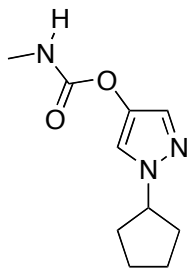
1-(pentan-2-yl)-1*H*-pyrazol-4-yl methylcarbamate (99a): To a solution of triphosgene (51.9 mg, 0.17 mmol) in dichloromethane (5.0 mL) was slowly added to a solution of **98a** (76.2 mg, 0.49 mmol) and diisopropylethylamine (0.09 mL, 0.49 mmol) in THF (5.0 mL), and the mixture was stirred at room temperature for 30 min. To the reaction mixture, a solution of methylamine (2 M in THF, 0.37 mL, 0.74 mmol) and diisopropylethylamine (0.19 mL, 1.11 mmol) in dichloromethane (1.0 mL) was added, and the reaction was allowed to proceed for an additional 30 min. The subsequent reaction mixture was partitioned between dichloromethane and water, and the organic phase was dried over anhydrous sodium sulfate and concentrated. The residue obtained was purified by column chromatography eluting with 20% ethyl acetate in hexanes to give the desired compound **99a** as clear oil (76.3 mg, 73%). <sup>1</sup>H NMR (500 MHz, Chloroform-*d*) δ 7.50 (s, 1H), 7.35 (s, 1H), 4.99 (s, 1H), 4.25-4.15 (m, 1H), 2.86 (d, *J* = 4.9 Hz, 3H), 1.90-1.79 (m, 1H), 1.71-1.59 (m, 1H), 1.44 (d, *J* = 6.8 Hz, 3H), 1.30-1.03 (m, 2H), 0.87 (t, *J* = 7.4 Hz, 3H).

<sup>13</sup>C NMR (126 MHz, Chloroform-*d*) δ 154.57, 135.33, 129.41, 118.03, 58.89, 39.33, 27.86, 21.26, 19.45, 13.84. HRMS (ESI) calcd for C<sub>10</sub>H<sub>18</sub>N<sub>3</sub>O<sub>2</sub> [M+H]<sup>+</sup> 212.1394, found 212.1396.

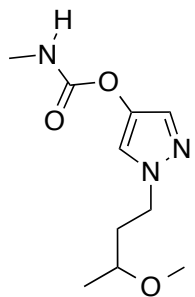
(AA-III-152)



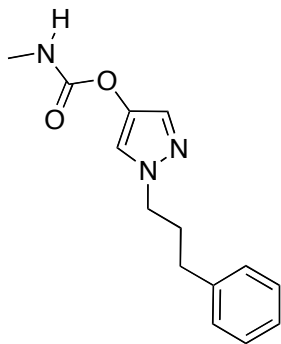
1-(pentan-3-yl)-1*H*-pyrazol-4-yl methylcarbamates (99b): To a solution of triphosgene (46.1 mg, 0.15 mmol) in dichloromethane (4.0 mL) was slowly added to a solution of **98b** (67.7 mg, 0.44 mmol) and diisopropylethylamine (0.08 mL, 0.44 mmol) in THF (4.0 mL), and the mixture was stirred at room temperature for 30 min. To the reaction mixture, a solution of methylamine (2 M in THF, 0.33 mL, 0.66 mmol) and diisopropylethylamine (0.17 mL, 0.99 mmol) in dichloromethane (1.0 mL) was added, and the reaction was allowed to proceed for an additional 30 min. The subsequent reaction mixture was partitioned between dichloromethane and water, and the organic phase was dried over anhydrous sodium sulfate and concentrated. The residue obtained was purified by column chromatography eluting with 20% ethyl acetate in hexanes to give the desired compound **99b** as clear oil (63.4 mg, 69%). <sup>1</sup>H NMR (500 MHz, Chloroform-*d*) δ 7.50 (s, 1H), 7.38 (s, 1H), 4.95 (s, 1H), 3.86-3.76 (m, 1H), 2.87 (d, *J* = 4.9 Hz, 3H), 1.91-1.71 (m, 4H), 0.78 (t, *J* = 7.3 Hz, 6H). <sup>13</sup>C NMR (126 MHz, Chloroform-*d*) δ 154.41, 135.17, 129.38, 118.82, 67.10, 28.38, 27.73, 10.66. HRMS (ESI) calcd for C<sub>10</sub>H<sub>18</sub>N<sub>3</sub>O<sub>2</sub> [M+H]<sup>+</sup> 212.1394, found 212.1400. (AA-III-152)



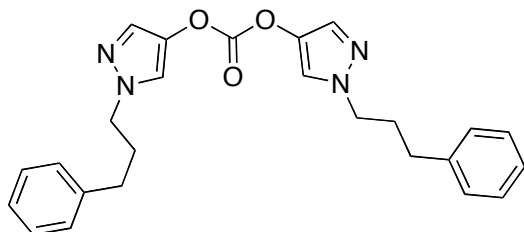
**1-cyclopentyl-1*H*-pyrazol-4-yl methylcarbamates (99c):** To a solution of triphosgene (79.0 mg, 0.27 mmol) in dichloromethane (8.0 mL) was slowly added to a solution of **98c** (122.5 mg, 0.81 mmol) and diisopropylethylamine (0.14 mL, 0.81 mmol) in THF (8.0 mL), and the mixture was stirred at room temperature for 30 min. To the reaction mixture, a solution of methylamine (2 M in THF, 0.61 mL, 1.21 mmol) and diisopropylethylamine (0.32 mL, 1.81 mmol) in dichloromethane (1.6 mL) was added, and the reaction was allowed to proceed for an additional 30 min. The subsequent reaction mixture was partitioned between dichloromethane and water, and the organic phase was dried over anhydrous sodium sulfate and concentrated. The residue obtained was purified by column chromatography eluting with 20% ethyl acetate in hexanes to give the desired compound **99b** as clear oil (96.8 mg, 58%). <sup>1</sup>H NMR (500 MHz, Chloroform-*d*) δ 7.53 (s, 1H), 7.37 (s, 1H), 4.97 (s, 1H), 4.57 (quintet, *J* = 7.1 Hz, 1H), 2.88 (d, *J* = 4.9 Hz, 3H), 2.18-2.09 (m, 2H), 2.04-1.95(m, 2H), 1.89-1.79 (m, 2H), 1.73-1.62 (m, 2H). <sup>13</sup>C NMR (126 MHz, Chloroform-*d*) δ 154.60, 135.38, 129.74, 118.52, 63.69, 32.98, 27.89, 24.24. This compound has been reported previously in literature.<sup>12</sup> (**AA-III-102**)



**1-(3-methoxybutyl)-1*H*-pyrazol-4-yl methylcarbamates (**99d**):** To a solution of **98d** (77.0 mg, 0.45 mmol) in DMF (1.0 mL) was added 1,1 carbonyldimidazole (73.4 mg, 0.45 mmol) and the mixture was stirred at room temperature for 1 hour. To the reaction mixture, methylamine hydrochloride salt (30.5 mg, 0.45 mmol) was added, and the reaction was allowed to proceed for an additional one hour. The subsequent reaction mixture was partitioned between ethyl acetate and water, and the organic phase was dried over anhydrous sodium sulfate and concentrated. The residue obtained was purified by column chromatography eluting with 2% methanol in dichloromethane to give the desired compound **99d** as a clear oil (54.4 mg, 53%). <sup>1</sup>H NMR (500 MHz, Chloroform-*d*) δ 7.48 (s, 1H), 7.36 (s, 1H), 5.02 (s, 1H), 4.14 (t, *J* = 7.5 Hz, 2H), 3.30 (s, 3H), 3.23-3.15 (m, 1H), 2.86 (d, *J* = 4.8 Hz, 3H), 2.07-1.97 (m, 1H), 1.94-1.86 (m, 1H), 1.12 (d, *J* = 6.1 Hz, 3H). <sup>13</sup>C NMR (126 MHz, Chloroform-*d*) δ 154.40, 135.22, 130.13, 120.21, 73.46, 56.06, 49.19, 37.04, 27.75, 18.77. HRMS (ESI) calcd for C<sub>10</sub>H<sub>17</sub>N<sub>3</sub>O<sub>3</sub> [M+H]<sup>+</sup> 228.1343, found 228.1329.

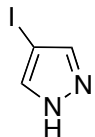


**1-(3-phenylpropyl)-1*H*-pyrazol-4-yl methylcarbamates (99e):** To a solution of triphosgene (39.4 mg, 0.132 mmol, 0.35 equiv) in dichloromethane (3.7 mL) was slowly added a solution of **98e** (76.0 mg, 0.38 mmol, 1.0 equiv) and diisopropylethylamine (0.07 mL, 0.38 mmol, 1.0 equiv) in THF (3.7 mL), and the mixture was stirred at room temperature for 30 min. To the reaction mixture, a solution of methylamine (0.28 mL (2 M in THF), 0.56 mmol, 1.5 equiv) and diisopropylethylamine (0.15 mL, 0.85 mmol, 2.25 equiv) in dichloromethane (1.0 mL) was added, and the reaction was allowed to proceed for an additional 30 min. The subsequent reaction mixture was partitioned between dichloromethane and water, and the organic phase was dried over anhydrous sodium sulfate and concentrated. The residue obtained was purified by column chromatography eluting with 20% ethyl acetate in hexanes to yield **99e** as clear oil (73.3 mg, 76%). <sup>1</sup>H NMR (500 MHz, Chloroform-*d*) δ 7.49 (s, 1H), 7.39 (s, 1H), 7.28 (t, *J* = 7.4 Hz, 2H), 7.22-7.14 (m, 3H), 4.94 (s, 1H), 4.05 (t, *J* = 7.0 Hz, 2H), 2.88 (d, *J* = 4.9 Hz, 3H), 2.61 (t, *J* = 7.6 Hz, 2H), 2.18 (quintet, *J* = 7.3 Hz, 2H). <sup>13</sup>C NMR (126 MHz, Chloroform-*d*) δ 154.50, 140.95, 135.54, 130.18, 128.62, 128.58, 126.24, 120.01, 52.16, 32.74, 31.74, 27.91. HRMS (ESI) calcd for C<sub>14</sub>H<sub>17</sub>N<sub>3</sub>O<sub>2</sub> [M+H]<sup>+</sup> 260.1394, found 260.1384. (**AA-III-126**)

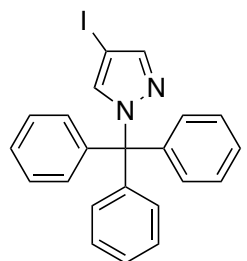


bis(1-(3-phenylpropyl)-1H-pyrazol-4-yl) carbonate (101e): An Impurity formed in 43% yield when old bottle of methylamine in THF was used.  $^1\text{H}$  NMR (500 MHz, Chloroform-*d*) 7.57 (s, 2H), 7.54 (s, 2H), 7.29 (t, *J* = 7.5 Hz, 4H), 7.23-7.14 (m, 6H), 4.08 (t, *J* = 7.0 Hz, 4H), 2.63 (t, *J* = 7.6 Hz, 4H), 2.21 (quintet, *J* = 7.3 Hz, 4H).  $^{13}\text{C}$  NMR (126 MHz, Chloroform-*d*)  $\delta$  150.44, 140.60, 135.47, 129.69, 128.54, 128.43, 126.19, 119.63, 52.17, 32.53, 31.55. (**AA-III-117A**)

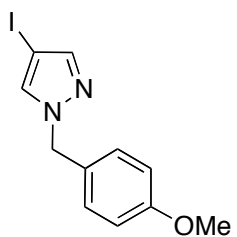
#### 6.4 Experimental section for chapter 3 section 3.6



4-iodo-1H-pyrazole (96): Adapted from the procedure of Rodríguez-Franco *et al.*<sup>14</sup> To a solution of pyrazole **91** (5.00 g, 73.4 mmol) in acetonitrile (400 mL) was added ceric ammonium nitrate (CAN,  $(\text{NH}_4)_2(\text{NO}_3)_6\text{Ce}$ ) (24.2 g, 44.1 mmol), and iodine (11.2 g, 44.1 mmol). The reaction mixture was stirred at room temperature for 3 hours followed by filtration to remove CAN. The filtrate was concentrated in vacuo and the crude residue obtained was triturated from hot hexane yielding **96** as an off white crystalline solid after a quick filtration (11.9 g, 83%); mp 107.8-109.0 °C.  $^1\text{H}$  NMR (500 MHz, Chloroform-*d*):  $\delta$  11.22 (s, 1H), 7.64 (s, 2H).  $^{13}\text{C}$  NMR (126 MHz, Chloroform-*d*)  $\delta$  138.93, 56.67. HRMS (ESI) calcd for  $\text{C}_3\text{H}_3\text{IN}_2$   $[\text{M}+\text{H}]^+$  194.9414, found 194.941. (**AA-IV-5**)

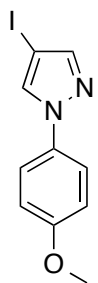


**4-iodo-1-trityl-1H-pyrazole (93f):** Adapted from the procedure of Anderson *et al.*<sup>15</sup> Kt-OBu (3.47 g, 30.9 mmol) was added to a solution of **96** in DMF (36.0 mL) at 0 °C and the reaction mixture was allowed to stir for 15 minutes. After 15 minutes, trityl chloride (5.00 g, 25.7 mmol) was added and the reaction was stirred for additional 1 hour at room temperature. The reaction mixture was then dumped into a flask containing cold water. The precipitates thus formed were filtered and recrystallization from hot hexane/THF provided **93f** as a white crystalline solid (9.56 g in two crops, 85%); mp 192-194 °C. <sup>1</sup>H NMR (400 MHz, Chloroform-*d*) δ 7.68 (s, 1H), 7.42 (s, 1H), 7.35-7.30 (m, 9H), 7.16-7.11 (m, 6H). <sup>13</sup>C NMR (101 MHz, Chloroform-*d*) δ 144.82, 142.82, 136.59, 130.23, 128.06, 127.96, 79.44, 55.78. The melting point of this compound matches the reported literature data.<sup>16</sup> (**AA-IV-7**)

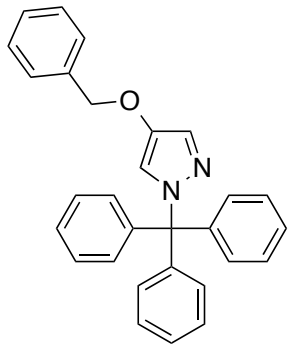


**4-iodo-1-(4-methoxybenzyl)-1H-pyrazole (93g):** Adapted from the procedure of Anderson *et al.*<sup>15</sup> Kt-OBu (694 mg, 6.19 mmol) was added to a solution of **96** in DMF (10.0 mL) at 0 °C and the reaction mixture was allowed to stir for 15 minutes. After 15 minutes, *p*-methoxybenzyl chloride (0.77 mL, 5.67 mmol) was added and the reaction was stirred for additional 1 hour at room temperature. The subsequent reaction mixture was partitioned between ethyl acetate and

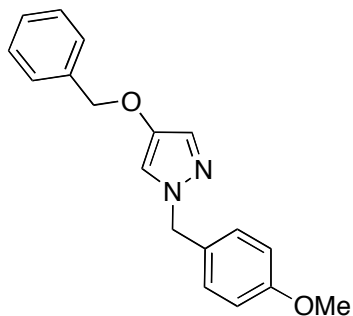
water, and the organic phase was dried over anhydrous sodium sulfate and concentrated. The residue obtained was purified by column chromatography eluting with 10% ethyl acetate in hexane to give the desired compound **93g** as white crystalline solid (1.53 g, 85%); mp 69.7–71.6 °C. <sup>1</sup>H NMR (500 MHz, Chloroform-d) δ 7.52 (s, 1H), 7.35 (s, 1H), 7.18 (d, *J* = 8.5 Hz, 2H), 6.88 (d, *J* = 8.5 Hz, 2H), 5.22 (s, 2H), 3.79 (s, 3H). <sup>13</sup>C NMR (126 MHz, Chloroform-d) δ 159.76, 144.53, 133.43, 129.62, 127.77, 114.42, 56.41, 56.14, 55.42. HRMS (ESI) calcd for C<sub>11</sub>H<sub>11</sub>IN<sub>2</sub>O [M+H]<sup>+</sup> 314.9989, found 314.9976. (**AA-III-135**)



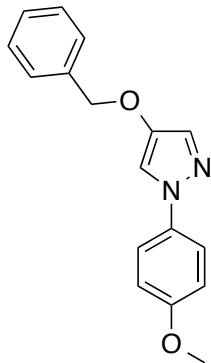
**4-iodo-1-(4-methoxyphenyl)-1*H*-pyrazole (93h):** Adapted from the procedure of Zhu et al.<sup>17</sup> A flamed dried round bottom flask was charged with **96** (232 mg, 1.20 mmol), K<sub>3</sub>PO<sub>4</sub> (363 mg, 1.71 mmol), 4-iodo anisole (200 mg, 0.85 mmol), CuI (33.0 mg, 0.17 mmol), and DMF (0.8 mL). The flask was purged with nitrogen, evacuated and back filled with nitrogen. The reaction mixture was allowed to stir at 40 °C for 2 days. The reaction mixture was allowed to cool to room temperature, diluted with ethyl acetate, filtered through a plug of silica gel and washed with ethyl acetate. The filtrate was concentrated and the resulting residue was purified by column chromatography over silica gel (10% ethyl acetate in hexanes) to provide the desired **93h** as a white solid (31.8 mg, 12%); mp 120.0–122.3 °C. (<sup>1</sup>H NMR (400 MHz, Chloroform-*d*) δ 7.85 (s, 1H), 7.68 (s, 1H), 7.53 (d, *J* = 9.1 Hz, 2H), 6.96 (d, *J* = 9.1 Hz, 2H), 3.84 (s, 3H). <sup>13</sup>C NMR (101 MHz, Chloroform-*d*) δ 158.82, 145.64, 133.46, 131.49, 121.01, 114.73, 58.30, 55.73. HRMS (ESI) calcd for C<sub>10</sub>H<sub>9</sub>IN<sub>2</sub>O [M+H]<sup>+</sup> 300.9832, found 300.9828. (**AA-III-176**)



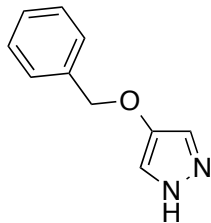
4-(benzyloxy)-1-trityl-1*H*-pyrazole (97f): Adapted from the procedure of Altman *et al.*<sup>11</sup> A round bottom flask was charged with CuI (162 mg, 0.85 mmol), 3,4,7,8-tetramethyl-1,10-phenanthroline (401 mg, 1.70 mmol), Cs<sub>2</sub>CO<sub>3</sub> (8.29 g, 25.4 mmol), **93f** (7.40 g, 16.9 mmol), benzyl alcohol (2.63 mL, 25.4 mmol), toluene (9.0 mL), and a magnetic stir bar under nitrogen. The reaction mixture was refluxed for 18 h, and then cooled to room temperature. Subsequently, the reaction mixture was diluted with ethyl acetate, and filtered through a plug of silica gel. The filtrate was concentrated yielding crude **97f** as an oil. On sonication, the crude solid **97f** crashes out of the oil. The residual benzyl alcohol and slight impurities were removed by washing the crude solid with hexane/methanol (150 mL/3 mL) to provide the desired **97f** as an off white solid (5.71 g, 81%); mp 155-157 °C. <sup>1</sup>H NMR (500 MHz, Chloroform-*d*) δ 7.44 (s, 1H), 7.35-7.32 (m, 4H), 7.30-7.26 (m, 10H), 7.15-7.11 (m, 6H), 7.02 (s, 1H), 4.85 (s, 2H). <sup>13</sup>C NMR (126 MHz, Chloroform-*d*) δ 144.28, 143.27, 136.86, 130.24, 128.60, 128.48, 128.20, 127.93, 127.76, 118.82, 78.76, 73.81. HRMS (ESI) calcd for C<sub>29</sub>H<sub>24</sub>N<sub>2</sub>O [M+Na]<sup>+</sup> 439.1781, found 439.1768. (**AA-IV-11**)



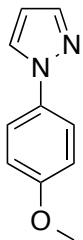
**4-(benzyloxy)-1-(4-methoxybenzyl)-1H-pyrazole (97g):** Adapted from the procedure of Altman et al.<sup>11</sup> A thick-walled sealable reaction tube was charged with CuI (41.5 mg, 0.22 mmol), 3,4,7,8-tetramethyl-1,10-phenanthroline (103 mg, 0.44 mmol), Cs<sub>2</sub>CO<sub>3</sub> (2.13 g, 6.54 mmol), **93g** (1.37 g, 4.36 mmol), benzyl alcohol (0.68 mL, 6.54 mmol), toluene (2.2 mL), and a magnetic stir bar. The reaction was purged with dry nitrogen and then quickly sealed with a teflon screwcap. The vessel was immersed in a 80 °C oil bath and stirred vigorously for 18 h. The reaction mixture was allowed to cool to room temperature, diluted with ethyl acetate, filtered through a plug of silica gel. The filtrate was concentrated and the resulting residue was purified by column chromatography over silica gel (10% ethyl acetate in hexanes) to provide the desired **97g** as a white solid (883 mg, 69%); mp 140.5-141.8 °C. <sup>1</sup>H NMR (500 MHz, Chloroform-d) δ 7.39-7.29 (m, 5H), 7.28 (s, 1H), 7.14 (d, *J* = 8.6 Hz, 2H), 7.01 (s, 1H), 6.86 (d, *J* = 8.6 Hz, 2H), 5.11 (s, 2H), 4.88 (s, 2H), 3.79 (s, 3H). <sup>13</sup>C NMR (126 MHz, Chloroform-d) δ 159.53, 145.83, 136.96, 129.24, 128.72, 128.64, 128.21, 127.77, 127.69, 115.12, 114.28, 73.87, 56.31, 55.41. HRMS (ESI) calcd for C<sub>18</sub>H<sub>18</sub>N<sub>2</sub>O<sub>2</sub> [M+H]<sup>+</sup> 295.1441, found 295.1412. (**AA-III-138**)



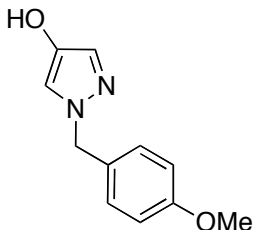
**4-(benzyloxy)-1-(4-methoxyphenyl)-1*H*-pyrazole (97h): Adapted from the procedure of Altman et al.<sup>11</sup>** A thick-walled sealable reaction tube was charged with CuI (12.3 mg, 0.06 mmol), 3,4,7,8-tetramethyl-1,10- phenantholine (30.6 mg, 0.13 mmol), Cs<sub>2</sub>CO<sub>3</sub> (634 mg, 1.95 mmol), **93h** (389 mg, 1.30 mmol), benzyl alcohol (0.20 mL, 1.95 mmol), toluene (0.65 mL), and a magnetic stir bar. The reaction was purged with dry nitrogen and then quickly sealed with a teflon screwcap. The vessel was immersed in a 80 °C oil bath and stirred vigorously for 40 h. The reaction mixture was allowed to cool to room temperature, diluted with ethyl acetate, filtered through a plug of silica gel. The filtrate was concentrated and the resulting residue was purified by column chromatography over silica gel (10% ethyl acetate in hexanes) to provide the desired **97h** as an off white solid (297 mg, 82%); mp 86-86.6 °C. <sup>1</sup>H NMR (400 MHz, Chloroform-*d*) δ 7.51 (s, 1H), 7.49 (d, *J* = 2.1 Hz, 2H), 7.47 (s, 1H), 7.42 (t, *J* = 6.3 Hz, 2H), 7.40-7.31 (m, 3H), 6.94 (d, *J* = 9.1 Hz, 2H), 5.00 (s, 2H), 3.82 (s, 3H). <sup>13</sup>C NMR (101 MHz, Chloroform-*d*) δ 158.10, 146.97, 136.83, 134.40, 129.63, 128.76, 128.36, 127.78, 120.24, 114.63, 112.68, 73.98, 55.70. HRMS (ESI) calcd for C<sub>17</sub>H<sub>16</sub>N<sub>2</sub>O<sub>2</sub> [M+H]<sup>+</sup> 281.1285, found 281.131. (**AA-III-179**)



**4-(benzyloxy)-1*H*-pyrazole (103):** Adapted from the procedure of Gellibert et al.<sup>18</sup> To a solution of **97f** (5.43 g, 13.04 mmol) in DCM (54.3 mL) was added trifluoroacetic acid (10.1 mL, 130.4 mmol) at 0 °C. The color of the reaction changes from colorless to yellow on addition of trifluoroacetic acid. To this solution was added triethylsilane (2.10 mL, 13.0 mmol), which was accompanied by a color change of the solution from yellow to colorless suggesting the scavenging of the trityl cation. The reaction mixture was stirred at room temperature for additional 1 hour before concentrating the solvents in vacuo. The crude residue was dissolved in toluene and the solvent was stripped off on rotavap to get rid of residual trifluoroacetic acid, this process was repeated twice. The crude residue obtained was triturated in hot hexane/ether and filtered yielding the first crop of pure product. The mother liquor was concentrated and triturated in hot ether, filtered yielding second crop of pure product **103** (1.47 g in two crops, 65%); mp 84.7-85.6 °C. <sup>1</sup>H NMR (500 MHz, Methanol-*d*<sub>4</sub>) δ 7.41-7.33 (m, 6H), 7.29 (t, *J* = 7.2 Hz, 1H), 4.94 (s, 2H). <sup>13</sup>C NMR (126 MHz, Methanol-*d*<sub>4</sub>) δ 138.57, 129.46, 129.02, 128.74, 122.06, 74.80. HRMS (ESI) calcd for C<sub>10</sub>H<sub>10</sub>N<sub>2</sub>O [M+H]<sup>+</sup> 175.0866, found 175.0855. (**AA-IV-13**)

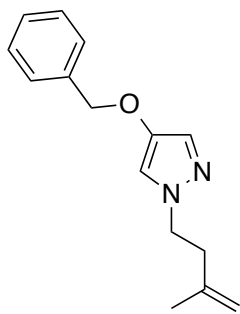


**1-(4-methoxyphenyl)-1*H*-pyrazole (104):** Adapted from the procedure of Xu et al.<sup>19</sup> A flamed dried round bottom flask was charged with pyrazole **91** (300 mg, 4.4 mmol), K<sub>3</sub>PO<sub>4</sub> (1.24 g, 5.29 mmol), 4-iodo anisole (200 mg, 0.85 mmol), CuI (33.0 mg, 0.17 mmol), and DMF (0.8 mL). The flask was purged with nitrogen, evacuated and back filled with nitrogen. The reaction mixture was allowed to stir at 40 °C for 2 days. The reaction mixture was allowed to cool to room temperature, diluted with ethyl acetate, filtered through a plug of silica gel and washed with ethyl acetate. The filtrate was concentrated and the resulting residue was purified by column chromatography over silica gel (10% ethyl acetate in hexanes) to provide the desired **104** as a white solid (31.8 mg, 12%). <sup>1</sup>H NMR (400 MHz, Chloroform-*d*) δ 7.81 (d, *J* = 2.0 Hz, 1H), 7.69 (d, *J* = 2.0 Hz, 1H), 7.58 (d, *J* = 9.0 Hz, 2H), 6.96 (d, *J* = 9.0 Hz, 2H), 6.42 (t, *J* = 2.0 Hz, 1H), 3.82 (s, 3H). <sup>13</sup>C NMR (101 MHz, Chloroform-*d*) δ 158.32, 140.67, 134.11, 126.89, 120.97, 114.60, 107.24, 55.64. The <sup>1</sup>H NMR and <sup>13</sup>C NMR for this compound matches the reported literature data.<sup>19</sup>



**1-(4-methoxybenzyl)-1*H*-pyrazol-4-ol (105):** Adapted from the procedure of Forbes et al.<sup>20</sup> A mixture of **103** (106 mg, 0.36 mmol), anisole (0.11 mL, 1.04 mmol), TFA (1.20 mL, 14.9 mmol),

and  $\text{H}_2\text{SO}_4$  (2 drops) was stirred at room temperature for 2 hours. Subsequently, the reaction mixture was concentrated in vacuo. Upon addition of ether for extraction, a solid precipitated out, which was filtered and washed with ether. The crude compound was identified as **106** using  $^1\text{H}$  NMR and  $^{13}\text{C}$  NMR.  $^1\text{H}$  NMR (500 MHz, Methanol- $d_4$ )  $\delta$  7.81 (d,  $J = 1.1$  Hz, 1H), 7.73 (d,  $J = 1.1$  Hz, 1H), 7.29 (d,  $J = 8.8$  Hz, 2H), 6.97 (d,  $J = 8.8$  Hz, 2H), 5.40 (s, 2H), 3.80 (s, 3H).  $^{13}\text{C}$  NMR (126 MHz, Methanol- $d_4$ )  $\delta$  161.94, 144.19, 130.88, 126.29, 123.82, 123.41, 115.63, 56.01, 55.83. HRMS (ESI) calcd for  $\text{C}_{11}\text{H}_{12}\text{N}_2\text{O}_2$   $[\text{M}+\text{H}]^+$  205.0899, found 205.0948.



**4-(benzyloxy)-1-(3-methylbut-3-en-1-yl)-1H-pyrazole (106):** To a mixture of sodium hydride (60% dispersion in mineral oil, 119 mg, 2.99 mmol) in THF (2.0 mL) at 0 °C was added **103** (400 mg, 2.30 mmol), and the subsequent mixture was kept stirring at room temperature for 1 h. To this mixture was added crude 3-methylbut-3-en-1-yl 4-methylbenzenesulfonate (1.66 g, 6.89 mmol), and the reaction was allowed to proceed at room temperature (25 °C) for 16 h. The solvent was concentrated and the residue was taken up in dichloromethane and washed with water, and then brine, and dried over sodium sulfate. The organic layer was evaporated and the residue was purified by silica gel column chromatography using 40% ethyl acetate in hexane to afford the **106** as clear oil (342 mg, 61%).  $^1\text{H}$  NMR (400 MHz, Chloroform- $d$ )  $\delta$  7.42-7.29 (m, 5H), 7.25 (d,  $J = 0.9$  Hz, 1H), 7.06 (d,  $J = 0.9$  Hz, 1H), 4.92 (s, 2H), 4.80-4.77 (m, 1H), 4.70-4.66 (m, 1H), 4.12 (t,  $J = 7.3$  Hz, 2H), 2.51 (t,  $J = 7.3$  Hz, 2H), 1.73 (dd,  $J = 1.5, 0.9$  Hz, 3H).  $^{13}\text{C}$

NMR (101 MHz, Chloroform-*d*) δ 145.32, 141.96, 137.08, 128.64, 128.19, 127.74, 127.36, 115.34, 112.60, 73.97, 51.44, 38.41, 22.48. (**AA-IV-26**)

## 6.5 Bibliography

1. Dragovich, P. S.; Bertolini, T. M.; Ayida, B. K.; Li, L.-S.; Murphy, D. E.; Ruebsam, F.; Sun, Z.; Zhou, Y., Regiospecific synthesis of 1,5-disubstituted-1*H*-pyrazoles containing differentiated 3,4-dicarboxylic acid esters via suzuki coupling of the corresponding 5-trifluoromethane sulfonates. *Tetrahedron* **2007**, *63*, 1154-1166.
2. Hilpert, H., Practical approaches to the matrix metalloproteinase inhibitor trocade® (Ro 32-3555) and to the TNF-α converting enzyme inhibitor ro 32-7315. *Tetrahedron* **2001**, *57*, 7675-7683.
3. Marer, F.; Hammann, I.; Homeyer, B.; Behrenz, W. N-methyl-0-pyrazol(4)yl-carbamic acid esters, process for their synthesis and their use as pesticides. . EP0023326 (A1), Feb 4, 1981.
4. Sasaki, I.; Toyoda, T.; Yoshinaga, H.; Natsutani, I.; Takahashi, Y. Preparation of (pyrazol-3-yl)methanamine derivatives as serotonin reuptake inhibitors having 5-HT2C antagonism. WO 2012008528A1, Jan 19, 2012.
5. Moreau, F.; Desroy, N.; Genevard, J. M.; Vongsouthi, V.; Gerusz, V.; Le Fralliec, G.; Oliveira, C.; Floquet, S.; Denis, A.; Escaich, S.; Wolf, K.; Busemann, M.; Aschenbrenner, A., Discovery of new Gram-negative antivirulence drugs: Structure and properties of novel *E. Coli* WaaC inhibitors. *Bioorg. Med. Chem. Lett.* **2008**, *18*, 4022-4026.
6. Desroses, M.; Jacques-Cordonnier, M.-C.; Llona-Minguez, S.; Jacques, S.; Koolmeister, T.; Helleday, T.; Scobie, M., A convenient microwave-assisted propylphosphonic

- anhydride (T3P®) mediated one-pot pyrazolone synthesis. *Eur. J. Org. Chem.* **2013**, *2013*, 5879-5885.
7. Chemistry of Heterocyclic Compounds (New York, N., United States)(Translation of Khimiya Geterotsiklicheskikh Soedinenii) Nam, N.; Grandberg, I., Condensation of n-3-substituted 5-pyrazolones with esters of  $\beta$ -keto acids. Synthesis of pyrano[2,3- c]pyrazol-6-ones. *Chem. Heterocycl. Compd.* **2006**, *42*, 326-330.
8. Balestra, M.; Bunting, H.; Chen, D.; Egle, I.; Forst, J.; Frey, J.; Isaac, M.; Ma, F.; Nugiel, D.; Slassi, A. Preparation of pyrazolones as metabotropic glutamate receptor agonists for the treatment of neurological and psychiatric disorders. WO 2006071730 A1, Jul 06, 2006. .
9. Buchi, J.; Ursprung, R.; Lauener, G., *N,N'*-dialkylpyrazolones. *Helv. Chim. Acta* **1949**, *32*, 984-992.
10. Kim, M. M.; Ruck, R. T.; Zhao, D.; Huffman, M. A., Green iodination of pyrazoles with iodine/hydrogen peroxide in water. *Tetrahedron Lett.* **2008**, *49*, 4026-4028.
11. Altman, R. A.; Shafir, A.; Choi, A.; Lichtor, P. A.; Buchwald, S. L., An improved Cu-based catalyst system for the reactions of alcohols with aryl halides. *J. Org. Chem.* **2007**, *73*, 284-286.
12. Maurer, F.; Hammann, I.; Homeyer, B.; Behrenz, W. 4-pyrazolyl *N*-methylcarbamates. EP 23326 A1 Feb 04, 1981.
13. Xue, F.; Seto, C. T., Fluorogenic peptide substrates for serine and threonine phosphatases. *Org. Lett.* **2010**, *12*, 1936-1939.

14. Rodríguez-Franco, M. I.; Dorronsoro, I.; Hernández-Higueras, A. I.; Antequera, G., A mild and efficient method for the regioselective iodination of pyrazoles. *Tetrahedron Lett.* **2001**, *42*, 863-865.
15. Anderson, E. D.; Boger, D. L., Inverse electron demand diels-alder reactions of 1,2,3-triazines: Pronounced substituent effects on reactivity and cycloaddition scope. *J. Am. Chem. Soc.* **2011**, *133*, 12285-12292.
16. Geyer, R.; Igel, P.; Kaske, M.; Elz, S.; Buschauer, A., Synthesis, SAR and selectivity of 2-acyl- and 2-cyano-1-hetarylalkyl-guanidines at the four histamine receptor subtypes: A bioisosteric approach. *MedChemComm* **2014**, *5*, 72-81.
17. Zhu, L.; Li, G.; Luo, L.; Guo, P.; Lan, J.; You, J., Highly functional group tolerance in copper-catalyzed *N*-arylation of nitrogen-containing heterocycles under mild conditions. *J. Org. Chem.* **2009**, *74*, 2200-2202.
18. Gellibert, F.; de Gouville, A.-C.; Woolven, J.; Mathews, N.; Nguyen, V.-L.; Bertho-Ruault, C.; Patikis, A.; Grygielko, E. T.; Laping, N. J.; Huet, S., Discovery of 4-{4-[3-(pyridin-2-yl)-1*H*-pyrazol-4-yl]pyridin-2-yl}-*N*-(tetrahydro-2*H*-pyran-4-yl) benzamide (GW788388): A potent, selective, and orally active transforming growth factor- $\beta$  type i receptor inhibitor. *J. Med. Chem.* **2006**, *49*, 2210-2221.
19. Xu, Z.-L.; Li, H.-X.; Ren, Z.-G.; Du, W.-Y.; Xu, W.-C.; Lang, J.-P., Cu(OAc)<sub>2</sub>.H<sub>2</sub>O-catalyzed *N*-arylation of nitrogen-containing heterocycles. *Tetrahedron* **2011**, *67*, 5282-5288.
20. Forbes, I. T.; Johnson, C. N.; Thompson, M., Syntheses of functionalised pyrido[2,3-*b*]indoles. *J. Chem. Soc., Perkin Trans. I* **1992**, 275-281.